EFFECT OF HIGH FREE STREAM TURBULENCE ON FILM COOLING
USING DOUBLE ROW OF 30° SLANT-HOLE INJECTORS

THESIS

Lilith I. Sorensen

AFIT/GAE/ENY/98M-03

19980423 065

Approved for public release; distribution unlimited

The views expressed in this thesis are those of the author and do not reflect the official policy or position of the Department of Defense or the U. S. Governmet.

EFFECT OF HIGH FREE STREAM TURBULENCE ON FILM COOLING USING

DOUBLE ROW OF 30° SLANT-HOLE INJECTORS

THESIS

Presented to the Faculty of the School of Engineering

of the Air Force Institute of Technology

Air University

In Partial Fulfillment of the

Requirements for the Degree of

Master of Science in Aeronautical Engineering

Lilith I. Sorensen, B. S.

March 1998

EFFECT OF HIGH FREE STREAM TURBULENCE ON FILM COOLING USING DOUBLE

ROW OF 30° SLANT-HOLE INJECTORS

Lilith I. Sorensen, B. S.

Approved:

_____
Chairman

11 May 98

_____

11 March 1998

_____

23 Mar 98

Acknowledgments

This study was a continuation of a project conducted at the Wright Research and Development Center (WRDC), Aero Propulsion and Power Laboratory, Components Branch (POTC) Turbine Engine Division. The test setup and data acquisition used for the study was done by Major Dino Ishikura.

I wish to express my deep appreciation and thanks to my faculty advisor Dr. Paul King for his technical guidance, encouragement, mentoring and patience throughout the time span spent to conduct this thesis research.

I would also like to thank Dr. Richard Rivir and Mr.Greg Cala from the Aero and Power Laboratory for providing assistance and the background information needed to continue the project.

Finally, I am deeply indebted to my husband, Scott and my children, Nichole and Raymond, for their support and understanding during this research.

Table of Contents

List of Figures

List of Tables

List of Symbols

b   - wall jet nozzle exit, (cm)

B   - blowing ratio

B_{opt} - optimum blowing ratio

CD   - coefficient of discharge

C_f - skin friction coefficient

C_p - specific heat at constant pressure (J/kg°K)

d   - injection hole diameter (cm))

D   - injection hole diameter (cm)

h   - heat transfer coefficient (W/m² °K)

h_o - heat transfer coefficient with film cooling (W/m² °K)

I   - momentum flux

J_u - integral time scale (s)

k   - conductivity (W/cm°K)

K   - Von Karman constant

l   - thickness (cm)

L   - integral length scale (cm)

M_j - wall jet momentum flux

P_{bar} - barometric pressure (N/m²)

P_{kiel} - kiel probe measured pressure (N/m²)

P_{tank} - pressure in main air supply plenum chamber (N/m²)

$P_{tankcool}$ - pressure in main coolant plenum chamber (N/m²)

P/D   - pitch to diameter ratio

Pr   - Prandlt number

q   - heat flux (W/m^2)

Re   - Reynolds number

R_{air} - gas constant for air (J/kg °K)

S   - spanwise hole spacing (cm)

St   - Stanton number

St_o - Stanton number with low free stream turbulence

t   - time (s)

T   - static temperature (°K)

T_{bs} - temperature at bottom surface of the plate (°K)

Thw   - free stream recovery temperature (°K)

Tr   - recovery temperature (°K)

T_{tank} - temperature in main air supply plenum chamber (°K)

$T_{tankcool}$ - temperature in coolant supply plenum chamber (°K)

Tu   - turbulence

T_w - wall temperature (°K)

$T\phi$ - air-coolant mixture temperature (°K)

u   - instantaneous velocity fluctuation (m/s)

u′   - velocity fluctuation (m/s)

u_o - local maximum velocity at a station (m/s)

U   - velocity (m/s)

U_j - wall jet nozzle exit velocity (m/s)

U_m - local maximum velocity at a station (m/s)

U_x - total velocity component in the x direction (m/s)

$U\tau$ - friction velocity (m/s)

U_{tau} - friction velocity (m/s)

U_∞ - free stream velocity at injection (unless otherwise specified, m/s)

U_{inf} - free stream velocity at injection (unless otherwise specified, m/s)

U_1 - free stream velocity (m/s)

v - kinematic viscosity (m^2/s^2)

x - longitudinal distance from nozzle exit to a station (cm)

X - longitudinal distance from injection (cm)

X_{inj} - longitudinal distance from nozzle exit to injection (cm)

X_L - longitudinal distance from nozzle exit to a station (cm)

y - vertical distance from the plate(m)

y_m - vertical distance where the profile velocity is a maximum (m)

$y_{m/2}$ - vertical distance where the profile velocity is half its maximum value (m)

z - lateral distance from the plate centerline (cm)

Greek Symbols

δ - boundary layer thickness (cm)

δ_* - displacement thickness(cm)

γ - friction factor

η - film cooling effectiveness

ν - kinematic viscosity (m^2/s)

ρ - density (kg/cm^3)

τ_w - wall shear stress (N/m^2)

Subscripts

aw   - adiabatic wall

c   - coolant

j   - nozzle exit

w   - wall

∞   - free stream

Abstract

Film cooling has an inherent complex flow structure due to the injection of coolant into the mainstream boundary layer. Phenomena such as film blow-off at high blowing rates are part of the experience when using discrete holes to inject the coolant. Inside a turbine, this flow structure is further complicated by the introduction of free stream turbulence. Knowledge of the effect free stream turbulence has on film cooling effectiveness serves to improve the prediction of coolant requirements during turbine operation .

In this study free stream turbulence levels from 7.3 % to 17.8 % are applied to film cooling over a flat plate with two rows of 30° slant-holes using a wall jet as the main stream air supply. Blowing ratios are varied from 0.25 to 2.0 and free stream velocities at injection range from 10 m/s to 85 m/s. A constant density ratio of 1.07 is kept throughout the experiment.

Results show that for different magnitudes of blowing ratio free stream turbulence has a different influence on effectiveness. At the forward stations, where blow-off was present at high blowing ratios, high free stream turbulence increased effectiveness. While at mid to aft stations for all blowing ratios high free stream turbulence decreased effectiveness.

A correlation for effectiveness with a non-dimensional group of film cooling parameters is offered. The effectiveness correlated best 10 to 15 diameters after injection where blow-off effects are no longer present, and before the very far downstream stations where uncertainties in the measurements were greater.

1. Introduction

1.1 Background

A common practice to improve the performance of advanced gas turbine engines is to increase engine operating temperatures in order to increase the thermodynamic efficiency. Current engine operating temperatures are in the neighborhood of 1750°K. To maintain structural integrity under such a high temperature environment cooling of turbine blades is still necessary, despite major material advances leading to the use of components made from nickel superalloys and ceramics. Consequently, film cooling continues to be an important technology development area.

Film cooling is applied through the injection of coolant onto the surface of the blade. This is done by bleeding air from the compressor and redirecting it to channels inside the turbine blade. The air is then injected onto the blade through holes on the surface of the blade. At present, less than 10 % of total engine compressor flow is used for cooling. The subtraction of this air from the main compressor flow produces unwanted work losses. The reduction of these losses is a big motivation for the achievement of better prediction of coolant requirements.

The parameter used to quantify the performance of film cooling, and therefore predict coolant requirements, is referred to as the adiabatic effectiveness and defined as:

$$\eta = \frac{T_{aw} - T_{\infty}}{T_c - T_{\infty}} \qquad (1\text{-}1)$$

where T_{aw} is the adiabatic wall temperature, T_{∞} is the free stream temperature and T_c is the coolant temperature. (For high speed flow the flow temperatures would be replaced by recovery

temperatures.) Additional insight into these parameters is provided in the following chapter on film cooling theory.

Another important parameter is the indicator of the mass flux ratio of coolant injection to free stream air, known as the blowing ratio and defined as:

$$B = \frac{\rho_c U_c}{\rho_\infty U_\infty} \qquad (1\text{-}2)$$

where ρ_c and ρ_∞ are the density of the coolant and free stream, respectively; and U_c and U_∞ are the velocities of the coolant and free stream, respectively.

In situations like blade cooling where high strength requirements exclude the use of a continuos slot and discrete hole injection is necessary, the blowing rate becomes a critical parameter in terms of film coverage of the plate. For high blowing rate injection, mainly $B > 1.0$, the cooling jets detach from the surface and penetrate into the mainstream. This leaves the immediate area after injection with little protection and allows mainstream air to come in contact with the surface. This occurrence is commonly known as blow-off, and is expected to have a marked effect on how free stream turbulence affects effectiveness in this experiment.

Like the blowing ratio, the choice of film cooling configuration parameters also has an impact on the magnitude of the effectiveness achieved. For instance, the more parallel to the surface the injection of coolant is, the better the coverage and reach of the film over the surface. Therefore, the smallest possible injection angle should be used. However, current manufacturing technology limits this angle to 30°. The number of injection hole rows used also affects the end effectiveness. In experiments by Han and Menhendale (1986), and Cirriello (1991), two rows of holes have been shown to be superior to one row. Another important configuration parameter is the injection hole pitch (P/D). A pitch of 3.0 produced higher effectiveness than a pitch of 5.4 in

studies by Jubran and Brow (1985) with two rows of holes 10D apart. Most film cooling studies have been performed at $P/D = 3.0$. The present work was done using $P/D = 4.0$, to provide data within the range of $3.0 < P/D < 5.4$ which could be used to find the largest P/D less than 5.4 that still produces comparable values of η. Relative placement of the rows with one another also affects the performance of film cooling. Afejuku et al. (1980 and 1983) tested in-line and staggered configurations and showed the latter configuration to be superior.

The ratios of thermodynamic properties, such as density, between coolant and free stream also affect the performance of film cooling. In studies by Goldstein et al. (1966 and 1974) and Perdersen et al. (1977) using Helium, Freon-12 and CO_2 to produce different density ratios ($DR = \rho_c/\rho_\infty$), maximum η occurred at a higher density ratio with higher B. During actual turbine operation the coolant density is considerably higher than that of the free stream; the density ratio can be as high as 2.0. In the present experiment the secondary flow equipment limits the density ratio to 1.07.

The complexity of the flow structure inherent in the film cooling process also plays a major role on the achieved effectiveness. Secondary flow injection into a free stream increases the boundary layer thickness, δ, which in turn decreases heat transfer to the surface (Goldstein, 1971). Injection also causes the main flow speed to decrease upstream of the injecting jets creating an increase of pressure at this location while a decrease in pressure occurs at the downstream side of injection (Goldstein, 1971). This phenomenon results in a deformation of the jets. Vortices are generated within the jets which produce an intermixing of the coolant and free stream. Coolant flow is expelled from the jet while free stream air is introduced into the coolant region. Additionally, the interface or shear region between coolant and mainstream is characterized by

large scale turbulent structures which promote intermixing between the flows (Kohli and Bogard, 1996).

In practice, the complexity of the flow interaction between primary and secondary flow during film cooling is further complicated by the presence of free stream turbulence. Turbine blades are typically subjected to free stream turbulence in excess of 20 %. Even though this is the case, a relatively small number of film cooling studies have been performed with high free stream turbulence. One of the first comprehensive studies was conducted by Kadotani and Goldstein in 1979. Using turbulence generation grids, Tu levels from 0.3 % to 20.6 % with a length scale of 0.06d to 0.3d were applied to film cooling with one row of injection holes. They concluded that the free stream turbulence affects the effectiveness through changes in boundary layer thickness, mixing between mainstream and injected flow, shape of the injected flow due to vortex formation, and penetration height of the injected flow. For different blowing ratios the predominant factor among those listed varied. They also found that as the flow moves downstream, the effect of free stream turbulence becomes smaller. In a later study by Jumper (1988), a wall jet was used to generate free stream turbulence of 14 % to 17 %. Film cooling was applied through a single row of 30° slant-hole injectors. He found that at low B free stream turbulence decreased η. In a more recent study, Bons et al. (1994) used a single row of 35° slant-hole injectors, P/D = 3.0 and DR = 0.95. Turbulence was generated by a grid for the low Tu (0.9 %) and by jets in cross-flow for the mid to high Tu (6.5 % to 17.4 %). Bons et al. (1994) found that the effect free stream turbulence has on effectiveness depends on the magnitude of the blowing ratio. For B between 0.55 and 0.95, where blow-off is not normally present, free stream turbulence decreased centerline η. At these blowing ratios the reduction in η was dominated by the increased dissipation of the coolant into the mainstream. For B > 0.95, where blow-off is present, high free stream turbulence increased centerline and midline effectiveness at the forward stations by reintroducing detached

coolant closer to the surface and by promoting the lateral spread of the coolant jets. Similar effects to all these described are expected in this study which includes a comparable set of parameters. Schmidt and Bogard (1996) conducted a study using a single row of 30° slant-hole injections, P/D = 6.5 and Tu levels of 0.3 %, 10 %, and 17 %. In their study, laterally averaged η decreased with high Tu levels for low B. Kohli and Bogard (1997) studied the effect of free stream turbulence on the coolant and mainstream flow interaction using a single row of 35° slant-hole injectors, P/D = 1.05 and Tu levels of 0.5 % and 20 %. They determined that the coolant dispersion was initially dominated by the shear layer generated turbulence, followed farther downstream by large turbulent structures from the free stream.

All of the studies mentioned above studied the effects of free stream turbulence on effectiveness using a single row of injectors. The present work will study the case for two rows of 30° slant-hole injectors, wall jet generated Tu levels of 7.3 %, 12.2 % to 17.8 %, DR = 1.07 and P/D = 4.0. Additionally, each set of measurements will be taken for five different free stream velocities at injection.

Better understanding of high free stream turbulence effects on the mechanics of film cooling, and how these effects are influenced by other film cooling parameters, will enable improved modeling of the process and therefore more accurate prediction of η.

1.2 Problem

The goal of this study is to investigate the effect free stream turbulence has on film cooling effectiveness as manifested in measurements for the case of two rows of 30° slant-hole injectors.

1.3 Scope

Effectiveness was generated for various values of Tu, B and U_∞ at injection

- Free stream turbulence was varied from 7.3 % to 17.8 %

- Blowing ratio was varied from 0.25 to 2.0

- U_∞ was varied from 10 m/s to 85 m/s

Density ratio was constant at 1.07.

1.4 Assumptions

In order to create a near-adiabatic wall condition, no power was applied to the plate from which surface temperatures were measured. At zero voltage, conduction and radiation losses are still present. Effectiveness was corrected for these losses in the normal direction to the plate. Losses in the lateral and longitudinal direction were assumed negligible.

1.5 Experimental Approach

Effectiveness was measured using a set-up designed to replicate film cooling conditions over a turbine blade using a practical range of parameters. A wall jet supplied the main stream air over the plate. The coolant air was injected through 2 rows of holes on the surface of the plate. The coolant temperature was an average of 10 to 20 degrees lower than the main stream air. With no power supplied to the plate, free stream and surface temperatures were collected along the plate.

This was done for each velocity and blowing ratio combination for all three levels of free stream turbulence.

1.6 Sequence of presentation

Following the introduction the film cooling effectiveness and wall jet characterization is presented, followed by a description of the experimental apparatus, experimental procedures and data reduction, results and discussion, and finally the conclusion.

2. Film Cooling Effectiveness and Wall Jet flow Characterization

2.1 Film cooling Effectiveness

Inside a turbine, film cooling is primarily used to reduce the convective heat transfer rate from the hot gases to an exposed blade. The secondary fluid not only produces an insulating layer which protects the surface of the blade, but it also acts as a heat sink by lowering the mean temperature in the boundary layer. The heat flux from the hot gases to the surface can be written

$$q = h_0 \left(T_{aw} - T_w \right) \qquad (2\text{-}1)$$

where h_0 is the heat transfer coefficient with film cooling, T_w is the wall temperature, and T_{aw} is the adiabatic wall temperature. The latter temperature is the surface temperature for the limiting case of a perfectly insulated surface where the heat flux would be zero. Without film cooling injection this adiabatic temperature would be the same as the free stream temperature or for high speed flow the recovery temperature. With injection, the resulting T_{aw} depends on the temperatures of the free stream and the coolant stream. To bypass this temperature dependence, the adiabatic wall temperature can be expressed in a dimensionless form called the film cooling effectiveness as:

$$\eta = \frac{T_{aw} - T_\infty}{T_c - T_\infty} \qquad (1\text{-}1)$$

where T_∞ is the free stream temperature and T_c is the temperature of the coolant at the point of injection (Goldstein, 1971). For high speed flows η is expressed as:

$$\eta = \frac{T_{aw} - T_{r\infty}}{T_{rc} - T_{r\infty}} \qquad\qquad (2\text{-}3)$$

where $T_{r\infty}$ is the free stream recovery temperature and T_{rc} is the recovery temperature of the coolant at injection. The limiting values of effectiveness are unity at the point of injection ($T_{aw} = T_{rc}$), and zero far downstream of injection where the secondary flow is greatly diluted and the wall temperature approaches the free stream recovery temperature.

2.2 Wall Jet Flow

2.2.1 General characteristics

When a fluid is blown parallel to a surface, it forms a configuration known as a wall jet. Figure 2-1. Shows the typical mean velocity distribution across a two-dimensional wall jet and defines the nomenclature. The wall jet is a two-layer shear flow that combines the characteristics of a boundary layer and a free jet. The region from the wall to Y_m is the inner layer, in which the flow exhibits similarities in structure with that of a conventional turbulent boundary layer. The region extending from Y_m to the outer edge of the flow is the outer layer (Launder and Rodi, 1983).

Modeling the high turbulence intensity of real engine blades under typical operating conditions in a laboratory is difficult. Many researchers, such as MacMullin et al. (1988), Maciejewski and Moffat (1989), Jumper et al. (1988), etc., used the aggressive flow characteristics of a wall jet over a flat plate at atmospheric pressure and temperature to generate a high turbulence level. MacMullin et al. (1988) determined that turbulence intensity in the wall jet boundary layer varied as a function of longitudinal distance along the plate and was largely independent of nozzle velocity. This is an important fact because a wide range of Reynolds number may be covered by varying the nozzle exit velocity, without much change in the local turbulence level. MacMullin et

al. used a round ASME nozzle to generate the free jet with high turbulence intensity level for his study.

Eckerle (1988) used a 7 cm x 48 cm short radius rectangular nozzle to create a wall jet. He found that the rectangular geometry reduced the edge effects observed in previous tests with a circular wall jet, in which a variation was observed in the velocity field and turbulence intensity in the lateral border of the jet. Eckerle (1988) also found a region in the centerline of the flow at a distance three times the nozzle diameter, where the velocity field and the turbulence intensity suffered perturbations. This could have been caused by the recirculation over the plate, due to induced flow over the settling chamber. For the present research, a new longer rectangular nozzle was used to eliminate this problem.

2.2.2 Applicable scaling laws

For the wall jet flow, the choice of scaling parameters or the application of a specific scaling law has not entirely been agreed on by researchers in the field. A study by Wygnanski et al. (1992) on the applicability of scaling laws to the turbulent wall jet provides valuable information on the subject. In the study, the wall jet flow was scaled by the local length and velocity scales, by outer flow variables, and by wall jet momentum flux.

For the initial scaling, Wygnanski et al. (1992) plotted velocity profiles for several values of Re_j in $Y/Y_{m/2}$ and U/U_m coordinates. A good collapse was obtained at Y locations far from the wall ($Y/Y_{m/2} \sim 1$), but near the wall the profiles were dependent on Re_j. This finding triggered their search for a different way of scaling the data which could sustain self-similarity for a range of Re_j.

Wygnanski et al. (1992) obtained a good collapse for all velocity profiles and all Re_j

through the use of outer variables, $Y/Y_{m/2}$ and $(U-U_m)/U_\tau$, where,

$$\frac{U-U_m}{U_\tau} = A\log\left(\frac{Y}{Y_m}\right) + A\Pi\left[w\left(\frac{Y}{Y_m}\right) - w(1)\right], \quad (2-4)$$

and

$$w\left(\frac{Y}{Y_m}\right) = 3\left(\frac{Y}{Y_m}\right)^2 - 2\left(\frac{Y}{Y_m}\right)^3$$

is a wake function curve fit (White, 1991), Π is Coles wake parameter equal to 0.45 for a flat plate

(White, 1991), and A is the universal constant of the inner scaling laws equal to 3.9 for the profiles

in this experiment. (In his 1992 paper Wygnanski et al. points out that several researchers, Myers

et al. (1963), Bradshaw and Gee (1962) and R. P. Patel (1962), question the universality of the

constant A and propose constants varying from 3.9 to 4.75). Wygnanski et al. (1992) showed that

outer variables correlate well beyond the maximum velocity point $(U = U_m)$ and well below the

location where the Reynolds stress, $(-\rho\overline{u'v'})$, vanishes near the solid wall. Equation 2-4 is also

known as the Outer Law.

Additionally, Wygnanski et al. (1992) scaled the flow by the wall jet momentum flux,

$M_j = U_j^2 b$, and compared his results with those of Narasimha et al.(1973). In their separate works

this scaling was shown to be independent of Re_j, for large values of the same parameter.

Wygnanski determined the threshold to be $Re_j > 5000$. For the present work Re_j values ranged

from 43,300 to 368,000 which fall well above the threshold value. Both researchers used the same

form of the following power law:

$$U_m \frac{\upsilon}{M_j} = A_u \left(X_L \frac{M_j}{\upsilon^2} \right)^n , \tag{2-5}$$

where X_L is distance in the flow direction measured from the nozzle exit to a station ($X_L = X_{inj}$) for

the current application, i. e., the distance from the nozzle exit to the coolant injection point). Each

study produced slightly different values for the exponent n, however, and also fairly different

values of the constant A_u. Wygnanski obtained $A_u = 1.473$ and n = -0.472, while Narasimha

obtained $A_u = 4.6$ and n = -0.506. Wygnanski attributes the differences in the constants to the

scatter in Narasimha's original data. The set of constant and exponent obtained by Wygnanski was

used in this experiment. Further detail on how the appropriate set was selected is given in Chapter

5.

The development of the wall jet scaling by momentum flux from Wygnanski's study also

included an equation for the Y location where η becomes half of its original value. This equation

takes the form

$$Y_{m/2} \frac{M_j}{\upsilon^2} = A_y \left(X_L \frac{M_j}{\upsilon^2} \right)^m , \tag{2-6}$$

where $A_y = 1.445$ and m = 0.881.

Also from the same development, the friction velocity, $U_\tau = \left(\tau_w / \rho \right)^{1/2}$, can be obtained

through a combination of equation (2-5) and equation (2-7)

$$\frac{\tau_w}{\rho} \left(\frac{\upsilon}{M_j} \right)^2 = A_\tau \left(X_L \frac{M_j}{\upsilon^2} \right)^k , \tag{2-7}$$

where $A_\tau = 0.146$ and k = -1.07, which yields

$$\frac{U_m}{U_\tau} = \frac{A_u}{A_\tau^{1/2}} \left(X_L \frac{M_j}{\upsilon^2} \right)^{n-k/2}$$

(2-8)

Finally, substituting the respective constants and exponents gives

$$\frac{U_m}{U_\tau} = 3.85 \left(X_L \frac{M_j}{\upsilon^2} \right)^{0.063}$$

(2-9)

The scaling of the wall jet flow by the momentum flux provided the means to obtain the

input parameters of equation (2-4) and later solve for U to generate velocity profiles. This is the

main capacity the wall jet scaling development is used for in the present work.

3. Experimental Apparatus

The equipment and set up described in this section were used for preliminary measurements to qualify the configuration of a rectangular nozzle and instrumented table, as well as for the collection of the data to be analyzed.

Previous research by Eckerle (1988), MacMullin (1986), and Jumper (1988) was conducted in the same facility in room 21 at WRDC/POTC, with small variations in configuration. To eliminate recirculation over the plate, due to induced flow over the settling chamber and surroundings, a long radius ASME rectangular nozzle was built and installed. An additional step was to add one 60 % open perforated plate in the settling chamber to break up the flow structure coming from the wall jet generator. The perforated plate was positioned upstream of the egg crate and honeycomb flow straightener already existent.

The complete table set up consists of a test section (flat plate), two extension tables, and an injection table. In the following subsections the flat plate and extension tables are described first, followed by the injection table, the traversing system, and finally the data acquisition system. Figures 3-1(a), (b) and (c) illustrate the complete apparatus layout.

3.1 Flat Plate and Extension Tables

The test section (flat plate) is used for the evaluation of the film cooling effectiveness from measurements of surface temperatures using embedded thermocouples (see Figure 3-2 for detailed layout). The plate is laid out into fourteen stations starting at $x/d = 5$ to 70 in increments of 5, where x is measured from the injection point and d is the diameter of the hole. At each station

there are eight laterally embedded thermocouples. The flat plate substrate consists of a 46.04 cm x 1.549 m stainless steel plate, insulated by fiberglass, wood, and Styrofoam with thickness of 0.476 cm, 3.65 cm, 15.24 cm, respectively, placed underneath the plate. This flat plate substrate is supported by a wood structure and is positioned immediately after the injection table.

Two extension tables measuring 1.22 m x 33.3 cm and 1.22 m x 1.33 m, are used to increase the distance from nozzle exit to the injection holes to a specific downstream location where the Tu intensity level is known. These tables are inserted directly between the nozzle exit and the injection table. Data was recorded at three different free stream turbulence levels,

- Tu = 7.3 % - no extension table, injection table at nozzle exit, X_{inj} = 34.69 cm.

- Tu = 12.2 % - one extension table inserted immediately upstream of the injection table, X_{inj} = 68.02 cm.

- Tu = 17.8 % - two extension tables inserted immediately upstream of the injection table, X_{inj} = 2.013 m.

3.2 Air Supply (Wall jet)

The main stream air is supplied by a compressor rated at 300 psi and 7.5 lb./sec., and passes through a gate valve into a cylindrical settling chamber with a diameter of 0.81 m and a length of 1.52 m. Inside the settling chamber the wall jet stagnation temperature was measured by a 24 gauge iron-constantan thermocouple. The wall jet is produced over a flat plate, at the outlet of a nozzle. The nozzle is an ASME long radius rectangular nozzle with a 48.0 cm by 6.5 cm cross section and a length of 38.0 cm. This apparatus is designed to provide clean flow (absence of oil and dirt), with uniform turbulence level and velocity fields at nozzle exit, steady flow, and absence of swirl.

Side walls to ensure the two dimensionality of the flow are positioned at both sides of the plate. The 15.2 cm height side walls are much higher than the boundary layer formed up to 3 m from the nozzle exit, therefore the two-dimesionality of the main flow is guaranteed. Moreover, despite the increase of the boundary layer by the secondary flow injection, the lateral wall is still high enough to avoid interference of room air from the sides into the region where the measurements were taken.

3.3 Injection Table

The injection table is a 1.22 m x 37.62 cm horizontal flat surface with a total of eleven injection holes distributed between two rows, 5 holes upstream and 6 holes downstream. The row-to-row distance is 3.64d, with the holes at the vertices of an isosceles triangle, as shown in Figure 3-5, and a pitch to diameter ratio of 4. The downstream edge of the second row serves as the reference line for measuring the distance from the nozzle exit to injection and from injection to each station.

The coolant flow is supplied by an A/M 32C-4 aircraft ground air conditioner unit. This unit is capable of supplying air at a constant temperature in the range of 20 to 100°F. Prior to injection, the coolant is delivered to a plenum chamber with measurements of 20 x 50 x 22 cm.

The secondary flow is injected through stainless steel tubes with an internal diameter of 1.83 cm. One end of the tubes is glued to the upper plate of the plenum chamber and the other end to the injection table, flush to the test surface. The film cooling injection tube length was established as three times the injection tube diameter. With this tube length the velocity profile of the cooling flow at the point of injection is not fully developed. This is a desirable condition since the objective is to simulate as close as possible an actual turbine application. If the tube is too long the velocity profile would be fully developed, and would influence the penetration of the cooling jet

into the main stream and the structure of the film cooling. The injection angle is 30° which is often used in actual turbine blades. This angle was also chosen because it facilitates comparison with results obtained by other researchers.

3.4 Traversing System

The traversing system included manual adjustment of the vertical and lateral probe location. A hot-film probe and a boundary layer thermocouple were held at the same height, side by side, on a support bar, 3.55 m in length. These thermocouples were used to collect velocity and temperature data of the main stream flow at the centerline of the flat table.

3.5 Data Acquisition System

The data acquisition hardware was controlled by a Hewlett Packard HP 9845C computer controller, which was connected directly through an HP-IB interface bus (IEEE-488 standard) to an 80 channel HP 3497A Data Acquisition Controller Unit and two HP 3478A digital multimeters. Velocity and turbulence intensity were calculated by the HP computer and the results stored on HP 9885M flexible disk drive, 8 in. floppy disks. The data acquisition software provided a real time display of the velocity and turbulence intensity profile.

Velocity measurements were obtained from a single hot-film sensor controlled by a Thermo-System Inc. (TSI) IFA-100 constant temperature anemometer. The anemometer RMS outputs were read by the HP 3478A multimeters. The HP 3497A controller unit read the thermocouple and DC anemometer voltages. The anemometer output was also connected in parallel to an HP 3562A Dynamic Signal Analyzer for autocorrelation integral time scale measurements. A standard model TSI 1210-20 hot-film probe was used throughout the test.

Additional equipment included a TransAmerica CEC 2500 Digital Barometer, which measured the laboratory ambient pressure; a TSI 1125 Calibrator for hot-film calibration; and a Tektronix 2430A Digital Oscilloscope to measure the frequency response and stability of the film anemometer.

4. Experimental Procedures and Data Reduction

Two major types of measurements were performed during this research: preliminary measurements (diagnostic or validation) and actual data collection measurements. The following section describes procedures and data reduction for all measurement collections. Since the author did not take part in the collection of the data the following descriptions were gathered in part by reconstructing the events based on the evidence revealed by the data records, information acquired from the thesis prospectus, and by accounts from researchers present at the time the experiment was taking place. Any small deviation from actual events is purely unintentional. The preliminary measurements taken to assess the two dimensionality of the main stream flow over the flat plate are described first, followed by the velocity and temperature profiles and finally the film cooling effectiveness measurements.

4.1 Preliminary Measurements

4.1.1 Two Dimensionality Analysis

An open flat plate measuring 2.4 m by 4.9 m was placed tangentially in front of a short rectangular nozzle without lateral constrains. The velocity distribution was determined at nine locations along the plate with coordinates x, y, z, where x is the distance from the nozzle, y is the height where the maximum velocity was achieved (local Y_m) and z is the lateral distance from centerline. The x distances along the plate were, x = 22.9, 45.7, 66.7, 100.0, 133.4, 166.7, 215.9, 279.4, and 333.4 cm. Figure 4-1 shows the results plotted in contour and three-dimensional plots.

The lateral traverse of velocity showed that only the region very close to the centerline ($|z| < 15$ cm) and close to the nozzle ($x < 45$ cm), i.e. the core region, had a near two-dimensional profile. Outside this region, the distribution had no level plateau of velocity, indicating that the flow over the open flat plate was not close to two-dimensional. The lateral jet spread was determined by the locus of lateral positions where the velocity is 50 % of the local centerline velocity. The value of the jet spread angle measured without side walls was about 6 degrees, as can be seen in Figure 4-2. The results indicated that a simple flat plate is unsuitable, and side walls are required to avoid lateral jet spread and/or induction of air. These results led to the experiment to check the two-dimensionality of the flow including side walls, described in the next section.

As part of the two dimensionality check, the velocity measurements were used to calculate the turbulence intensity, integral length scale and velocity fluctuation. The turbulence intensity (Tu) is defined as:

$$Tu = \frac{u'}{U} \qquad (4\text{-}1)$$

where U is the mean velocity, and the rms velocity fluctuation (u') is defined as:

$$u' = \sqrt{\overline{u^2}} \qquad (4\text{-}2)$$

in which u is the instantaneous velocity fluctuation. The total velocity component in the x direction (U_x) is defined as :

$$U_x = U + u \qquad (4\text{-}3)$$

The integral length scale (L) is defined as:

$$L = UJ_u \tag{4-4}$$

where J_u is the integral time scale defined as:

$$J_u = \int_0^\infty \frac{U_x(t)U_x(t+\tau)}{\overline{u^2}} d\tau \tag{4-5}$$

where τ is the time increment.

Figures 4-3, 4-4, and 4-5 show the resulting turbulence intensity level, integral length scale, and velocity fluctuation in contour and three-dimensional plots. The figures show that all these parameters change considerably in the longitudinal and lateral direction.

4.1.2 Two Dimensionality with Side walls

The boundary layer velocity was acquired with the previously described apparatus. The velocity fluctuation, turbulence intensity, and integral length scale were evaluated as described in the previous section. Here a long radius ASME rectangular nozzle was used, with two side walls 45 cm apart, exactly the width of the rectangular nozzle. The side wall height was 15.2 cm. This wall height assured that the flow was contained in the channel, since the maximum thickness (Y_m) measured previously was only 5.1 cm at a distance 3 m downstream of the nozzle exit.

The results from the experiments with side walls were plotted in contour plots, and are shown in Figure 4-6. In all plots the contour lines are approximately perpendicular to the mean flow, showing that two-dimensional flow was achieved.

4-3

4.2 Velocity and Temperature Profiles (no film cooling injection)

Two velocity profile data sets were collected at U_j = 55.8 m/s to characterize the main stream flow vertically. One set was taken at 14 stations with 30 data points each ranging from Y = 0.508 cm to 17.78 cm and a Y increment of 0.254 cm. At each Y location turbulence intensity and velocity fluctuations were measured. A temperature profile was also taken at all 14 stations along the plate. A second velocity profile set was taken at 6 stations with 20 data points each ranging from 0.53 mm to 10.53 mm (did not include Y_m point) and a Y increment of 0.1 mm. The coefficient of friction (C_f) and the friction velocity (U_τ) were calculated at each station for this set of profile data.

4.3 Film Cooling Effectiveness Tests

Surface temperature measurements were taken at 14 stations with coordinates x, y, z, where x is the longitudinal distance from injection, y is the vertical distance (y = 0) and z is the lateral distance from the centerline. Eight lateral measurements were taken at each station from which an average T_w was calculated. Using T_w average and the corresponding free stream temperature at x, y, 0, a laterally averaged η was calculated. Effectiveness was obtained for five different U_∞ at injection values, 10, 18, 37, 60, and 85 m/s, at three Tu levels 7.3 %, 12.2 %, and 17.8 %, with a B range of 0.25 to 2.0. There was no heat applied to the plate in an attempt to create a near adiabatic surface condition. A correction was then applied to account for any losses still present due to conduction and radiation. This correction approach is based on similar procedures outlined by Mick and Mayle (1988) and Ligrani et. al., (1992), wherein the adiabatic film cooling effectiveness (equation 2-3) is rewritten including a correction term as

$$\eta = \frac{T_w - T_{r\infty}}{T_{rc} - T_{r\infty}} + \frac{q_{rad} + q_{cond}}{h_0 (T_{rc} - T_{r\infty})} \qquad (4\text{-}6)$$

where T_w is the actual measured wall temperature and h_0 is the heat transfer coefficient with film

cooling. The latter parameter was not available for this experiment and was estimated using a

Stanton number correlation (Kays and Crawford, 1980)

$$St_0 \, Pr^{0.4} = 0.0287 \, Re_x^{-0.2} \qquad (4\text{-}7)$$

and an expression to account for the effects of free stream turbulence on the Stanton number by

Simonich (1978)

$$\frac{St}{St_0} = 1 + 5Tu \qquad (4\text{-}8)$$

The derivation of equation (4-6) is presented in Appendix A.

Kinematic and thermodynamic properties of the main stream and secondary flow were

obtained through a mixture of direct measurements and calculations. Free stream pressure and

temperature measurements were taken at centerline with a Kiel probe and boundary layer

thermocouple located at Y_m where U_∞ is at a maximum. From these measurements the free stream

velocity was calculated. Coolant temperatures were calculated from coolant tank total temperature

and coolant velocity values. The coolant velocity, was calculated using the coefficient of discharge

and coolant tank pressure and density values. The secondary flow injection was kept at a

temperature 10 to 20 degrees lower than the free stream. Wall temperatures were registered using

thermocouples imbedded in the plate. A description for the uncertainties in the measurements and

the propagation of these to the calculation of the effectiveness is presented in Appendix B.

The procedure for collecting the data was the following:

1. Set U_∞ at injection by adjusting the pressure in the main tank

2. Set film cooling flow by adjusting the pressure in the cooling tank, which in turn sets the discharge coefficient (see Appendix C for CD correlation used)

3. When desired conditions are met, take measurements for T_m, $T_{r\alpha}$, P_{kiel}, T_{tank}, $T_{tankcool}$, P_{tank}, $P_{tankcool}$.

4. Reduce data (for thermocouple data reduction program see Appendix C)

The above procedure was repeated for each blowing rate for a given U_∞ at injection value and Tu level. The blowing rate was changed by resetting U_c (adjusting to desired coefficient of discharge) while keeping U_∞ at injection at a set value. The density ratio was maintained at slightly above one (~1.07). After the desired range of blowing rates was covered, U_∞ at injection would be changed next for the same Tu level until data was collected for all blowing rates. After data for all combinations of U_∞ and B had been collected an extension table was inserted to relocate the injection holes to the respective longitudinal location, X_{inj} for the next turbulence level to be tested. The turbulence level achieved at a specific X_{inj} was independent of the value of nozzle jet exit velocity set. In other words it did not matter whether U_∞ at injection was set to 10 m/s or 60 m/s, the turbulence level at $X_{inj} = 2.01$ m continued to be 17.8 %. This finding was determined by McMullin et al. (1988) who also used a wall jet (round ASME nozzle) as a source of free stream turbulence during his heat transfer research.

4.3.1 Reconstruction of free stream temperature data

Subsequent inspection of the free stream temperature data by this author revealed that the thermocouple used to record the free stream temperature, $T_{r\infty}$, , was positioned too close to the coolant jet stream and at high blowing rates, when the jet stream penetrated further into the main

stream, the temperature being registered was that of a mixture of coolant and main stream flow, not of the main stream alone. As a result, free stream temperature values needed to be replaced in all film cooling effectiveness calculations. Since the data could not be collected again (the test apparatus had been disassembled) an alternate way to obtain free stream temperature values was devised. Using the total temperature in the main air source plenum chamber, T_{tank}, and free stream velocities, new $T_{r\infty}$ values were calculated (for calculation details see Appendix D). The recovery temperature for low B values was also reconstructed because there was no way of knowing at which blowing ratio the free stream temperature measurements began to be tainted by the coolant.

The above mentioned misplacement of the free stream thermocouple could have been avoided by taking a temperature profile along the plate with injection at high and low blowing rates to locate the best position for the thermocouple for the respective blowing rate.

It was also found that the film cooling effectiveness was calculated using static temperature values instead of recovery temperature values which were verified to be necessary at the higher U_∞ and U_c conditions used in this experiment. Therefore, all relevant temperatures (T_∞, and T_c) were converted to recovery values and η values recalculated.

5. Results and Discussion

For this research, laterally averaged film cooling effectiveness was generated from the collection of surface and free stream temperatures acquired while injecting cooled air over an adiabatic plate through two rows of 30° slant-hole injectors. The data was obtained for five values of free stream velocities at injection from a rectangular slot (10, 18, 37, 60 and 85 m/s), three free stream turbulence levels (7.3 %, 12.2 % and 17.8 %), and blowing ratios from 0.25 to 2.0.

This chapter presents the results of the experiment and offers a discussion of the behaviors observed. The chapter is divided into two parts. The first part deals with the effect of free stream turbulence on film cooling effectiveness. The second part presents the development of a film cooling effectiveness correlation.

5.1 Effect of Free Stream Turbulence on Film Cooling Effectiveness

The effects of free stream turbulence on film cooling effectiveness involve a complex process, influenced by many factors. Film cooling effectiveness is affected by the presence of turbulence in the free stream through the enhanced mixing of the coolant with the main stream air. As the cooling air is injected, turbulence in the free stream spreads the air laterally, encouraging a uniform distribution of the injecting jets, and also vertically. For flows attached to the surface this vertical spreading usually implies a decrease in effectiveness as the coolant is diffused away from the surface; but as shown later in this section, effectiveness increases with increased turbulence if the flow has lifted from the surface due to a high blowing ratio. The method and the degree to

which free stream turbulence affects the performance of film cooling is influenced by such parameters as longitudinal distance from the injection holes (x/d), blowing ratio (B) and free stream velocity (U_∞). Various combinations of these parameters create different flow regimes, and the flow regime created determines the manner in which free stream turbulence affects film cooling effectiveness.

Two major regimes were detected, one for B < 0.75, where the cooling stream remains attached to the surface of the plate at all x/d and one for B ≥ 0.75, where the cooling stream lifts off from the surface of the plate and reattaches at x/d ≤ 15. To facilitate the discussion of the turbulence effects on film cooling effectiveness, the sections that follow are divided according to these different regimes, specifically:

- Effectiveness variation with x/d for B < 0.75 and B ≥ 0.75

- Local effectiveness variation with blowing rate for x/d ≤ 15 and x/d >15

All plots include data for Tu = 7.3 % and Tu = 12.2 %, and many include Tu = 17.8 % also. For further reference, Appendix E contains the plots of cases for specific combinations of B and U_∞ at injection that fall within the range of a particular section but are not directly referred to in the discussion.

5.1.1 Effectiveness Variation with x/d for B < 0.75

In the low range of blowing ratios 0.25 ≤ B < 0.75, a rapid monotomic decrease in effectiveness with x/d occurred, with lower Tu values generally yielding higher values of effectiveness, as can be seen in Figure 5-1. Generally, for low blowing ratios, high free stream turbulence has a detrimental effect as turbulent mixing diverts streamwise propagation of the lower

momentum injection (lower U_c) away from the plate, dissipating any amount of coolant reaching the end of the plate. In their study on the interaction between the coolant jet and mainstream flow (B = 0.4), Kohli and Bogard (1997) found that high free stream turbulence not only dispersed coolant away from the wall but also thrusted free stream air through the core of the coolant jet. This exchange of free stream and coolant fluid elements started at injection and became more pronounced downstream (x/d > 3) where elements of free stream flow penetrated through to the wall.

Only for low B (B ≤ 0.5) at extreme downstream regions, did the low Tu case not produce higher values of η. In Figures 5-1, 5-2 and 5-3 for U_∞ = 10, 37 and 85 m/s respectively, the Tu = 12.2 % case achieves a value of η higher than the Tu = 7.3 % case starting at x/d of 30 to 50 and continuing to the end of the plate. Bons et al. (1992) found (for a single row of holes) similar effectiveness enhancement at large x/d (starting at x/d ≈ 30) for B = 1.47, where the Tu = 6.5 % case produced higher values of centerline η than the Tu = 0.9 % case. He attributes this enhancement to the earlier merging of the cooling jet streams at higher Tu levels. For B > 0.5, higher effectiveness with low Tu occurred to the end of the measurement surface

5.1.2 Effectiveness Variation with x/d for B ≥ 0.75

As B increases above 0.75, a transition occurs between attached flow and blow-off (Figure 3), a condition where the cooling jet tends to detach at the forward stations and penetrate into the main stream. For the transition blowing rates, 0.75 < B < 1.0, the higher Tu cases keep the flow attached while for the lowest Tu case some degree of blow-off is possible, indicated by the presence of maximums in Figures 5-4 and 5-5. The progression from attached flow to blow-off can also be seen in Figures 5-6, 5-7 and 5-8 for the higher free stream velocity at injection,

U_∞ = 18 m/s, and in Figures 5-9, 5-10 and 5-11 for U_∞ = 37 m/s. As seen in these latter six figures, higher free stream velocities tend to delay the onset of blow-off to values of B nearer to unity; and always with the high Tu case the most resistive to blow-off for any velocity. Also for the transition blowing rates (B < 1.0) higher free stream velocities result in only small changes in effectiveness values (see Figures 5-4 and 5-10).

For higher blowing ratios (at or greater than unity), Figure 5-12 (B = 1.25 and U_∞ = 10 m/s) is representative of the overall trend in effectiveness with x/d. For the early stations effectiveness increased, reached a maximum, with a greater maximum for the high Tu cases, and decreased as the flow moved down the plate. The region of effectiveness increase between x/d = 5 and 10 is an indication that cooling flow is being reattached (brought closer to the surface) by the mixing action of the free stream turbulence. Figure 5-12 also shows that higher levels of turbulence cause an earlier reattachment of blow-off.

Once the cooling flow is reattached, indicated by a maximum, effectiveness is reduced downstream for the highest Tu flow as seen earlier for low B (B < 0.75) (see Figure 5-12). Again, low values of effectiveness for higher Tu develop as a result of the increased vertical dissipation of the film cooling air caused by the greater mixing action. Effectiveness values continue to have approximately the same differential between high and low Tu at stations toward the end of the plate. Each of the high free stream turbulence effects, early reattachment of blow-off, and accelerated effectiveness decay, was seen at similar downstream locations (x/d = 10~15) for midline η by Bons et al. (1994) in their work with only one row of holes but with similar magnitudes of free stream turbulence. The effectiveness in the present study was laterally averaged, therefore similarities with midline η are appropiate.

For very high blowing ratios up to 2.0, the various Tu-related differences in effectiveness are greatly reduced (curves come to a near-collapse in Figure 5-13) but overall levels of effectiveness are higher for higher blowing ratios. Thus for very high blowing ratios any free stream turbulence is limited in ability to improve effectiveness during blow-off.

Finally, an increase in U_∞ did not have a significant influence on the relative or absolute effects of free stream turbulence on effectiveness discussed above. See Figures 5-5 and 5-11.

Table 5-1. Summary of η variation with turbulence

Low B		High B pre blow-off reattach (forward stations)		High B post blow-off attach (mid to aft stations)	
Tu ↑	η ↓	Tu ↑	η ↑	Tu ↑	η ↓

5.1.3 Local Effectiveness Variation with Blowing Rate

5.1.3.1 Forward Stations (x/d ≤ 15)

A view of local film cooling effectiveness variation with B offers the opportunity to observe the effects of free stream turbulence on η from a different perspective. Figures 5-14 and 5-15 for x/d = 5 and 10, show the variation with B for U_∞ = 10 m/s. At these forward stations with B < 0.75, the coolant film is attached. (These figures are representative of what also happens at U_∞ = 18 m/s.) The resulting effectiveness decreases with increased levels of turbulence. From temperature profiles at low (0.9 %)and high (17.6 %) free stream turbulence levels and injection at a low blowing rate, Bons et al. (1994) was able to verify (for a single row of holes) substantial temperature dissipation due to greater mixing for the high Tu cases.

For the transition blowing ratio and beyond, B > 0.75, high free stream turbulence increases the value of effectiveness. As stated earlier in this chapter, high blowing rate injection produces blow-off at the forward stations as the higher momentum flow penetrates deeper into the mainstream. In this situation the dispersed film is more effectively redirected towards the plate due to the greater mixing of the higher free stream turbulence level. Also, for the higher blowing ratio, η generally tends to increase as B is increased.

At the intermediate station, $x/d = 15$, for B < 0.75 high free stream turbulence causes a decrease in effectiveness while a lack of sensitivity to Tu is seen for B > 0.75. Figure 5-16 shows the curves for Tu = 17.8 %, Tu = 12.2 % and Tu = 7.3 % merged at virtually the same effectiveness values.

At higher free stream velocities the limitations of the injection equipment restricted the maximum blowing ratio to 1.0 for $U_\infty = 37$ m/s , 0.68 for $U_\infty = 60$ m/s and 0.5 for $U_\infty = 85$ m/s. Higher free stream velocities, however, did not alter the influence of free stream turbulence on η previously discussed at lower velocities. In Figures 5-18, 5-18, 5-19, 5-20, 5-21, 5-22 for B < 0.75 and with $U_\infty = 37$, 60 and 85 m/s, respectively, the lower Tu level generally produces the higher effectiveness value. In Figures 5-17 and 5-18 for B > 0.75 the higher Tu level produces the higher effectiveness value.

Free stream turbulence did not significantly affect the optimum blowing ratio (B_{opt}) value. At $x/d = 5$ for $U_\infty = 18$ m/s (see Figure 5-23), B_{opt} changed from 0.25 to 0.50 when Tu increased from 7.3 % to 12.2%. When Tu increased further to 17.8 %, B_{opt} remained at 0.50. At $5 < x/d < 15$ B_{opt} remained at 2.0 for all Tu levels. Similar insensitivity was observed for $U_\infty = 10$, 37, 60, 85 m/s.

5.1.3.2 Aft stations (x/d > 15)

At x/d > 15, Figures 5-24, 5-25, 5-26, and 5-27 suggest that the film is in contact with the surface for any blowing rate and thus experiences a larger amount of vertical dissipation at higher turbulence. (i.e., for a given blowing ratio, B, as the longitudinal distance along the plate increases the mass of coolant reaching the end of the plate decreases). Also for higher blowing ratios η increases but is less dramatically affected by turbulence than at low blowing ratios. For instance, in Figure 5-24 for x/d = 20, for B = 0.25, η is very sensitive to Tu. As the flow moves further aft this sensitivity decreases but η is always higher for the low Tu case.

There are several instances at x/d $\geq$ 45 for the higher free stream velocity of U_∞ = 85 m/s where higher turbulence (Tu = 12.2 %) produces higher values of η than lower turbulence (Tu = 7.3 %). This occurrence again signals the fact that at very aft stations for low B, the medium Tu level of 12.2 % seems to be optimum.

As noted, in general η increases with B for all Tu levels for the higher velocities, 60 m/s and 85 m/s, however towards the middle and end of the plate there are some sharp dips in η registered for low blowing ratio, B = 0.35. Figures 5-28 - 5-31 show the effect (data was not collected for Tu = 12.2 %). For stations further aft (Figures 5-32, 5-33, 5-34) this dip in η becomes more pronounced with streamwise distance along the plate. At this time there is insufficient data to identify the causes for these isolated decreases in effectiveness for high free stream velocities with low blowing rates. Another uncharacteristic decrease in effectiveness occurs at x/d $\geq$ 65 for Tu = 7.3 % as B approaches 0.68 for U_∞ = 60 (Figure 5-35) and 0.50 for U_∞ = 85 m/s (Figure 5-36). Although these decreases fall within the uncertainty band of $\pm$ 0.015 for small values of η and low B, the fact that these decreases continue to show up in subsequent

stations strengthens the argument that these are true representations of the physics present in the flow and not an error in data collection.

The optimum blowing ratio did not change with free stream turbulence for x/d > 15. Figure 5-23 for $U_\infty = 18$ m/s shows that B_{opt} remained at 2.0 for all Tu levels. Similar insensitivity was observed for $U_\infty = 10, 37, 60, 85$ m/s.

5.2 Film Cooling Effectiveness Correlation

Film cooling effectiveness correlated with a grouping of film cooling parameters as

$$\eta = A_1 \, Re_{\delta^*}{}^b \left(\frac{X}{Bd}\right)^c Tu^f \qquad (5-1)$$

where X is longitudinal distance measured from the injection point and d is the diameter of the injection hole. The inclusion of Re_{δ^*} required $U_{(y)}$ distributions to determine δ^* at injection. Due to a lack of velocity profiles for all conditions, two methods were used to generate the required $U_{(y)}$ distributions. The velocity profile correlation known as the Outer Law (equation 2-4), valid when wall jet similarity is present, was used for injection at x/b ≥ 30. Here x is the longitudinal distance measured from the jet nozzle to a station and b is the height of the nozzle slot. For injection at x/b < 30, velocity profiles were available from test set up measurements and were curve fitted using a self-preserving wall jet distribution (i.e., preserving the proportionality of the distribution shape for a given flow). Even though the local velocity distributions are not fully self-preserving at these early stations, this wall jet distribution provides better profile shapes than other curve fitting distributions previously used.

During the preliminary search for an appropriate correlation grouping an effort was made to correlate effectiveness with different combinations of B, X, I and S without success. The details of this undertaking are given in Appendix F.

The following sections begin with a discussion on the film cooling parameter grouping $Re_{\delta*}{}^b[(X/Bd)]^c$, followed by a detailed description of the two velocity profile generation methods, the displacement thickness calculation, and finally, the development of the correlation.

5.2.1 Effectiveness Correlation with $Re_{\delta*}{}^b[X/(Bd)]^c$

The grouping $Re_{\delta*}{}^b[(X/Bd)]^c$ was used to correlate effectiveness for several reasons. The method used to generate different free stream Tu levels (wall jet) required that the starting length prior to injection be increased for increased Tu levels. The parameter $Re_{\delta*}$ would therefore account for the effect of the differences in displacement thickness prior to injection for various Tu levels. Furthermore, this grouping and others similar to it, with the term $[X/(Bd)]^c$ by itself or multiplied by a form of Re, had been successfully used in other effectiveness correlations (Goldstein, Shavit, and Chen, 1965).

The Reynolds number based on displacement thickness was calculated for several U_∞ velocities for each Tu level. The calculation of the displacement thickness for each of these conditions required velocity profiles. As mentioned earlier, velocity profiles were not available for all of the five free stream velocities used in the experiment; therefore, an alternate way to generate velocity profiles was developed based on the only profile available, collected during preliminary test set-up for $U_j = 55.8$m/s. Two sets of velocity profiles for $U_j = 55.8$m/s enabled the method, one

at 14 station locations with a Y increment of 0.254 cm and another at 6 station locations with a Y increment of 0.1 mm,.

The procedure entailed the use of the self-similarity principle for a wall jet. The use of self-similarity considerations which are appropriate for values of x/b > 20 to 30 (Narasimha et al., 1973, and Wygnanski et al., 1992), excluded the generation of velocity profiles for Tu =7.3 % and Tu = 12.2 %. Cooling injection for these two turbulence levels was at x/b = 5.4 and x/b = 10.5, both of which are upstream of the region in question. Therefore, the method used to generate velocity profiles based on self-similarity applies only for Tu = 17.8 %, with injection at x/b = 31.7.

5.2.1.1 Velocity profiles for film cooling injection with Tu = 17.8 %

The Outer Law (equation 2-4) was evaluated for its suitability to produce velocity profiles for the present wall jet flow. To ascertain the degree of self-similarity of the flow, fourteen station velocity profiles were plotted in Outer Law variables, $Y/Y_{m/2}$ and $(U-U_m)/U_\tau$, for $Y^+ > 30$ (i.e. the region where the logarithmic velocity distribution applies). The collapse of the profiles was fair except for the earliest stations, x/b = 5, 10 and 15, with the first of these showing the most obvious separation (see Figure 5-37).

For a closer look at the region near the wall, Figure 5-38 shows a plot of the three station profiles with the best collapse, x/b = 35, 41 and 47, along with the Outer Law equation. As expected, self-similarity was not exhibited by the profiles at the forward stations. However, at x/b = 25 the profile seemed to collapse with the others at several Y locations. Therefore, it is safe to assume that for this wall jet self-similarity begins between x/b = 25 and x/b = 35.

Based on the collapse using the Outer Law variables, and the fact that self-similarity has been shown to be independent of Re_j when plotting profiles in this manner (Wygnanski et al.,

1992), the Outer Law was considered a suitable technique to generate velocity profiles for

x/b = 31.7 (Tu =17.8 %) and different values of free stream velocity.

5.2.1.1.1 Determination of U_m, Y_m and U_τ

To use equation 2-4, the values of U_m, Y_m and U_τ were produced using power laws

developed through the momentum flux scaling of the flow by Wygnanski et al.(1992).

Figure 5-39 shows equation 2-5 plotted using two sets of the constant A_u and the exponent n. One

set corresponds to the power law given by Wygnanski et al.(1992) and the other set belongs to the

power law given by Narasimha et al. (1973), who also scaled the flow by M_j. To select which set

was appropriate to use for the wall jet flow in this study the equation was plotted using

$U_j = 55.8$ m/s for x/b = 5, 15, 25, 35, 41, and 47, along with the respective measured profile

parameters in power law variables for the same stations. The measured values lie closest to

Wygnanski's power law expression for x/b = 35, 41, and 47. The point for x/b = 15 intercepts the

power law curve, but at this early station similarity has not truly been achieved and the flow would

not normally be following any structured behavior. Consequently, Wygnanski's power law was

considered suitable to generate values of U_m for profiles at x/b = 31.7 (Tu =17.8 %).

The Y location for U_m was determined using the relation $Y_m = 0.015Y_{m/2}$, obtained from

Wygnanski's development and due to Launder and Rodi (1981). The values for $Y_{m/2}$ and U_τ in

turn were found using equation 2-6 and 2-8, respectively, also from the same development.

These equations completed the method for generating velocity profiles at X_{inj} for the

different free stream velocities. The overall procedure consisted of inputting U_j and X_{inj} into

equations (2-5), (2-6), and (2-8) to obtain U_m, $Y_{m/2}$ ($Y_m = 0.15$ $_{Ym/2}$) and U_τ respectively. These

quantities would then be inputted into equation (2-4) to generate $U_{(Y)}$ at the specified X_{inj} .

To verify this new procedure, six station profiles at $U_j = 55.8$ m/s were plotted along with

equation 2-4 generated at the same U_j and X_{inj} value. Figures 5-40 and 5-41 show the match of the

generated profile with the measured profile to be fairly good at $X_{inj} = 2.30$m (x/b = 35) and near

perfect at $X_{inj} = 2.67$m (x/b = 41). This was so in spite of the fact that the calculated U_m, Y_m and

U_τ differed from the measured values by 3.9 %, 5 % and 15 %, respectively, at $X_{inj} = 2.30$m and by

2.8 %, 4.7 % and 15.8%, respectively, at $X_{inj} = 2.67$m. Table 5-2 shows the corresponding

numerical values.

Table 5-2. Wall jet flow parameters measured and calculated from power laws

	Measured values for $U_j = 55.8$ m/s		Calculated values using power laws	
	$X_{inj} = 2.30$ m	$X_{inj} = 2.67$ m	$X_{inj} = 2.30$ m	$X_{inj} = 2.67$ m
U_m (m/s)	31.7	29.2	30.4	28.38
Y_m (cm)	1.8	2.1	1.7	2.0
U_τ (m/s)	1.12	1.03	1.33	1.23

5.2.1.2 Velocity profiles for injection with Tu = 7.3 % and Tu = 12.2 %

The velocity profiles for the Tu = 7.3 % and Tu = 12.2 % cases could not be generated

using equation 2-4 which required similarity of the flow. A means to include effectiveness values

in the correlation for this Tu levels was to calculate δ^* for Re_{δ^*} using distributions from existing

velocity profiles at locations near injection. For Tu = 7.3 % and Tu = 12.2 %, coolant was

injected at x = 34.69 cm (x/b = 5.4) and x = 68.02 cm (x/b = 10.5), respectively. One set of

velocity profiles for $U_j = 55.8$ m/s was measured at 14 stations, two of which were x = 32.3 cm

(x/b = 5.03) and x = 64.6 cm (x/b = 10.06). These profiles were curve fitted using a self-preserving wall jet distribution of the from:

$$U = \frac{\tau_0^{1/2}}{k}\left[\log\left(\frac{z}{z_0}\right) - \frac{z}{(\eta_1 l_0)}\right],\qquad(5\text{-}2)$$

where, $\eta_1 l_0 = Y_m$, k is Von Karman's constant equal to 0.41(White, 1991), τ_0 is the kinematic wall stress (Townsend, 1976) and z is vertical distance from the wall. The parameters τ_0, and z_0, were calculated using points from the velocity profile measured for $U_j = 55.8$ m/s (see Appendix G for sample calculations).

Equation (5-2) applies to the inner layer of the wall jet, that is, the region from the surface of the plate to Y_m, where the maximum velocity (U_m) is reached. For both locations x/b = 5.03 and x/b = 10.06, the fit of the self-preserving distribution to the velocity profile was fair at the Y locations closest to Y_m and deteriorated at locations closer to the wall. Although, for x/b = 5.03 this deviation of the velocity profile from the self-preserving distribution at the near-wall region was greater (see Figures 5-42 and 5-43). It should be noted that the fact that these velocity profiles were measured at Y increments of 0.254 cm contributes to the inaccuracy of the fit.

Effectiveness values for Tu = 7.3 % and Tu = 12.2 % used in the correlation were not directly measured. The free stream velocity settings at injection for which effectiveness measurements were taken did not include the U_∞ at injection values of 51.95 m/s and 54.56 m/s corresponding to x/b = 5.03 and x/b = 10.06 when $U_j = 55.8$ m/s . Therefore, the effectiveness at these two U_∞ values used in the correlation was obtained from plots of η with U_∞ (See Figure 5-44 for an example plot).

5.2.1.3 Displacement Thickness Calculation

From the velocity profiles obtained, displacement thickness at injection was calculated for

U_∞ = 10 m/s, 18 m/s, and 60 m/s (nominal U_∞ values at X_{inj} = 2.01 m) with Tu = 17.8 %; for

U_∞ = 54.46 m/s with Tu = 7.3 %; and U_∞ = 51.95 m/s with Tu = 12.2 %. $U_{(Y)}$ profiles generated

with the Outer Law were valid only as low as $Y^+ > 30$ ($Y^+ = (YU_\tau)/\nu$); therefore, to calculate

displacement thickness down to $Y^+ = 0$ an approximation by Reichardt (Bejan, 1984)

$$\frac{U}{U_\tau} = 2.5\ln\left(1+0.4y^+\right)+7.8\left(1-e^{\frac{-y^+}{11}}-\frac{y^+}{11}e^{-0.33y^+}\right) \qquad (5\text{-}3)$$

was used to generate profiles for this very thin region. The addition of this small region was done

for completeness; the actual contribution to the displacement thickness was relatively small (an

average of 13.2 % of δ^*). Calculated values of displacement thickness and Re_{δ^*} are presented in

the following tables.

TABLE 5-3. Input parameters and results with Outer Law equation (Y at $Y^+ = 30 < Y < Y_m$) and

Reichardt's approximation ($0 < Y < Y$ at $Y^+ = 30$)

X_{inj} (m)	U_j (m/s)	Tu (%)	U_∞ (m/s)	Y_m (cm)	U_τ (m/s)	δ^* (cm)	Re_{δ^*}
2.01	18.93	17.8	10.34	1.97	0.521	0.2635	1816
2.01	29.96	17.8	16.63	1.77	0.792	0.2236	2479
2.01	94.4	17.8	56.43	1.34	2.32	0.1459	5489

TABLE 5-4. Input parameters and results with self-preserving wall jet distribution

equation ($0 < Y < Y_m$)

X_{inj} (cm)	U_j (m/s)	Tu (%)	U_o (m/s)	τ_o (m²/s²)	$\eta_{\frac{1}{2}}l_o$ (cm)	z_o (cm)	δ^* (cm)	Re_{δ^*}
68.02	55.8	12.2	51.95	7.79	2.032	7.373×10^{-11}	0.1402	4849
34.69	55.8	7.3	54.46	1.79	1.778	2.150×10^{-10}	0.1296	4720

5.2.2 Development of Correlation using $Re_{\delta*}{}^b[X/(Bd)]^c Tu^f$

A discrete least square approximation with two independent variables was performed to find the constant A_1 and the exponents b and c (see equation 5-1), using effectiveness values from the first eight cases listed in Table 5-5. These cases all have the same Tu level. The goal was to find coefficients for one Tu level, then introduce the other two levels and observe whether any separation in the collapse occurred. If separation of the collapse was apparent then the value of the exponent f for the turbulence term would be sought.

TABLE 5-5. Listing of conditions included in effectiveness correlation with $Re_{\delta*}{}^b[X/(Bd)]^c Tu^f$

Case	U_∞ (m/s)	B	Tu (%)
1	56.43	0.25	17.8
2	56.43	0.50	17.8
3	56.43	0.75	17.8
4	10.34	0.50	17.8
5	10.34	0.75	17.8
6	16.63	0.25	17.8
7	16.63	0.50	17.8
8	16.63	0.75	17.8
9	54.46	0.25	7.3
10	54.46	0.50	7.3
11	54.46	0.75	7.3
12	51.95	0.25	12.2
13	51.95	0.50	12.2
14	51.95	0.75	12.2
15	10.34	1.75	17.8
16	16.63	1.50	17.8

The approximating function in two variables is arrived at by taking the natural log of

$$\eta = A_1 \, \mathrm{Re}_{\delta^*}^{\ b} \left(\frac{X}{Bd} \right)^{c} \tag{5-3}$$

which gives

$$\ln \eta = \ln A_1 + b \ln \mathrm{Re}_{\delta^*} + c \ln \left(\frac{X}{Bd} \right) \tag{5-4}$$

and assigning the corresponding term to the form

$$y = a + bx + cz \tag{5-5}$$

so that the dependent variable is assigned as $y = \ln \eta$, the two independent variables are assigned as $x = \ln \mathrm{Re}_{\delta^*}$ and $z = \ln(X/Bd)$, and the coefficients are assigned as $a = \ln A_1$, $b = b$ and $c = c$.

The approximation produced values of $b = 0.089$, $c = -0.613$ and constant $A_1 = 0.596$. The exponent c was of the same order of magnitude as those found by Seban (1960), Scesa (1954), Wieghardt (1946), Nishiwaki et al. (1961), and Goldstein et al. (1965), whose exponent c ranged from -0.5 to -0.88 in film cooling effectiveness correlations without free stream turbulence including the term $[X/(Bd)]^c$. In the correlations by Nishiwaki et al. and Goldstein et al. the term $[X/(Bd)]^c$ was multiplied by $\mathrm{Re}_x^{\ b}$ and $\mathrm{Re}_{\delta^*}^{\ b}$, respectively. The exponent b in these correlations was also less than one as it was for this study. A plot of the parameters showed a grouping of data points. Although the grouping was fairly good, closer examination revealed that it was fragmented into three distinct turbulence levels. The turbulence term was then included and the exponent f, along with a new constant A_1 were found through iteration. The resulting correlation is:

$$\eta = 0.345 \, \mathrm{Re}_{\delta^*}^{\ 0.089} \left(\frac{X}{Bd} \right)^{-0.613} Tu^{-0.3} \tag{5-6}$$

Figure 5-45 shows a plot of η for cases 1-14 in Table 5-5 along with the correlation

equation (5-6). The blowing ratios used were all less than unity because most of the previous

correlations referenced were successful in this blowing ratio range. The effectiveness correlates

fairly good with the major scatter towards the end of the plate. The effectiveness values which lie

closest to equation (5-6) are generally the cases for B = 0.50 and B = 0.75 with Tu = 12.2 % and

Tu = 17.8 %

The possibility of extending the correlation to blowing ratios greater than unity was

explored by including the last two cases in Table 5, B = 1.50 and B = 1.75. Figure 5-46 shows

that these high blowing ratio cases fell practically on the correlation line, with the exception of the

blow-off region of the data (x/d < 15). As it stands, equation (5-6) is considered to be a suitable

correlation for $0.5 < \lambda < 1.0$, where $\lambda = Re_{\delta *}{}^{0.089}[X/(Bd)]^{-0.613} Tu^{-0.3}$. This interval excludes the

blow-off region of the flow, where the flow may need to be modeled perhaps by a momentum flux

term to account for the higher momentum injection at high B; and the far downstream region of the

flow, where uncertainties were largest when measuring small values of effectiveness for low B.

Another possibility of why the far downstream region of the correlation shows a greater

separation is that in this region the turbulence present in the flow was at a somewhat higher level

than at injection. Perhaps as high as 20 % judging from the 2-D validation test contours.

Substituting a more representative level of Tu in the correlation for stations far from injection may

produce a better collapse of the data at these far downstream stations. Unfortunately, Tu contours

for the corresponding test runs from which an accurate turbulence increase could be extracted were

not available.

For comparison purposes effectiveness values from three separate works, Bons (1992),

Jumper (1988) and Jabbari et al.(1978), were included in Figure 5-47. Bons' effectiveness values

for only one row of holes with Tu = 11.5 % fell under the correlation region; this result was

expected since one row of holes has been shown to produce lower effectiveness (Han and Mehendale, 1986, Cirriello, 1991). Jumper's effectiveness values also for one row of holes with Tu = 17 % fell within the grouping (except for a few very high values in the region close to injection). This result was unexpected since the previous one row values fell well below the correlation region. Although Jumper's hole configuration did have both a smaller P/D ratio and injection angle than Bons' configuration; it is not entirely clear whether those differences would account for such a large increase in effectiveness. Jabbari's effectiveness for two rows of holes, with free stream turbulence of less than 1 % and B = 0.50 and B = 0.20, fell on the correlation region as expected.

6. Conclusions

The objective of the present research was to investigate how the blowing ratio influences the effects of free stream turbulence on the film cooling effectiveness. Free stream and surface temperature measurements were taken along a flat plate for three different Tu levels, five free stream velocities and a blowing ratio ranging from 0.25 to 2.0.

The method by which free stream turbulence affects effectiveness was strongly dominated by two main factors: blowing ratio and location of the flow along the plate. For high blowing ratios at locations soon after injection high free stream turbulence levels counteract the effects of blow-off. The greater mixing action with high free stream turbulence forces detached coolant elements back down towards the surface of the plate increasing the effectiveness.

At mid to aft stations for all blowing ratios high free stream turbulence generally decreases the effectiveness. In these locations where the coolant stream is attached to the surface the mixing action of the higher turbulence dissipates the coolant away from the surface.

Far downstream of injection where the lowest Tu level (7.3 %) is expected to achieve the greater value of effectiveness, the medium Tu level (12.2 %) produced the highest values instead. This occurrence suggested that far downstream there may be an optimum level of free stream turbulence which produces the best effectiveness.

Free stream velocity was found not to have a significant influence on the impact of free stream turbulence on effectiveness. The main outcome of varying the free stream velocity was a change on the location a particular trend would take effect. For instance, if η began to increase with blowing rate as the flow moved further downstream, this trend change would begin to take place further upstream as U_∞ was increased. Another more subtle effect was the retardation of the

onset of blow-off for high B as U_∞ increased. Principally, changes in U_∞ did not change how free stream turbulence affected the film cooling effectiveness.

A correlation of effectiveness with $Re_\delta^b (X/Bd)^e Tu^f$ is offered which incorporates all Tu levels used. Effectiveness correlated best at 10 to 15 diameters after injection where blow-off effects are no longer present, and before the very far downstream stations where uncertainties in the measurements were greater.

Recommendation

An optimum level of free stream turbulence seemed to be evident at far downstream regions of the flow. Studies focused on the flow structures of the coolant-mainstream interaction at large x/d may help identify the turbulence qualities which produce higher effectiveness at these stations.

7. References

1. Afejuku, W. O, Hay, N. and Lampard, D. "Film Cooling Effectiveness of Double Rows of Holes", Journal of Engineering for Power, 102(3):601-606, July, 1980.

2. Afejuku, W. O, Hay, N. and Lampard, D. "Measured Coolant Distributions Downstream of a Single and Double Rows of Film Cooling Holes", ASME Paper 82-GT-144, 1983.

3. Bons, J. P., MacArthur, C. D. and Rivir, R. B. "The Effect of High Freestream Turbulence of Film Cooling Effectiveness", ASME Journal of Turbomachinery, 118:814-825, 1994.

4. Ciriello, S. "Heat Transfer, Adiabatic Effectiveness and Injectant Distributions Downstream of Single and Double Rows of Film-Cooling Holes with Simple and Compound Angles", Master Thesis Naval Postgraduate School, Monterey, March, 1991.

5. Eckerle, W. A. "Measurement of the Velocity Field and Heat Transfer Coefficients Associated with Rectangular Wall Jet", Final Report, USAF Contract No. F49620-87-R-0004, September, 1988.

6. Goldstein, R. J., Shavit, G. and Chen, T. S. "Film-Cooling Effectiveness with Injection Through a Porous Section", Journal of Heat Transfer: 353-361, August, 1965.

7. Goldstein, R. J., Rask, R. B. and Eckert, E. R. G. "Film Cooling with Helium Injection into an Incompresible Air Flow", International Journal of Heat and Mass Transfer, 09(12):1341-1350, December, 1966.

8. Goldstein, R. J. "Film Cooling", in: Advances in Heat Transfer, edited by T. F. Irvine and J. P. Hartnett, Academic Press, New York and London, PP321-379, 1971.

9. Goldstein, R. J., Eckert, E. R. G. and Burggraf, F. "Effects of Hole Geometry and Density on Three-Dimensional Film Cooling", International Journal of Heat and Mass Transfer, 17(5):595-606, May, 1974.

10. Han, J. C. and Menhendale, A. B. "Flat Plate Film Cooling with Steam Injection Through One Row and Two Rows of Inclined Holes", ASME Paper 86-GT-105, 1986.

11. Jabbari, M. Y. and Goldstein, R. J. "Adiabatic Wall Temperature and Heat Transfer Downstream of Injection Through Two Rows of Holes", Journal of Engineering for Power, 100:303-307, April, 1978.

12. Jumper, G. W. " Film Cooling Effectiveness on a Flat Plate in High Free-Stream Turbulence Using Single Row of 30° Slant-Hole Injectors", Master Thesis ,AFIT/GAE/AA/87-D, December, 1987.

13. Jubran, B. A. and Brown, A. "Film Cooling from Two Rows of Holes Inclined in the Streamwise and Spanwise Directions", Journal of Engineering for Gas Turbine and Power, 107(1): 84-91, January, 1985.

14. Kadotani, K. and Goldstein, R. J. "On the Nature of Jets Entering a Turbulent Flow Part B - Film Cooling Performance", Journal of Engineering for Power, 101(3): 466-470, July, 1979.

15. Kays, W. M. and Crawford, M. E. Convective Heat and Mass Transfer (Second Edition), New York: Mc Graw-Hill Book Company, 1980.

16. Kline , S. J. and McClintock, F. A. "Describing Uncertainties in Single-Sample Experiments", Mechanical Engineering:3-8, January, 1953.

17. Kohli, A. and Bogard, D. G. "Effects of Very High Free-Stream Turbulence on the Jet-Mainstream Interaction in a Film Cooling Flow", ASME Paper 97-GT-121, 1997.

18. Lauder, B. E. and Rodi, W. "The Turbulent Wall Jet - Measurements and Modeling", Annual Review of Fluid Mechanics, 15:429-459, 1983.

19. Ligrani, P. M., Cirriello, S. and Bishop, D. T. "Heat Transfer, Adiabatic Effectiveness, and Injectant Distributions Downstream of a Single Row and Two Staggered Rows of Compound Angle Film-Cooling Holes", Journal of Turbomachinery, 114: 687-700, October, 1992.

20. Maciejewski, P. K. and Moffat, R. J. "Heat Transfer with Very High Free-Stream Turbulence", Report no. HMT-42, Stanford University, December, 1989.

21. MacMullin, R. "Effects of Free-Stream Turbulence from a Circular Wall Jet on Flat Plate Heat Transfer and Boundary Layer Flow", Master Thesis, AFIT/GA/AA/86 D-10, December, 1986.

22. Mick, W. J. and Mayle, R. E. "Stagnation Film Cooling and Heat Transfer, Including Its Effect Within the Hole Pattern", Journal of Turbomachinery, 110:66-72, January, 1988.

23. Narasimha, R., Narayan, K. Y. and Parthasarathy, S. P. "Parametric Analysis of Turbulent Wall Jets in Still Air", Aeronautical Journal, 77: 355-359, July, 1973.

24. Perdersen, D. R., Eckert, E. R. G. and Goldstein, R. J. "Film Cooling with Large Density Difference Between the Mainstream and Secondary Fluid Measured by the Heat-Mass Transfer Analogy", Journal of Heat Transfer, 99(11):620-627, November, 1977.

25. Scmidt, D. L. and Bogard, D. G. "Effects of Freestream Turbulence and Surface Roughness on Film Cooling", ASME Paper 96-GT-462, 1996.

26. Simonich, J. C. and Bradshaw P. "Effect of Free-Stream Turbulence on Heat Transfer through a Turbulent Boundary Layer", Journal of Heat Transfer, 100: 671-676, November, 1978.

27. Townsend, A. A. Structure of Turbulent Shear Flow:New York, Cambrige University Press, 1976.

28. White, F. M. Viscous Fluid Flow (Second Edition): New York, McGraw-Hill, Inc.,1991

8. Figures Referenced in Main Document
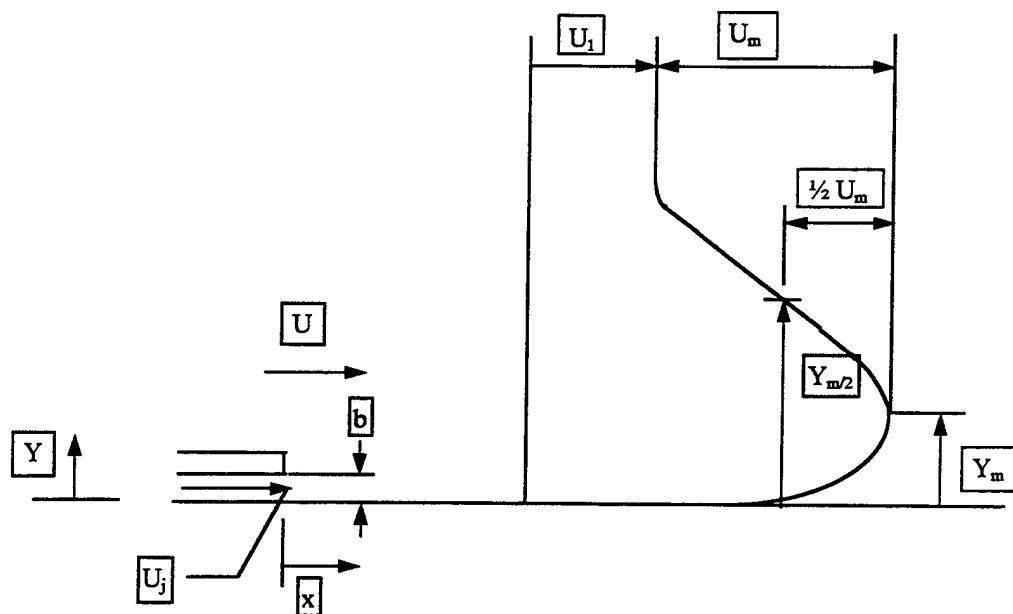
Figure 2-1. Turbulent Wall Jet Configuration
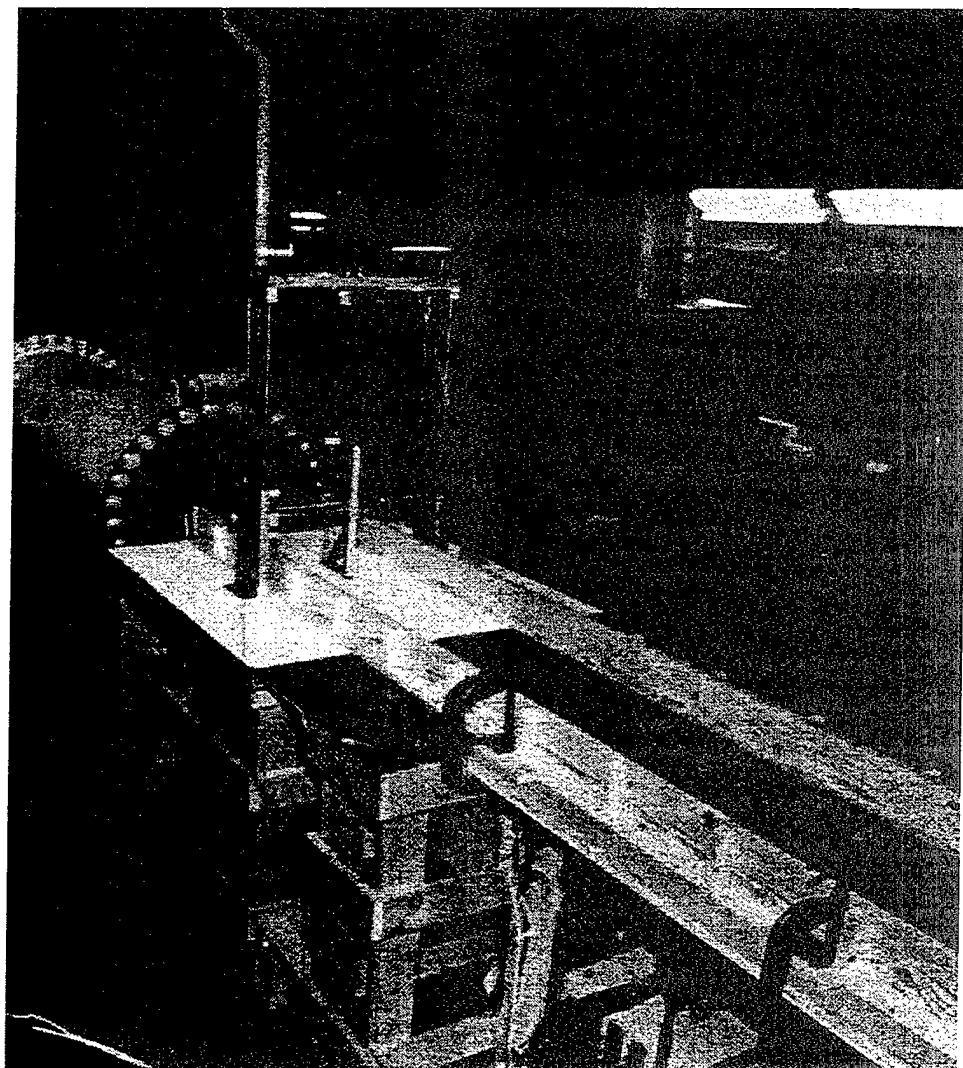
Figure 3-1. Complete Apparatus Layout (view a)
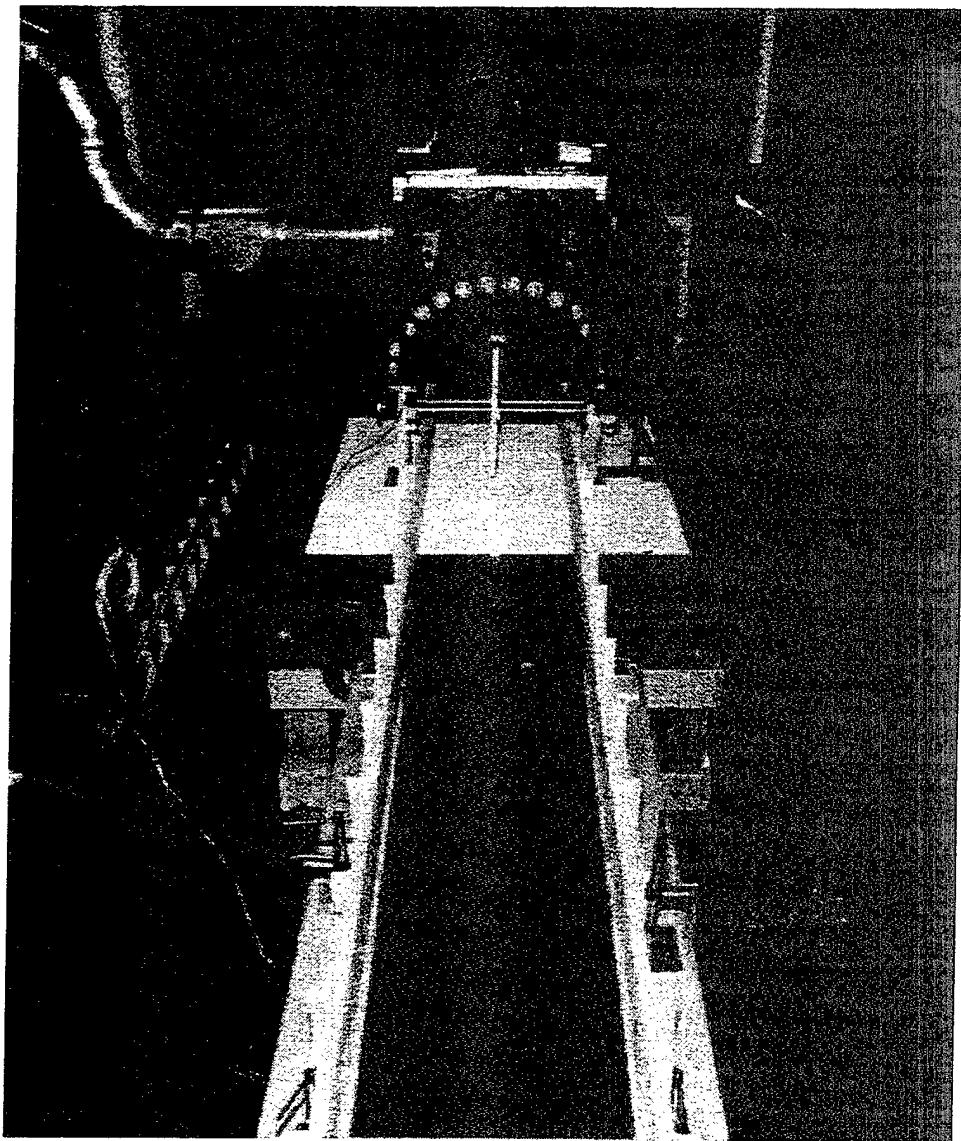
Figure 3-2. Complete Apparatus Layout (view b)
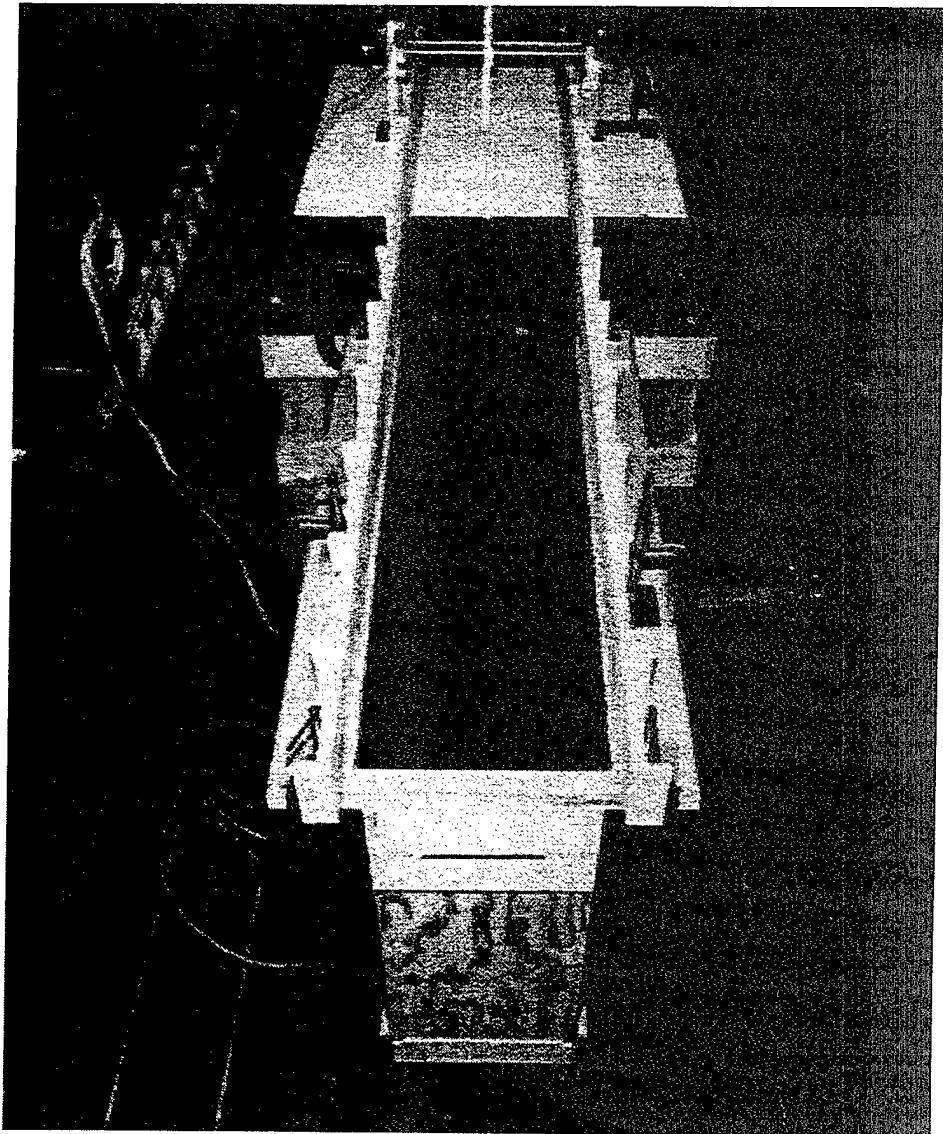
Figure 3-3. Complete Apparatus Layout (view c)
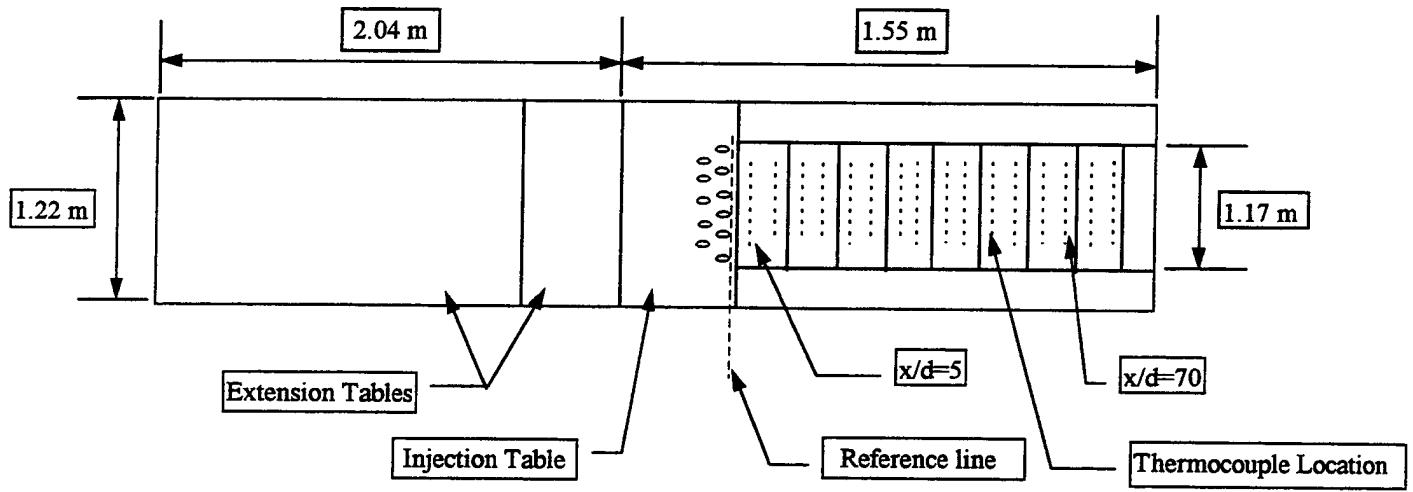
Figure 3-4. Thermocouple and Table Layout
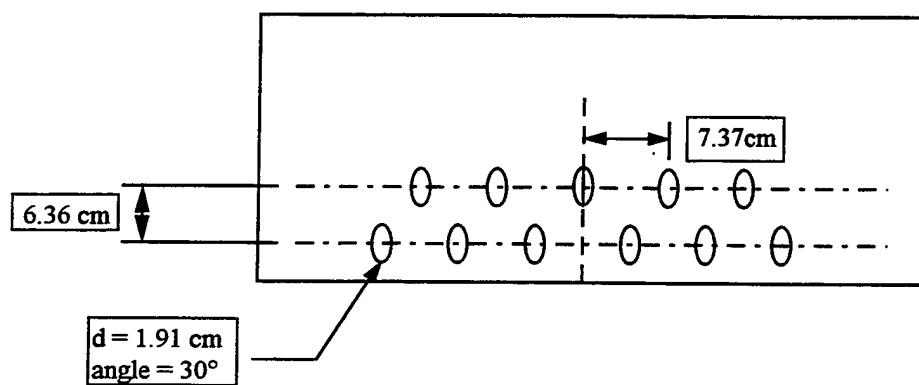
Figure 3-5 Injection Section of Flat Plate

Normalized Velocity Profile
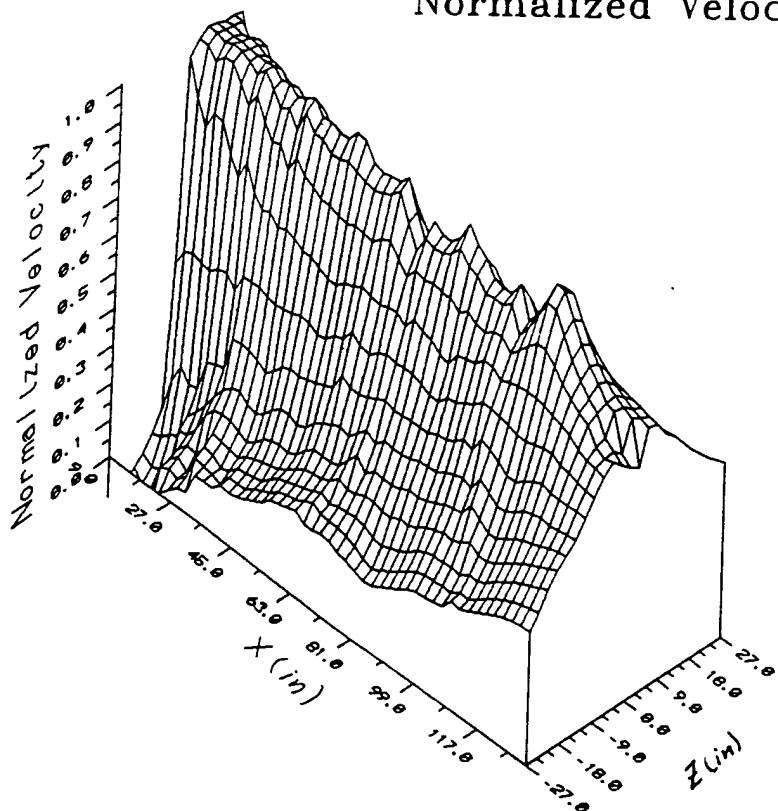
Normalized Velocity Contour
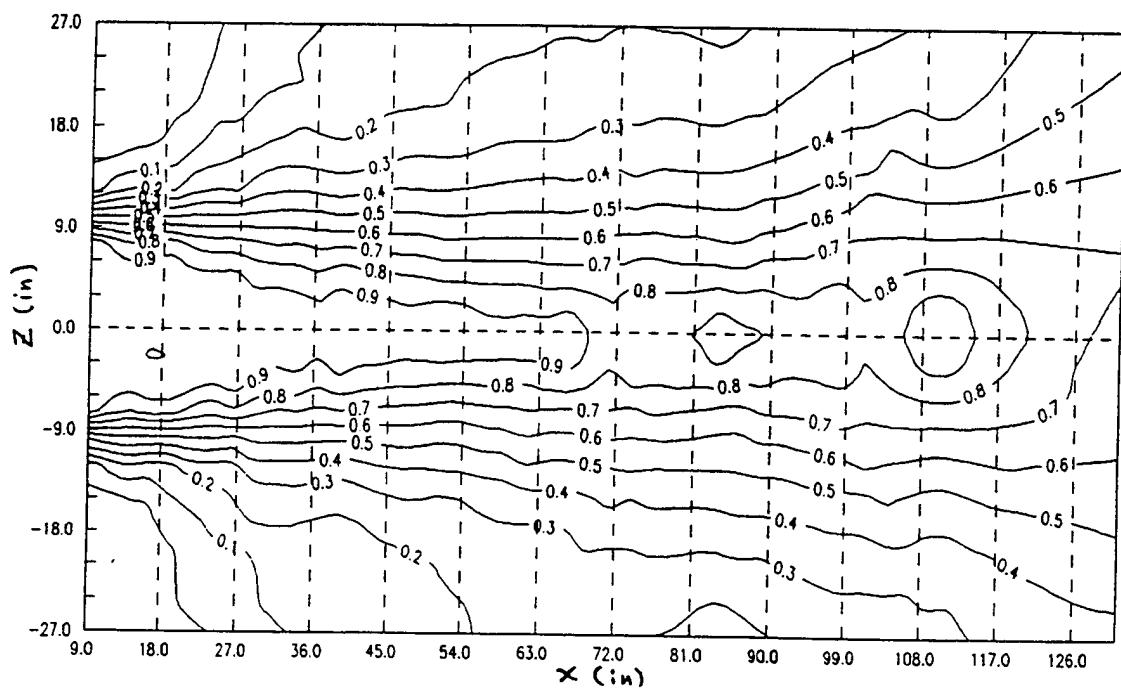
Figure 4-1. Velocity Results for Wall Jet without Side Walls

Normalized Velocity Contour
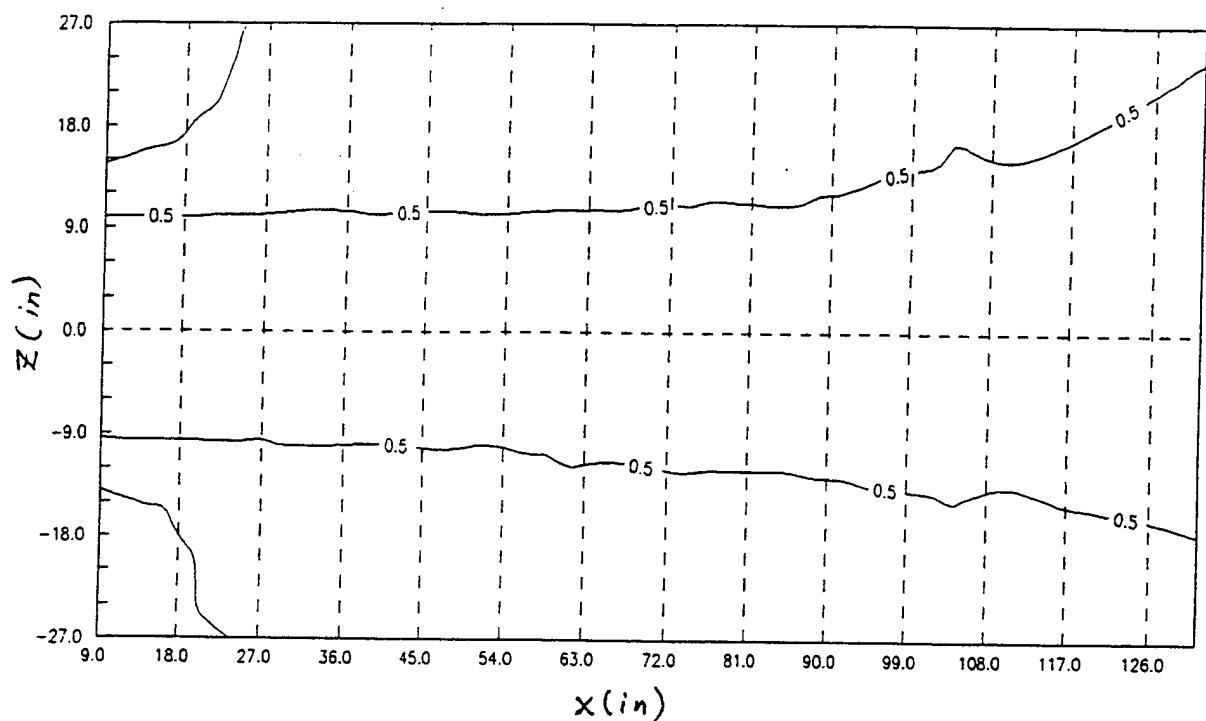
Figure 4-2. Contour Plot of Latteral Jet Spread

Turbulence Intensity Profile
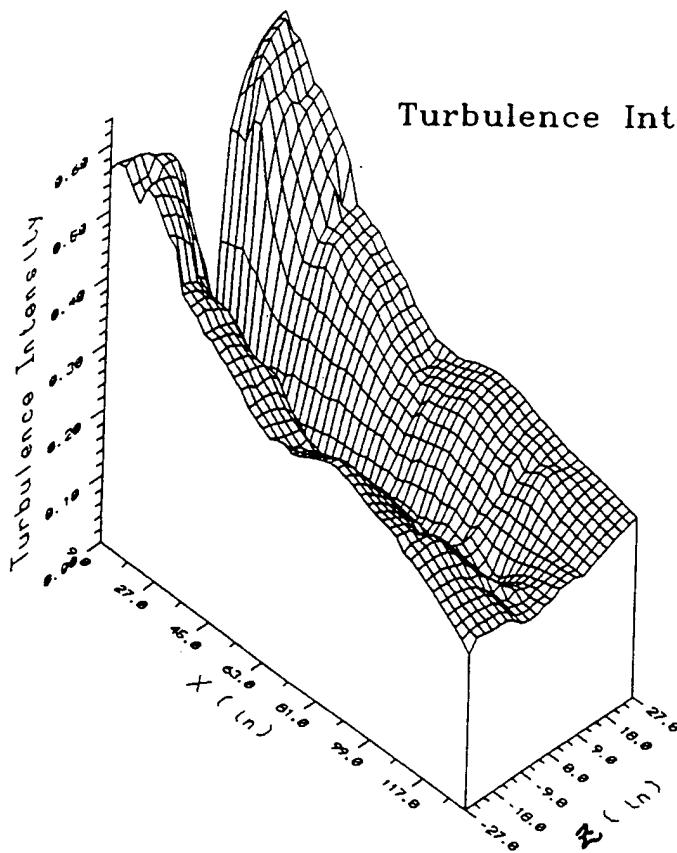
Turbulence Intensity Contour
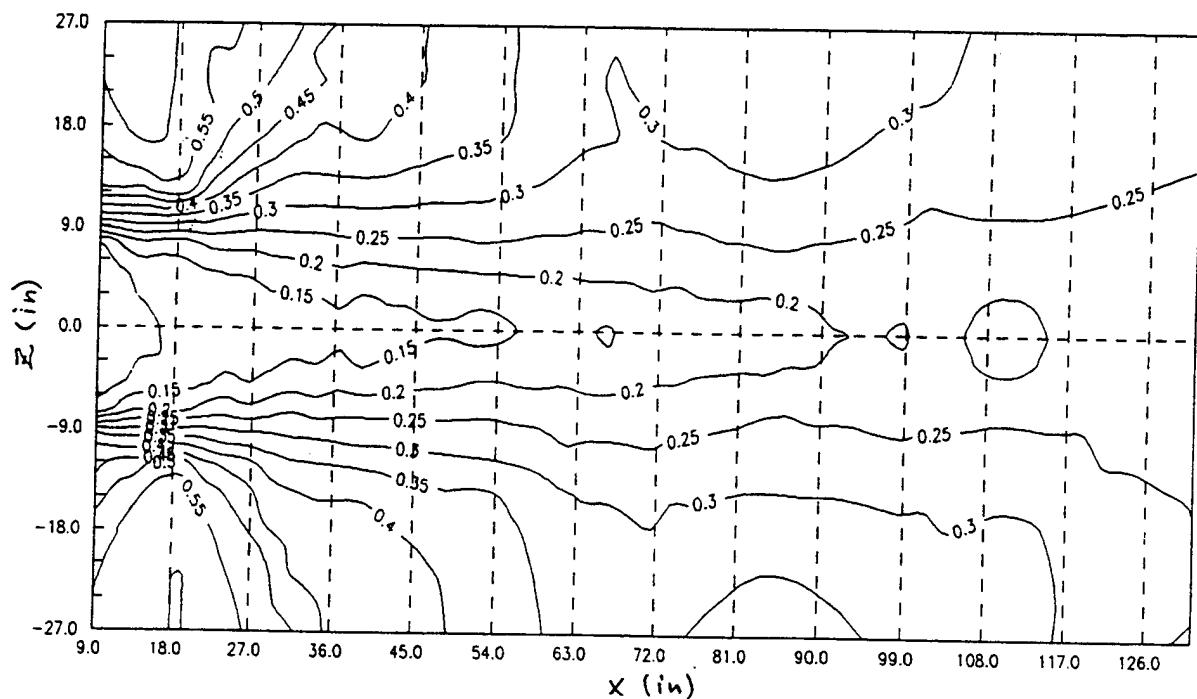
Figure 4-3. Turbulence Intensity Level Contour without Side Walls

Length Scale Profile
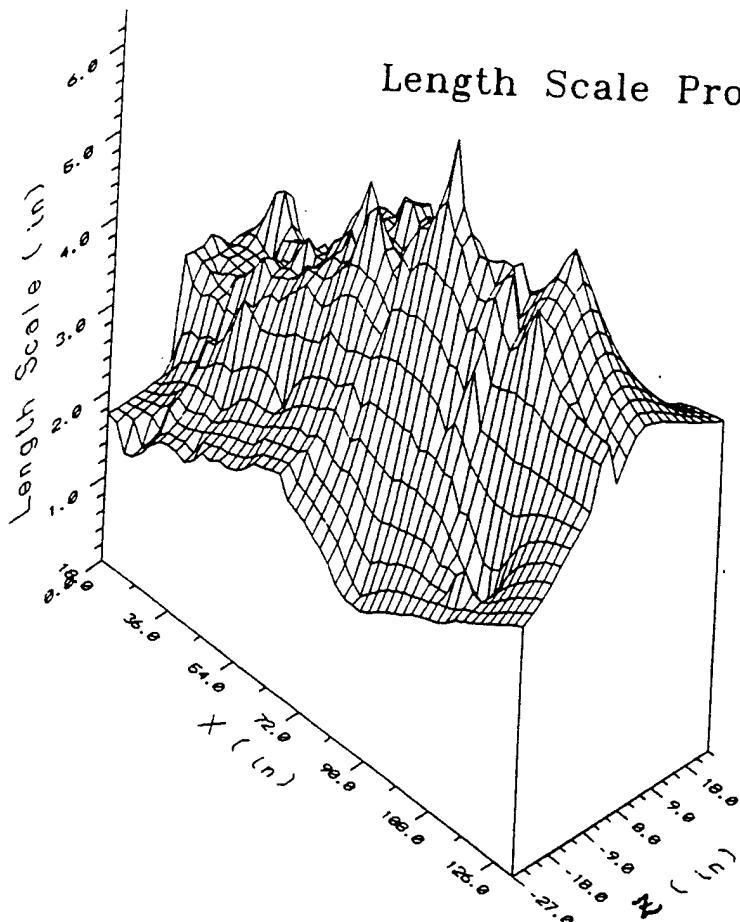
Length Scale Contour (in)
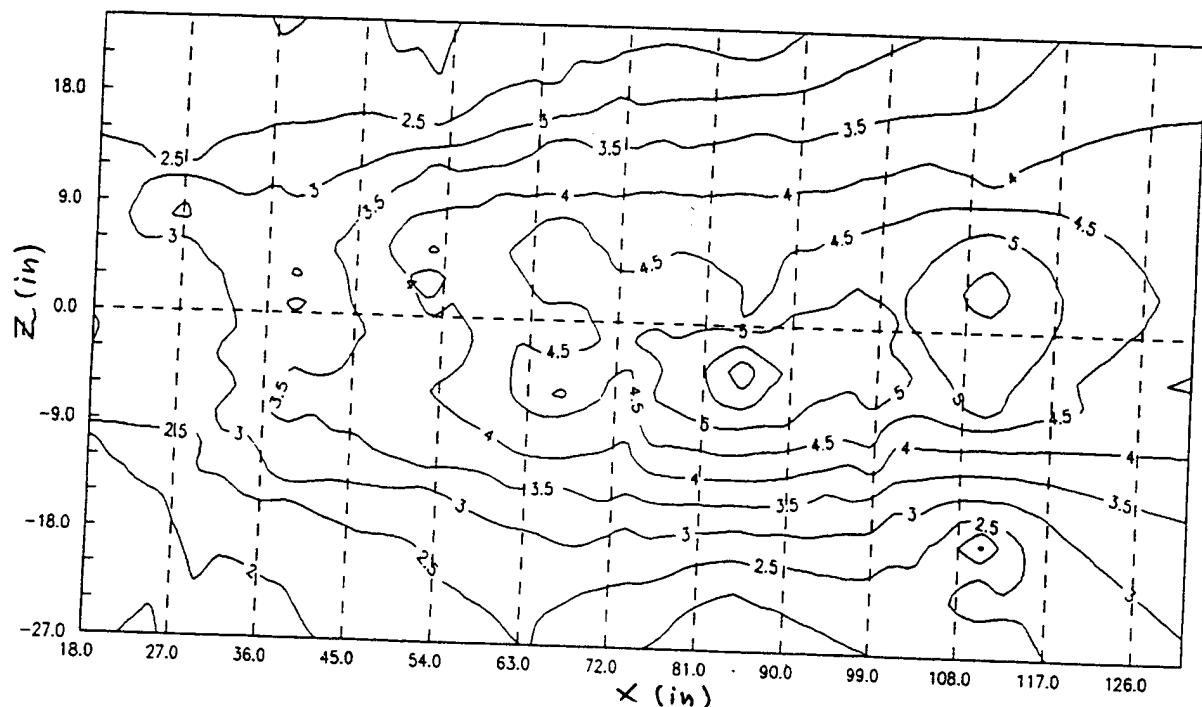
Figure. 4-4. Integral Length Scale Contour without Side Walls

Velocity Fluctuation Profile
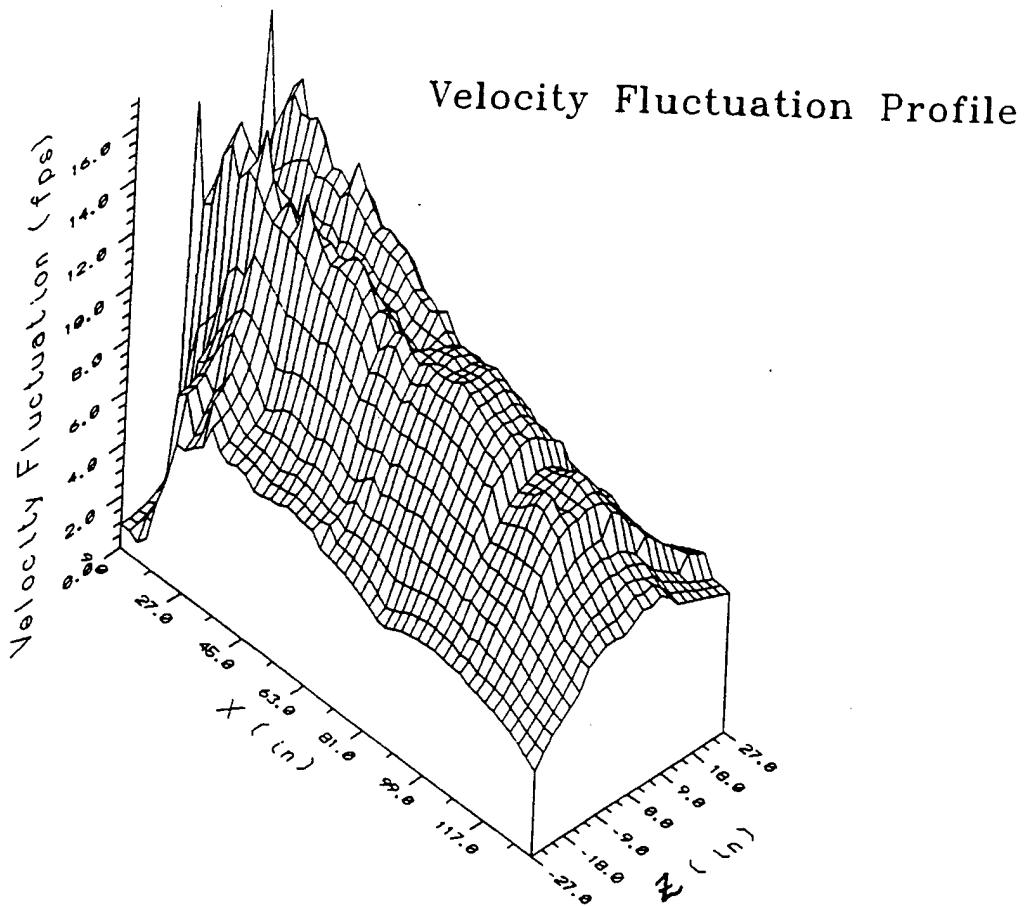
Velocity Fluctuation Contour (fps)
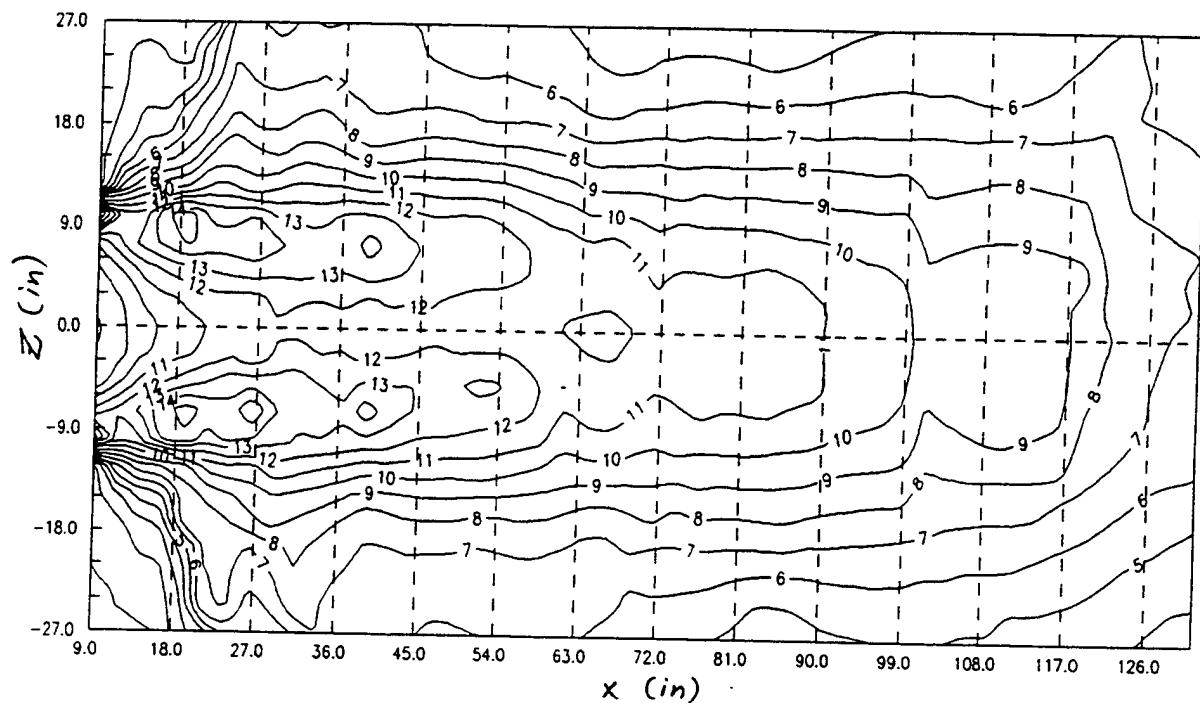
Figure 4-5. Velocity Fluctuation Contour without Side Walls

8-11

Velocity Contour (fps)
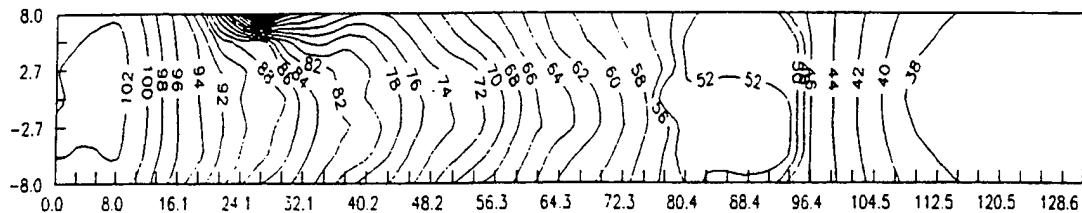
Velocity fluctuation (fps)
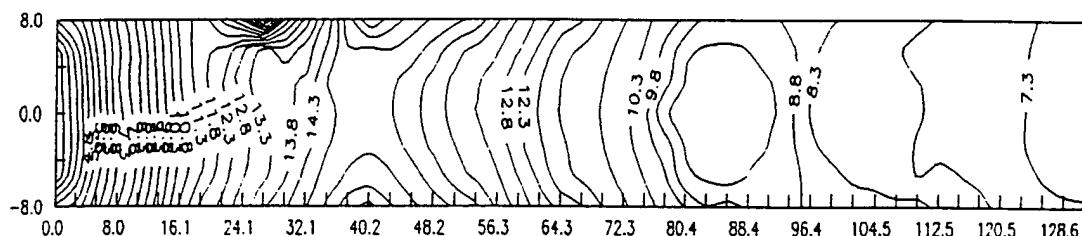
Turbulence Contour
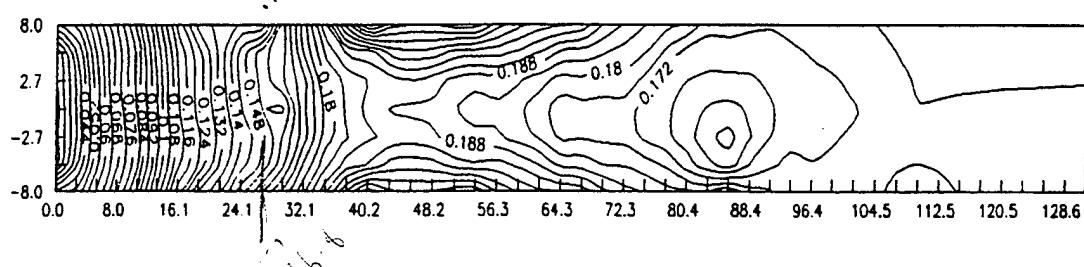
Length scale (in)
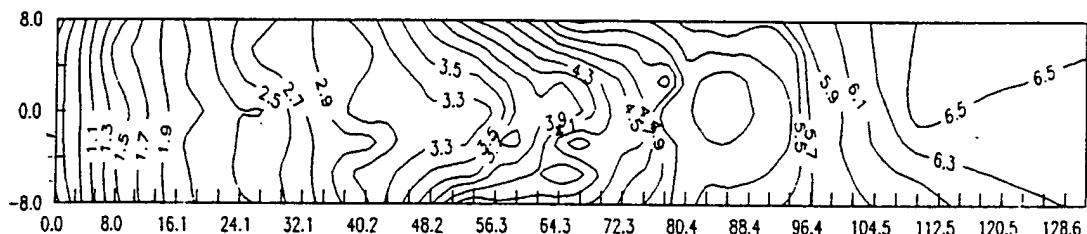
Figure 4-6. Results of Experiments with Side Walls
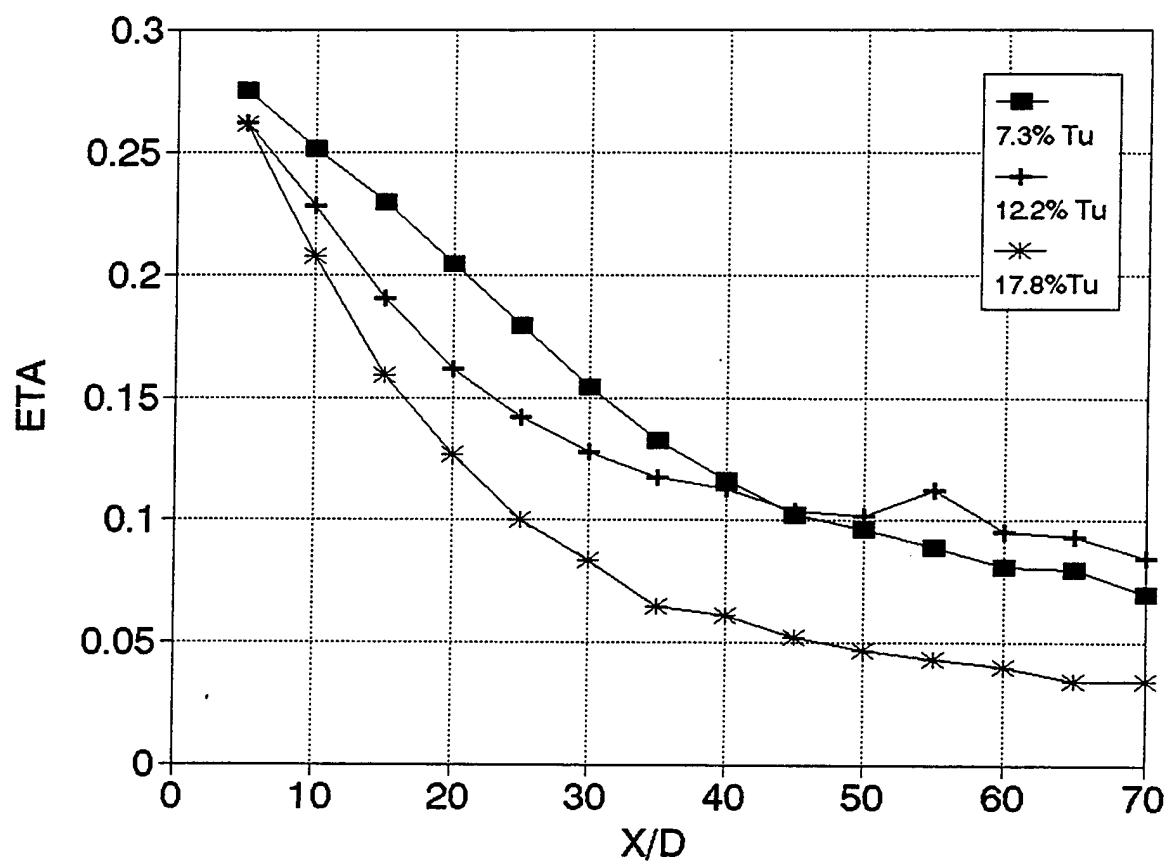
Figure 5-1. Effect of Free Stream Turbulence on Film Cooling Effectiveness
B = 0.50, Free stream velocity at injection = 10 m/s
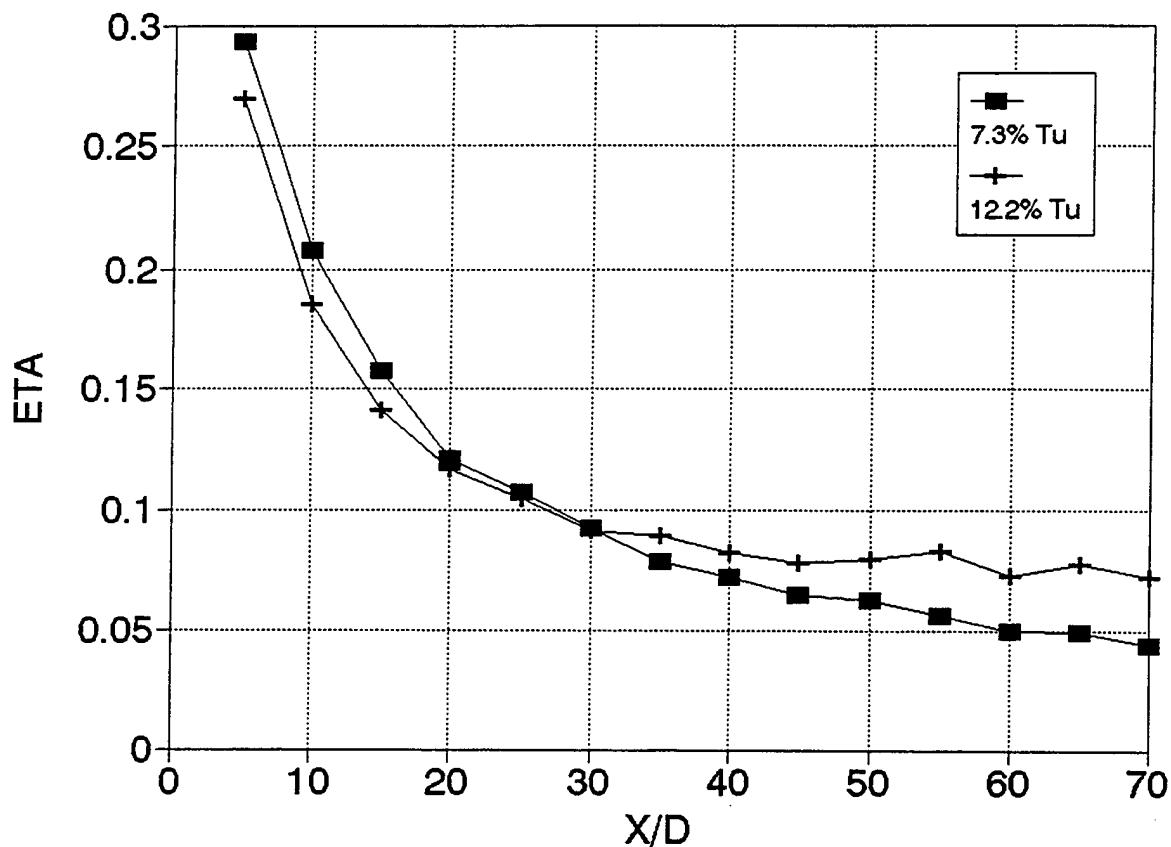
Figure 5-2. Effect of Free Stream Turbulence on Film Cooling Effectiveness
B = 0.25, Free stream velocity at injection = 37 m/s
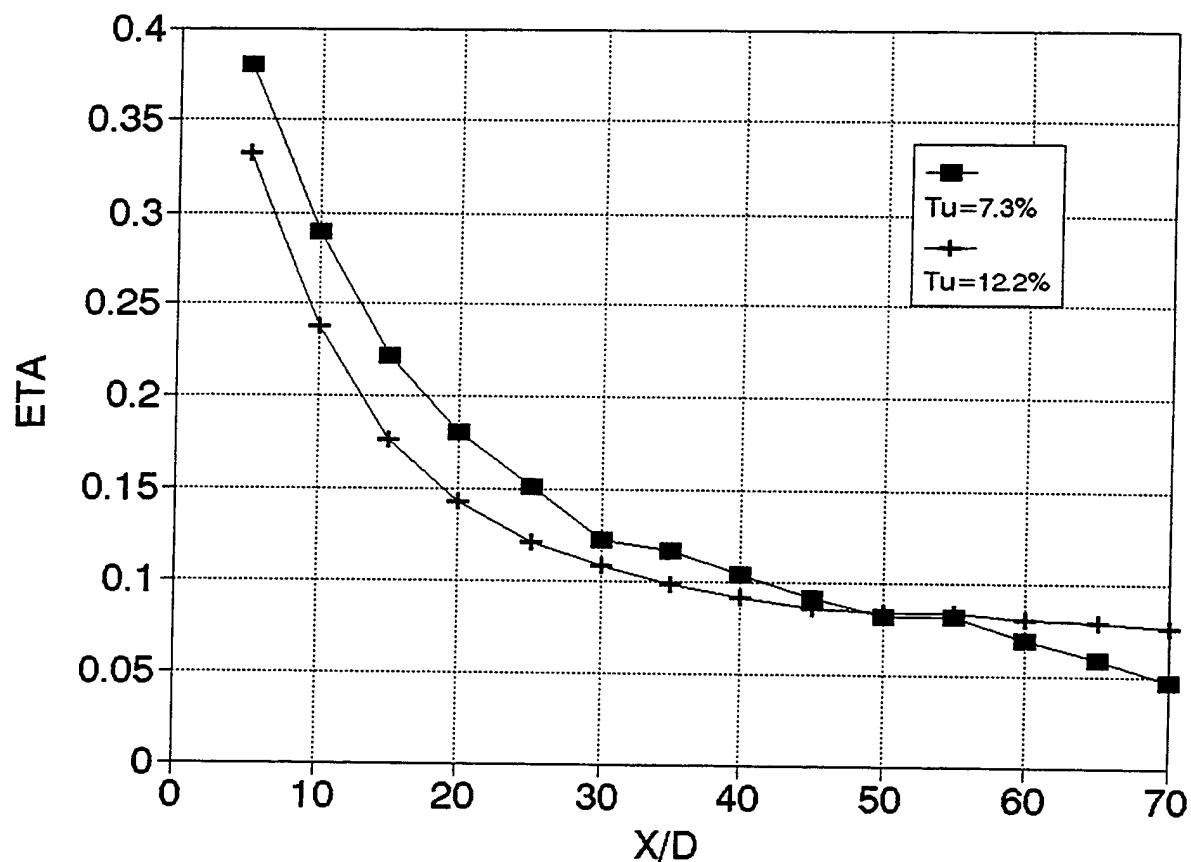
Figure 5-3. Effect of Free Stream Turbulence on Film Cooling Effectiveness
B = 0.50, Free stream velocity at injection = 85 m/s
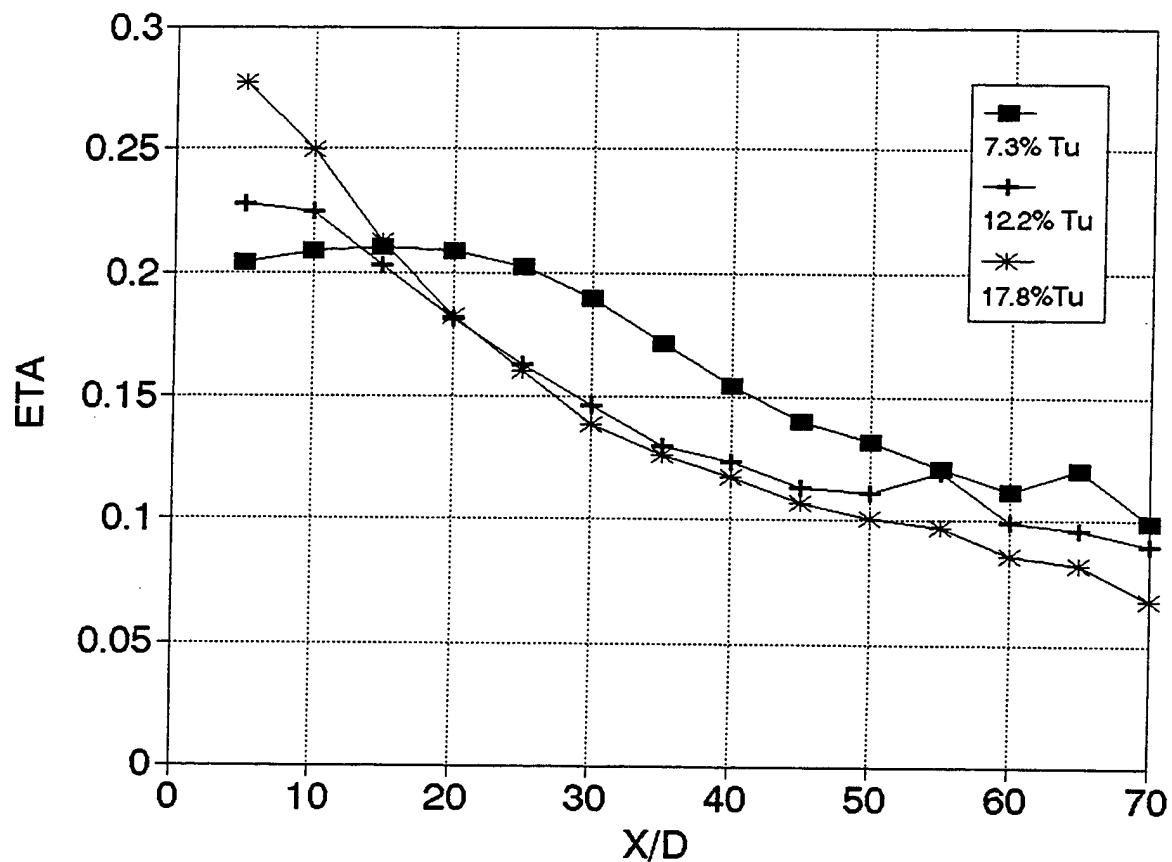
Figure 5-4. Effect of Free Stream Turbulence on Film Cooling Effectiveness
B = 0.75, Free stream velocity at injection = 10 m/s
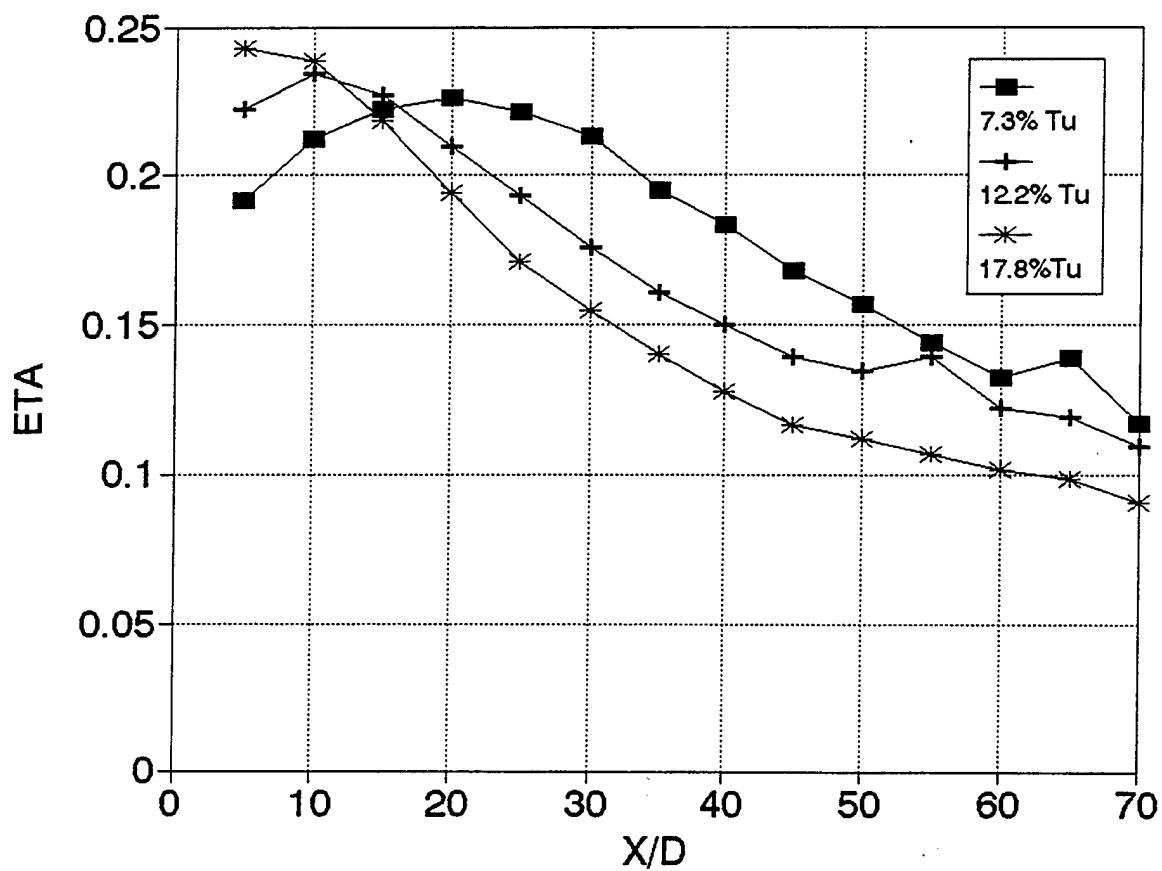
Figure 5-5. Effect of Free Stream Turbulence on Film Cooling Effectiveness
B = 1.0, Free stream velocity at injection = 10 m/s
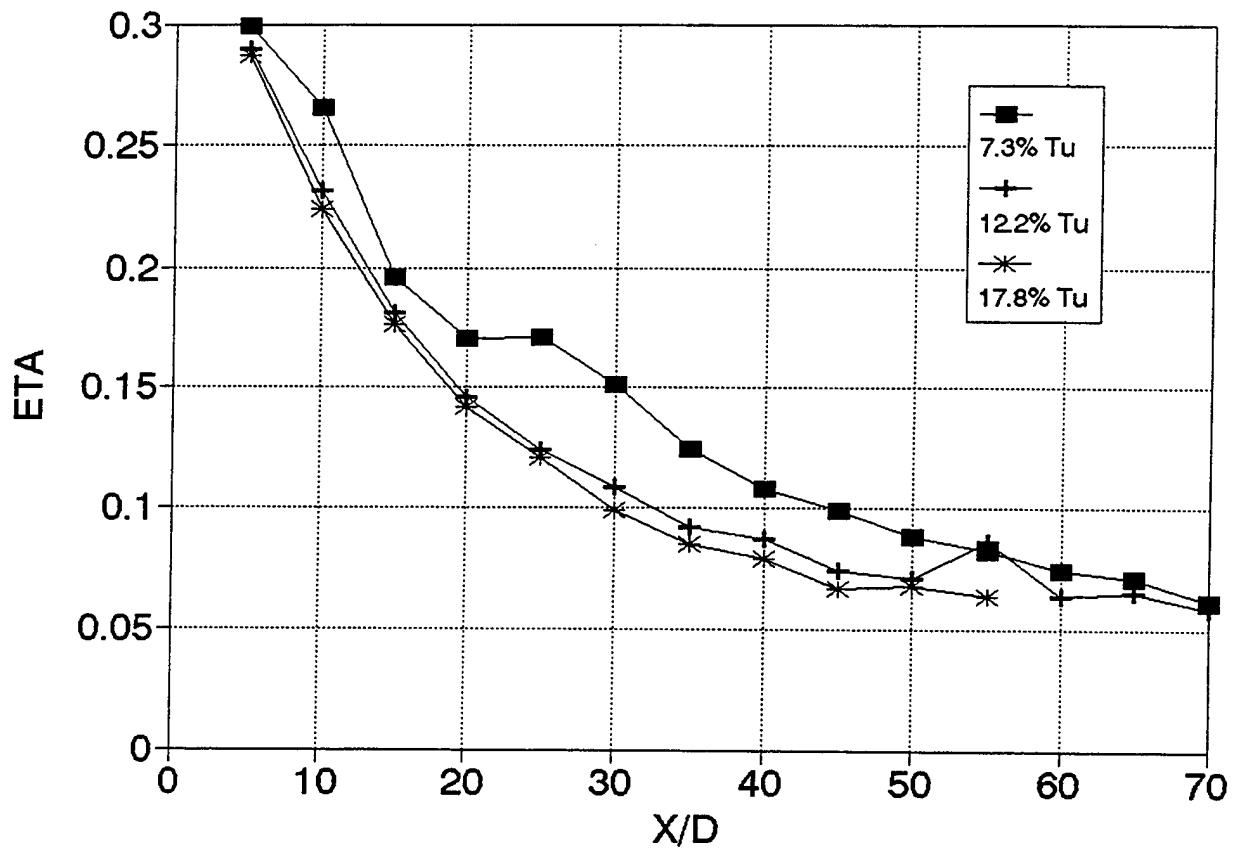
Figure 5-6. Effect of Free Stream Turbulence on Film Cooling Effectiveness
B = 0.50, Free stream velocity at injection = 18 m/s
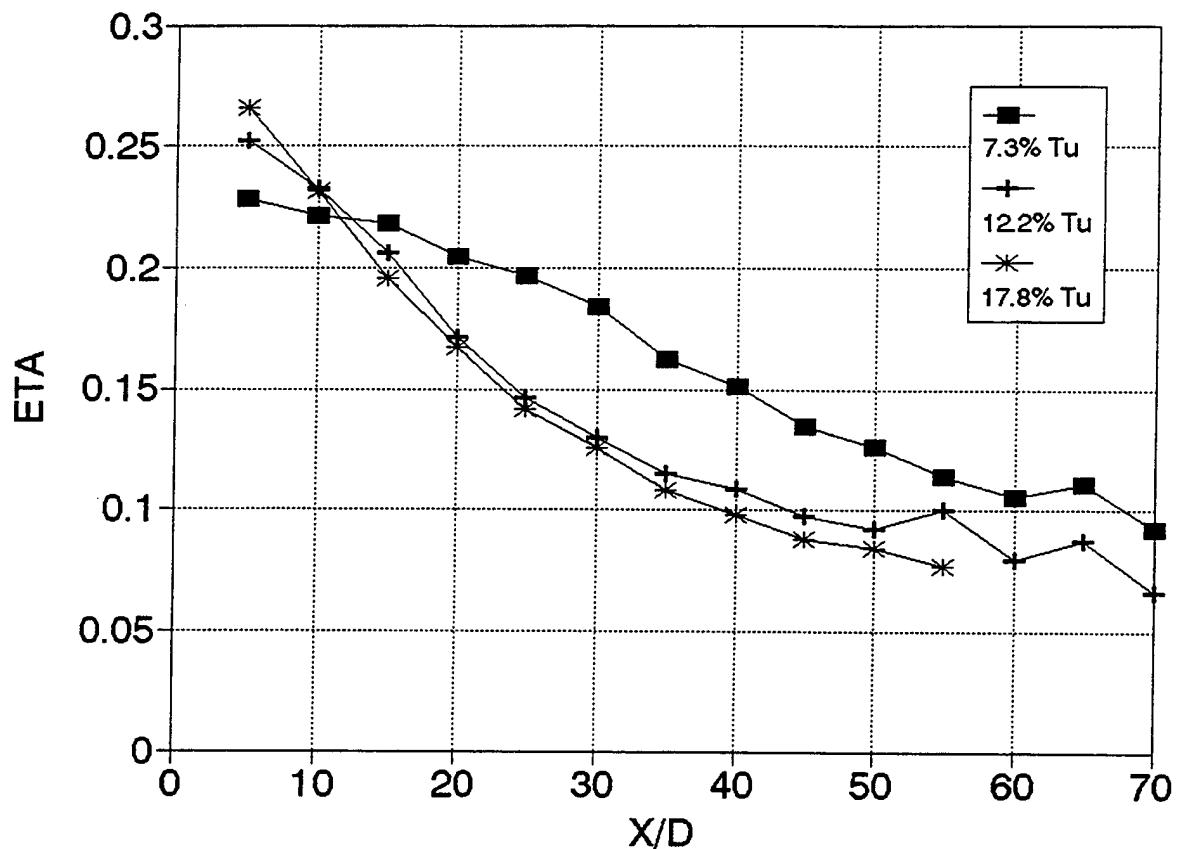
Figure 5-7. Effect of Free Stream Turbulence on Film Cooling Effectiveness
B = 0.75, Free stream velocity at injection = 18 m/s
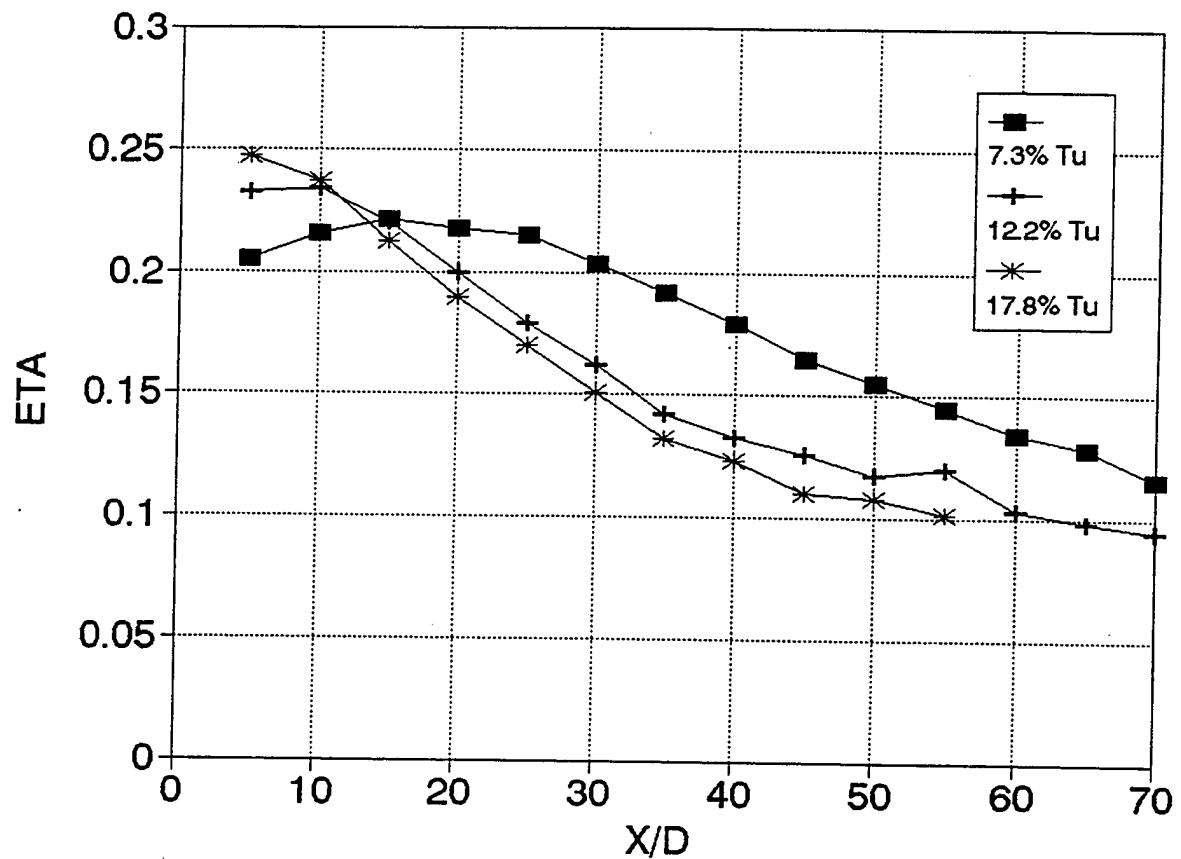
Figure 5-8. Effect of Free Stream Turbulence on Film Cooling Effectiveness
B = 1.0, Free stream velocity at injection = 18 m/s
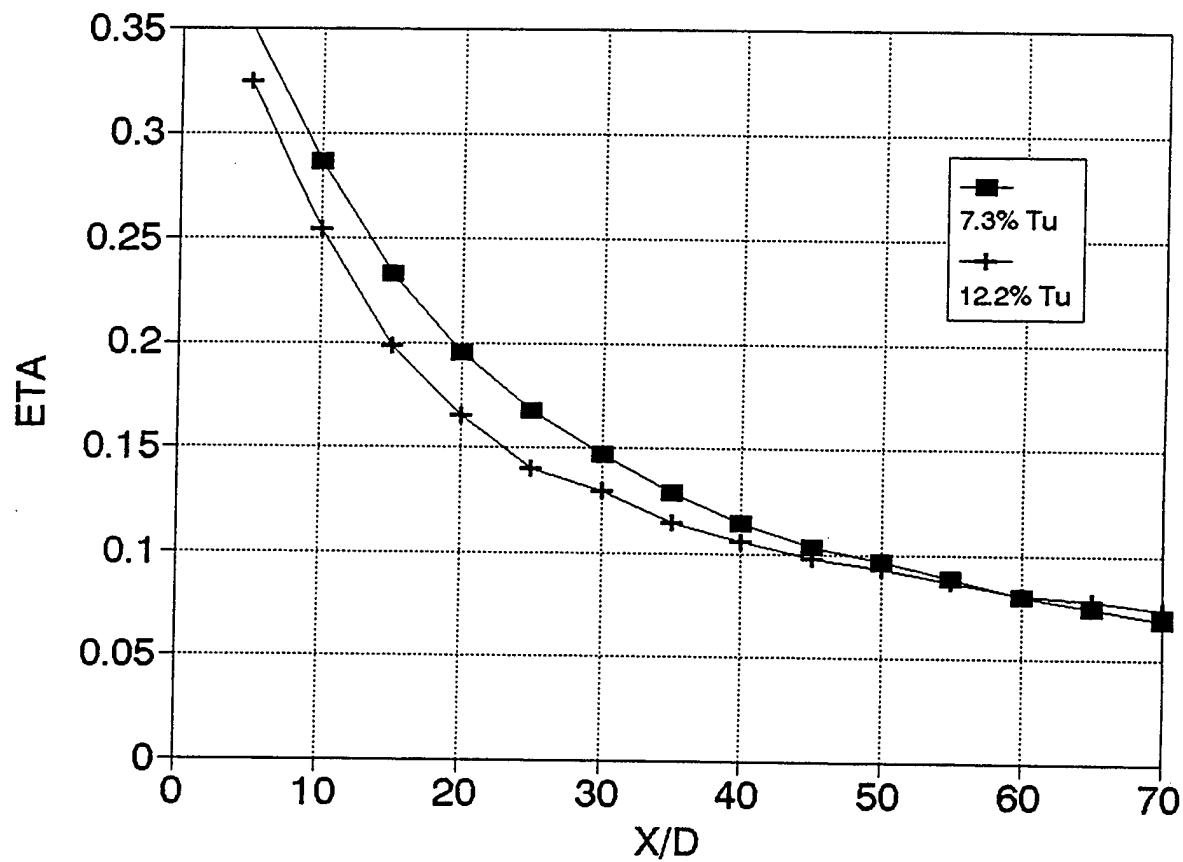
Figure 5-9. Effect of Free Stream Turbulence on Film Cooling Effectiveness
B = 0.50, Free stream velocity at injection = 37 m/s
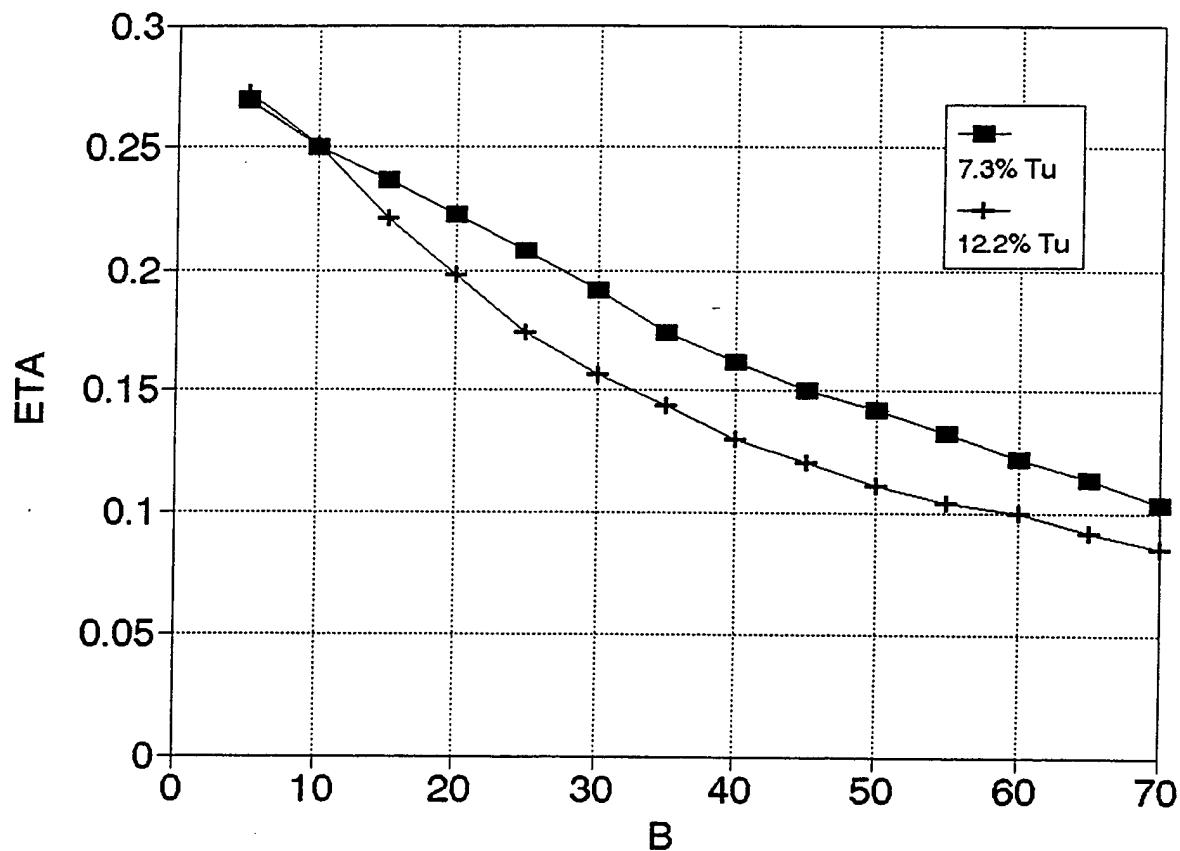
Figure 5-10. Effect of Free Stream Turbulence on Film Cooling Effectiveness
B = 0.75, Free stream velocity at injection = 37 m/s
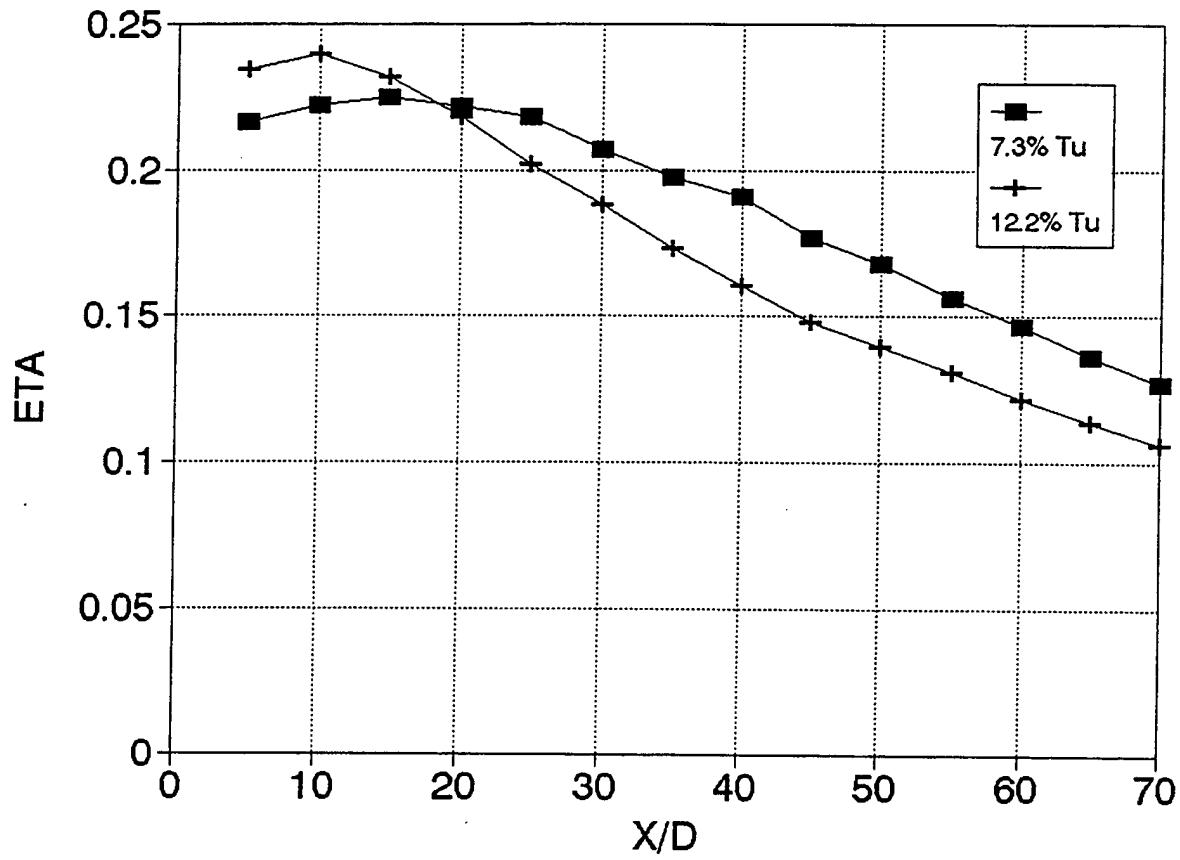
Figure 5-11. Effect of Free Stream Turbulence on Film Cooling Effectiveness
B = 1.0, Free stream velocity at injection = 37 m/s
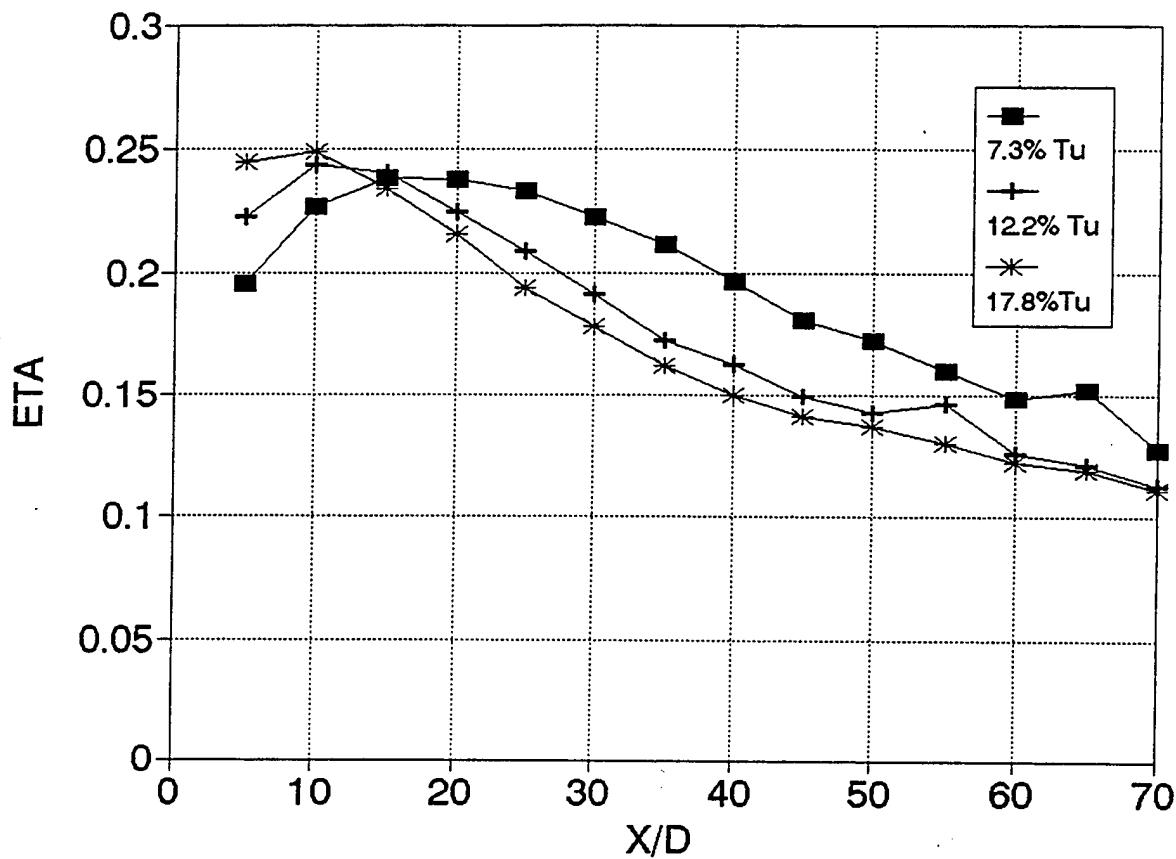
Figure 5-12. Effect of Free Stream Turbulence on Film Cooling Effectiveness
B = 1.25, Free stream velocity at injection = 10 m/s
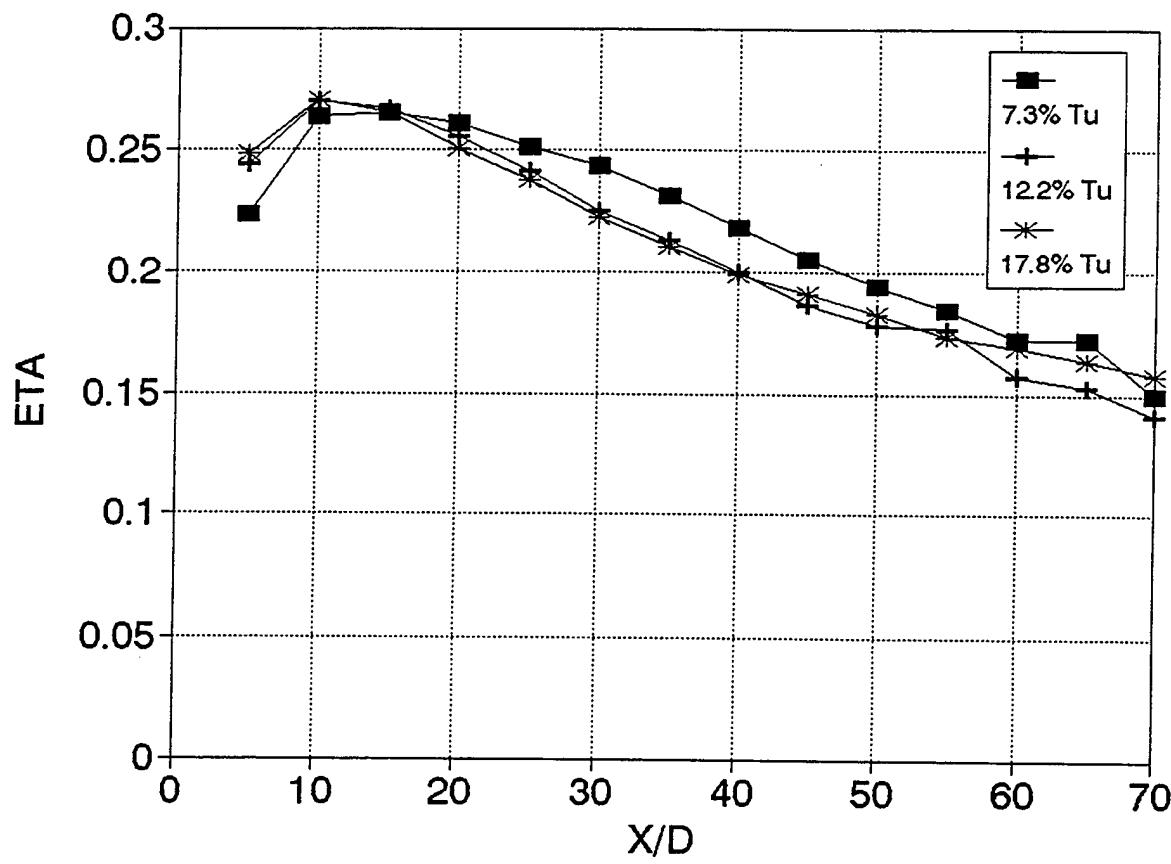
Figure 5-13. Effect of Free Stream Turbulence on Film Cooling Effectiveness
B = 2.0, Free stream velocity at injection = 10 m/s
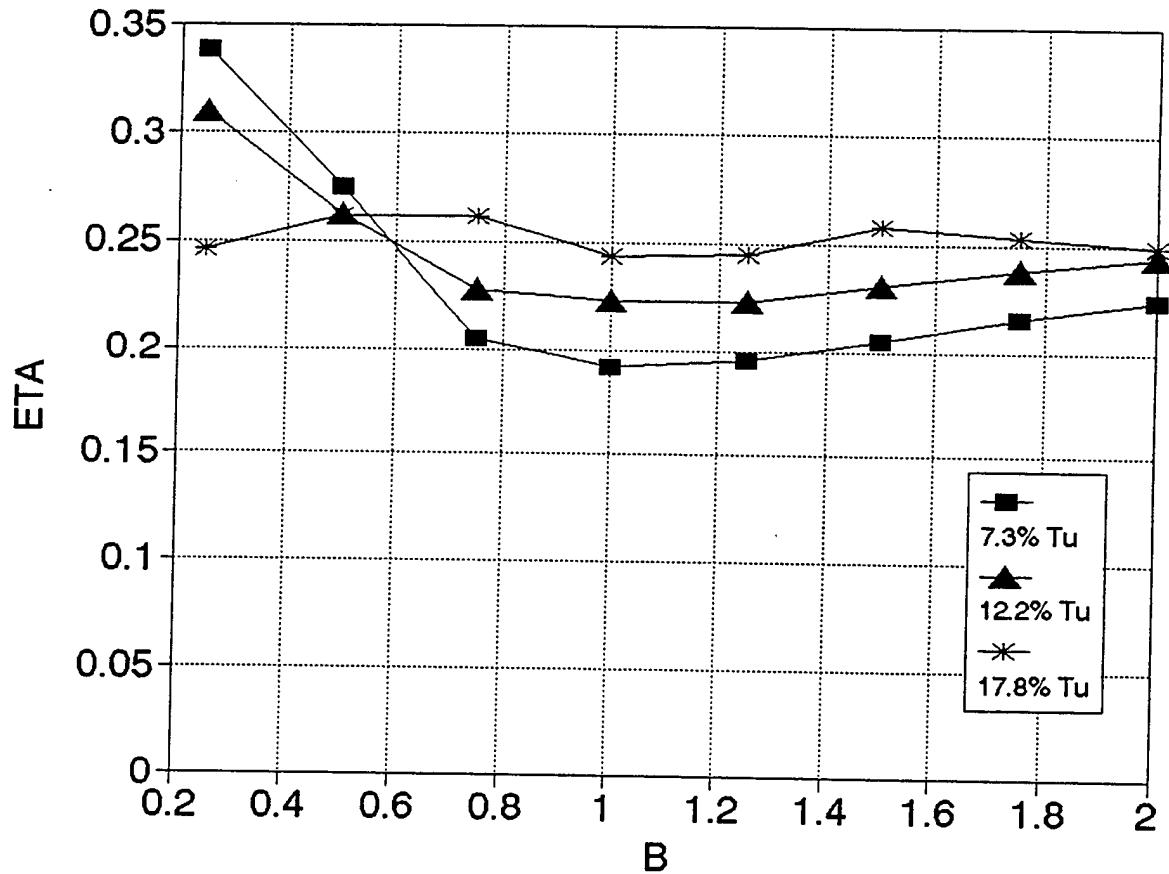
Figure 5-14. Effect of Free Stream Turbulence on Film Cooling Effectiveness
X/D = 5, Free stream velocity at injection = 10 m/s
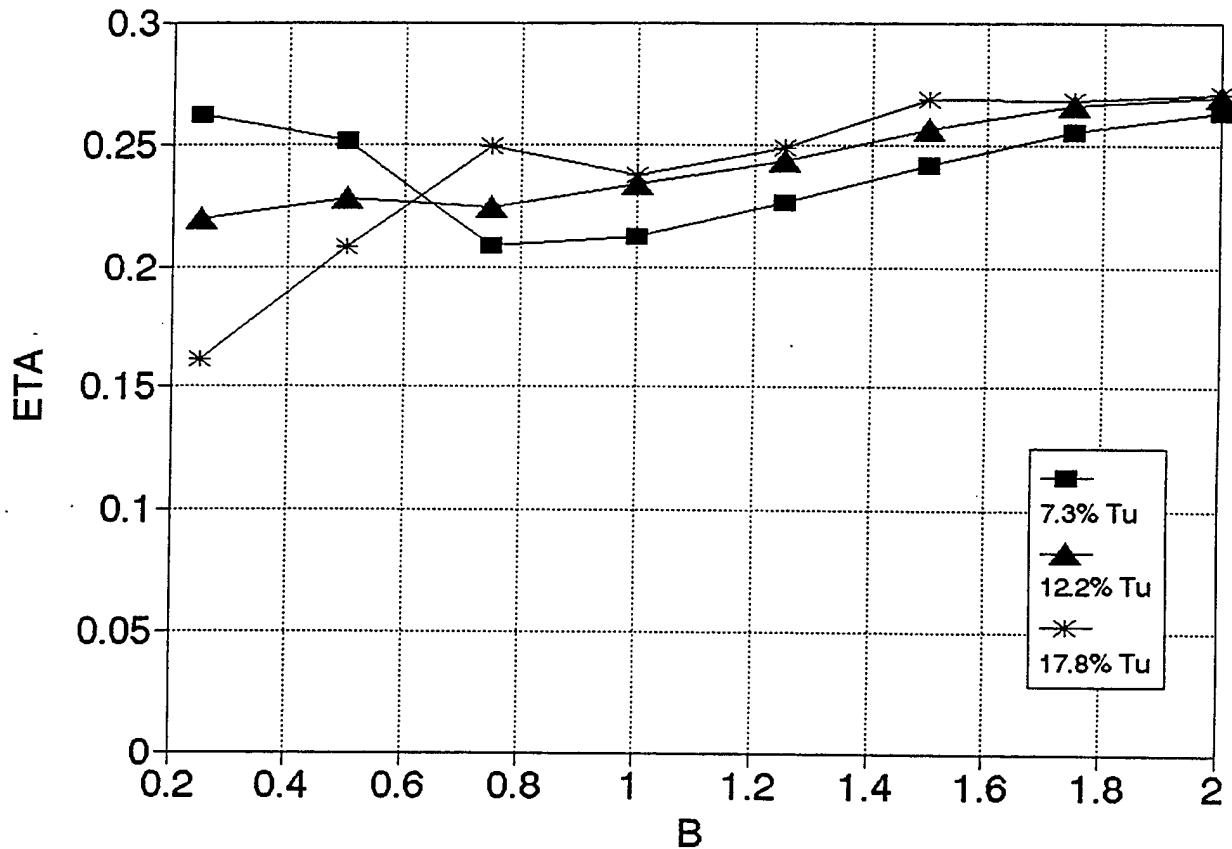
Figure 5-15. Effect of Free Stream Turbulence on Film Cooling Effectiveness
X/D = 10, Free stream velocity at injection = 10 m/s
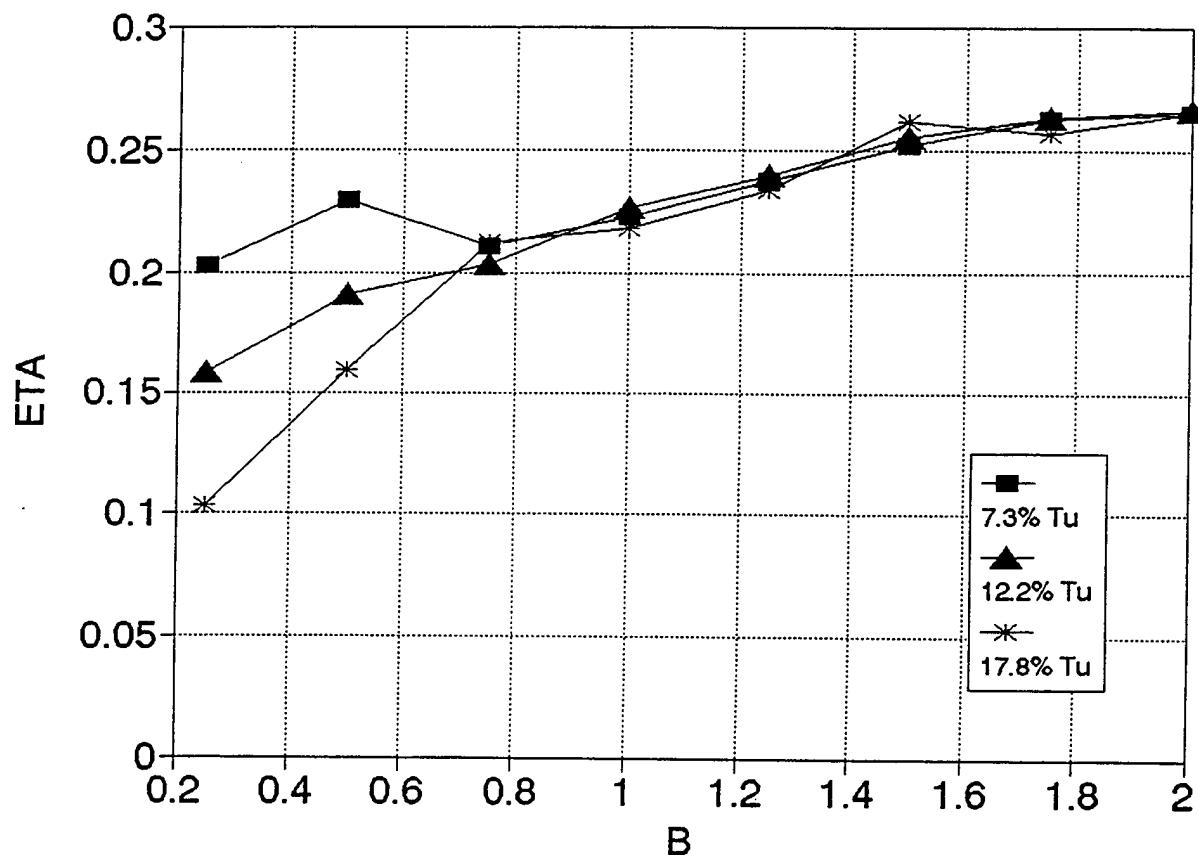
Figure 5-16. Effect of Free Stream Turbulence on Film Cooling Effectiveness
X/D = 15, Free stream velocity at injection = 10 m/s
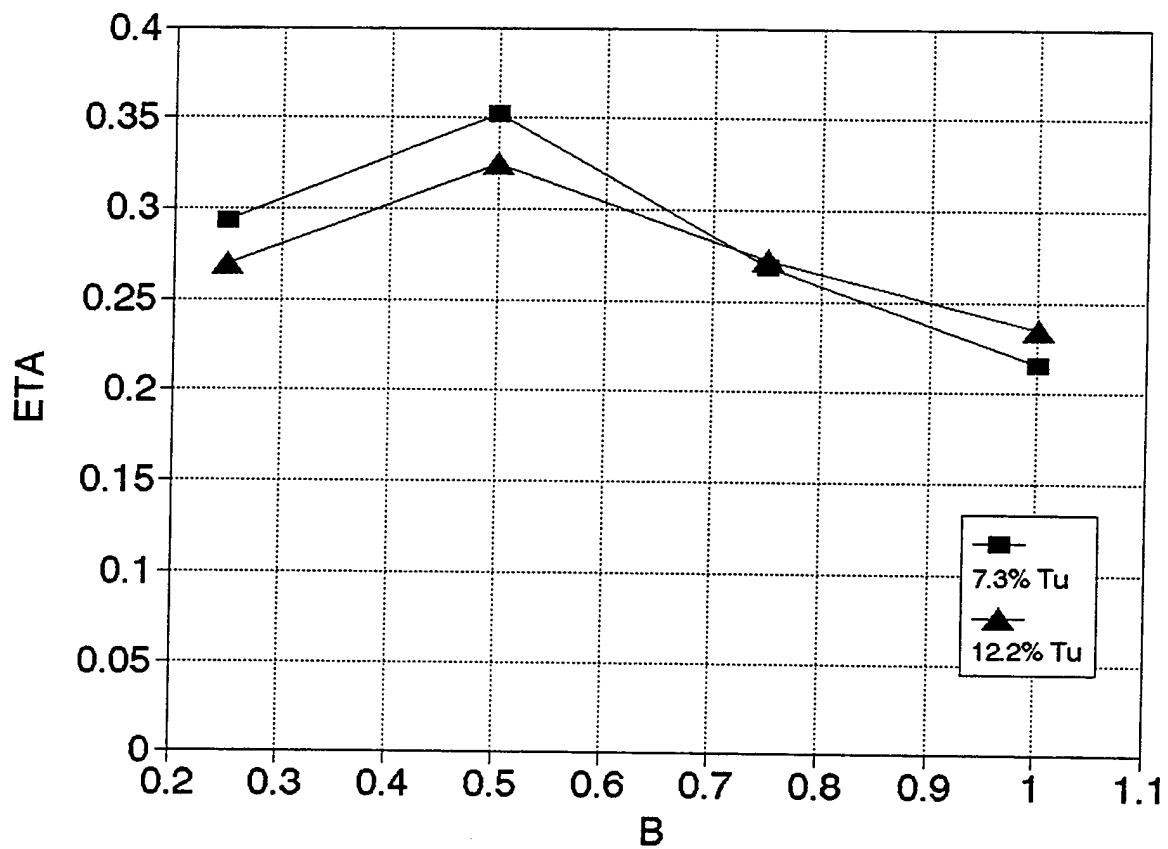
Figure 5-17. Effect of Free Stream Turbulence on Film Cooling Effectiveness
X/D = 5, Free stream velocity at injection = 37 m/s
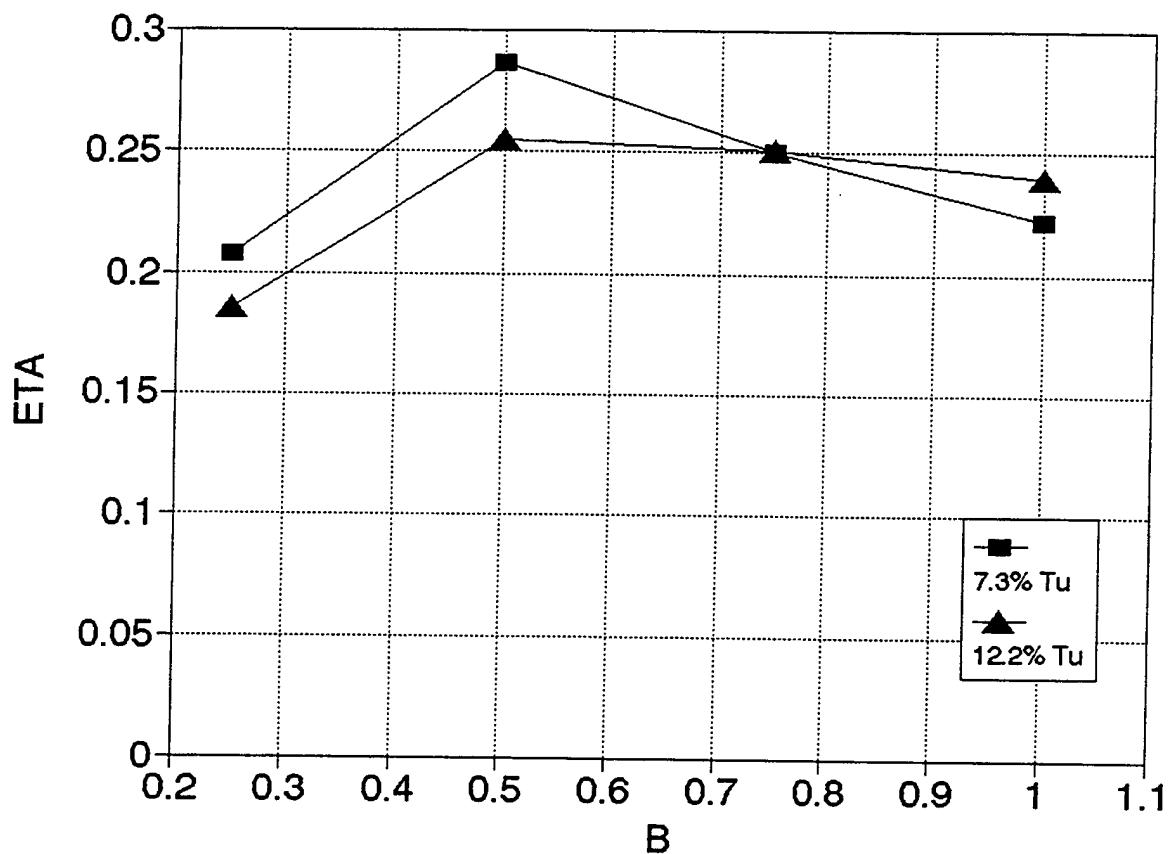
Figure 5-18. Effect of Free Stream Turbulence on Film Cooling Effectiveness
X/D = 10, Free stream velocity at injection = 37 m/s
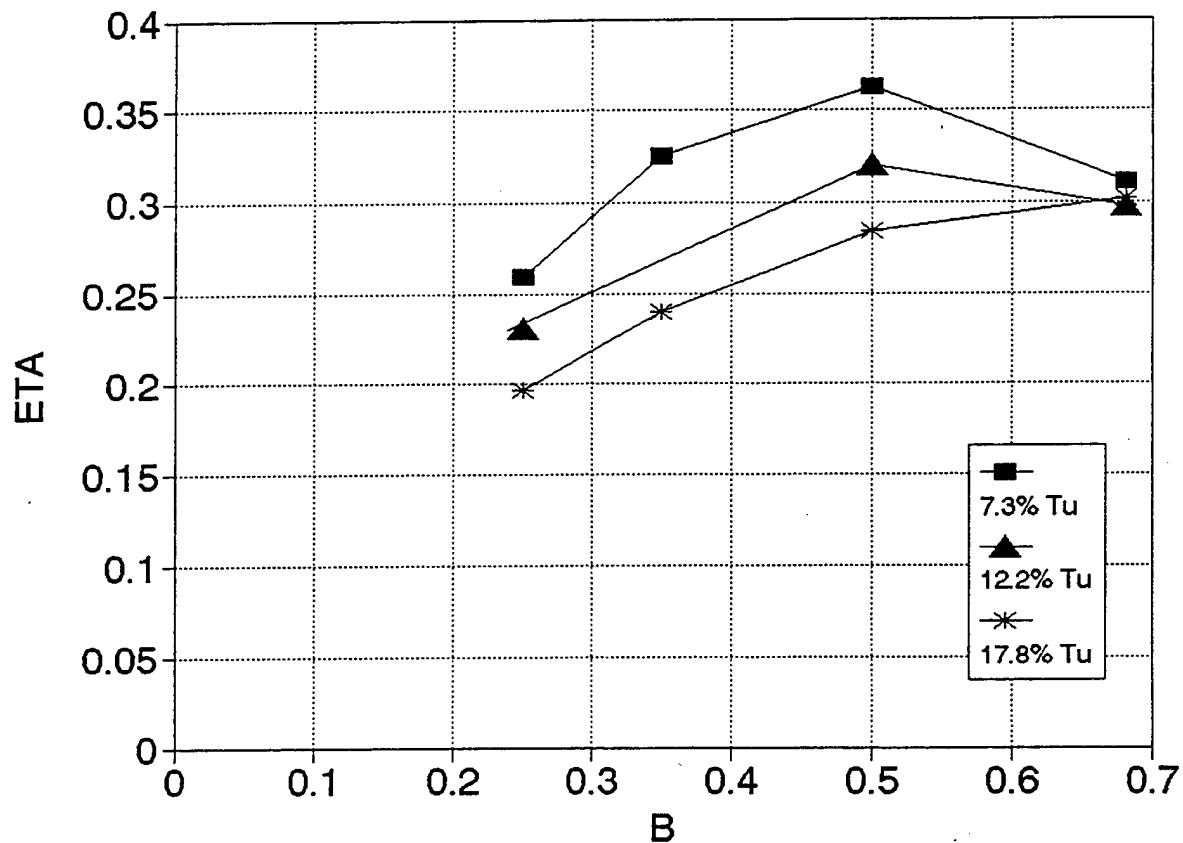
Figure 5-19. Effect of Free Stream Turbulence on Film Cooling Effectiveness
X/D = 5, Free stream velocity at injection = 60 m/s
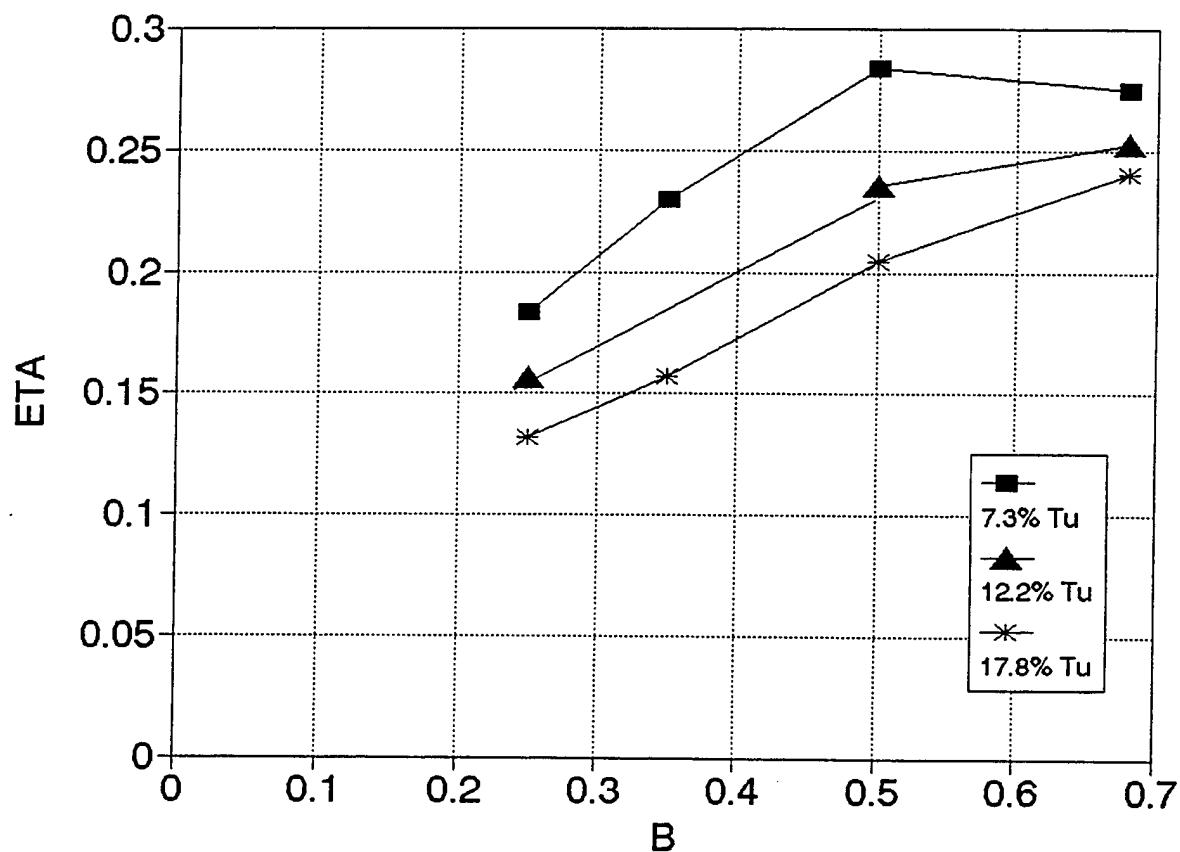
Figure 5-20. Effect of Free Stream Turbulence on Film Cooling Effectiveness
X/D = 10, Free stream velocity at injection = 60 m/s
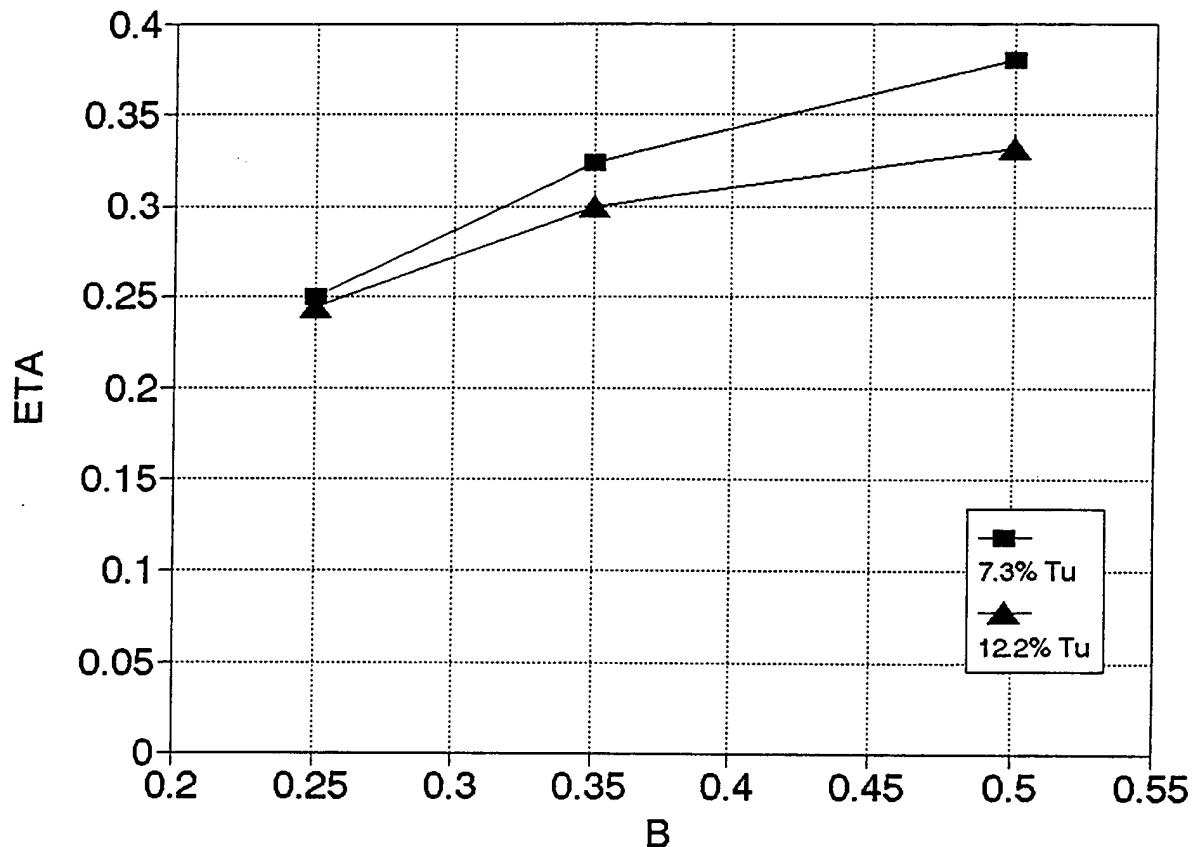
Figure 5-21. Effect of Free Stream Turbulence on Film Cooling Effectiveness
X/D = 5, Free stream velocity at injection = 85 m/s
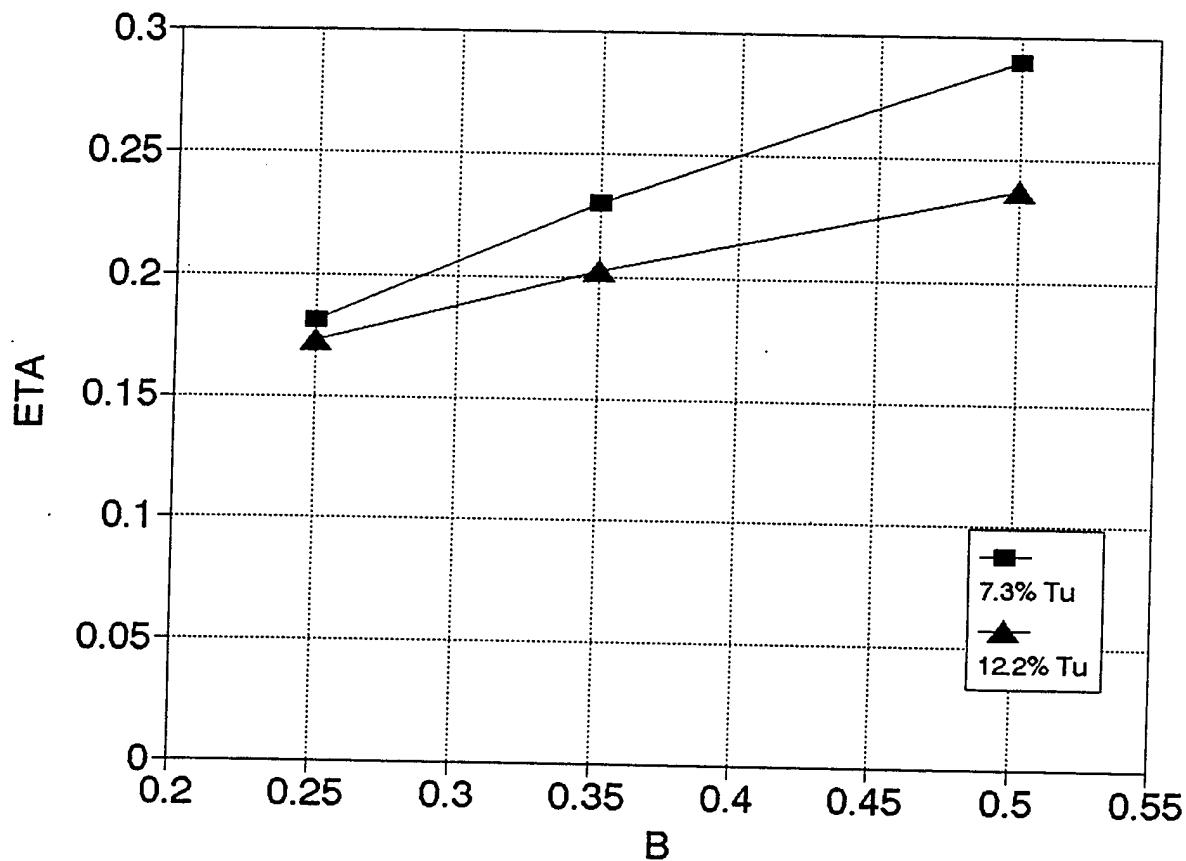
Figure 5-22. Effect of Free Stream Turbulence on Film Cooling Effectiveness
X/D = 10, Free stream velocity at injection = 85 m/s
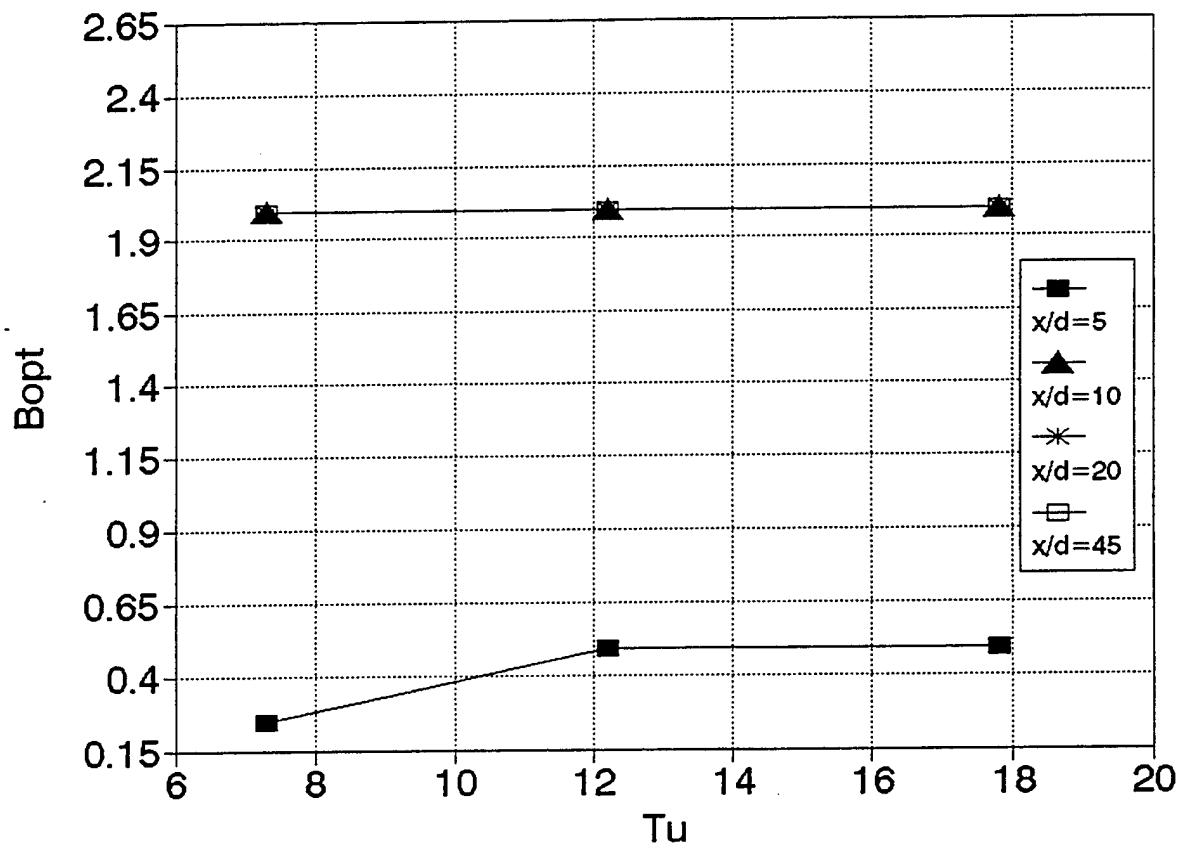
Figure 5-23. Effect of Free Stream Turbulence on Optimum Blowing Ratio
Free stream velocity at injection = 18 m/s
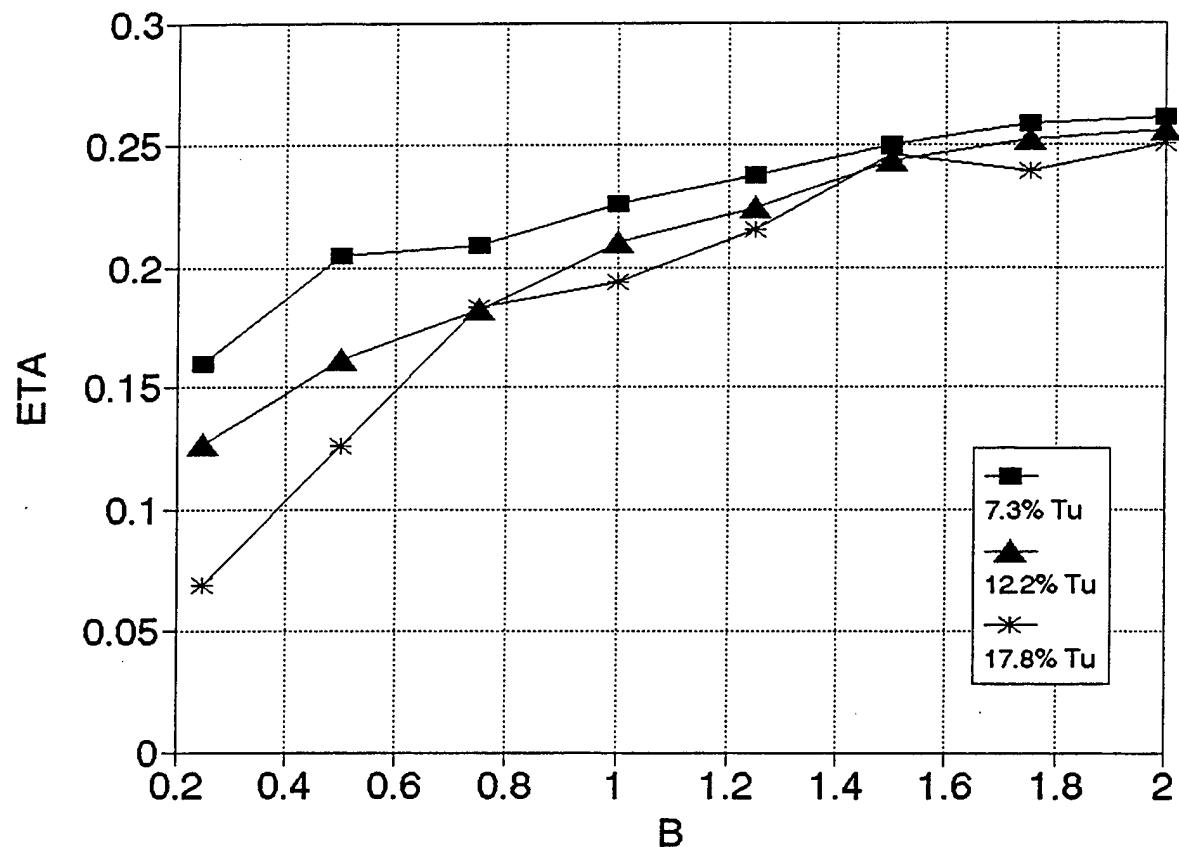
Figure 5-24. Effect of Free Stream Turbulence on Film Cooling Effectiveness
X/D = 20, Free stream velocity at injection = 10 m/s
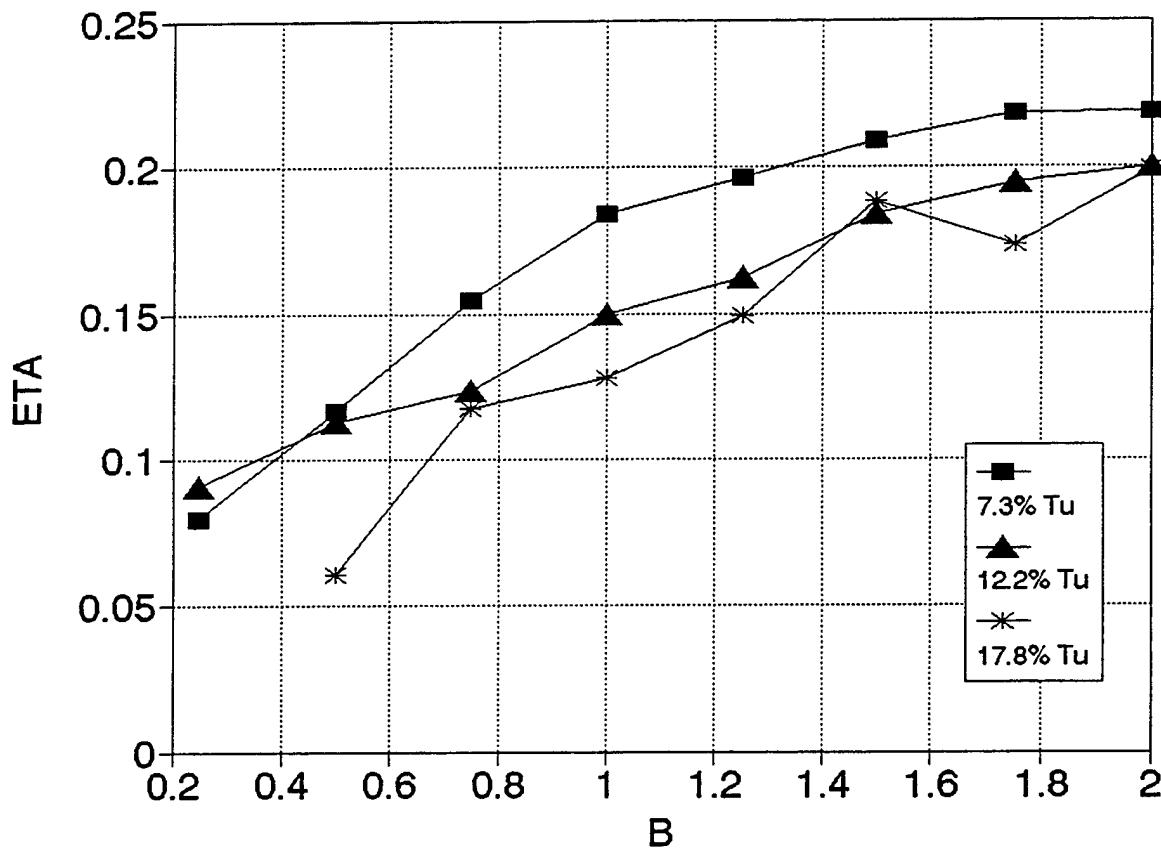
Figure 5-25. Effect of Free Stream Turbulence on Film Cooling Effectiveness
X/D = 40, Free stream velocity at injection = 10 m/s
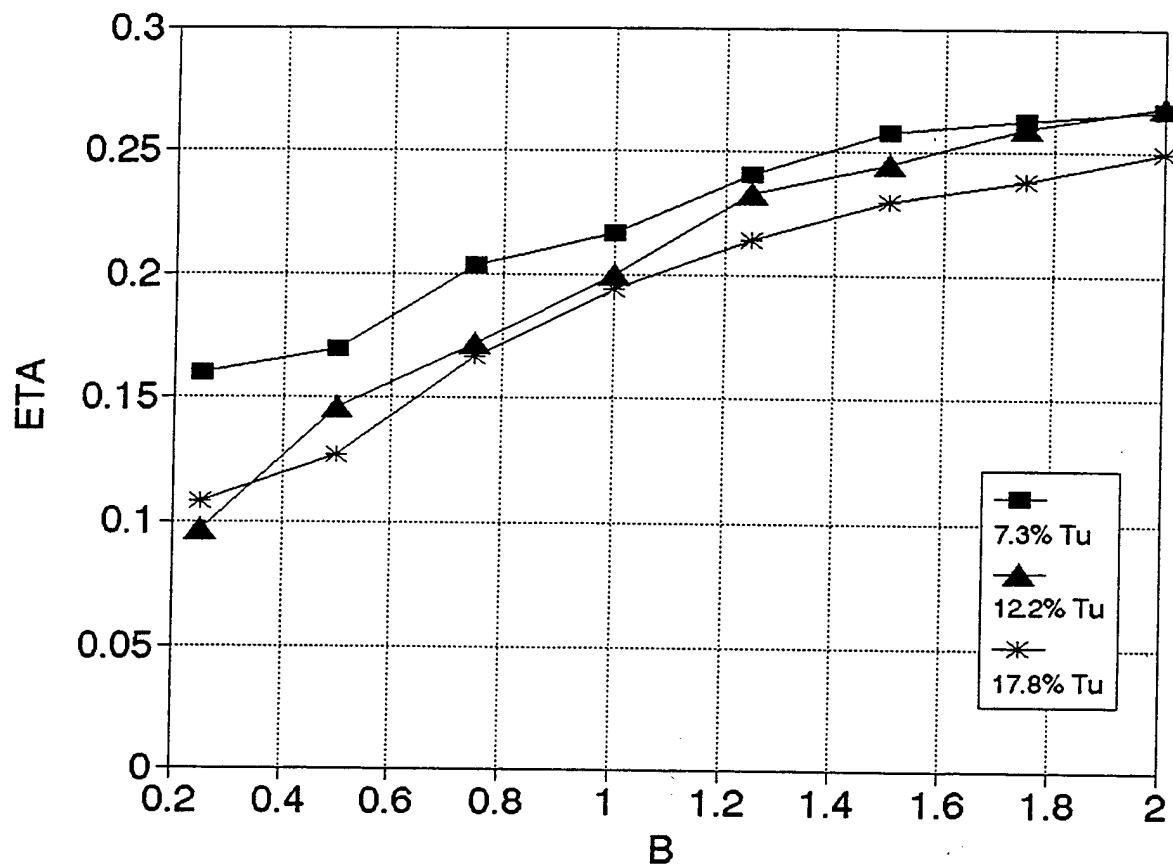
Figure 5-26. Effect of Free Stream Turbulence on Film Cooling Effectiveness
X/D = 20, Free stream velocity at injection = 18 m/s
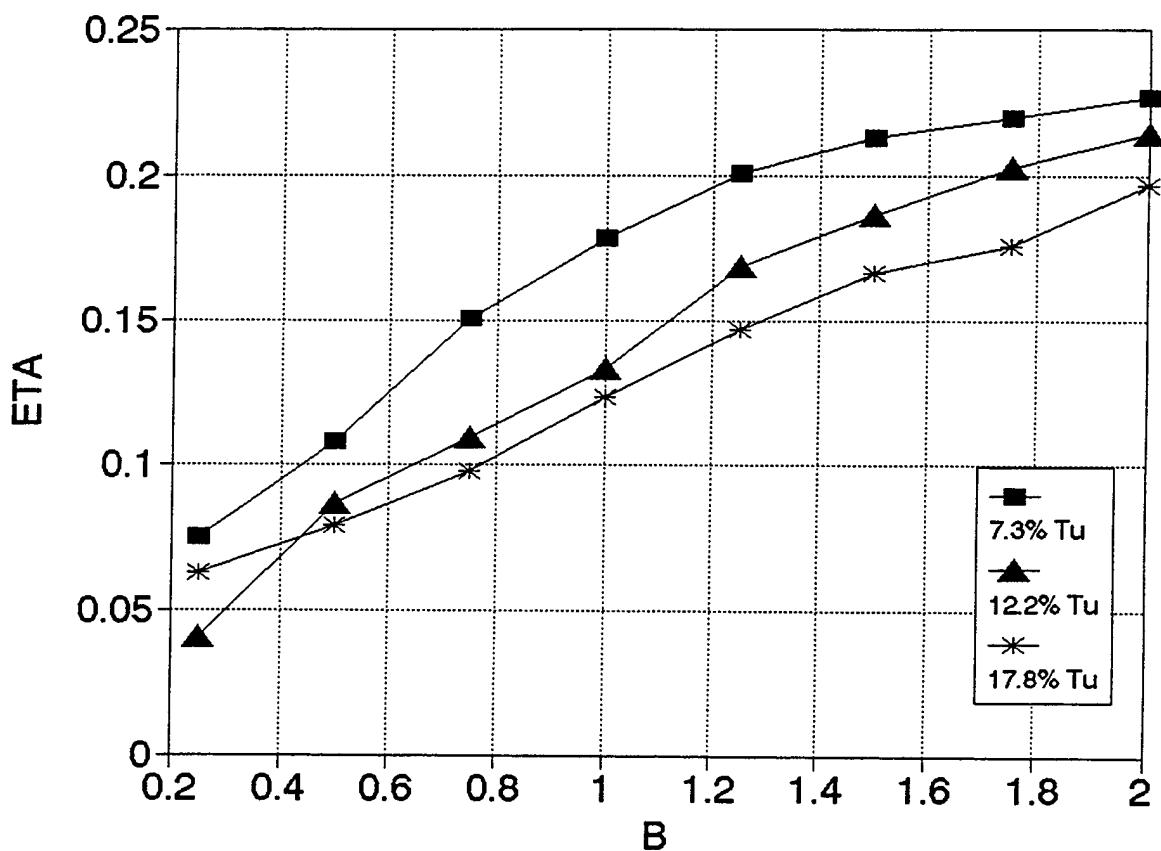
Figure 5-27. Effect of Free Stream Turbulence on Film Cooling Effectiveness
X/D = 40, Free stream velocity at injection = 18 m/s
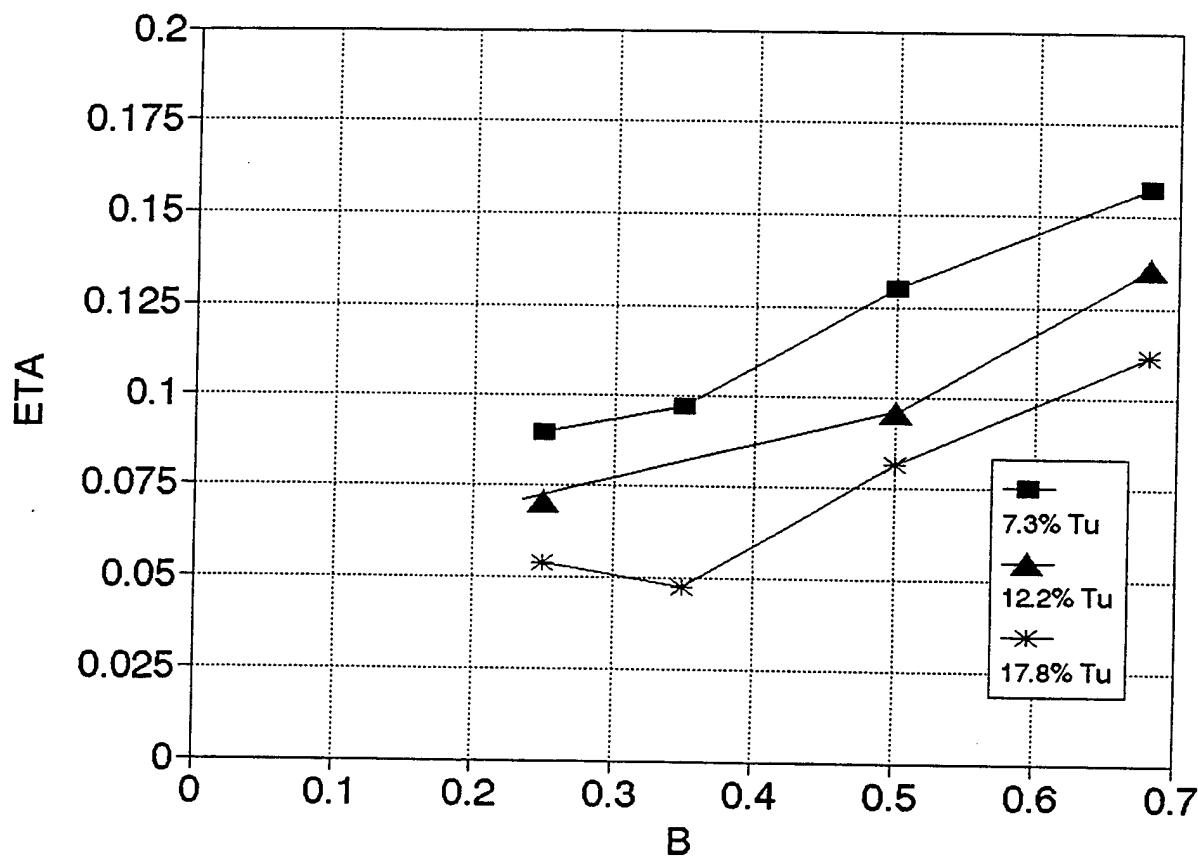
Figure 5-28. Effect of Free Stream Turbulence on Film Cooling Effectiveness
X/D = 30, Free stream velocity at injection = 60 m/s
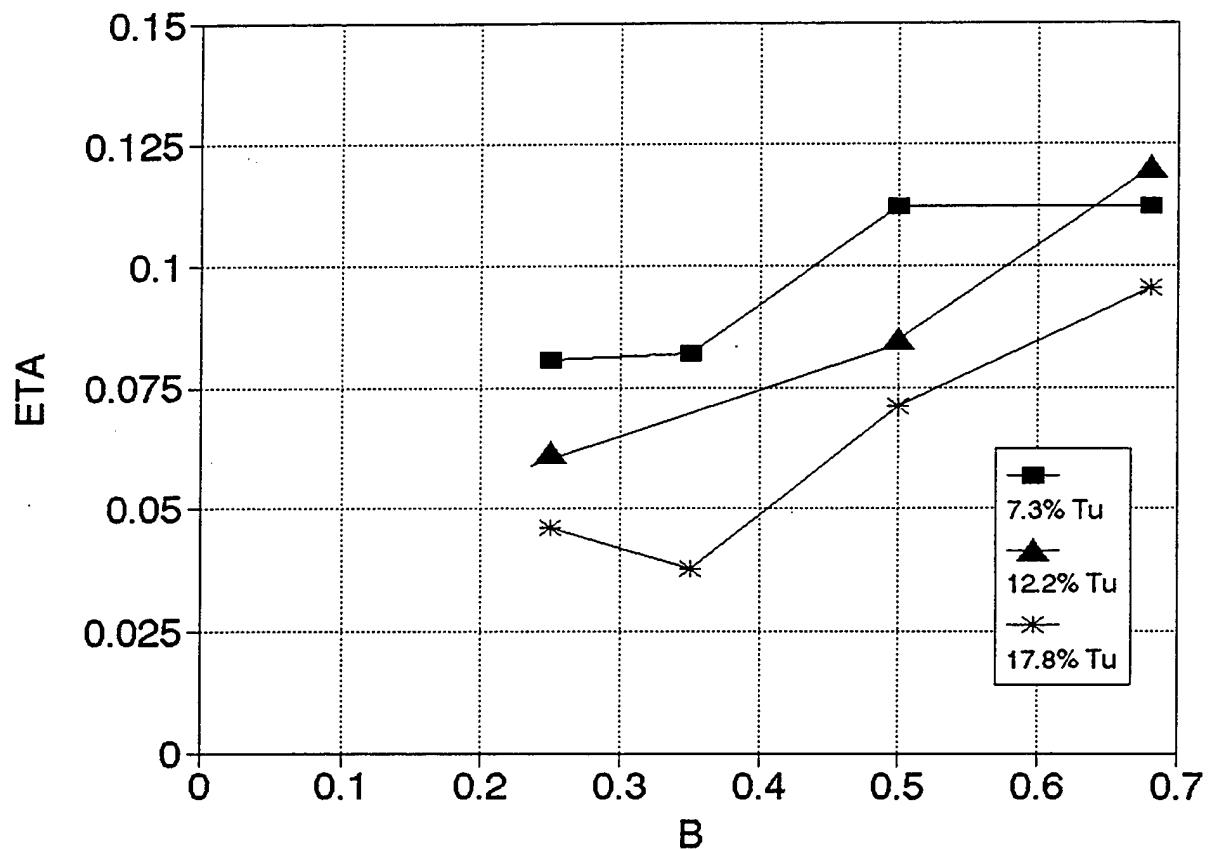
Figure 5-29. Effect of Free Stream Turbulence on Film Cooling Effectiveness
X/D = 35, Free stream velocity at injection = 60 m/s
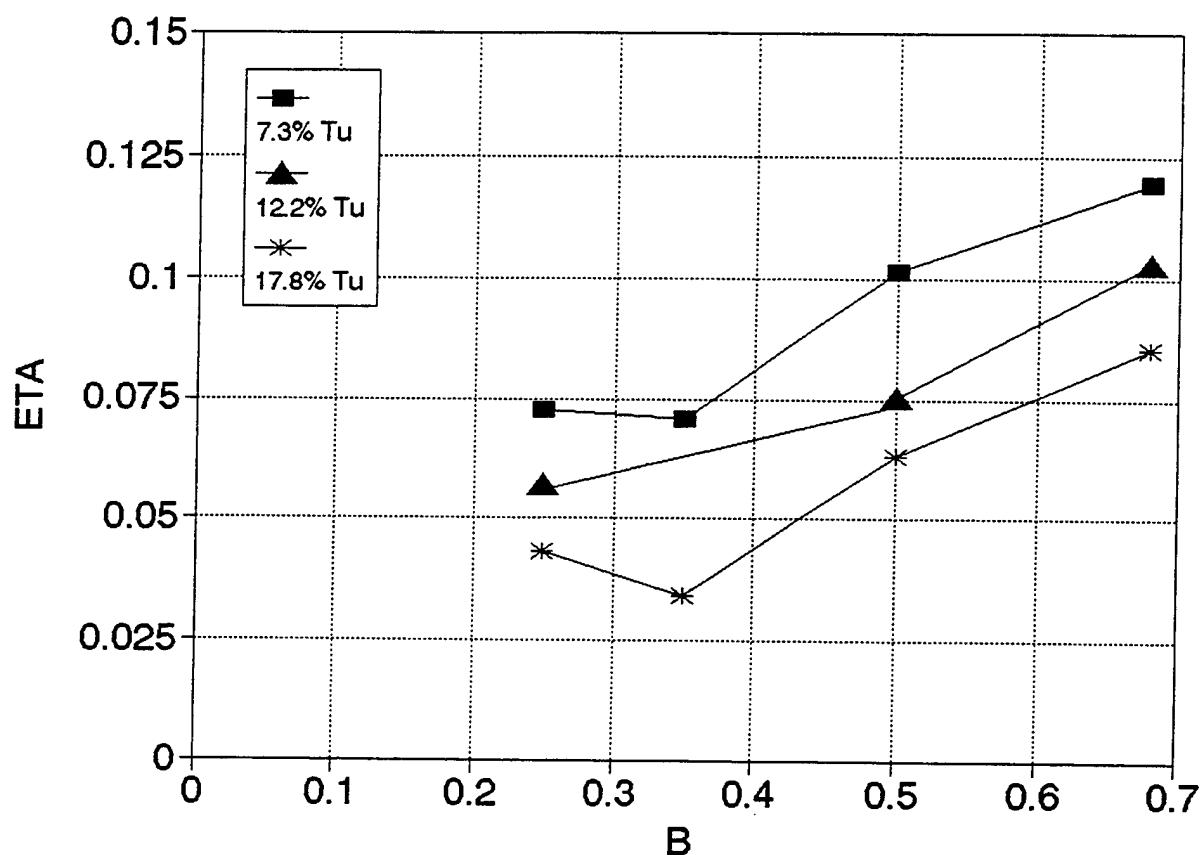
Figure 5-30. Effect of Free Stream Turbulence on Film Cooling Effectiveness
X/D = 40, Free stream velocity at injection = 60 m/s
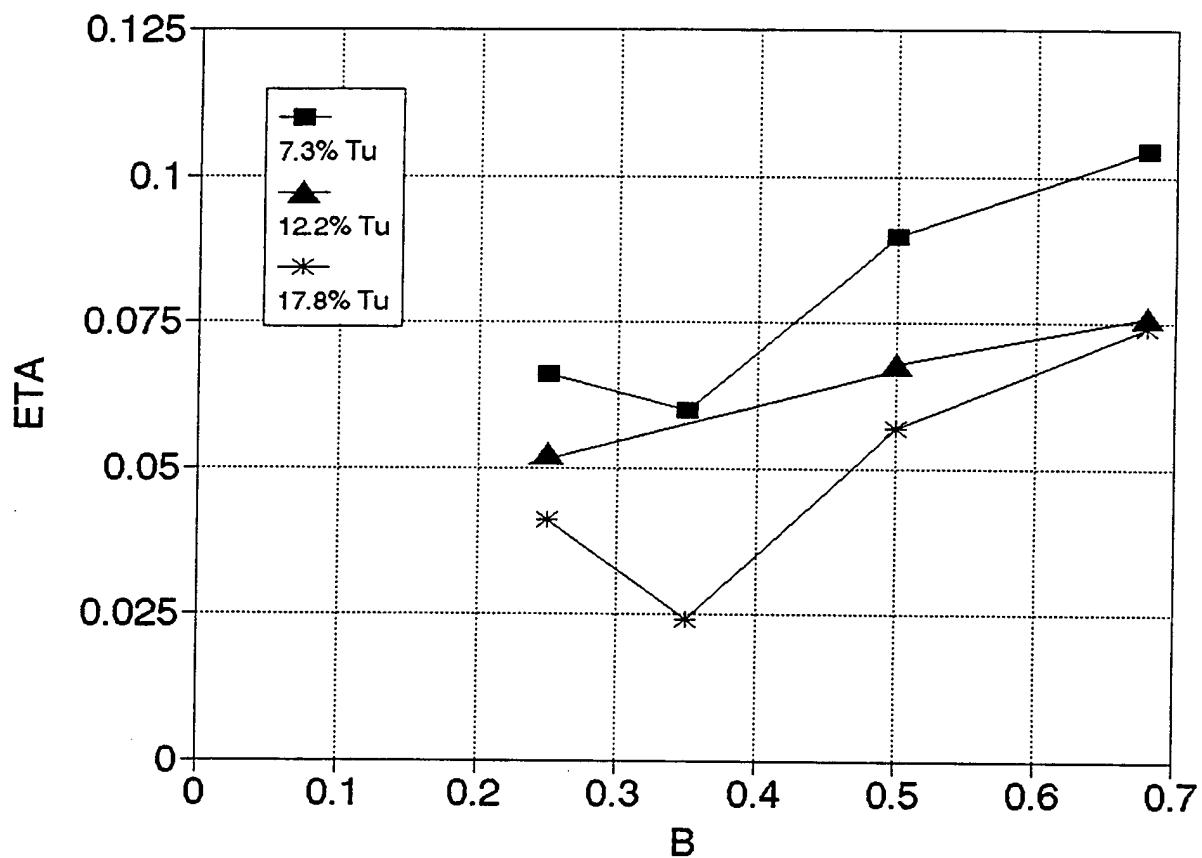
Figure 5-31. Effect of Free Stream Turbulence on Film Cooling Effectiveness
X/D = 45, Free stream velocity at injection = 60 m/s
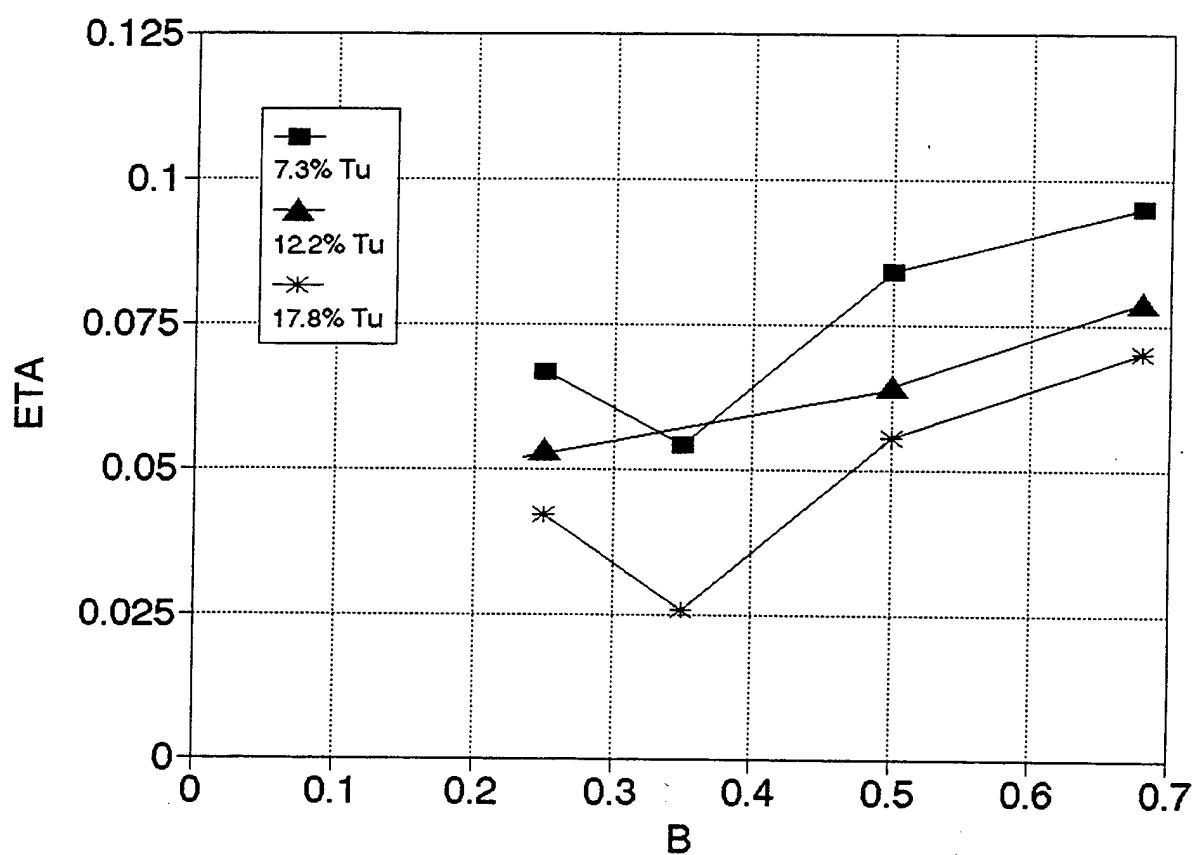
Figure 5-32. Effect of Free Stream Turbulence on Film Cooling Effectiveness
X/D = 50, Free stream velocity at injection = 60 m/s
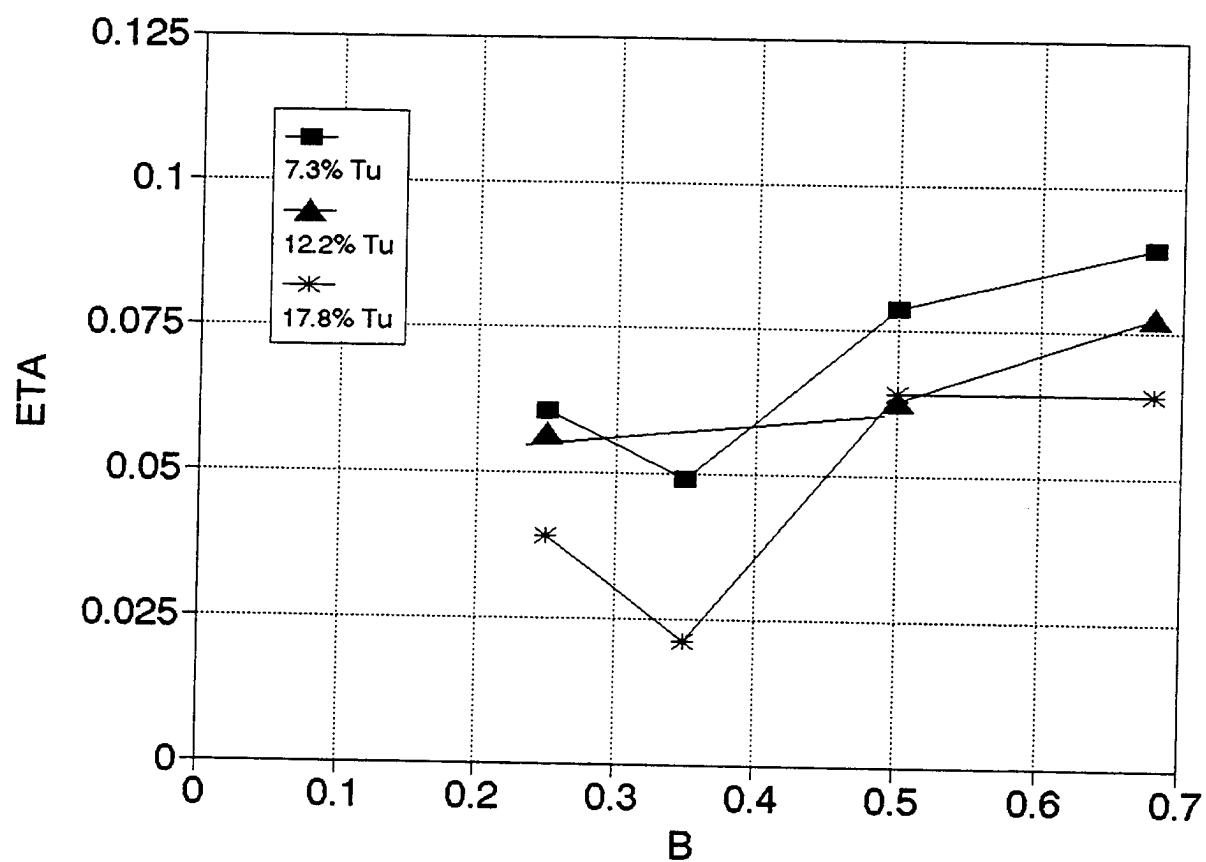
Figure 5-33. Effect of Free Stream Turbulence on Film Cooling Effectiveness
X/D = 55, Free stream velocity at injection = 60 m/s
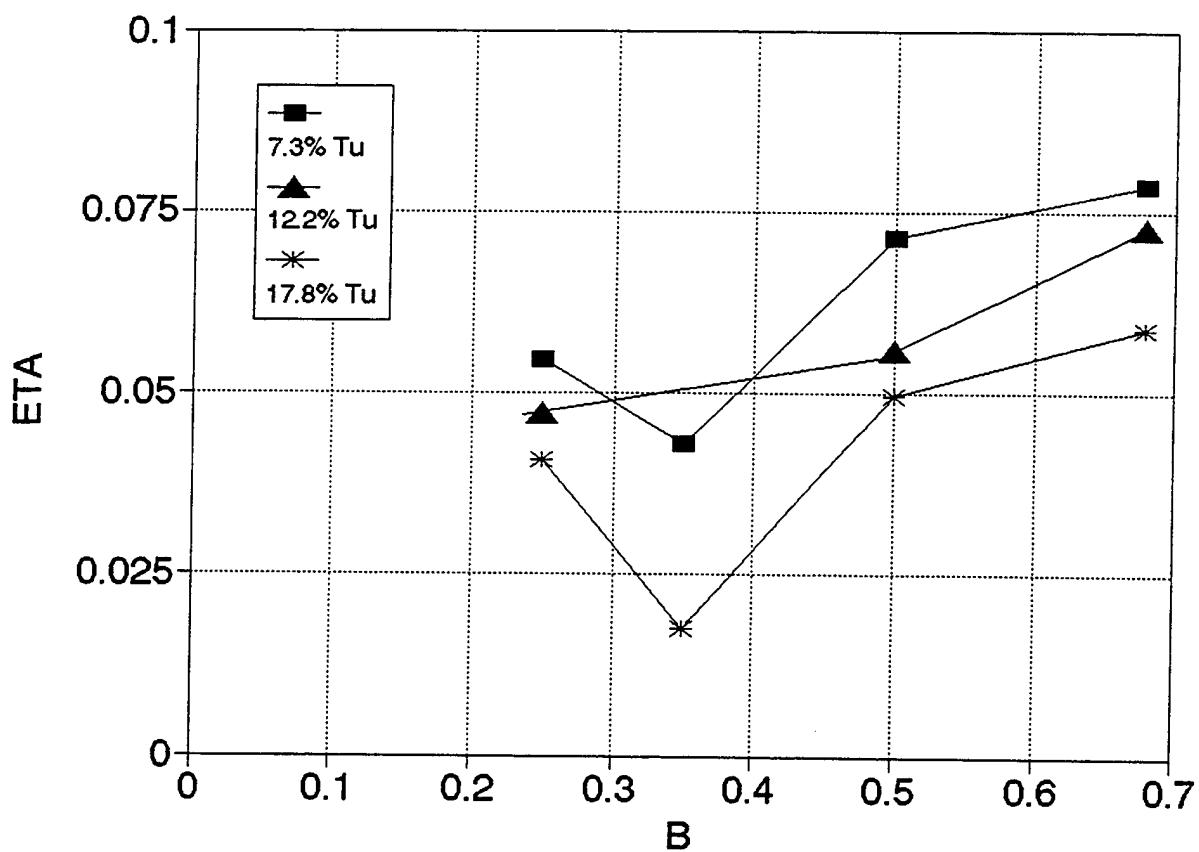
Figure 5-34. Effect of Free Stream Turbulence on Film Cooling Effectiveness
X/D = 60, Free stream velocity at injection = 60 m/s
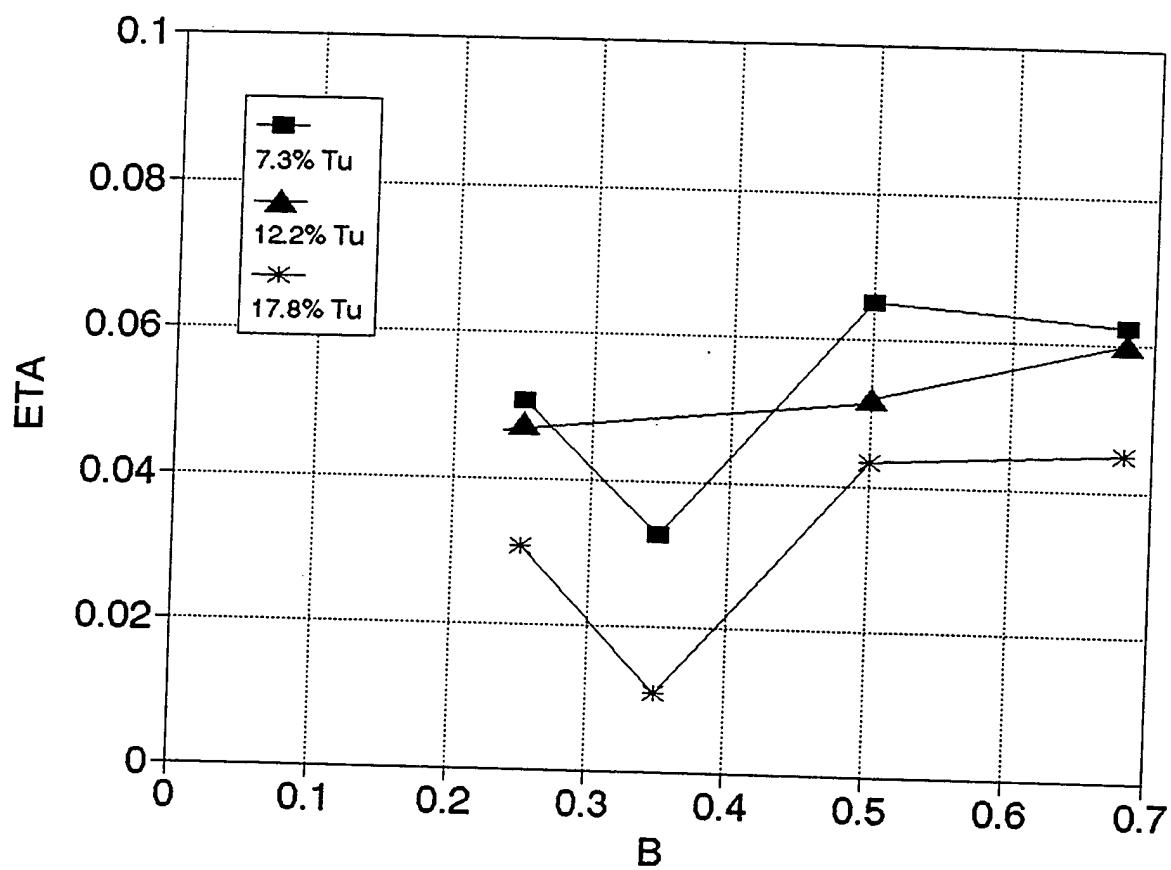
Figure 5-35. Effect of Free Stream Turbulence on Film Cooling Effectiveness
X/D = 70, Free stream velocity at injection = 60 m/s
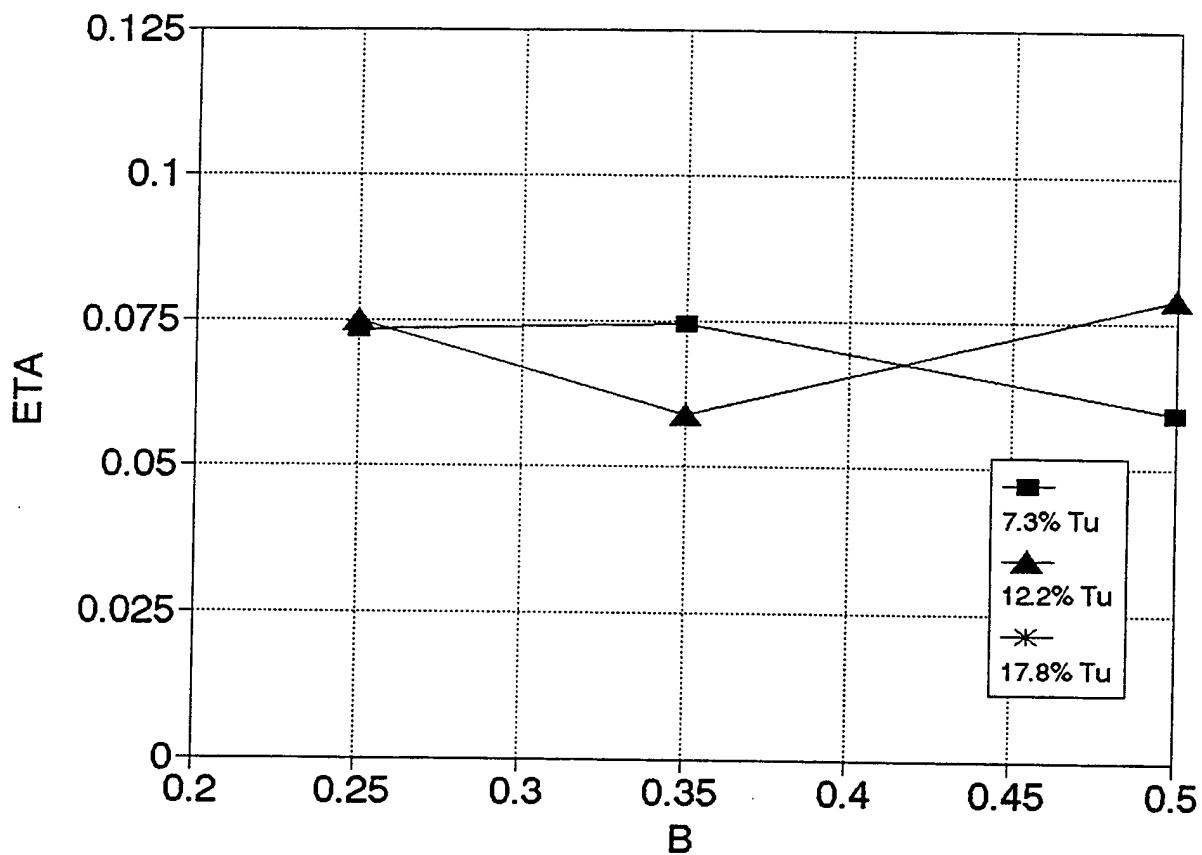
Figure 5-36. Effect of Free Stream Turbulence on Film Cooling Effectiveness
X/D = 65, Free stream velocity at injection = 85 m/s
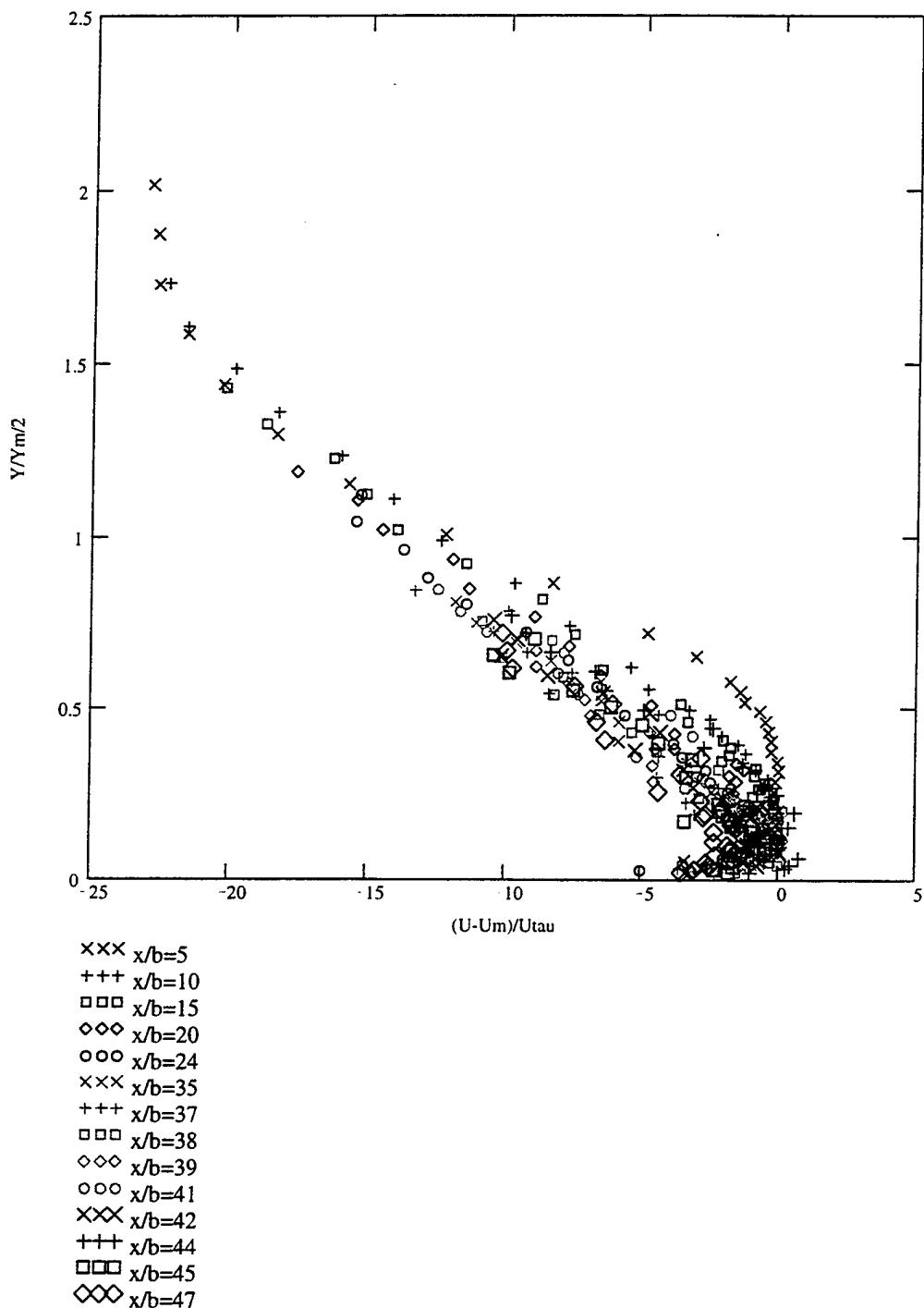
Figure 5-37. Velocity Profile Scaling Using Outer Law Variahles
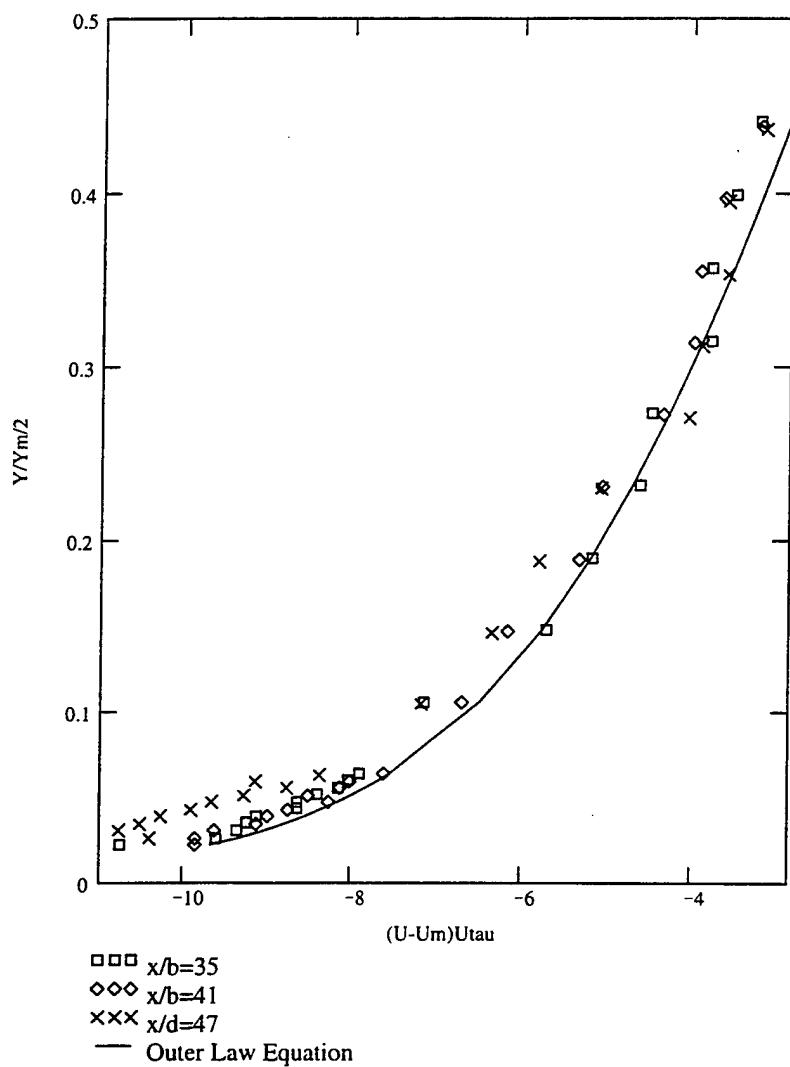
Figure 5-38. Near-Wall Velocity Profile Scaling Using Outer Law Variables
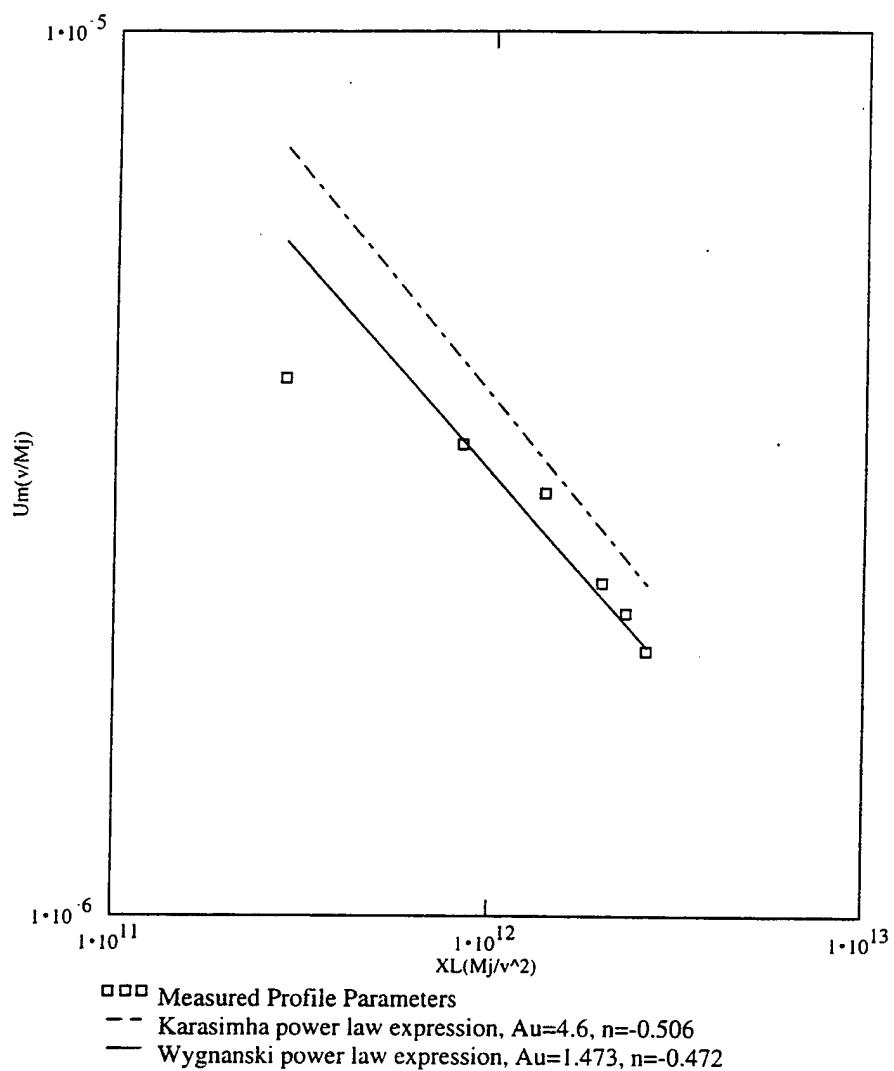
Figure 5-39. Wall Jet Momentum Scaling

The figure shows a log-log plot with:
- Y-axis: Um(v/Mj), ranging from $1 \cdot 10^{-6}$ to $1 \cdot 10^{-5}$
- X-axis: XL(Mj/v^2), ranging from $1 \cdot 10^{11}$ to $1 \cdot 10^{13}$

Legend:
□□□ Measured Profile Parameters
– – Karasimha power law expression, Au=4.6, n=-0.506
— Wygnanski power law expression, Au=1.473, n=-0.472
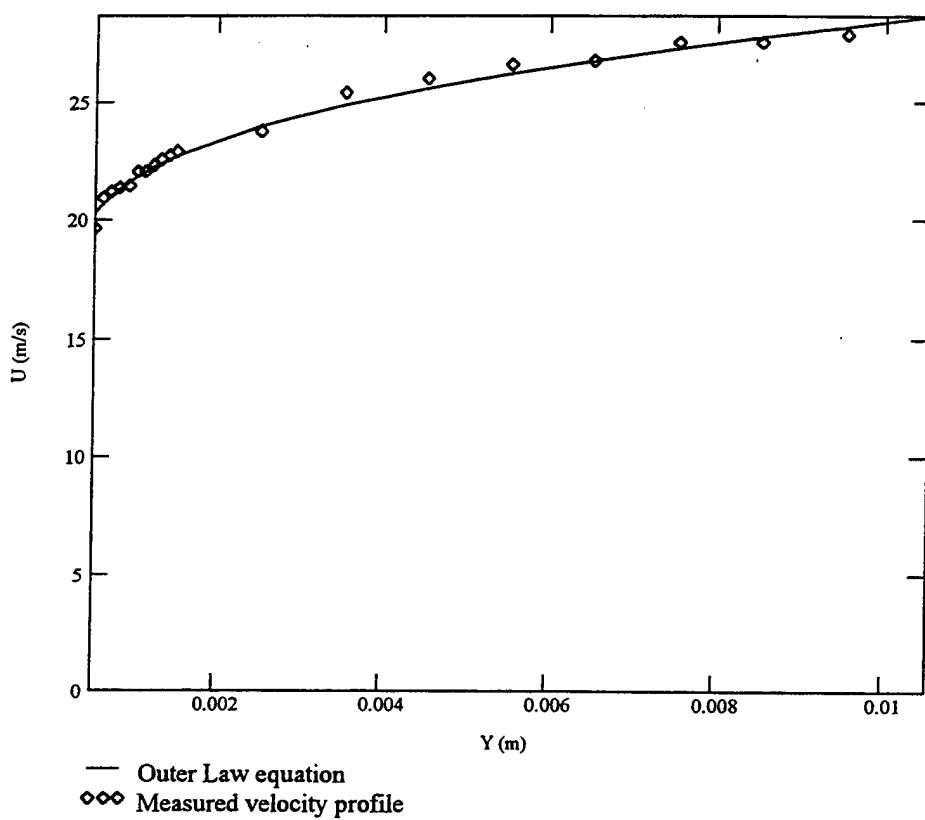
Figure 5-40. Comparison of Velocity Profile Generated with Outer Law Equation
and Measured Velocity Profile (x/b = 35, Uinf = 55.8 m/s)
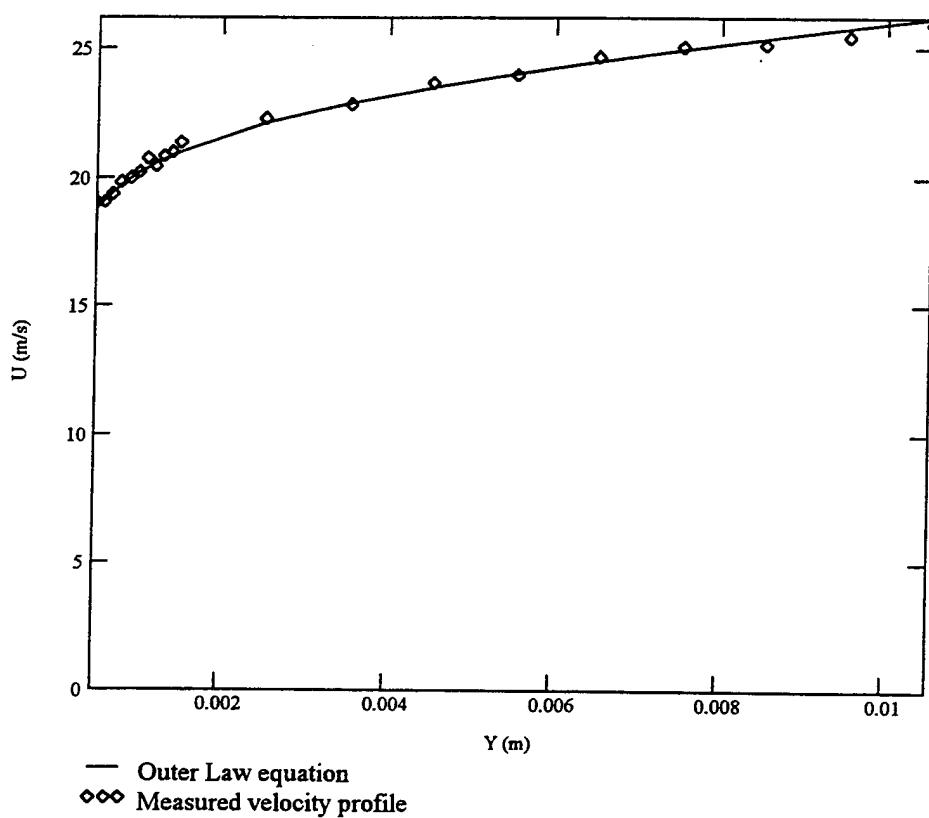
Figure 5-41. Comparison of Velocity Profile Generated with Outer Law Equation
and Measured Velocity Profile (x/b = 41, Uinf = 55.8 m/s)
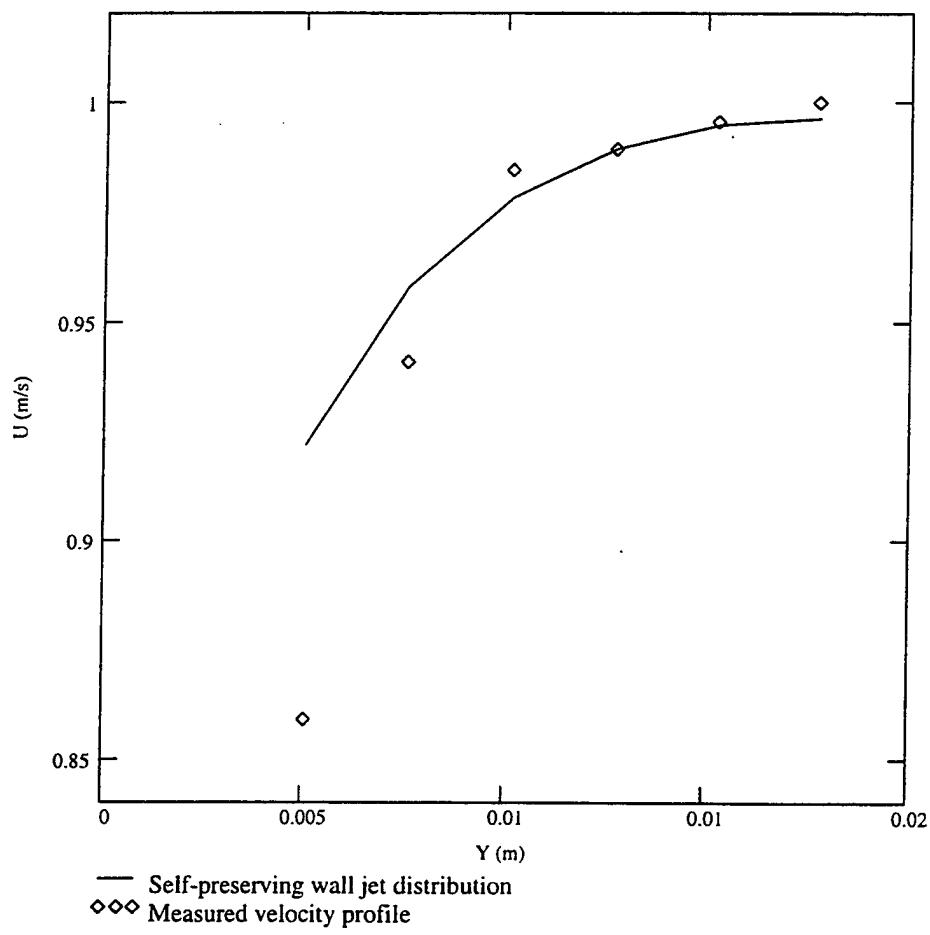
Figure 5-42 Velocity Profile Distribution Fit (x/b = 5.03, Uinf = 55.8 m/s)
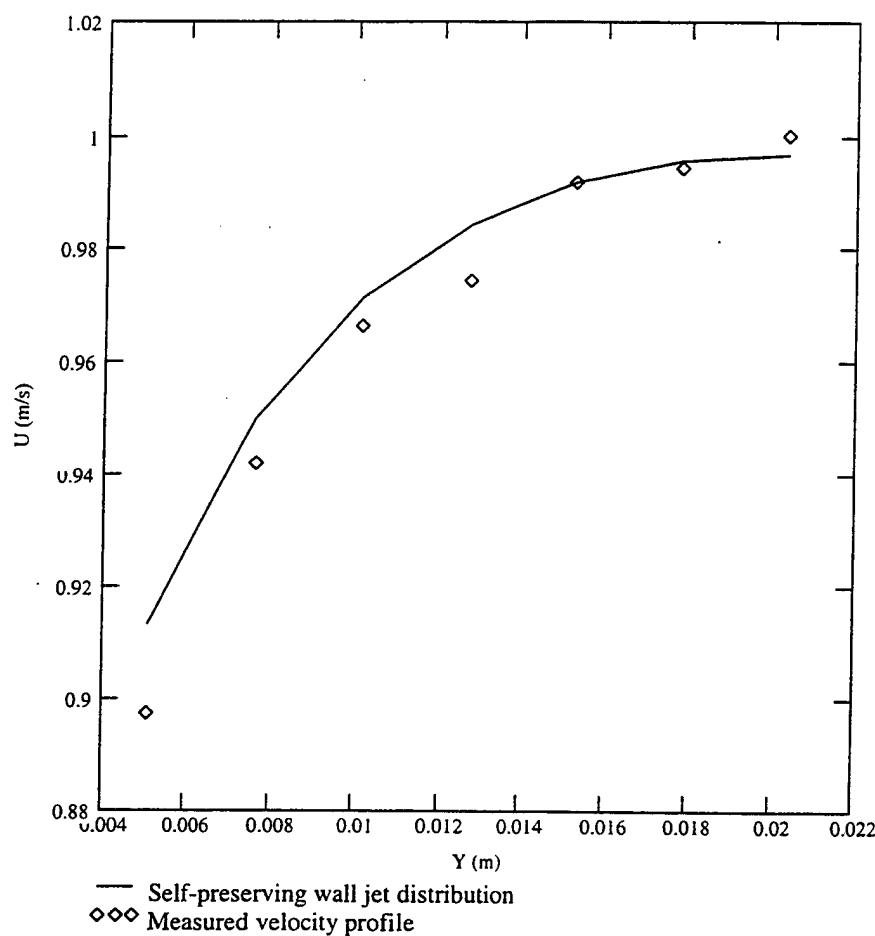
Figure 5-43. Velocity Profile Distribution Fit (x/b = 10.06, Uinf = 55.8 m/s)
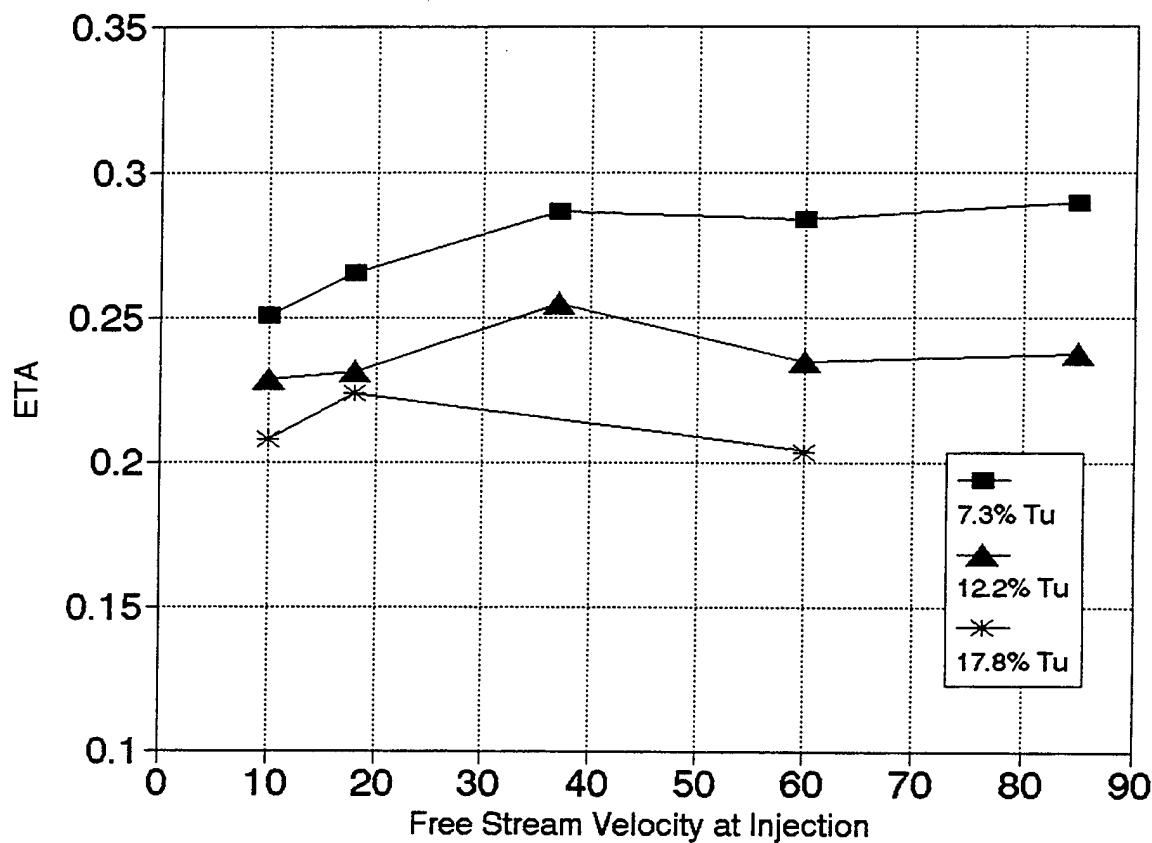
Figure 5-44. Effect of Free Stream Velocity on Film Cooling Effectiveness
X/D = 10, B = 0.50
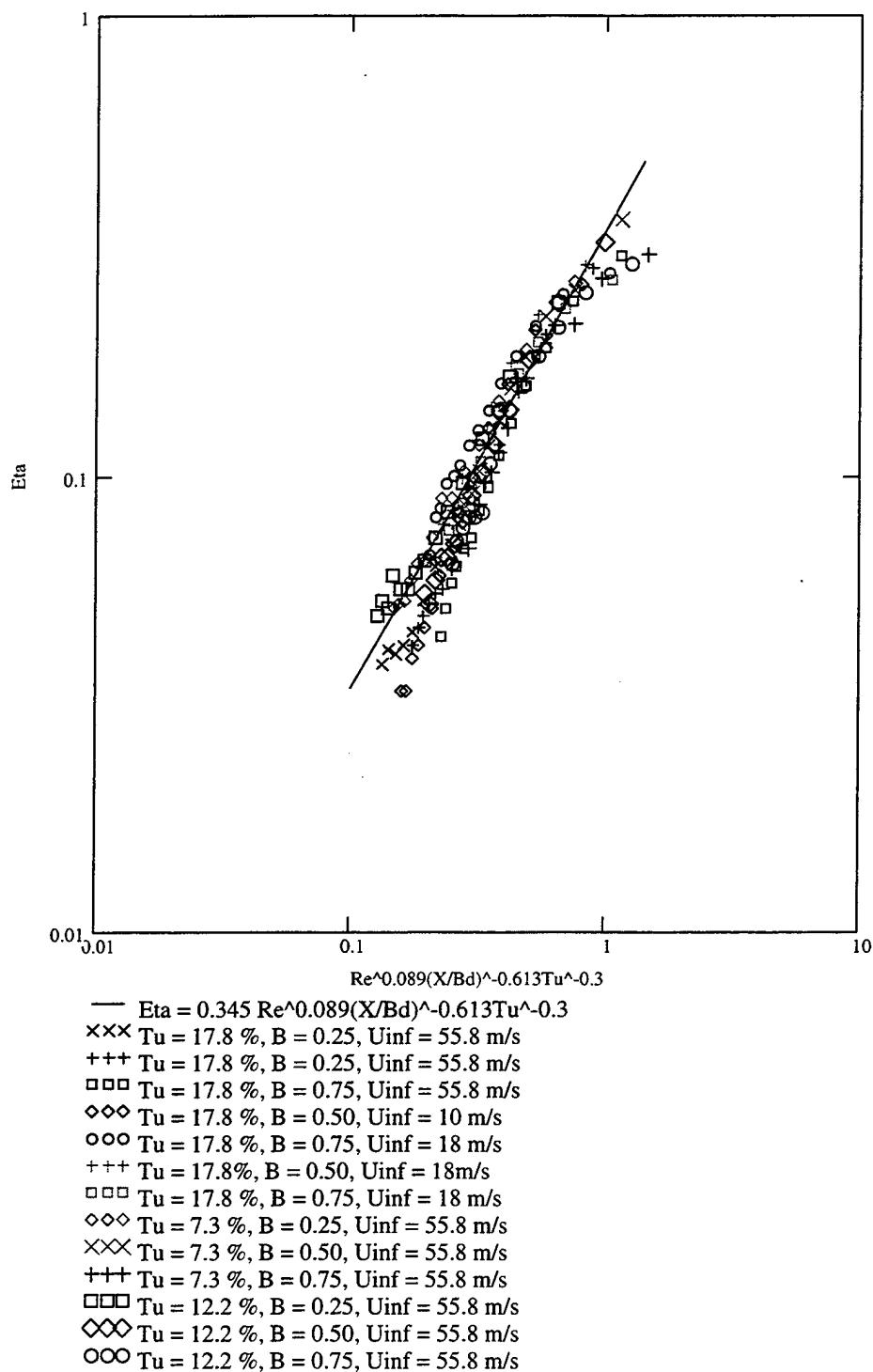
Figure 5-45. Effectiveness Correlation with Non-dimensional Grouping of Film
Cooling Parameters 0.25 <B < 0.75
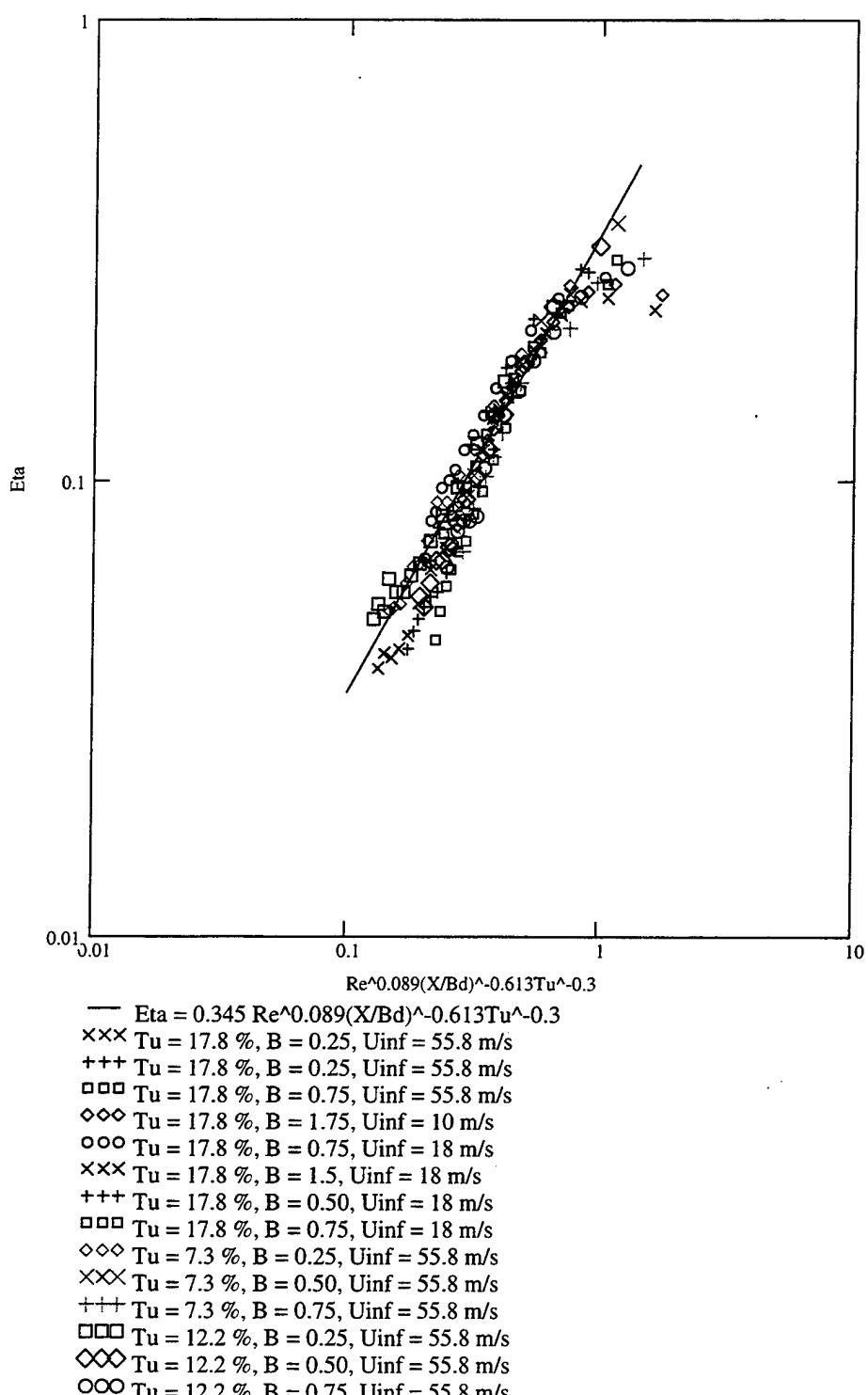
Figure 5-46. Effectiveness Correlation with Non-dimensional Grouping of Film
Cooling Parameters 0.25 < B < 1.75

Eta

0.1

0.01

0.01   0.1   1   10

Re^0.089(X/Bd)^-0.613Tu^-0.3

— Eta = 0.345 Re^0.089(X/Bd)^-0.613Tu^-0.3
××× Tu = 17.8 %, B = 0.25, Uinf = 55.8 m/s
+++ Low Tu, B = 0.50, Uinf = 30 m/s (Jabbari)
□□□ Tu=17.8 %, B = 0.75, Uinf = 55.8 m/s
◇◇◇ Tu = 17.8%, B = 1.75, Uinf = 10 m/s
ooo Tu = 17.8 %, B = 0.75, Uinf = 10 m/s
××× Tu = 17.8 % B = 1.5, Uinf = 18 m/s
+++ Low Tu, B = 0.20, Uinf = 30 m/s (Jabbari)
□□□ Tu = 17.8 %, B = 0.75, Uinf = 18 m/s
◇◇◇ Tu = 7.3 %, B = 0.25, Uinf = 55.8 m/s
ooo Tu = 11.5 %, B = =0.75, Uinf = 13.96 m/s (Bons)
××× Tu = 7.3 %, B = 0.75, Uinf = 55.8 m/s
+++ Tu = 12.2 %, B = 0.25, Uinf = 55.8 m/s
□□□ Tu = 12.2 %, B = 0.50, Uinf = 55.8 m/s ·
◇◇◇ Tu = 12.2 %, B = 0.75, Uinf = 55.8 m/s
ooo Tu = 17.0 %, Red = 24.7K, 0.25<B <2.4, (Jumper)

**Figure 5-47. Effectiveness Correlation Comparison Between Very Low
and High Free Stream Tu and One and Two Rows of Holes
0.20 < B < 2.4**

Appendix A : Derivation of the Corrected Effectiveness Equation

To obtain the adiabatic effectiveness, surface temperature measurements were taken on a plate with no power applied. This set up produces a near-adiabatic condition. The term near-adiabatic is used because the plate will experience loss of energy through conduction and radiation despite the insulation placed under the plate and the low emissivity of the plate material.

A correction to account for the non-adiabatic effects was calculated and applied to each effectiveness value obtained. The correction was typically 1 to 5 % of the final effectiveness value with the largest percentages obtained towards the end of the plate.

From a one-dimensional heat balance on an element of the surface one obtains

$$q_{rad} + q_{cond} + q_{conv} = 0 \tag{A-1}$$

where q_{rad} is the radiated heat from the surface to the environment, q_{cond} is the conducted heat flux through the surface, and q_{conv} is the convective heat flux from the surface to the fluid. The above equation can be expressed in terms of the respective temperatures as

$$\varepsilon\sigma(T_w^{\,4} - T_\infty^{\,4}) + h_o(T_w - T_\phi) + k\left(\frac{T_w - T_{bs}}{l}\right) = 0 \tag{A-2}$$

where T_w is the measured surface temperature, T_∞ is the free stream temperature, T_ϕ is the temperature resulting from a mixture of the free stream temperature and the coolant temperature (i.e., the temperature T_w would be if the plate was truly adiabatic), T_{bs} is the temperature at the bottom surface of the plate, and h_o is the heat transfer coefficient with injection. Defining $\Delta T = T_w - T_\phi$ and solving yields

$$\Delta T = -\left(\frac{\varepsilon\sigma\left(T_w^4 - T_\infty^4\right) + k\left(\frac{T_w - T_{bs}}{l}\right)}{h_o} \right) \tag{A-3}$$

The adiabatic wall temperature T_{aw} can be expressed as the combination of the measured temperature and ΔT, $T_{aw} = T_w - \Delta T$. Substituting this expression in the adiabatic effectiveness equation

$$\eta = \frac{\left(T_{aw} - T_\infty\right)}{\left(T_c - T_\infty\right)} \tag{A-4}$$

gives

$$\eta = \frac{\left(T_w - \Delta T - T_\infty\right)}{\left(T_c - T_\infty\right)} \tag{A-5}$$

Finally substituting equation A-3 into A-5 yields the corrected effectiveness

$$\eta = \frac{\left(T_w - T_\infty\right)}{\left(T_c - T_\infty\right)} + \frac{\left(q_{rad} + q_{cond}\right)}{h_o\left(T_c - T_\infty\right)} \tag{A-6}$$

where

$$q_{rad} = \varepsilon\sigma(T_w^4 - T_\infty^4)$$
$$q_{cond} = k\frac{(T_w - T_{bs})}{\ell}$$

The heat transfer coefficient in equation A-6 was obtained from a Staton number approximation due to Kays and Crawford (1980)

$$St_o\,\mathrm{Pr}^{0.4} = 0.0287\,\mathrm{Re}_x^{-0.2} \tag{A-7}$$

This approximation was adjusted for the appropriate level of free stream turbulence using a relation by Simonich (1978)

$$\frac{St}{St_o} = 1 + 5Tu \qquad \text{(A-8)}$$

Appendix B : Description of the Uncertainty

The uncertainty present in the calculation of effectiveness was described by a method for single-sample experiments presented by Kline and McClintock (1953). In this method the uncertainty interval for the result (in this case effectiveness) is

$$w_R = \left[\left(\frac{\partial R}{\partial v_1}w_1\right)^2 + \left(\frac{\partial R}{\partial v_2}w_2\right)^2 + \ldots + \left(\frac{\partial R}{\partial v_n}w_n\right)^2\right]^{1/2} \qquad \text{(B-1)}$$

where the result R is a function of n independent variables, $v_1, v_2, \ldots v_n$, and $w_1, w_2, \ldots w_n$ are the uncertainty intervals for the independent variables. This equation is referred to as the second-power equation.

The function R for this experiment is the effectiveness equation expressed in terms of directly measured parameters as:

$$\eta = \frac{T_w - \left[T_{\tan k} - \frac{(r-1)}{2C_p}\left(\frac{T_{hw}}{P_{bar}} - \frac{110.42 P_{kiel}{}^{3/2} T_{hw}}{P_{bar}{}^2}\right)^2\right]}{T_{\tan kcol} - \frac{R_{air}(r-1)CD^2 P_{\tan kcool} T_{\tan kcool}}{C_P(P_{\tan kcool} + P_{bar})} - \left[T_{\tan k} - \frac{(r-1)}{2C_P}\left(\frac{T_{hw}}{P_{bar}} - \frac{110.42 P_{kiel}{}^{3/2} T_{hw}}{P_{bar}{}^2}\right)^2\right]}$$

where

T_w is the temperature measured at the surface of the plate

T_{tank} is the total temperature measured in the air supply tank

$T_{tankcool}$ in the total temperature measured in the coolant tank

T_{hw} is the temperature measured in the free stream at the maximum velocity point

$P_{tankcool}$ is the total pressure measured in the coolant tank

P_{bar} is the ambient barometric pressure

P_{kiel} is the pressure measured at the maximum velocity point

CD is the coolant coefficient of discharge

Table B-1 presents the respective uncertainty intervals for each measured variable. The uncertainty intervals were estimated base on knowledge acquired through experience using instrumentation devices.

TABLE B-1. Uncertainty intervals for the independent variables in the effectiveness equation

Variable	Uncertainty Interval
T_w	$\pm 0.1°K$
T_{tank}	$\pm 0.1°K$
$T_{tankcool}$	$\pm 0.1°K$
T_{hw}	$\pm 0.1°K$
$P_{tankcool}$	± 260 Pa
P_{bar}	± 130 Pa
P_{kiel}	± 260 Pa

The uncertainty interval for the effectiveness was calculated for three different combinations of U_∞, Tu, B, and x/d. Uncertainty intervals along with the respective combination of parameters are presented in the following table:

TABLE B-2. Uncertainty intervals for the effectiveness at specific locations and conditions

U_∞ (m/s)	Tu (%)	B	x/d	Uncertainty interval
18	17.8	1.75	10	0.008
37	12.2	0.25	50	0.015
10	7.3	0.25	5	0.021

Appendix C : Data Reduction Program

This Appendix contains the Q-Basic program used to perform cooling jet calculations,

main flow calculations and flow calculations at nozzle exit

```
DEC!ARE SUB Tempss (filename$, Pbar!, Thw!, PrAvg!(), Temp!(), Qconv!())
   DECLARE SUB FC (filename$, Pbar!, Tinf!, Tmpf!, TankTempF!, CoolTankTempF!, Temp!(), PrAvg!(), Cmnt2$, Twavg!, Tstat!, Tstatcool!,
   DECLARE FUNCTION Cp! (Temp!)
   DECLARE SUB StaAvg (filename$, Temp!(), chan!(), NTC3497%, NTC3852%)
   'Created by Dino Ishikura
   'Data reduction for TC
   LS : COLOR 11, 0
      CONST Rair = 287.074          'Gas constant for air J/(kg.K)
      CONST HgtoPa = 3386.4         'convert pressure from in_Hg to Pa
      CONST H2OtoPa = 248.7         'convert pressure from in_H2O to Pa
      CONST rec = .862
   OPTION BASE 1
   n% = 150                 ' Max number of thermocouple
   DIM chan(n%), Temp(n%), X(n%), Y(n%), Z(n%), Ttype(n%), Status(n%)
   DIM Qrad(n%), Qconv(n%)
   DIM PrVAvg(3), PrAvg(3)
   DIM StaTback(16), StaTsum(16), StaTavg(16), StaTCcount%(16), StaTcen(16)
   INPUT "Enter directory name <c:\filmcool\>: ", dirname$
   IF dirname$ = "" THEN
      'dir$ = "c:\filmcool\"
      dir$ = "c:\filmcool\v10\"
   ELSE
      dir$ = dirname$
   END IF
   dir$ = "c:\filmcool\3ht60_60\"

   INPUT "Enter initial file number: ", init%
   INPUT "Enter final file number: ", final%
   CLS : COLOR 14, 0
   PRINT "Main Menu"
   PRINT " 1 - Process temperature for spreadsheat     "
   PRINT " 2 - Process station temperature average     "
   PRINT " 3 - Process Film Cooling data               "
   INPUT "Select option #: ", opt%
   'opt% = 3
   INPUT "Enter output file name: ", outname$
   ou1% = FREEFILE
   OPEN dir$ + outname$ + ".dat" FOR OUTPUT AS #ou1%
   ou2% = FREEFILE
   OPEN dir$ + "f" + outname$ + ".dat" FOR OUTPUT AS #ou2%
   'sta% = 15
   sta% = 0
   FOR k% = init% TO final%
      'sta% = sta% - 1
      sta% = sta% + 1
      ans$ = LTRIM$(STR$(k%))
      filename$ = dir$ + ans$
      filein$ = filename$ + "hf.tcd"
      Unit% = FREEFILE
      OPEN filein$ FOR INPUT AS #Unit%
      DO
         IF NOT EOF(Unit%) THEN
            INPUT #Unit%, Title1$
'           WRITE Title1$
            INPUT #Unit%, Ftype%, Filnum, Id$, TIME1$, DATE1$, Cmnt1$, Cmnt2$
'           WRITE Ftype%, Filnum, Id$, TIME1$, DATE1$, Cmnt1$, Cmnt2$

            '
            ' /Exprm/  Experiment conditions
            '
            INPUT #Unit%, Pbar, Tinf, Jetdp, CoolJetdp, Tmpf, Probetemp, TankTempF, CoolTankTempF
'           WRITE Pbar, Tinf, Jetdp, CoolJetdp, Tmpf, Probetemp, TankTempF, CoolTankTempF

            '
            ' /PlateT/, /Table/  Heated plate data
            '
            INPUT #Unit%, NStations%, NperStation%, NTCtotal%, NTC3497%, NTC3852%
'           WRITE NStations%, NperStation%, NTCtotal%, NTC3497%, NTC3852%

            '
            ' /TC Temperature Data/
            '
            FOR indx% = 1 TO NTCtotal%
               INPUT #Unit%, chan(indx%), Temp(indx%), X(indx%), Y(indx%), Z(indx%), Ttype(indx%), Status(indx%), Qrad(indx%), Qconv(i
'              WRITE #Unit1%, chan(indx%), Temp(indx%), X(indx%), Y(indx%), Z(indx%), Ttype(indx%), Status(indx%), Qrad(indx%), Qconv
            NEXT indx%

            '
            ' /Pressure Data/
            '
            INPUT #Unit%, Title2$
            WRITE Title2$
            FOR i% = 1 TO 3
               INPUT #Unit%, PrVAvg(i%), PrAvg(i%)
'              WRITE PrVAvg(i%), PrAvg(i%)
            NEXT i%

            '
```

```
              ' /Heated table parameters/
              '
              INPUT #Unit%, Title3$
               WRITE Title3$

              INPUT #Unit%, PlateV, PlateArea, RShunt, ShuntV, TPlateAvg
               WRITE PlateV, PlateArea, RShunt, ShuntV, TPlateAvg
          ELSE
              EXIT DO
          END IF
       LOOP
       CLOSE #Unit%
       SELECT CASE opt%
          CASE 1
             CALL Tempss(filename$, Pbar, Tmpf, PrAvg(), Temp(), Qconv())
          CASE 2
             CALL StaAvg(filename$, Temp(), chan(), NTC3497%, NTC3852%)
          CASE 3
             'CALL FC(filename$, Pbar, Tinf, Tmpf, TankTempF, CoolTankTempF, Temp(), PrAvg(), Cmnt2$, eta, sta%)
             CALL FC(filename$, Pbar, Tinf, Tmpf, TankTempF, CoolTankTempF, Temp(), PrAvg(), Cmnt2$, Tw, Tinf, Tcool, eta, sta%)
             'xd = ((sta% - 1) * 3.63 + 83.31) / 2.54
             'IF sta% = 0 THEN eta = 0
             'PRINT #ou1%, filename$, xd, eta
             PRINT #ou1%, filename$, Tw, Tinf, Tcool, eta
             PRINT #ou2%, sta%, Tinf
          CASE ELSE: BEEP
       END SELECT
    END IF
  NEXT k%
  CLOSE #ou1%, #ou2
  BEEP: PRINT : PRINT ">>>> DONE <<<<"
  END


FUNCTION Cp (Temp)
    ' Curve fit using:   Tmin = 250 K
    '                    Tmax = 500 K
    '                    Reference: Table A.1 (Kays/Crawford)
    Cp = 1022! - .167572 * Temp + .000360722# * Temp * Temp
END FUNCTION


SUB FC (filename$, Pbar, Tinf, Tmpf, TankTempF, CoolTankTempF, Temp(), PrAvg(), Cmnt2$, Twavg, Tstat, Tstatcool, eta, sta%)

     Ptankmain1 = PrAvg(1)
        IF Ptankmain1 < 0 THEN Ptankmain1 = 0
     PKiel1 = PrAvg(2)
        IF PKiel1 < 0 THEN PKiel1 = 0
     Ptankcool1 = PrAvg(3)
        IF Ptankcool1 > .2 THEN
           CD = .66 - .1532 / Ptankcool1 + .01634 / (Ptankcool1 * Ptankcool1)
        ELSE
           Ptankcool1 = 0
           CD = 0
        END IF

     'Convert pressure from inH2O to Pascal
     Pbar = Pbar * HgtoPa
     Ptankmain = Ptankmain1 * H2OtoPa
     Pkiel = PKiel1 * H2OtoPa
     Ptankcool = Ptankcool1 * H2OtoPa

     'rename to mneumonic temperature names
     Thw1 = Tmpf
     Ttanklarge1 = TankTempF
     Ttankcool1 = CoolTankTempF
     Tceiling1 = Tinf

     'Convert temperature from deg Farenheit to deg Kelvin
     Thw = (Thw1 - 32) / 1.8 + 273.15
     Ttanklarge = (Ttanklarge1 - 32) / 1.8 + 273.15
     Ttankcool = (Ttankcool1 - 32) / 1.8 + 273.15
     Tceiling = (Tceiling1 - 32) / 1.8 + 273.15

     ' Cooling jet calculation
     Denstankcool = (Ptankcool + Pbar) / (Rair * Ttankcool)
     VjetcoolTheo = SQR(2! * Ptankcool / Denstankcool)
     Vjetcool = CD * VjetcoolTheo
     Tstatcool = Ttankcool - Vjetcool * Vjetcool / (2 * Cp(Ttankcool))
     Densjetcool = Pbar / (Rair * Tstatcool)
     Gcool = Densjetcool * Vjetcool

     ' Main flow calculation
     ' n iterations over main flow static temperature
     n% = 3
     Dens = Pbar / (Rair * Thw)
     Vel = SQR(2! * Pkiel / Dens)      'first approach
     Tstat = Thw - rec * Vel * Vel / (2 * Cp(Thw))

     FOR i% = 1 TO n%
```

```
            PkielSTP = Pkiel * (101325! / Pbar) * (Tstat / 288.15)
            Dens = Pbar / (Rair * Tstat)
            Vel = SQR(2! * PkielSTP / Dens)        'first approach
            Tstat = Thw - rec * Vel * Vel / (2 * Cp(Tstat))
        NEXT i%
        Ginf = Dens * Vel
        IF Ginf <> 0 THEN
            B = Gcool / Ginf
        ELSE
            B = 0
        END IF


        ' Flow calculation at nozzle exit
        Denstanklarge = (Pbar + Ptankmain) / (Rair * Ttanklarge)
        Velexit = SQR(2! * Ptankmain / Denstanklarge)        'first approach
        'INPUT "Enter TC station #: ", sta%
        PRINT filename$
        ou% = FREEFILE
        OPEN filename$ + "fc.dat" FOR OUTPUT AS #ou%
        IF sta% = 0 THEN
            WRITE #ou%, Pbar / HgtoPa, DATE$, TIME$
            PRINT #ou%, "              Lge Tank     Cool Tank   NozExit  Infinity    Cool jet    "
            PRINT #ou%, USING "Pressure (inH2O)    #.##        #.##                      #.##        #.##"; Ptankmain1; Ptankcool1; PKiel1; Pt
            PRINT #ou%, USING "Temperature (K)   ###.##       ###.##                   ###.##     ###.##"; Ttanklarge; Ttankcool; Tstat; Tsta
            PRINT #ou%, USING "Density (kg/m^3)   #.###        #.###                    #.###      #.###"; Denstanklarge; Denstankcool; Dens
            PRINT #ou%, USING "Velocity (m/s)                             ##.##        ##.##       ##.##"; Velexit; Vel; Vjetcool
            PRINT #ou%, USING "Discharge Coefficient = #.### "; CD
            PRINT #ou%, USING "Gcool       = ###.## kg.m/s     Ginf        = ###.## kg.m/s  "; Gcool; Ginf
            PRINT #ou%, USING "Blowing ratio = #.## "; B
        ELSE
            PRINT #ou%, Cmnt2$
            WRITE #ou%, Pbar / HgtoPa, DATE$, TIME$
            PRINT #ou%,
            PRINT #ou%, "Station Temperature in deg. Farenheit"
            Twavg = 0: n% = 0
            FOR i% = 1 TO 7
                PRINT #ou%, Temp((sta% - 1) * 8 + i%);
                T = Temp((sta% - 1) * 8 + i%)
                IF T > 32 AND T < 120 THEN
                    Twavg = Twavg + Temp((sta% - 1) * 8 + i%)
                    n% = n% + 1
                ELSE
                    Temp((sta% - 1) * 8 + i%) = 0
                END IF
            NEXT i%
            PRINT #ou%,
            IF n% <> 0 THEN Twavg = (Twavg / n% + 459.95) / 1.8     'Kelvin
            'PRINT #ou%, Cmnt2$
            'WRITE #ou%, Pbar / HgtoPa, DATE$, TIME$
            'PRINT #ou%,
            PRINT #ou%, "Station "; sta%; " - Avg wall temperature = "; Twavg
            PRINT #ou%, "Static Flow Temp = "; Tstat
            PRINT #ou%, "Static cool jet Temp = "; Tstatcool
            eta = (Twavg - Tstat) / (Tstatcool - Tstat)
            PRINT #ou%, USING "FC effectiveness = ###.### %"; eta * 100
            PRINT #ou%,
            PRINT #ou%, "; Lge; Tank; Cool; Tank; NozExit; Infinity; Cool; jet; "; ""
            PRINT #ou%, USING "Pressure (inH2O)    #.##        #.##                      #.##        #.##"; Ptankmain1; Ptankcool1; PKiel1; Pt
            PRINT #ou%, USING "Temperature (K)   ###.##       ###.##                   ###.##     ###.##"; Ttanklarge; Ttankcool; Tstat; Tsta
            PRINT #ou%, USING "Density (kg/m^3)   #.###        #.###                    #.###      #.###"; Denstanklarge; Denstankcool; Dens
            PRINT #ou%, USING "Velocity (m/s)                             ##.##        ##.##       ##.##"; Velexit; Vel; Vjetcool
            PRINT #ou%, USING "Discharge Coefficient = #.### "; CD
        END IF

    CLOSE #ou%
END SUB

    SUB StaAvg (filename$, Temp(), chan(), NTC3497%, NTC3852%)
    DIM StaTback(16), StaTsum(16), StaTavg(16), StaTCcount%(16), StaTcen(16)
    fileout$ = filename$ + "hwT.dat"
    Unit1% = FREEFILE
    PRINT " >> processing ", filename$
    OPEN fileout$ FOR OUTPUT AS #Unit1%

    Tlow = 32
    Thigh = 200
    Xlimit = 100
    NTCtotal% = NTC3497% + NTC3852%

    FOR i% = 1 TO 16
        StaTCcount%(i%) = 0
        StaTsum(i%) = 0
    NEXT i%

    '
    ' Calculate Station Average Temperature. First thermocouples were
    ' classified by station number. It was selected SELECT CASE command
    ' insteady of formula in order to be more flexible to change HP
```

```basic
          ' channel number.
          FOR indx% = 1 TO NTC3497%      ' NTC3852%
              IF Temp(indx%) > Tlow AND Temp(indx%) < Thigh THEN
                  SELECT CASE chan(indx%)
                      CASE 0 TO 6: sta% = 1
                      CASE 8 TO 14: sta% = 2
                      CASE 16 TO 22: sta% = 3
                      CASE 24 TO 30: sta% = 4
                      CASE 32 TO 38: sta% = 5
                      CASE 40 TO 46: sta% = 6
                      CASE 48 TO 54: sta% = 7
                      CASE 56 TO 62: sta% = 8
                      CASE 64 TO 70: sta% = 9
                      CASE 72 TO 78: sta% = 10
                      CASE 80 TO 86: sta% = 11
                      CASE 88 TO 94: sta% = 12
                      CASE 7: StaTback(1) = Temp(indx%): GOTO ignore1
                      CASE 15: StaTback(2) = Temp(indx%): GOTO ignore1
                      CASE 23: StaTback(3) = Temp(indx%): GOTO ignore1
                      CASE 31: StaTback(4) = Temp(indx%): GOTO ignore1
                      CASE 39: StaTback(5) = Temp(indx%): GOTO ignore1
                      CASE 47: StaTback(6) = Temp(indx%): GOTO ignore1
                      CASE 55: StaTback(7) = Temp(indx%): GOTO ignore1
                      CASE 63: StaTback(8) = Temp(indx%): GOTO ignore1
                      CASE 71: StaTback(9) = Temp(indx%): GOTO ignore1
                      CASE 79: StaTback(10) = Temp(indx%): GOTO ignore1
                      CASE 87: StaTback(11) = Temp(indx%): GOTO ignore1
                      CASE 95: StaTback(12) = Temp(indx%): GOTO ignore1
                      CASE ELSE: GOTO ignore1
                  END SELECT
                  StaTCcount%(sta%) = StaTCcount%(sta%) + 1
                  StaTsum(sta%) = StaTsum(sta%) + Temp(indx%)
              END IF
ignore1:
          NEXT indx%

          FOR indx% = NTC3497% + 1 TO NTCtotal%
              IF Temp(indx%) > Tlow AND Temp(indx%) < Thigh THEN
                  SELECT CASE chan(indx%)
                      CASE 0 TO 6: sta% = 13
                      CASE 8 TO 14: sta% = 14
                      CASE 16 TO 19, 100 TO 102: sta% = 15
                      CASE 104 TO 110: sta% = 16
                      CASE 7: StaTback(13) = Temp(indx%): GOTO ignore2
                      CASE 15: StaTback(14) = Temp(indx%): GOTO ignore2
                      CASE 103: StaTback(15) = Temp(indx%): GOTO ignore2
                      CASE 111: StaTback(16) = Temp(indx%): GOTO ignore2
                      CASE ELSE: GOTO ignore2
                  END SELECT
                  StaTCcount%(sta%) = StaTCcount%(sta%) + 1
                  StaTsum(sta%) = StaTsum(sta%) + Temp(indx%)
              END IF
ignore2:
          NEXT indx%

'     PRINT "i%, StaTsum(i%), StaTCcount%(i%), StaTavg(i%), StaTcen(i%), StaTback(i%)"
      FOR i% = 1 TO 16
          StaTavg(i%) = StaTsum(i%) / StaTCcount%(i%)
          StaTcen(i%) = Temp((i% - 1) * 8 + 4)
          'WRITE i%, StaTsum(i%), StaTCcount%(i%), StaTavg(i%), StaTcen(i%), StaTback(i%)
          'WRITE #Unit1%, i%, StaTsum(i%), StaTCcount%(i%), StaTavg(i%), StaTcen(i%), StaTback(i%)
          WRITE #Unit1%, i%, StaTavg(i%), StaTcen(i%), StaTback(i%)
      NEXT i%
      CLOSE #Unit1%
END SUB

    SUB Tempss (filename$, Pbar, Thw, PrAvg(), Temp(), Qconv())
    Pkiel = PrAvg(3) * H2OtoPa
    Pbar = Pbar * HgtoPa
    Thw = (Thw - 32) / 1.8 + 273.15

    fileout$ = filename$ + "hfT.prn"
    Unit1% = FREEFILE
    LOCATE 10, 1: PRINT " >> processing ", filename$

    OPEN fileout$ FOR OUTPUT AS #Unit1%

    Tlow = 32
    Thigh = 200
    Xlimit = 100
      rint Temperature to a file in 16 columns
     R i% = 1 TO 8
      'PRINT i% - 4;
      PRINT #Unit1%, i% - 4;
      FOR j% = 1 TO 16
          indx% = (j% - 1) * 8 + i%
          IF Temp(indx%) > Tlow AND Temp(indx%) < Thigh THEN
              'PRINT Temp(indx%); ",";
```

```
                PRINT #Unit1%, Temp(indx%); ",";
            ELSE
                'PRINT CHR$(34); CHR$(34); ",";
                PRINT #Unit1%, CHR$(34); CHR$(34); ",";
            END IF
        NEXT j%
        'PRINT
        PRINT #Unit1%,
    NEXT i%
    PRINT #Unit1%,

    'print Qconv to a file in 16 columns
    FOR i% = 1 TO 8
        'PRINT i% - 4;
        PRINT #Unit1%, i% - 4;
        FOR j% = 1 TO 16
            indx% = (j% - 1) * 8 + i%
            IF Temp(indx%) > Tlow AND Temp(indx%) < Thigh THEN
                'PRINT Temp(indx%); ",";
                PRINT #Unit1%, Qconv(indx%); ",";
            ELSE
                'PRINT CHR$(34); CHR$(34); ",";
                PRINT #Unit1%, CHR$(34); CHR$(34); ",";
            END IF
        NEXT j%
        'PRINT
        PRINT #Unit1%,
    NEXT i%
    Dens = Pbar / (Rair * Thw)
    Vel = SQR(2 * Pkiel / Dens)         'first approach
    Tstat = Thw - rec * Vel * Vel / (2 * Cp(Thw))
    PkielSTP = Pkiel * (101325 / Pbar) * (Tstat / 288.15)
    Dens = Pbar / (Rair * Tstat)
    Vel = SQR(2 * PkielSTP / Dens)
    Tstat = Thw - rec * Vel * Vel / (2 * Cp(Tstat))
    WRITE #Unit1%, Vel, Tstat

    CLOSE #Unit1%
END SUB
```

Appendix D : Free stream recovery temperature reconstruction

The free stream recovery temperature, $T_{r\infty}$, was reconstructed using the total temperature (plenum temperature) and free stream velocity values. This reconstruction was necessary because the thermocouple used to measure the free stream recovery temperature was placed too close to the coolant stream and the temperature registered was not that of the coolant stream but of a mixture of free stream air and coolant.

The velocity term contribution was subtracted from the total temperature measured in the plenum and later added after multiplying the term by the recovery factor as follows:

$$T_{r\infty(new)} = T_{\tan k} - \frac{U_{\infty}^{2}}{2C_{p}} + r\frac{U_{\infty}^{2}}{2C_{p}} \tag{D-1}$$

where

T_{tank} is the temperature measured inside the air supply plenum chamber

U_{∞} is the free stream velocity at each station

r is the recovery factor (0.862)

Effectiveness was recalculated with the new free stream recovery temperatures for every combination of Tu, B and U_{∞}. The new effectiveness values were more in the order of what was expected based on other research seen, than the effectiveness obtained with the measured $T_{r\infty}$ values.

Appendix E : Plots of Effectiveness with Film Cooling Parameters

This Appendix contains figures of effectiveness with X/D and effectiveness with B for the combinations of Tu, B and U_∞ not directly referenced in the main document. Figures are arranged by ascending order of free stream velocity at injection value first, and blowing ratio or station location second.
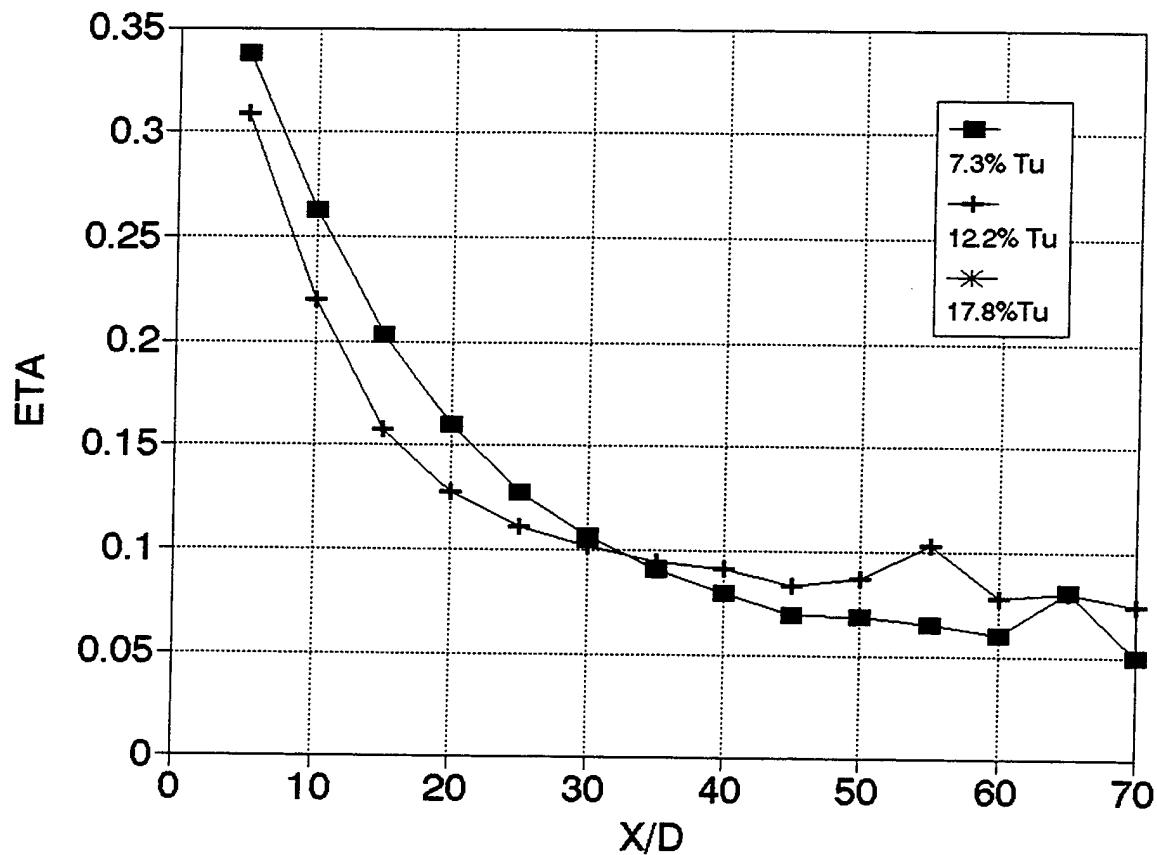
Figure E-1. Effect of Free Stream Turbulence on Film Cooling Effectiveness
B = 0.25, Free stream velocity at injection = 10 m/s
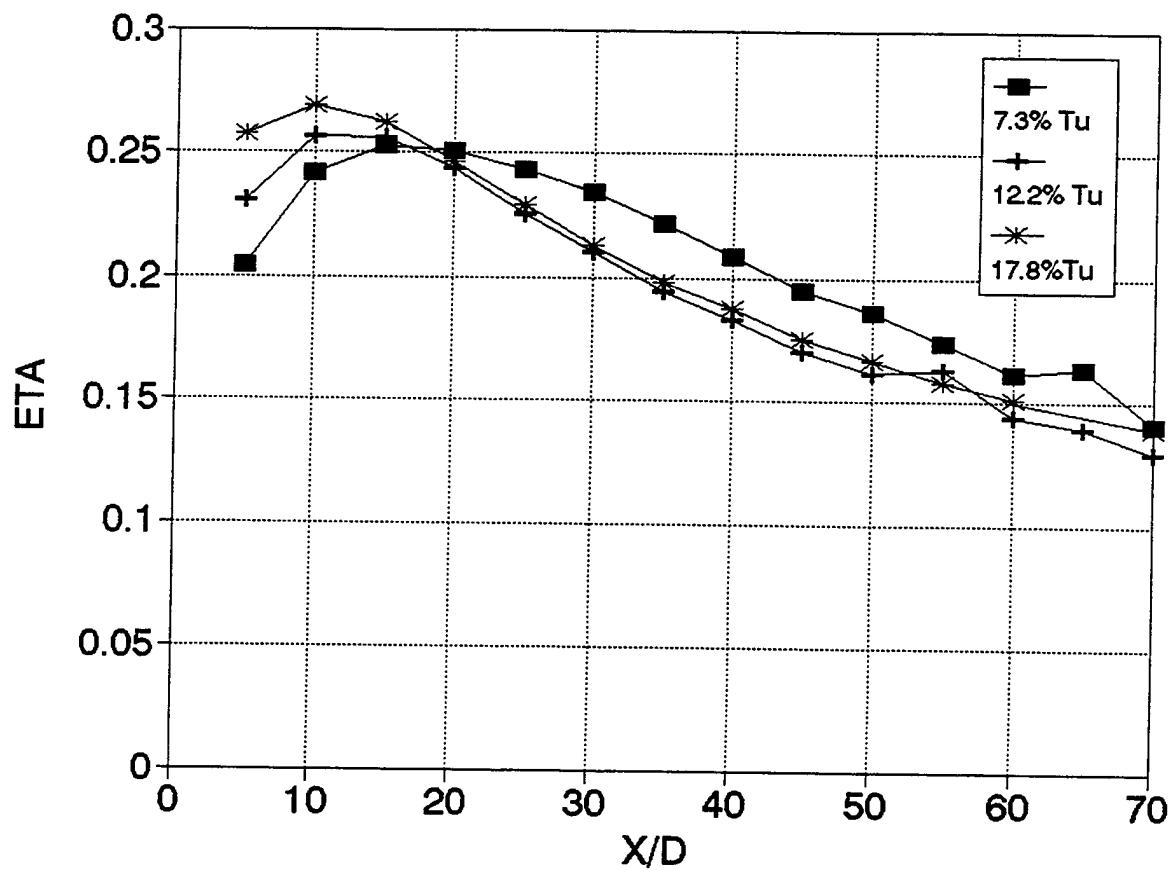
Figure E-2. Effect of Free Stream Turbulence on Film Cooling Effectiveness
B = 1.50, Free stream velocity at injection = 10 m/s
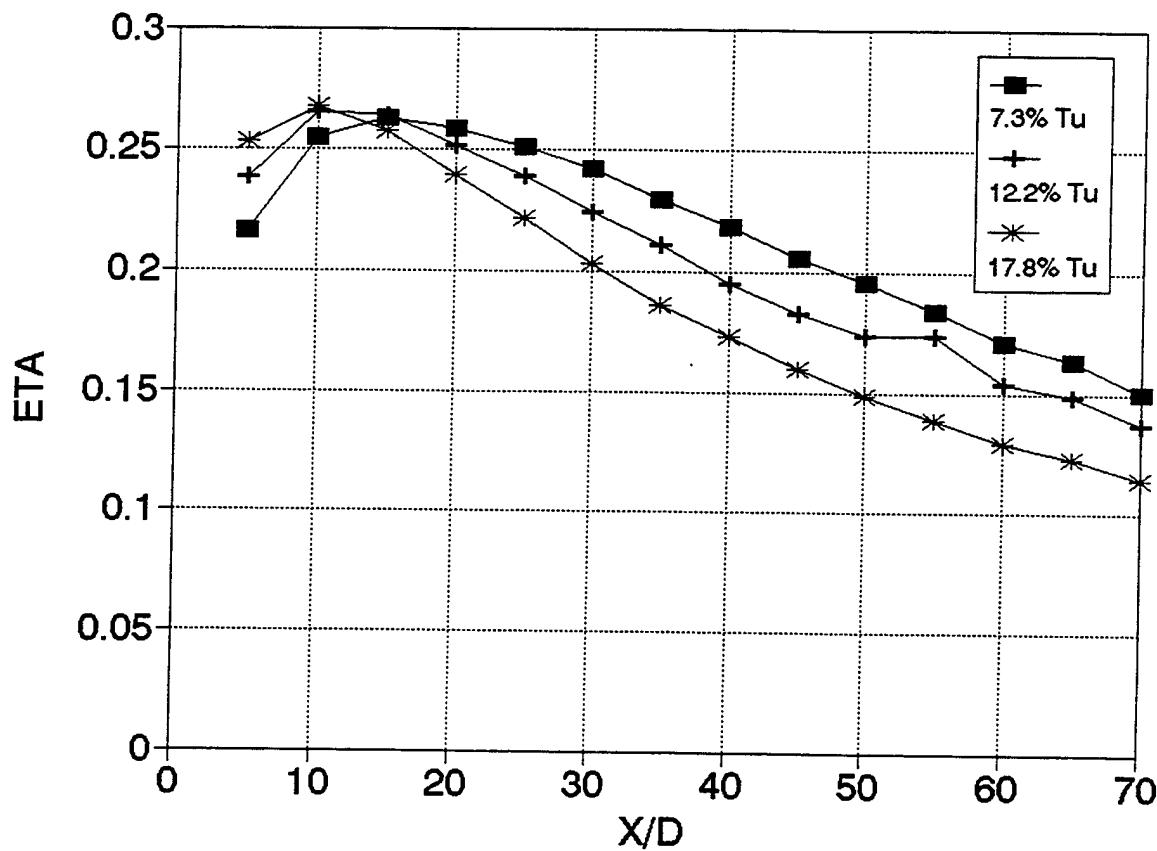
Figure E-3. Effect of Free Stream Turbulence on Film Cooling Effectiveness
B = 1.75, Free stream velocity at injection = 10 m/s
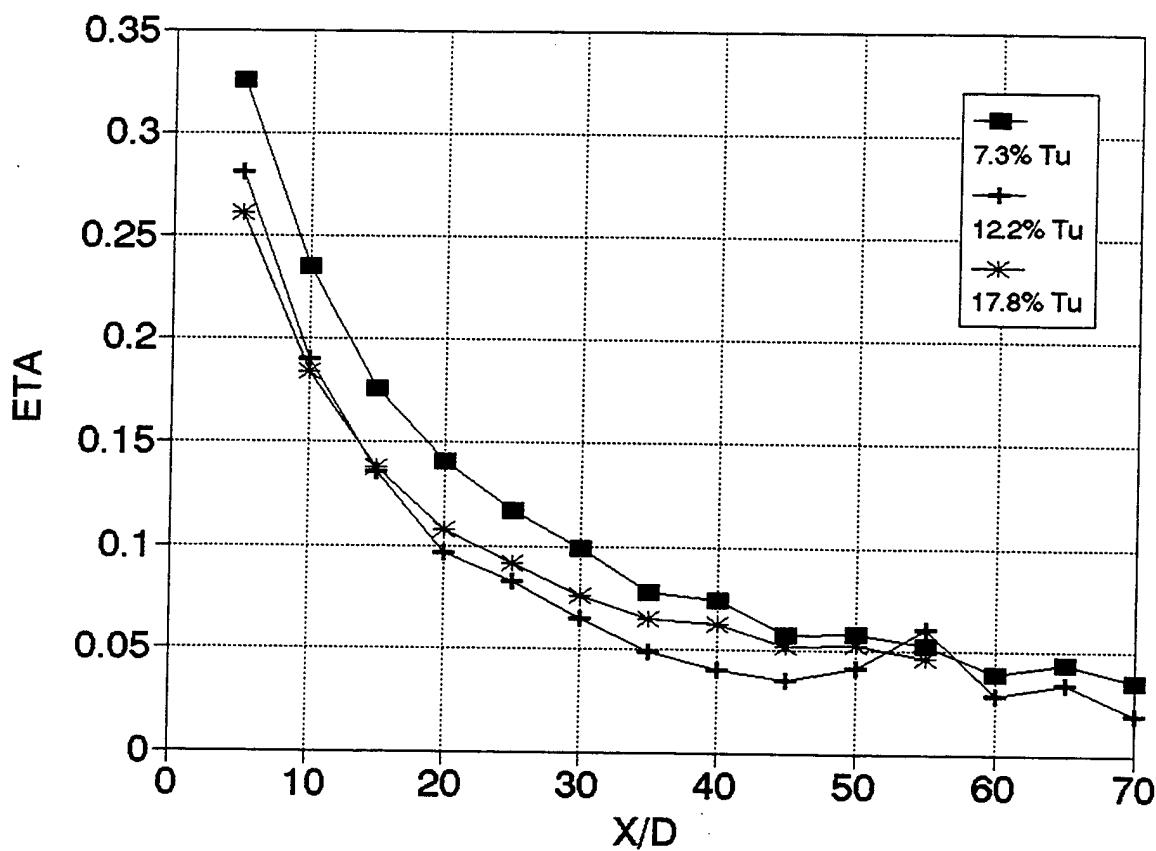
Figure E-4. Effect of Free Stream Turbulence on Film Cooling Effectiveness
B = 0.25, Free stream velocity at injection = 18 m/s
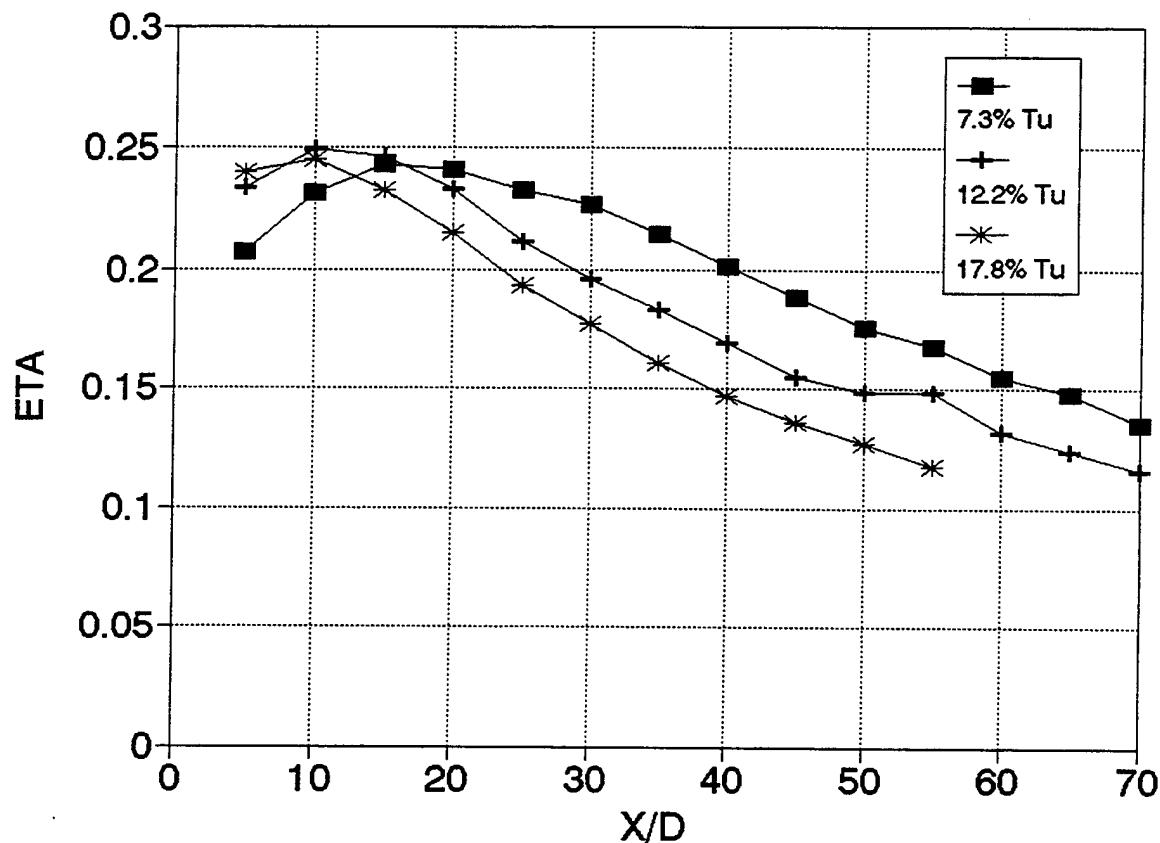
Figure E-5. Effect of Free Stream Turbulence on Film Cooling Effectiveness
B = 1.25, Free stream velocity at injection = 18 m/s
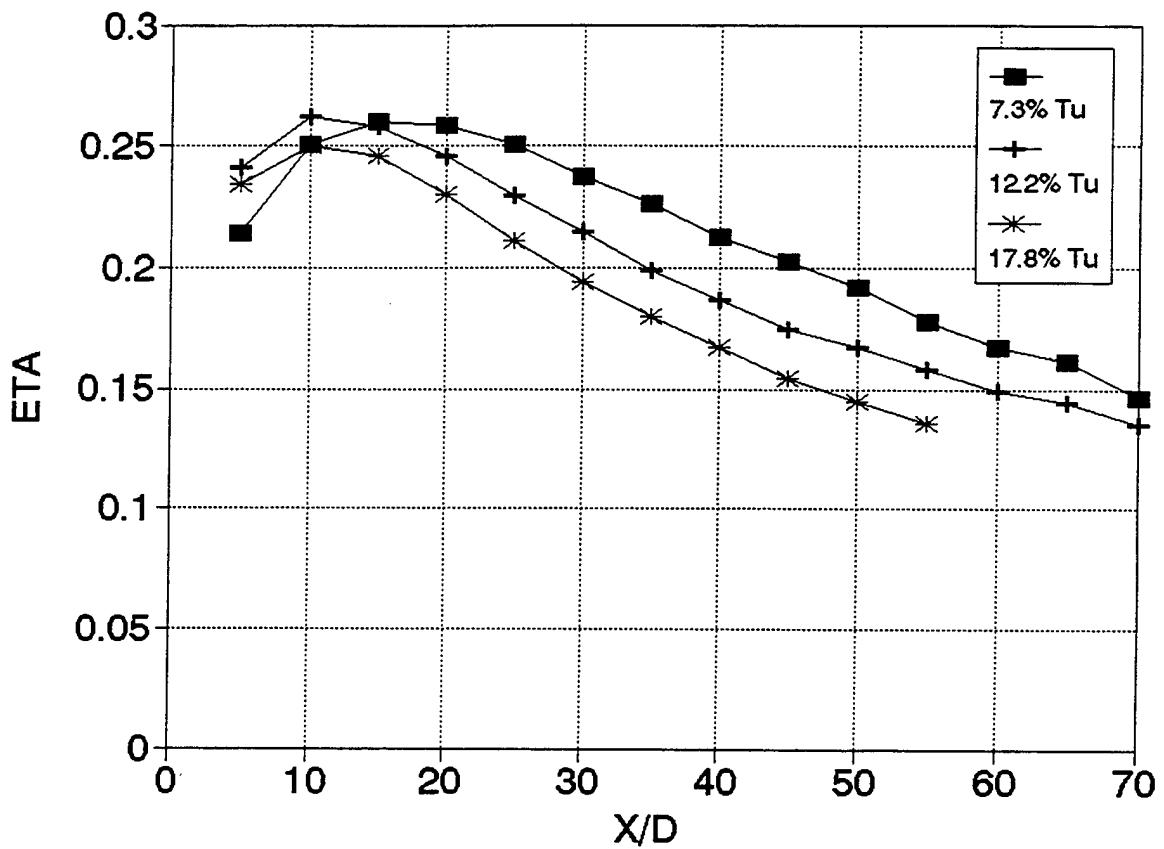
Figure E-6. Effect of Free Stream Turbulence on Film Cooling Effectiveness
B = 1.50, Free stream velocity at injection = 18 m/s
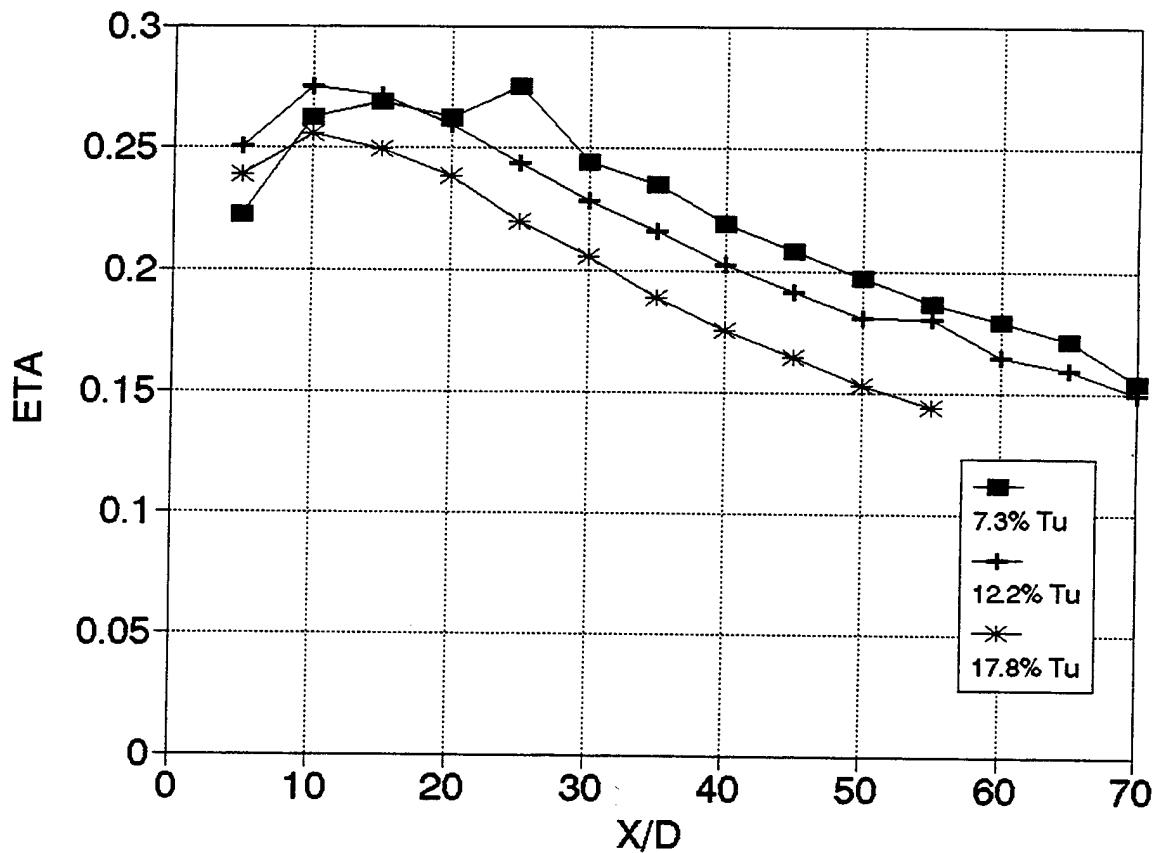
Figure E-7. Effect of Free Stream Turbulence on Film Cooling Effectiveness
B = 1.75, Free stream velocity at injection = 18 m/s
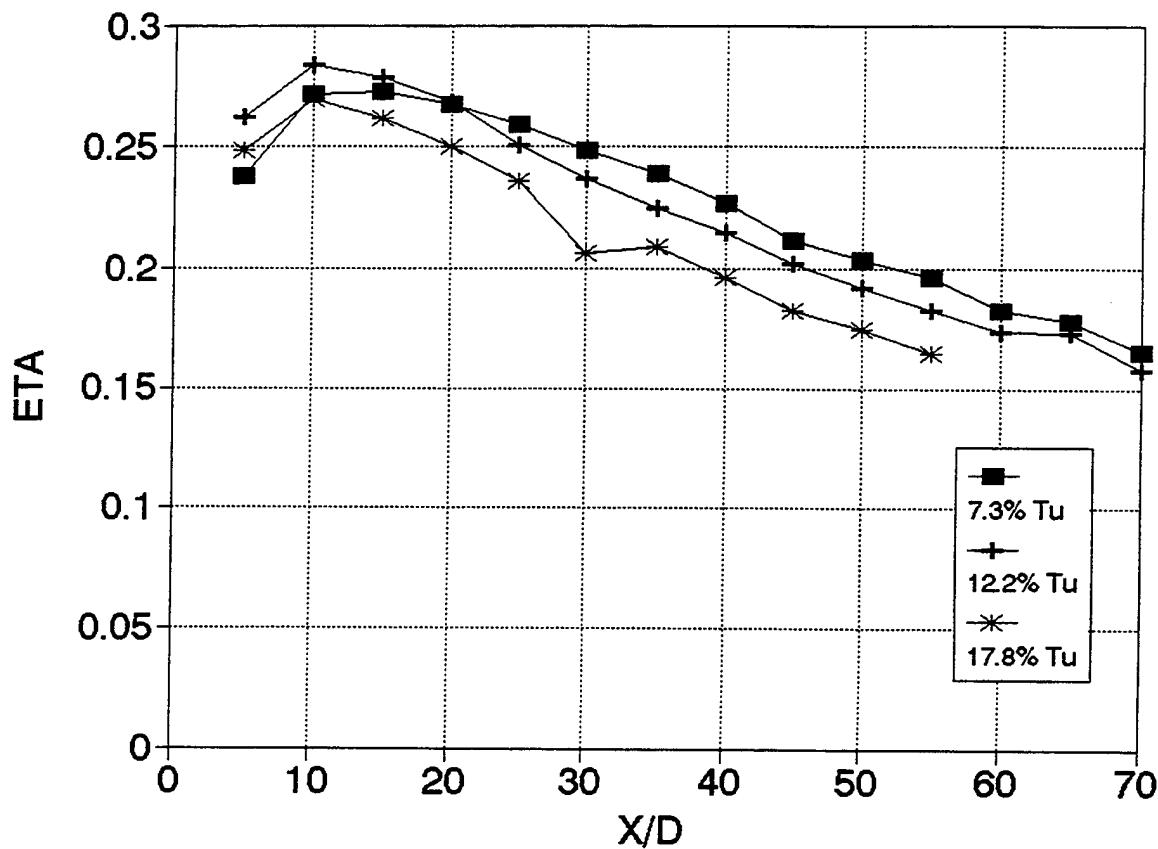
Figure E-8. Effect of Free Stream Turbulence on Film Cooling Effectiveness
B = 2.0, Free stream velocity at injection = 18 m/s
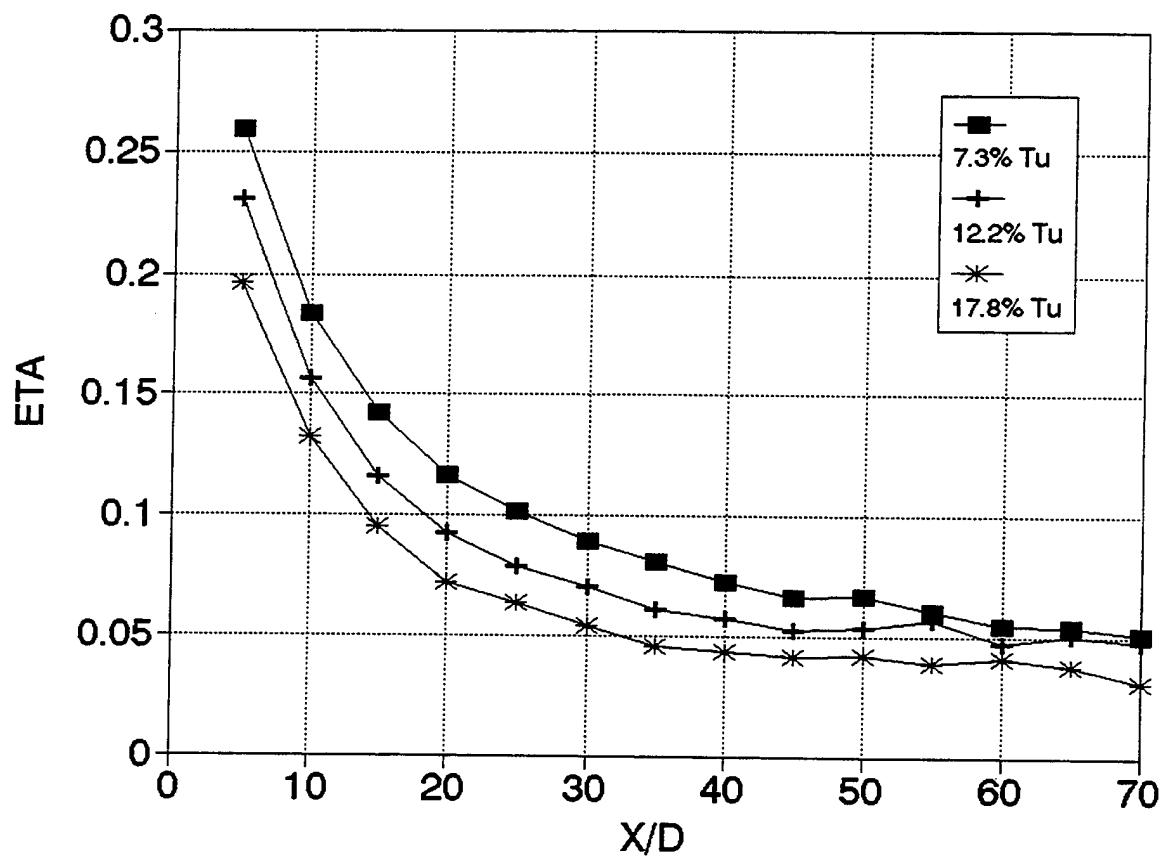
Figure E-9. Effect of Free Stream Turbulence on Film Cooling Effectiveness
B = 0.25, Free stream velocity at injection = 60 m/s
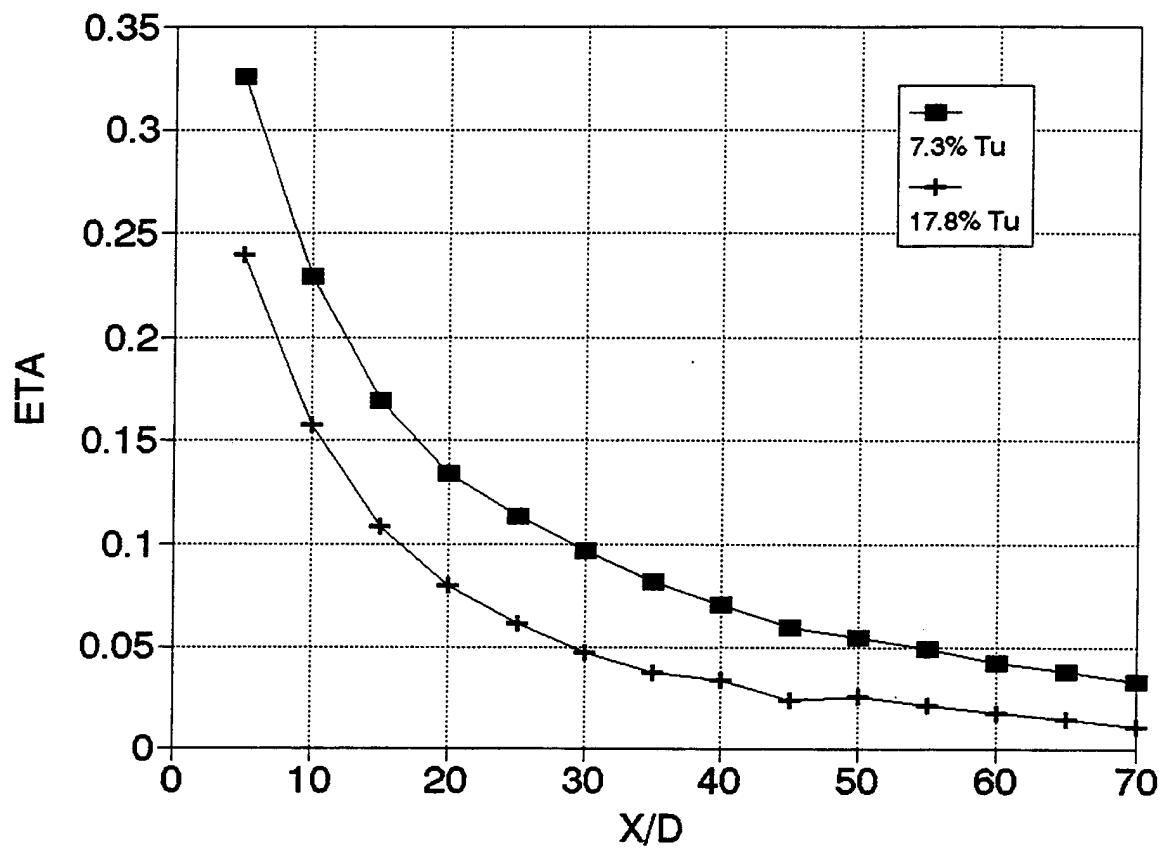
Figure E-10. Effect of Free Stream Turbulence on Film Cooling Effectiveness
B = 0.35, Free stream velocity at injection = 60 m/s
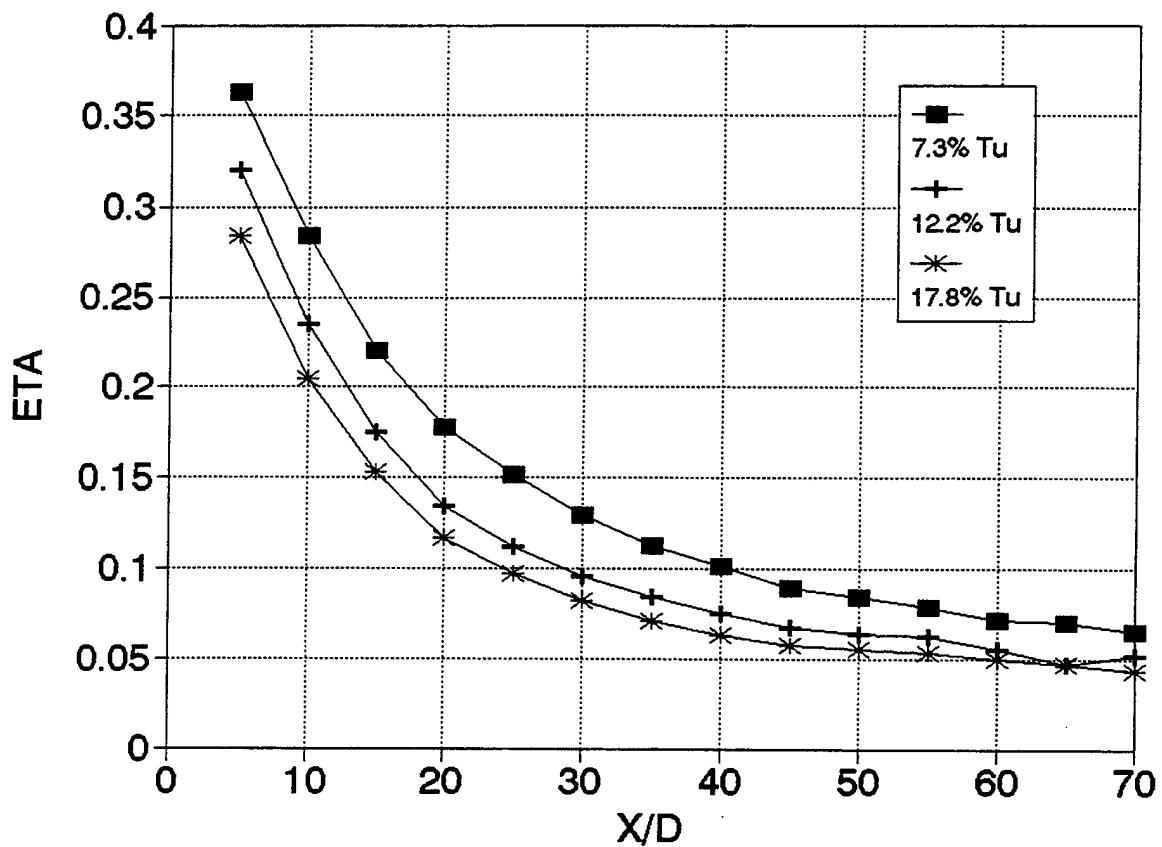
Figure E-11. Effect of Free Stream Turbulence on Film Cooling Effectiveness
B = 0.50, Free stream velocity at injection = 60 m/s
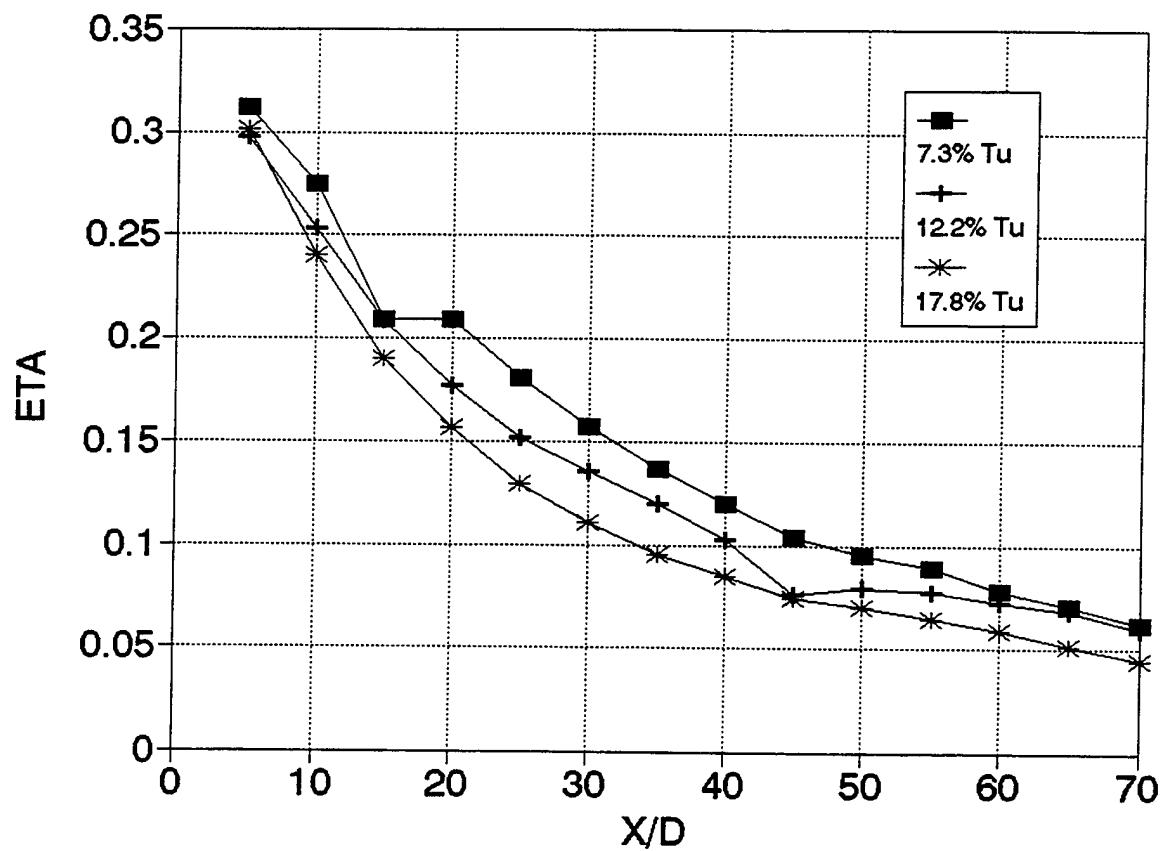
Figure E-12. Effect of Free Stream Turbulence on Film Cooling Effectiveness
B = 0.68, Free stream velocity at injection = 60 m/s
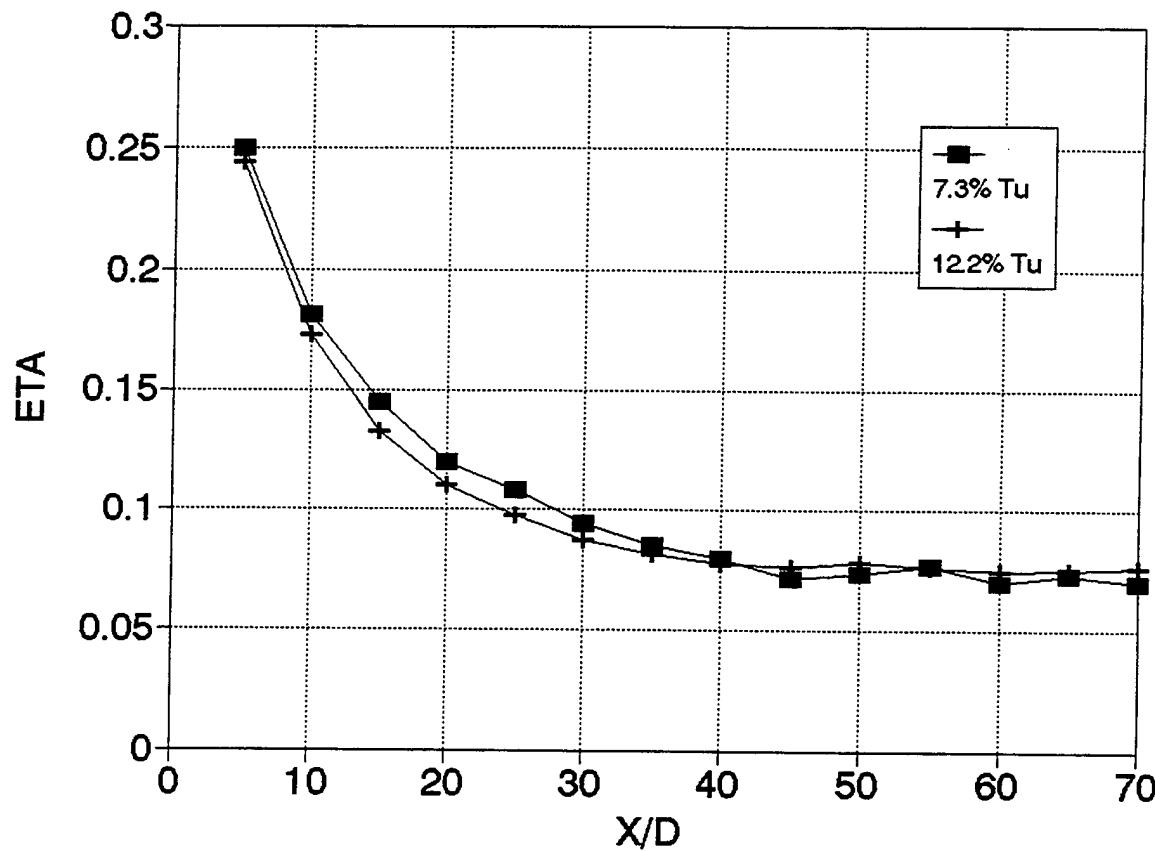
Figure E-13. Effect of Free Stream Turbulence on Film Cooling Effectiveness
B = 0.25, Free stream velocity at injection = 85 m/s
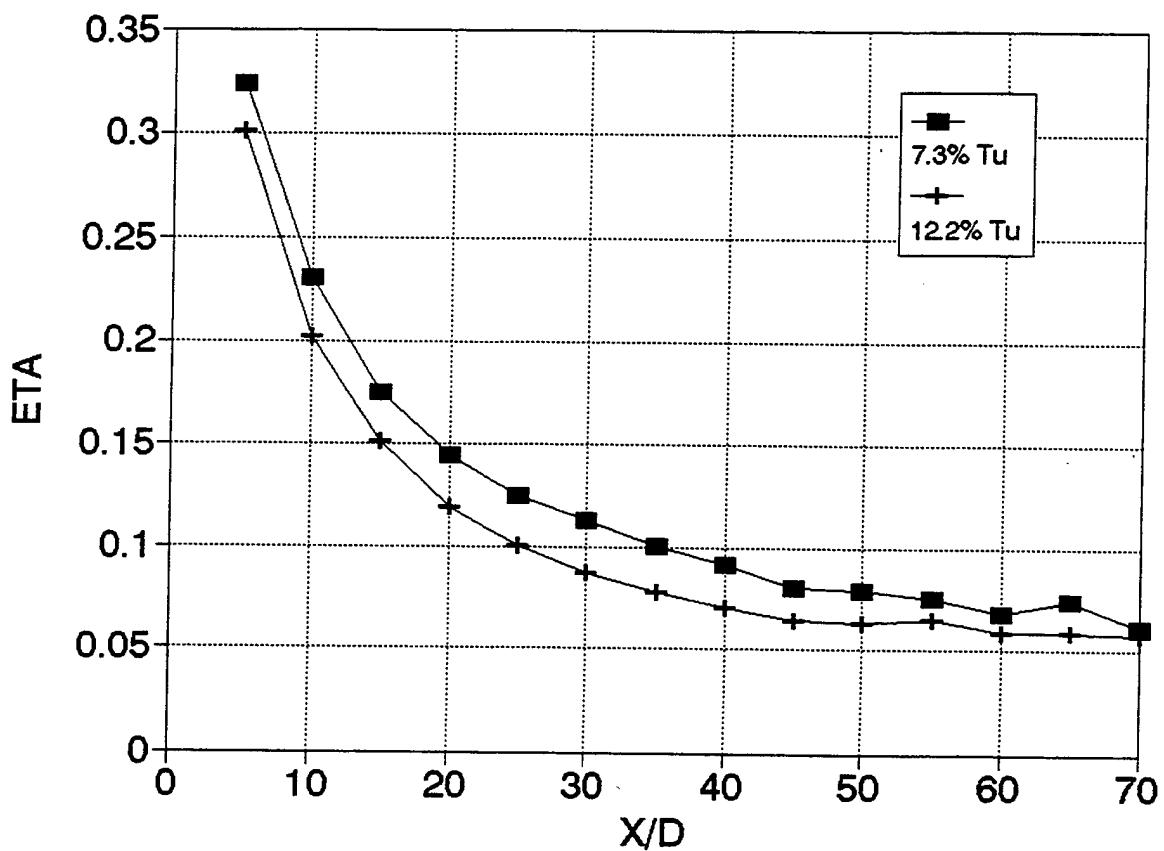
Figure E-14. Effect of Free Stream Turbulence on Film Cooling Effectiveness
B = 0.35, Free stream velocity at injection = 85 m/s
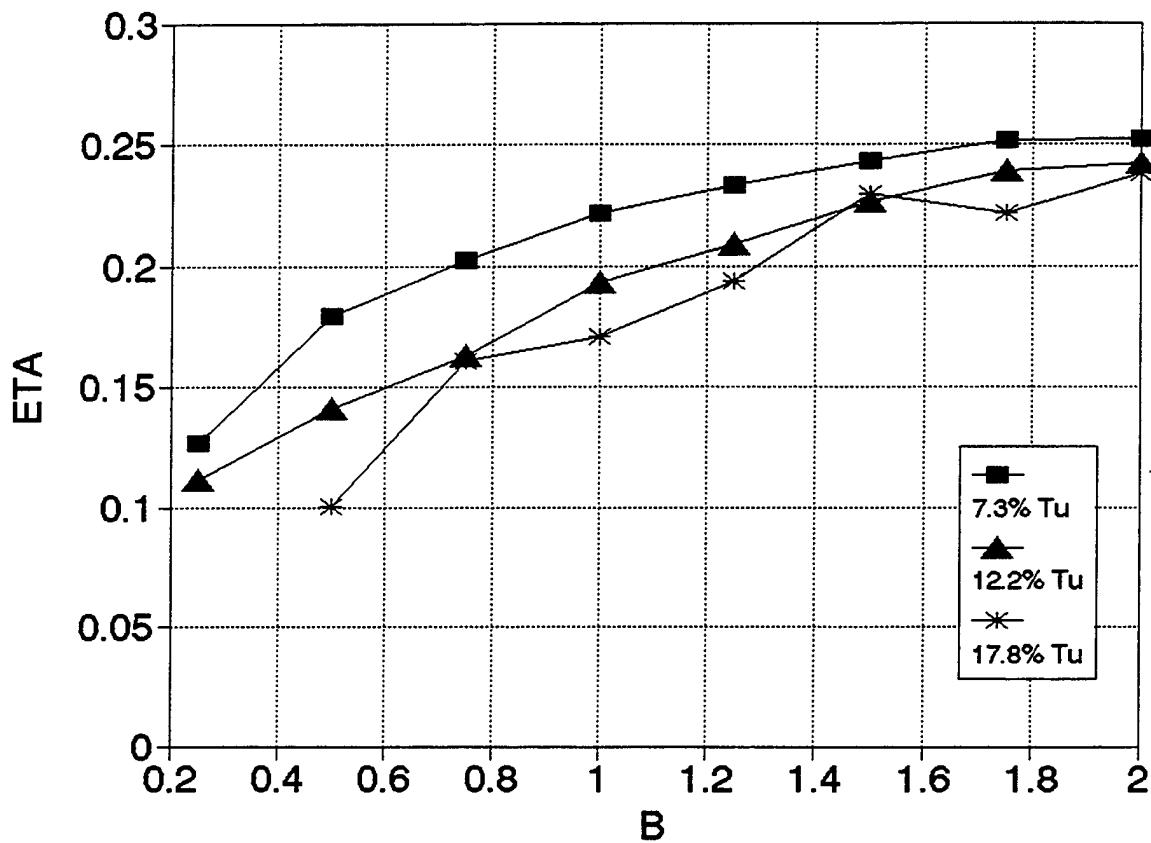
Figure E-15. Effect of Free Stream Turbulence on Film Cooling Effectiveness
X/D = 25, Free stream velocity at injection = 10 m/s
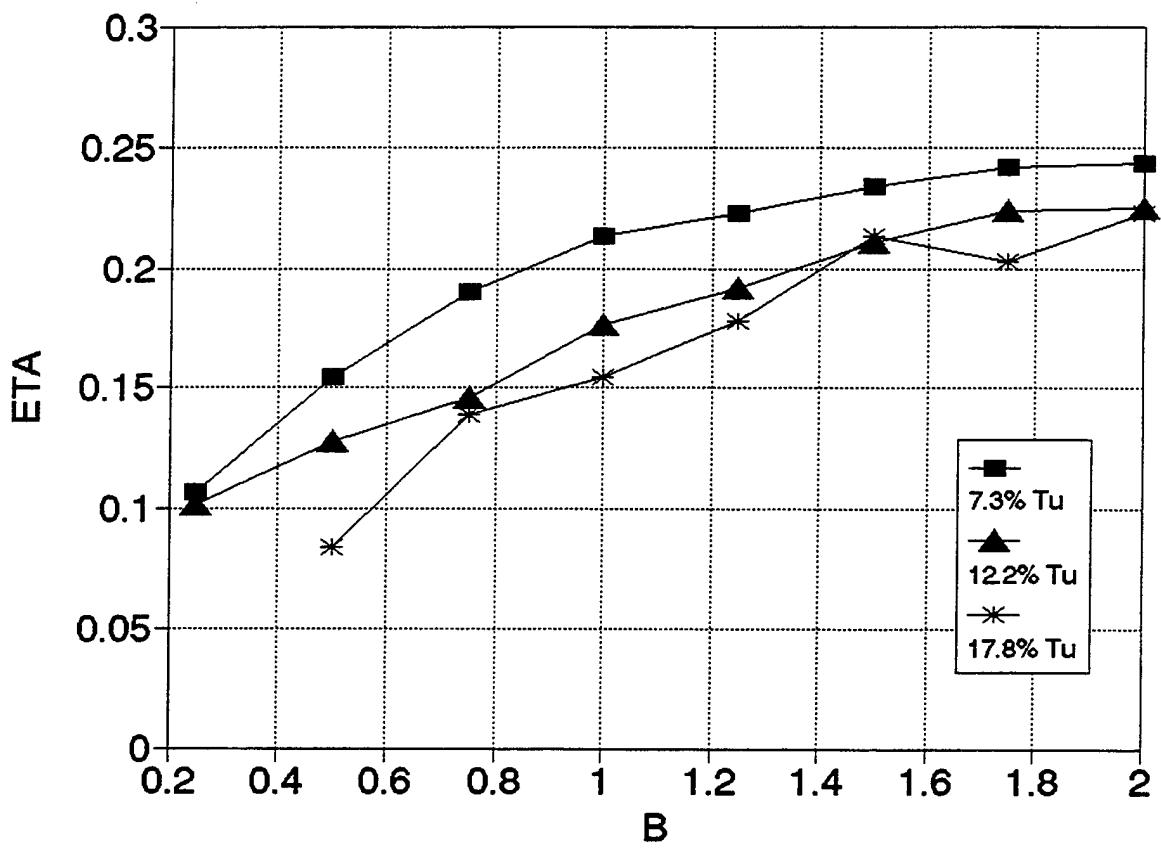
Figure E-16. Effect of Free Stream Turbulence on Film Cooling Effectiveness
X/D = 30, Free stream velocity at injection = 10 m/s
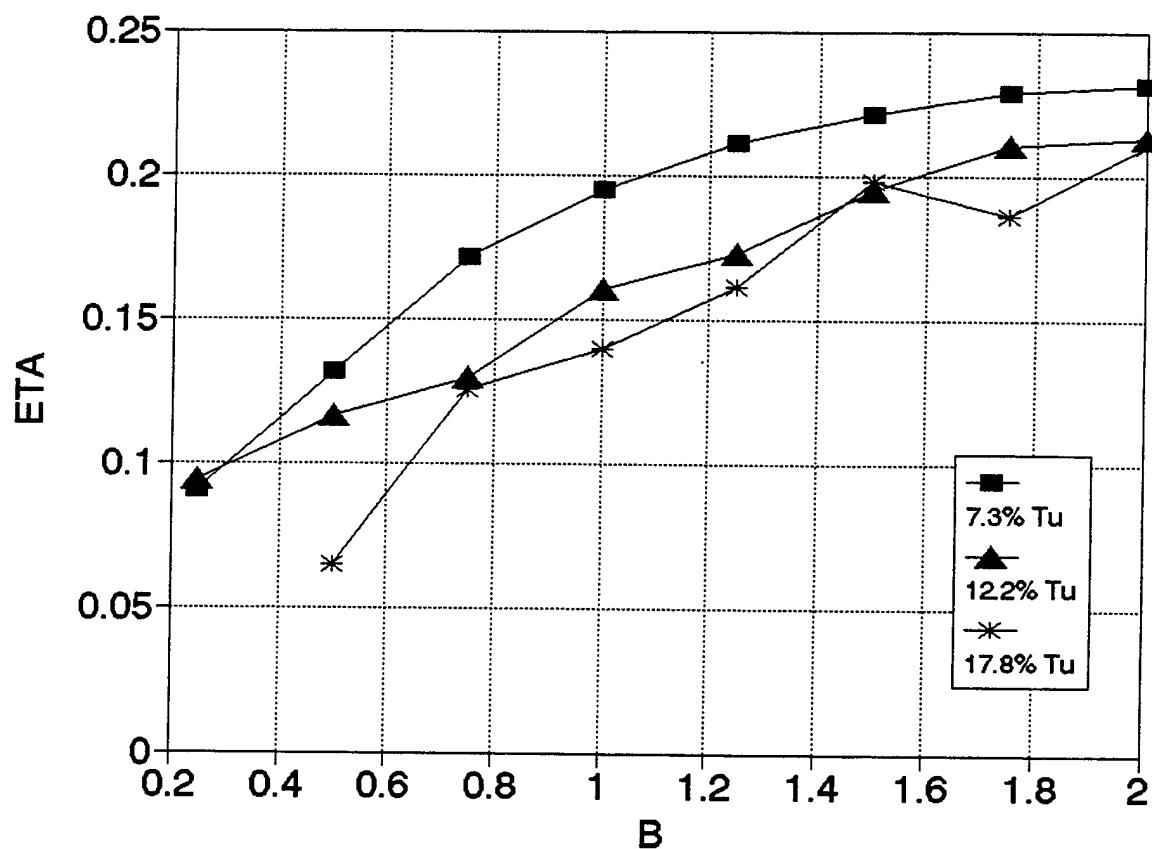
Figure E-17. Effect of Free Stream Turbulence on Film Cooling Effectiveness
X/D = 35, Free stream velocity at injection = 10 m/s
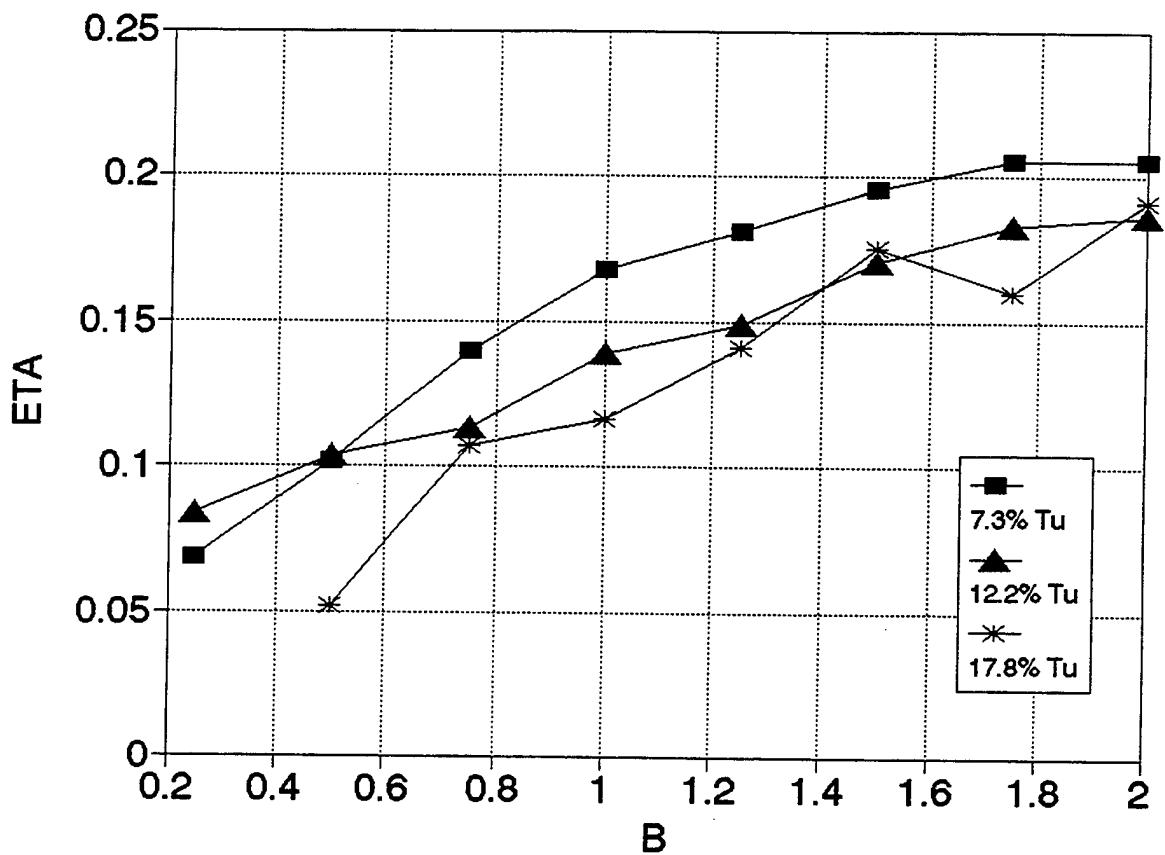
Figure E-18. Effect of Free Stream Turbulence on Film Cooling Effectiveness
X/D = 45, Free stream velocity at injection = 10 m/s
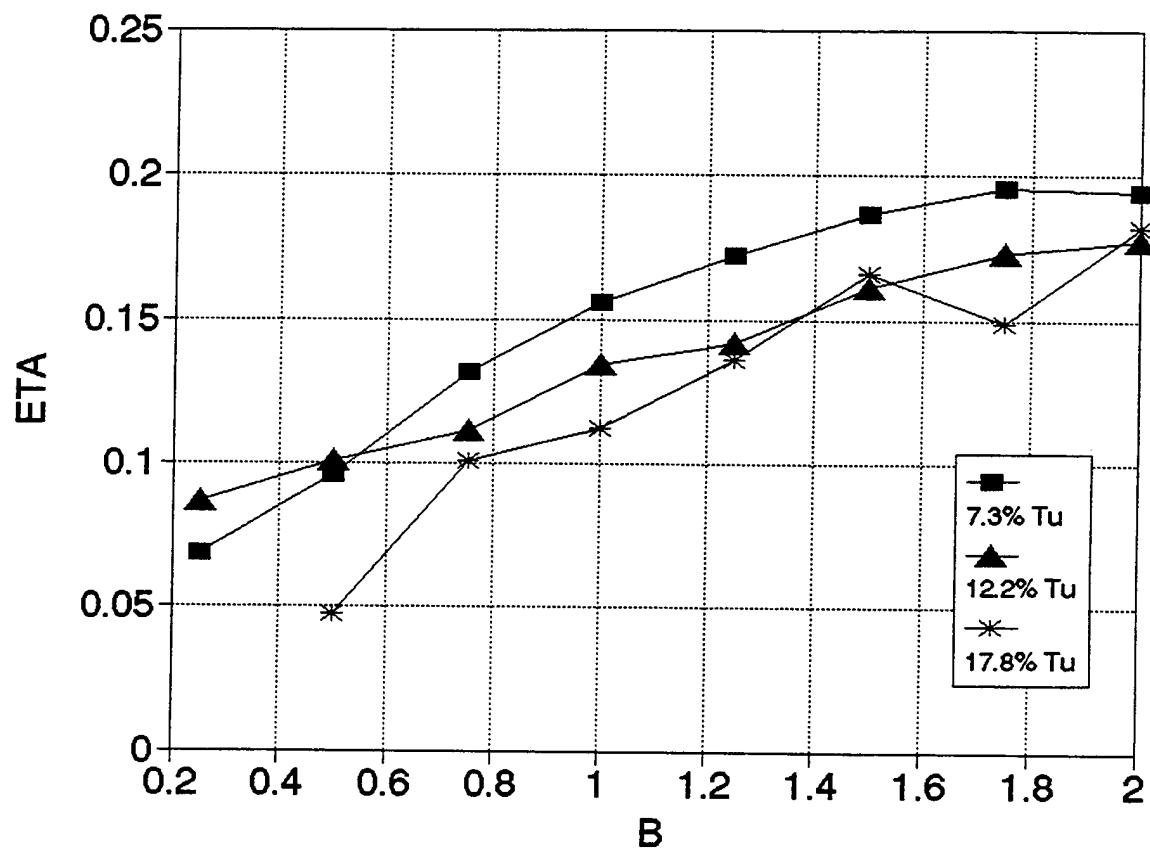
Figure E-19. Effect of Free Stream Turbulence on Film Cooling Effectiveness
X/D = 50, Free stream velocity at injection = 10 m/s
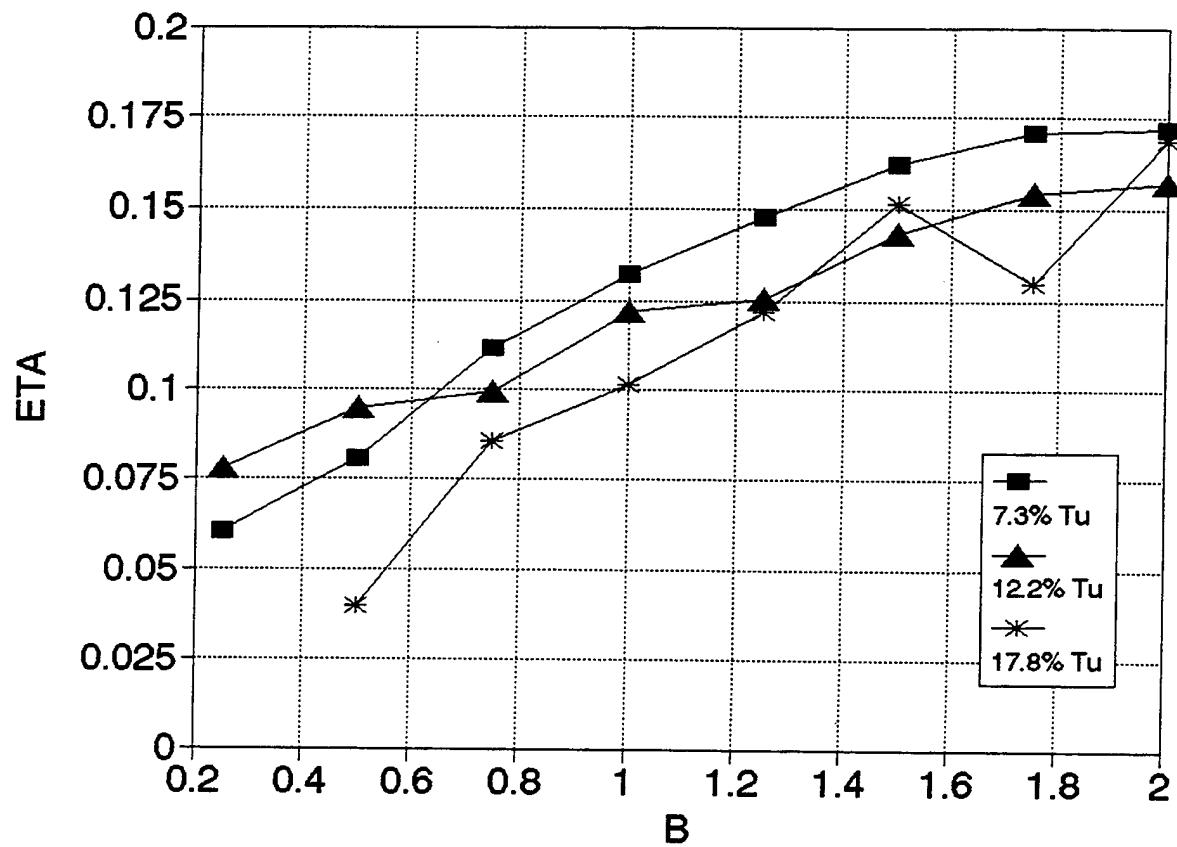
Figure E-20. Effect of Free Stream Turbulence on Film Cooling Effectiveness
X/D = 55, Free stream velocity at injection = 10 m/s
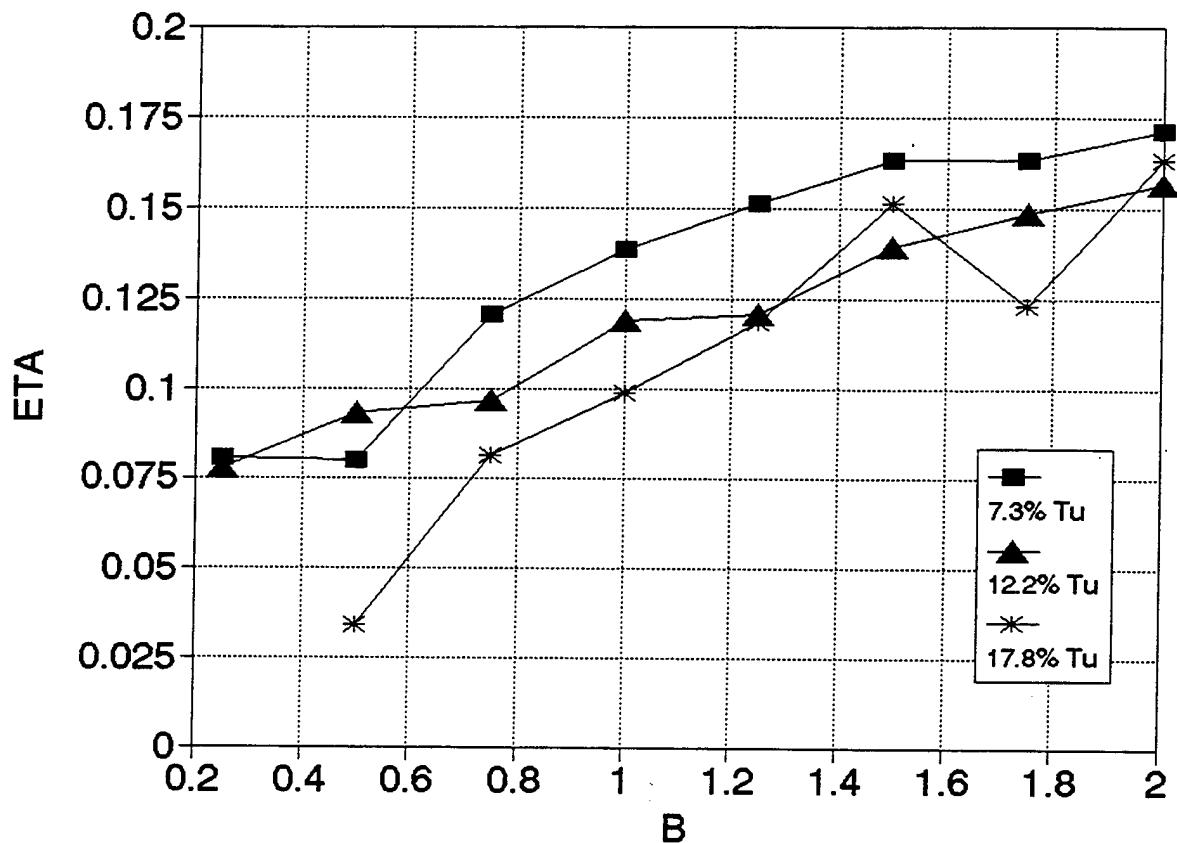
Figure E-21. Effect of Free Stream Turbulence on Film Cooling Effectiveness
X/D = 60, Free stream velocity at injection = 10 m/s
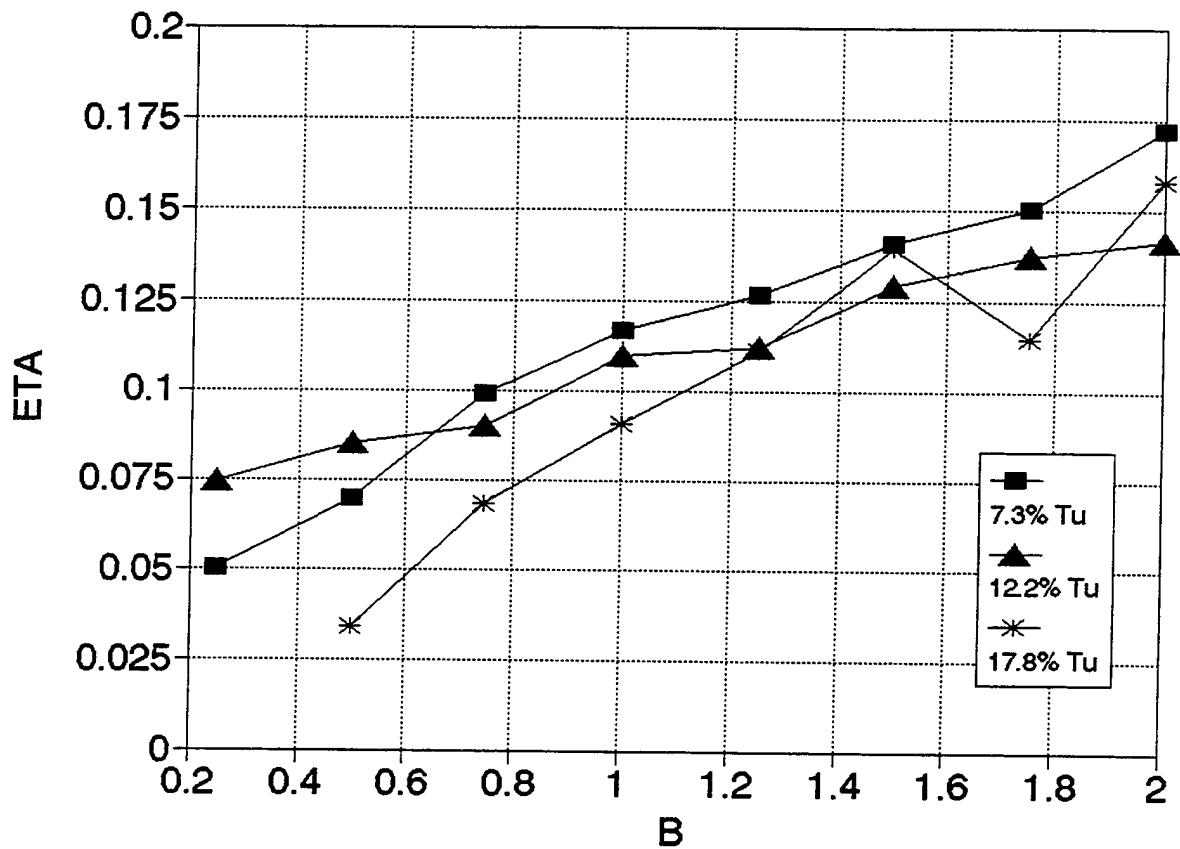
Figure E-22. Effect of Free Stream Turbulence on Film Cooling Effectiveness
X/D = 65, Free stream velocity at injection = 10 m/s
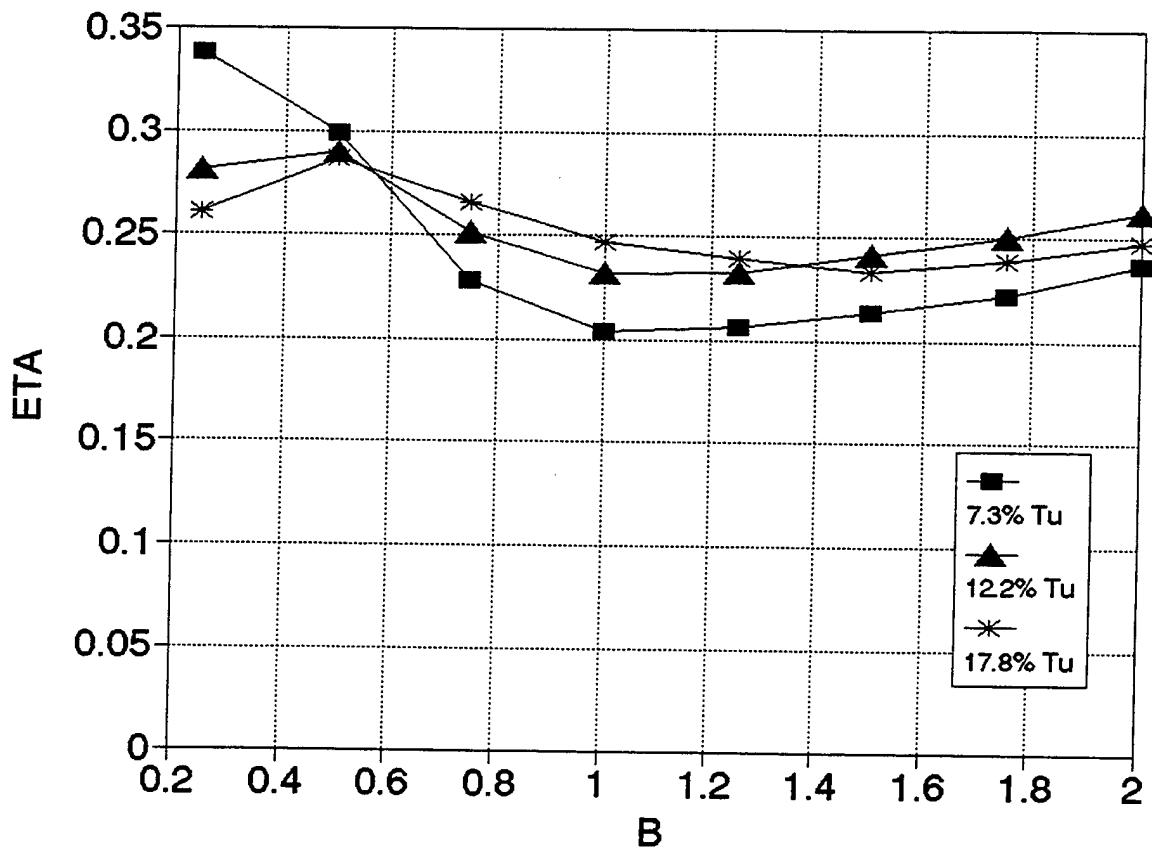
Figure E-23. Effect of Free Stream Turbulence on Film Cooling Effectiveness
X/D = 70, Free stream velocity at injection = 10 m/s
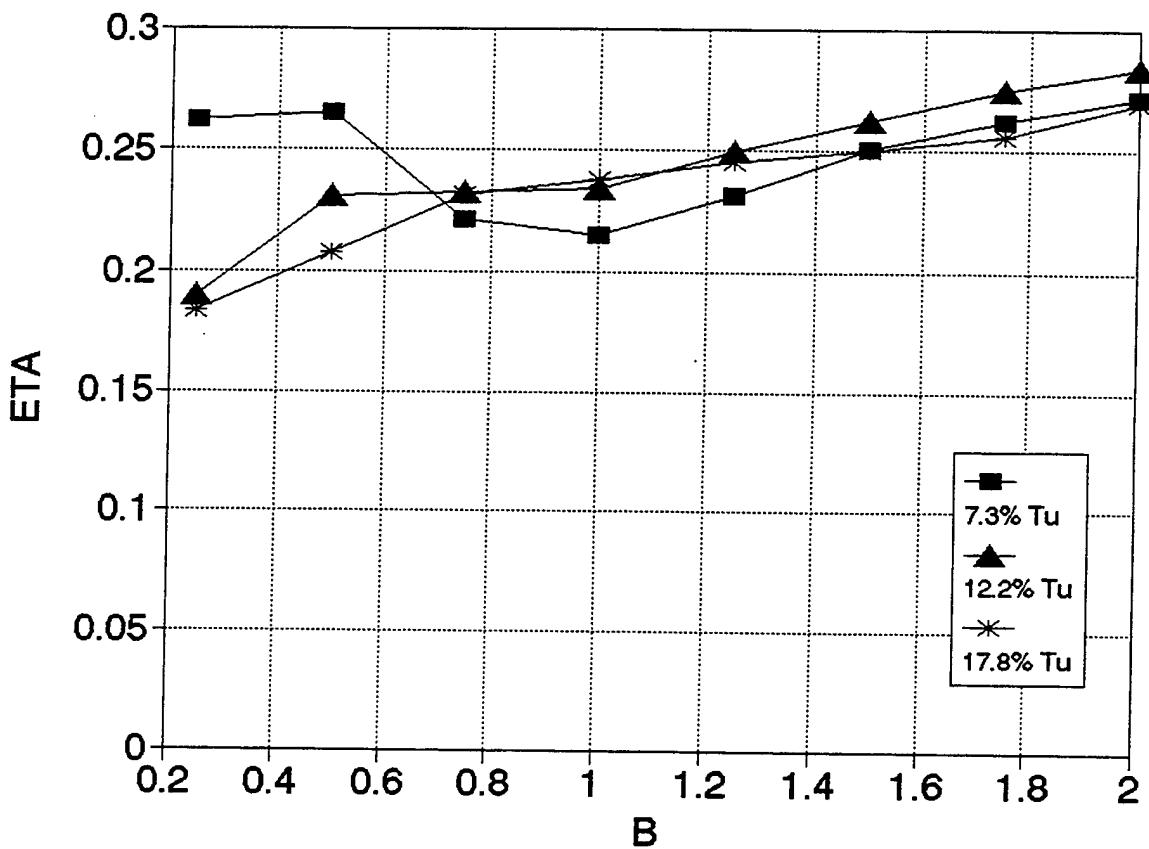
Figure E-24. Effect of Free Stream Turbulence on Film Cooling Effectiveness
X/D = 5, Free stream velocity at injection = 18 m/s
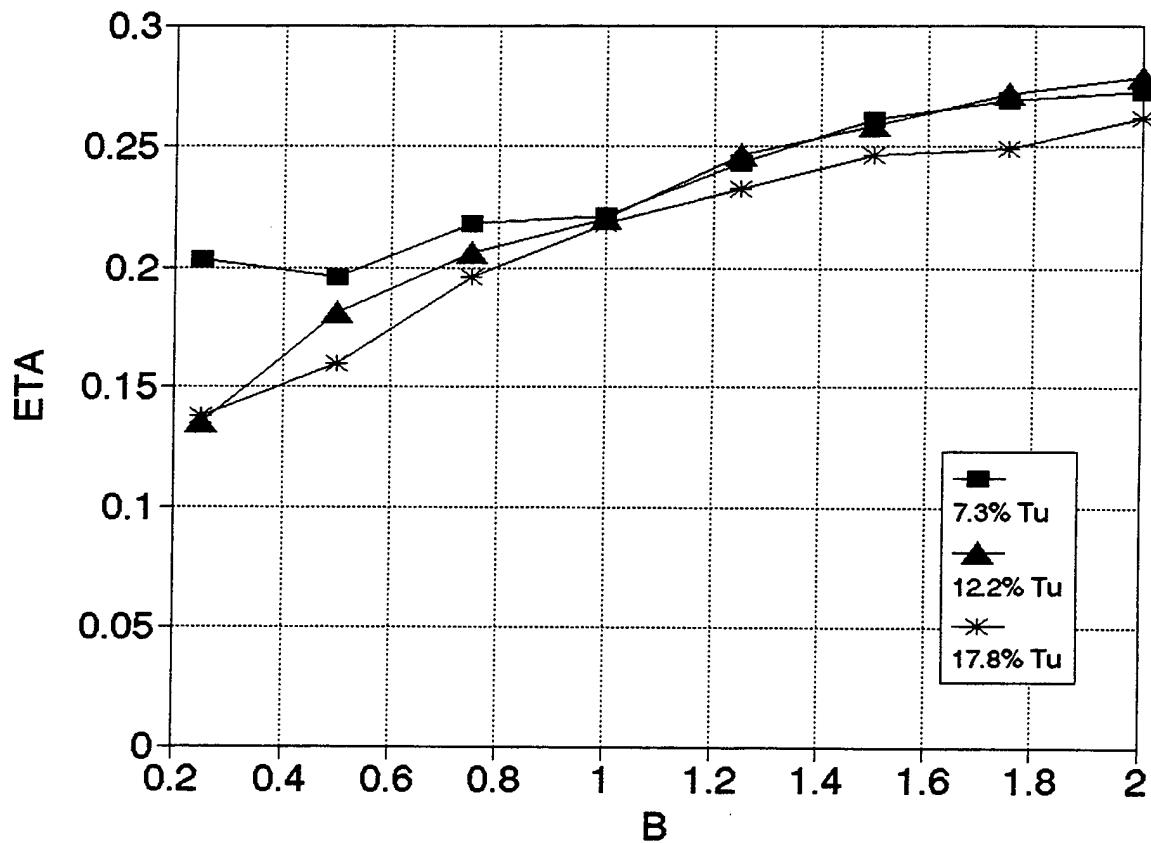
Figure E-25. Effect of Free Stream Turbulence on Film Cooling Effectiveness
X/D = 10, Free stream velocity at injection = 18 m/s
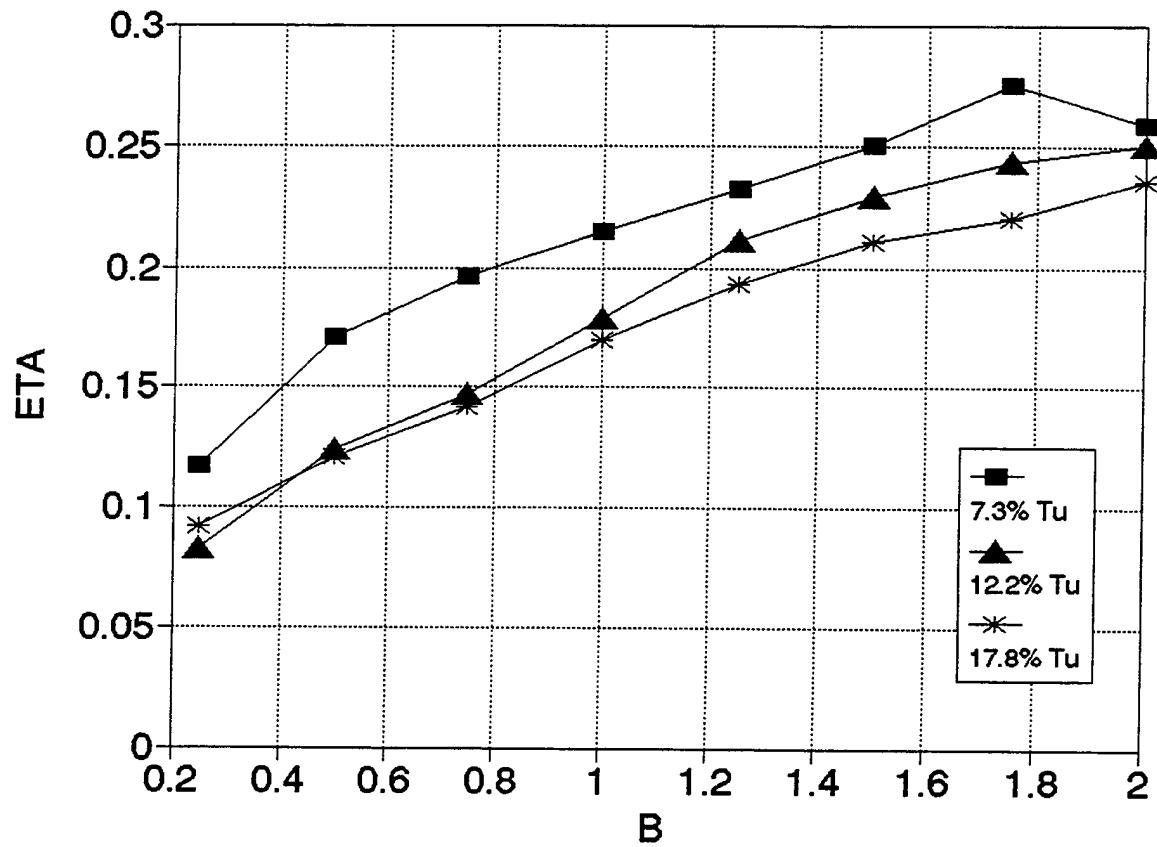
Figure E-26. Effect of Free Stream Turbulence on Film Cooling Effectiveness
X/D = 15, Free stream velocity at injection = 18 m/s
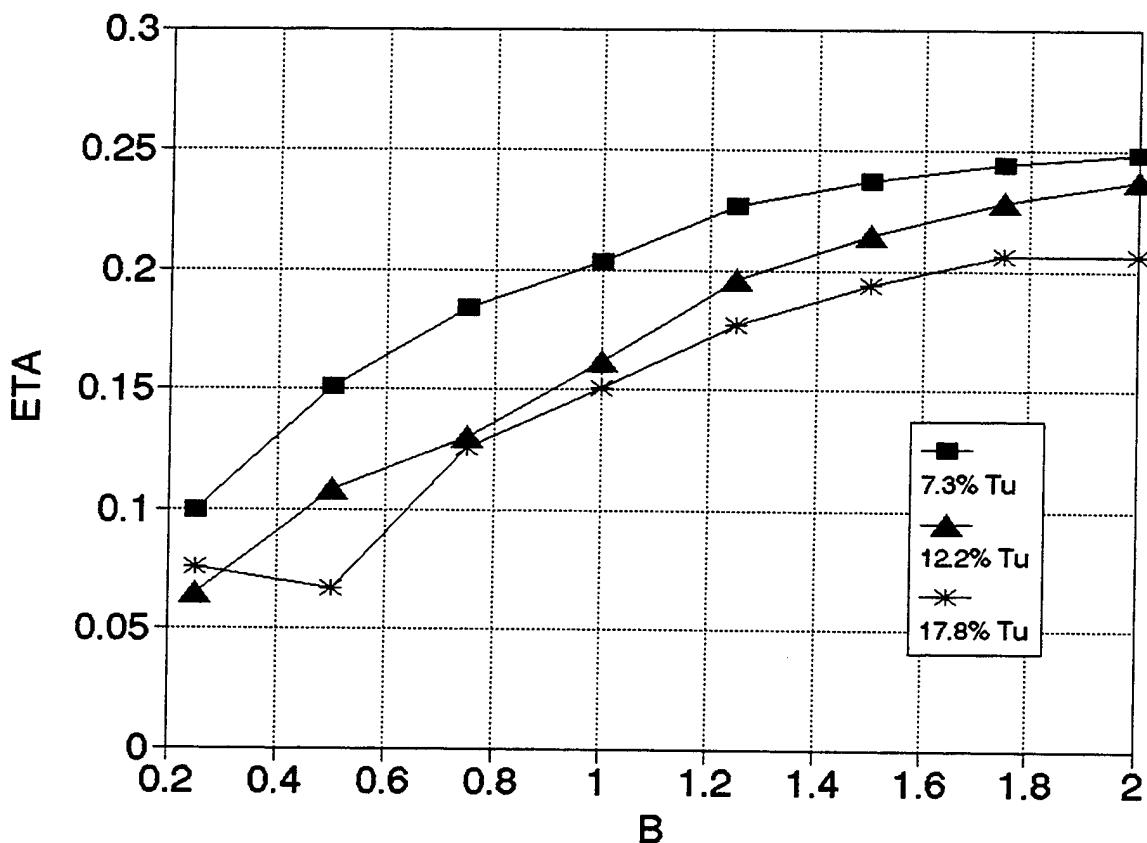
Figure E-27. Effect of Free Stream Turbulence on Film Cooling Effectiveness
X/D = 25, Free stream velocity at injection = 18 m/s
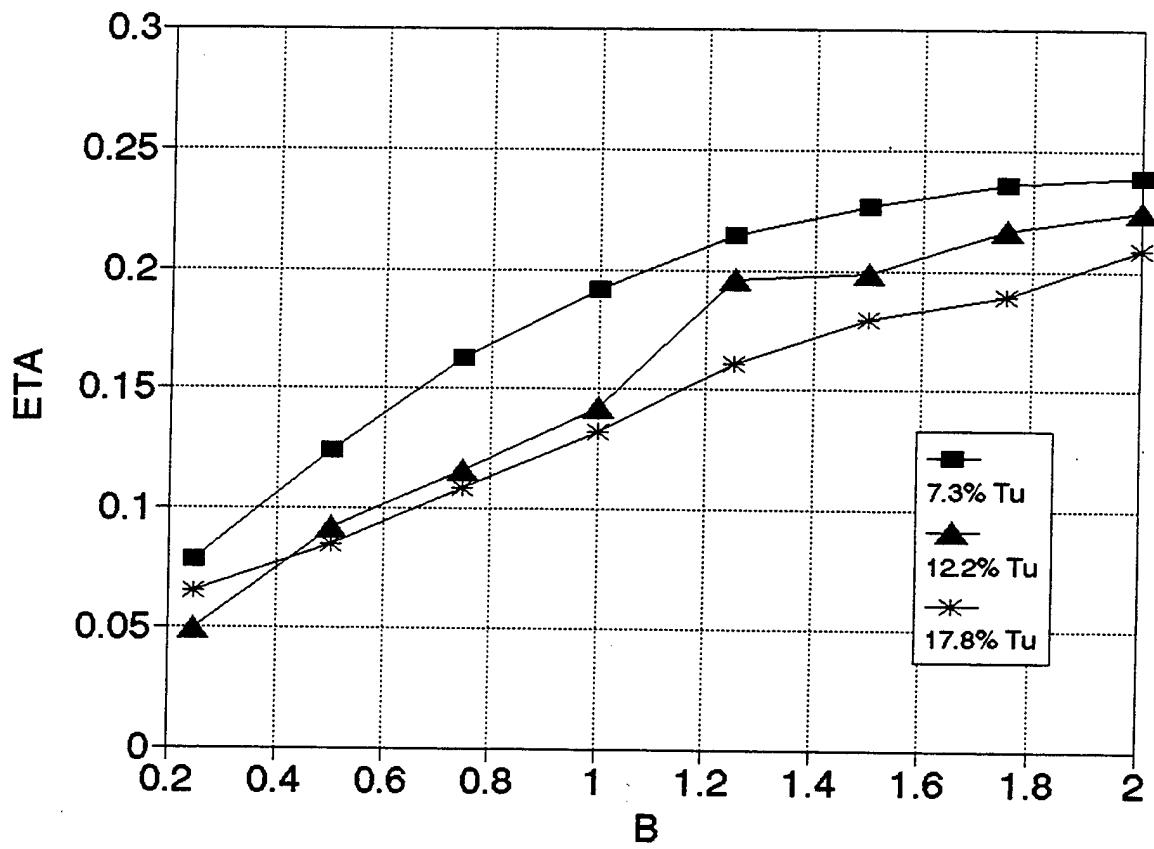
Figure E-28. Effect of Free Stream Turbulence on Film Cooling Effectiveness
X/D = 30, Free stream velocity at injection = 18 m/s
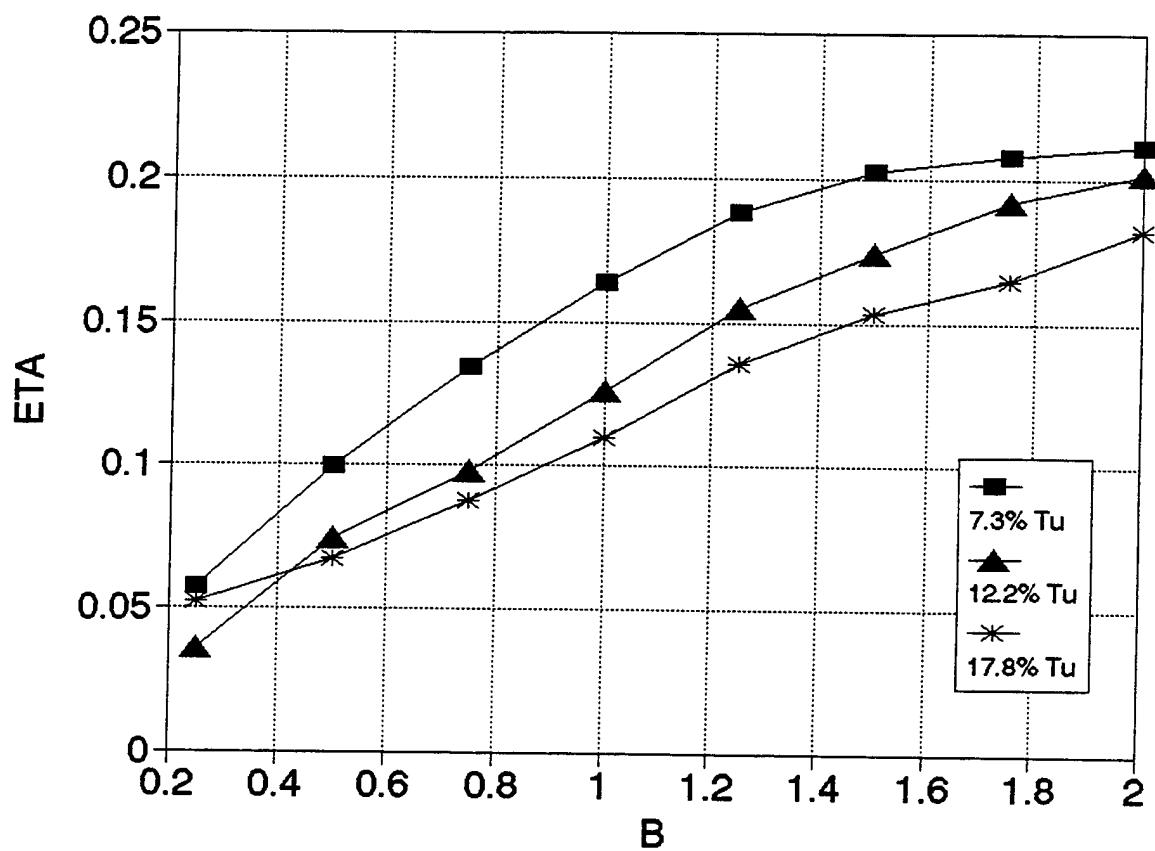
Figure E-29. Effect of Free Stream Turbulence on Film Cooling Effectiveness
X/D = 35, Free stream velocity at injection = 18 m/s
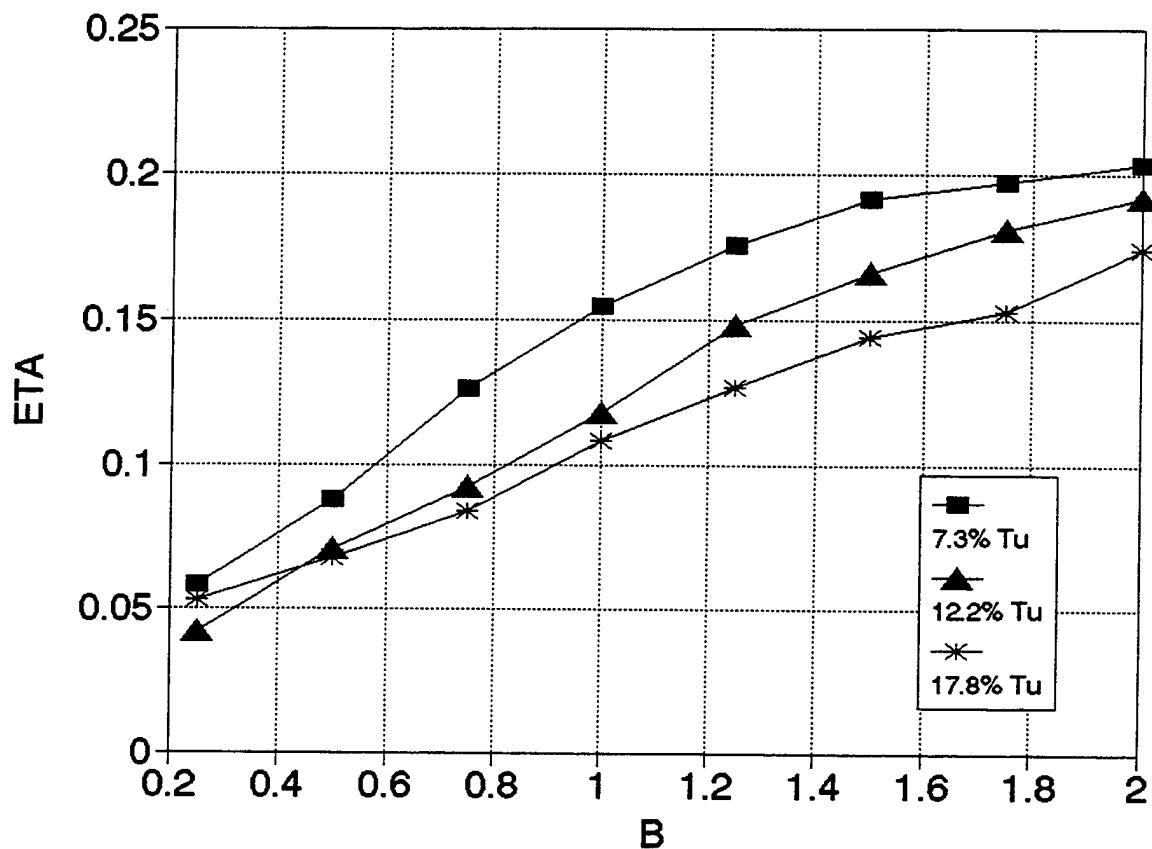
Figure E-30. Effect of Free Stream Turbulence on Film Cooling Effectiveness
X/D = 45, Free stream velocity at injection = 18 m/s
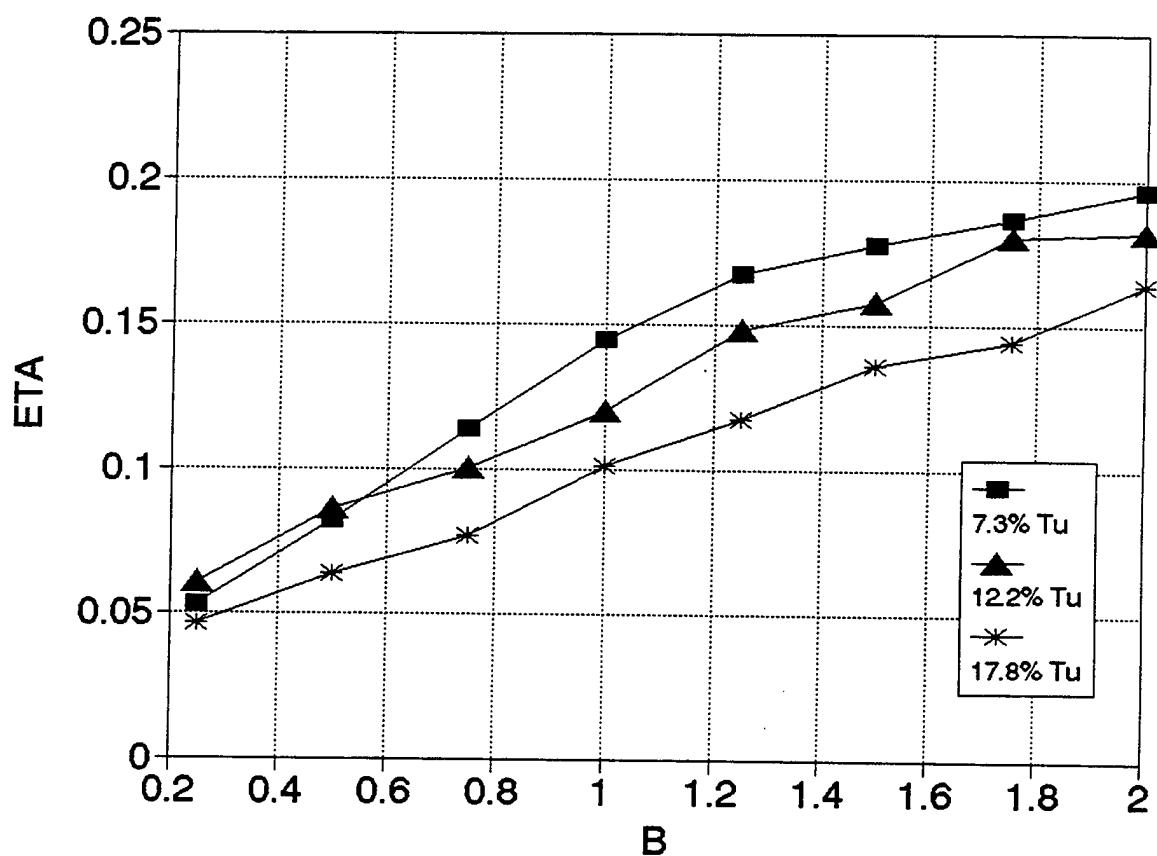
Figure E-31. Effect of Free Stream Turbulence on Film Cooling Effectiveness
X/D = 50, Free stream velocity at injection = 18 m/s
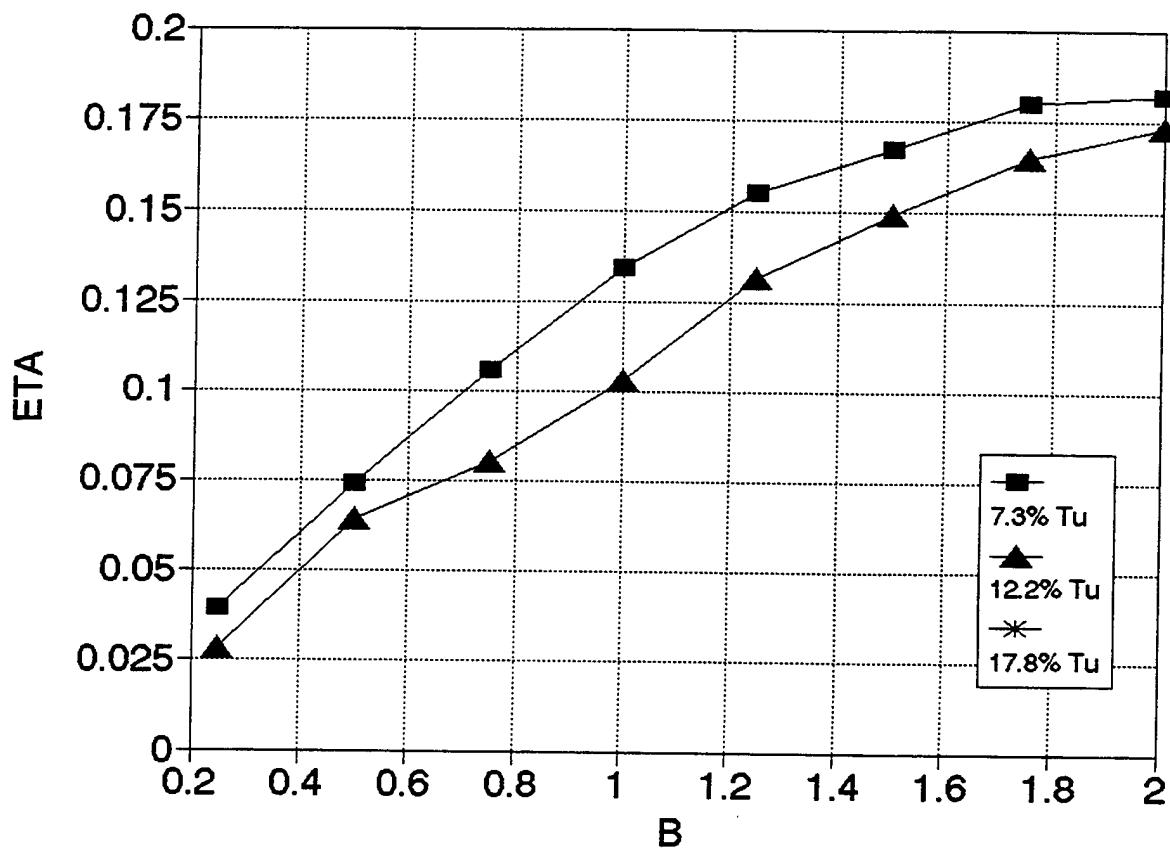
Figure E-32. Effect of Free Stream Turbulence on Film Cooling Effectiveness
X/D = 55, Free stream velocity at injection = 18 m/s
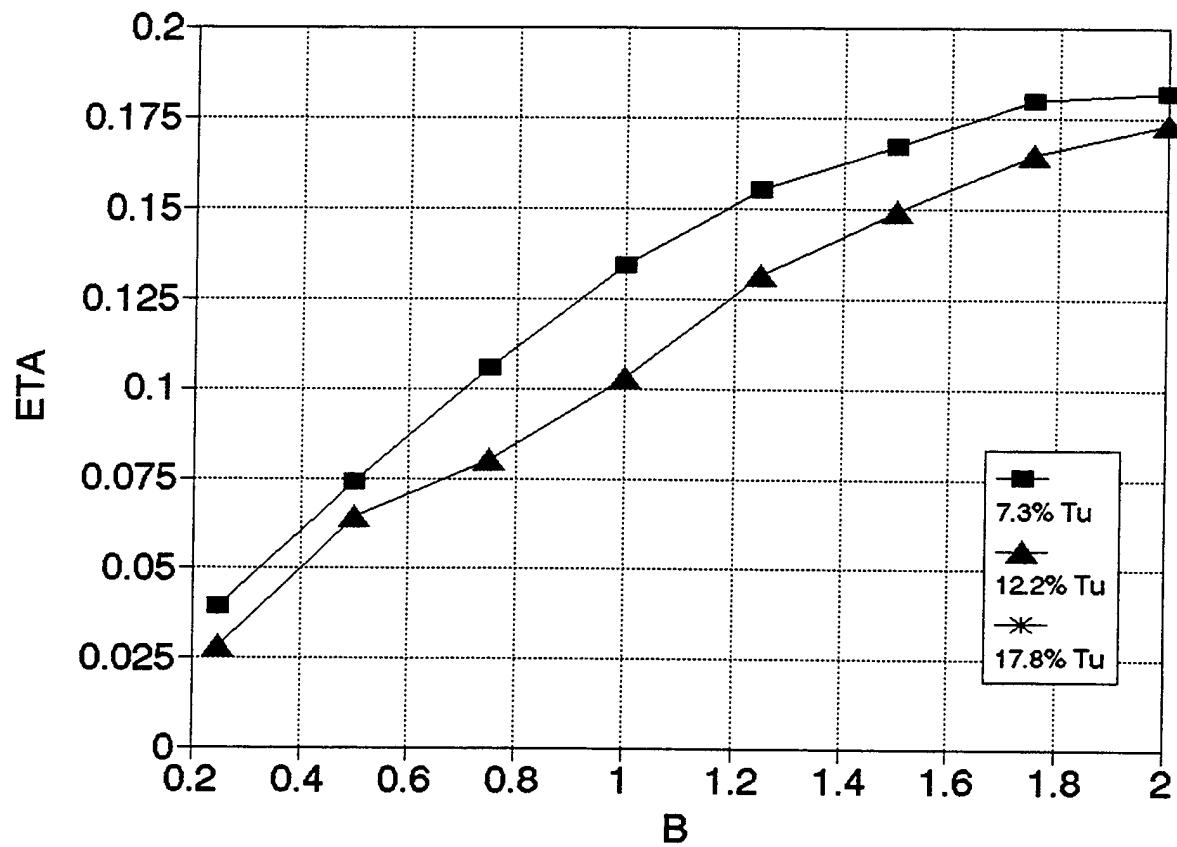
Figure E-33. Effect of Free Stream Turbulence on Film Cooling Effectiveness
X/D = 60, Free stream velocity at injection = 18 m/s
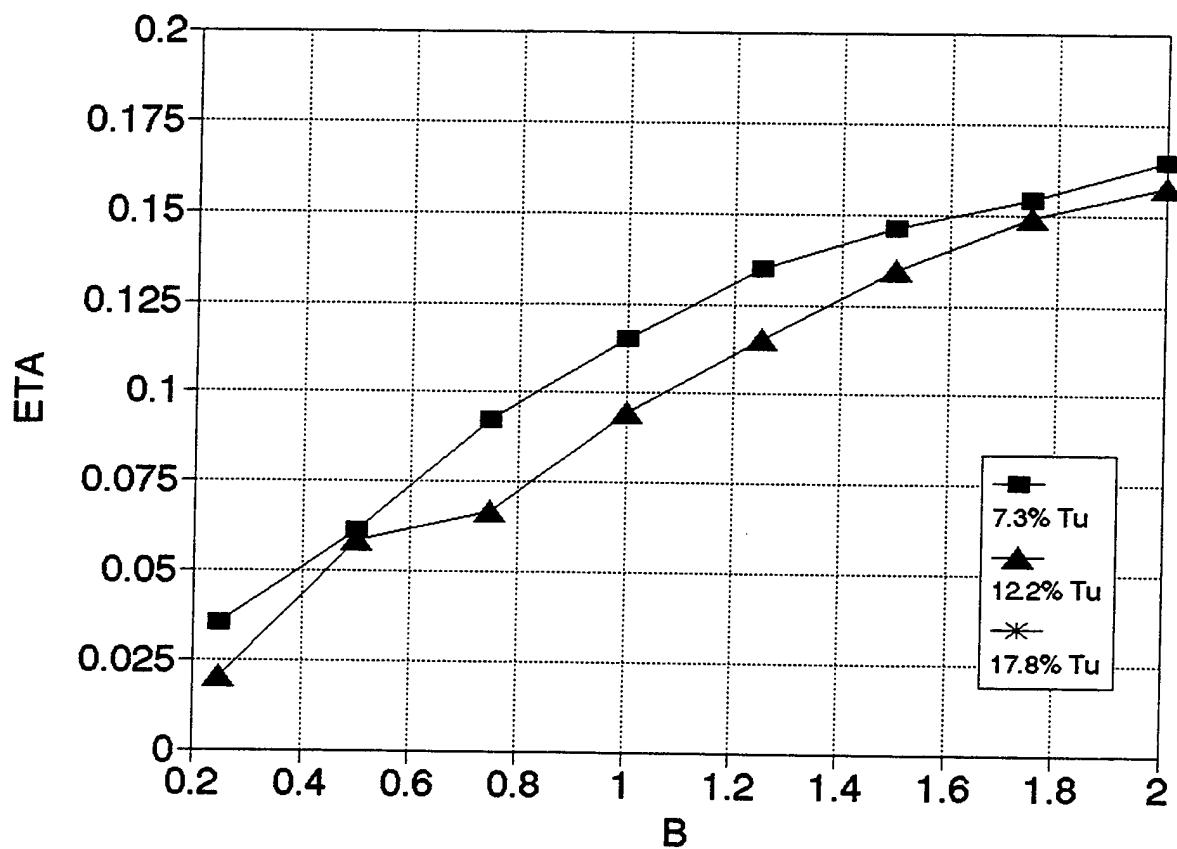
Figure E-34. Effect of Free Stream Turbulence on Film Cooling Effectiveness
X/D = 65, Free stream velocity at injection = 18 m/s
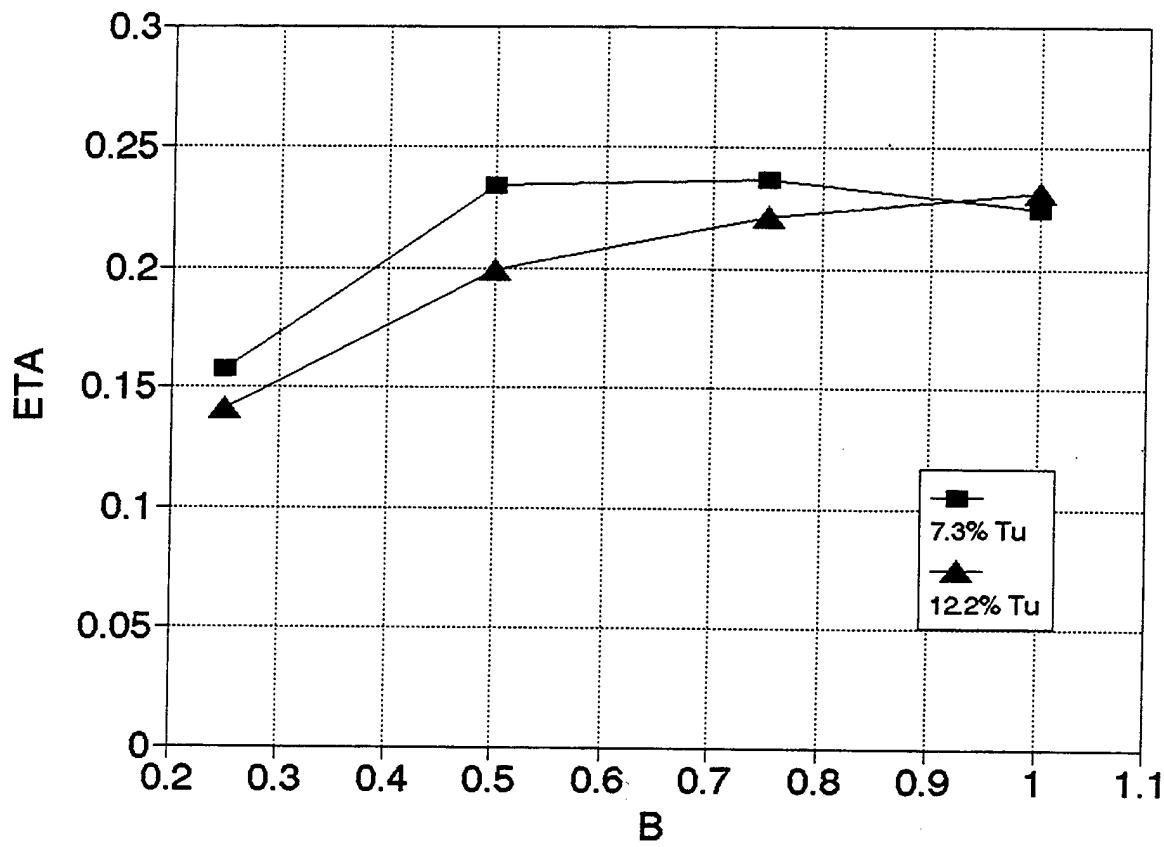
Figure E-35. Effect of Free Stream Turbulence on Film Cooling Effectiveness
X/D = 70, Free stream velocity at injection = 18 m/s
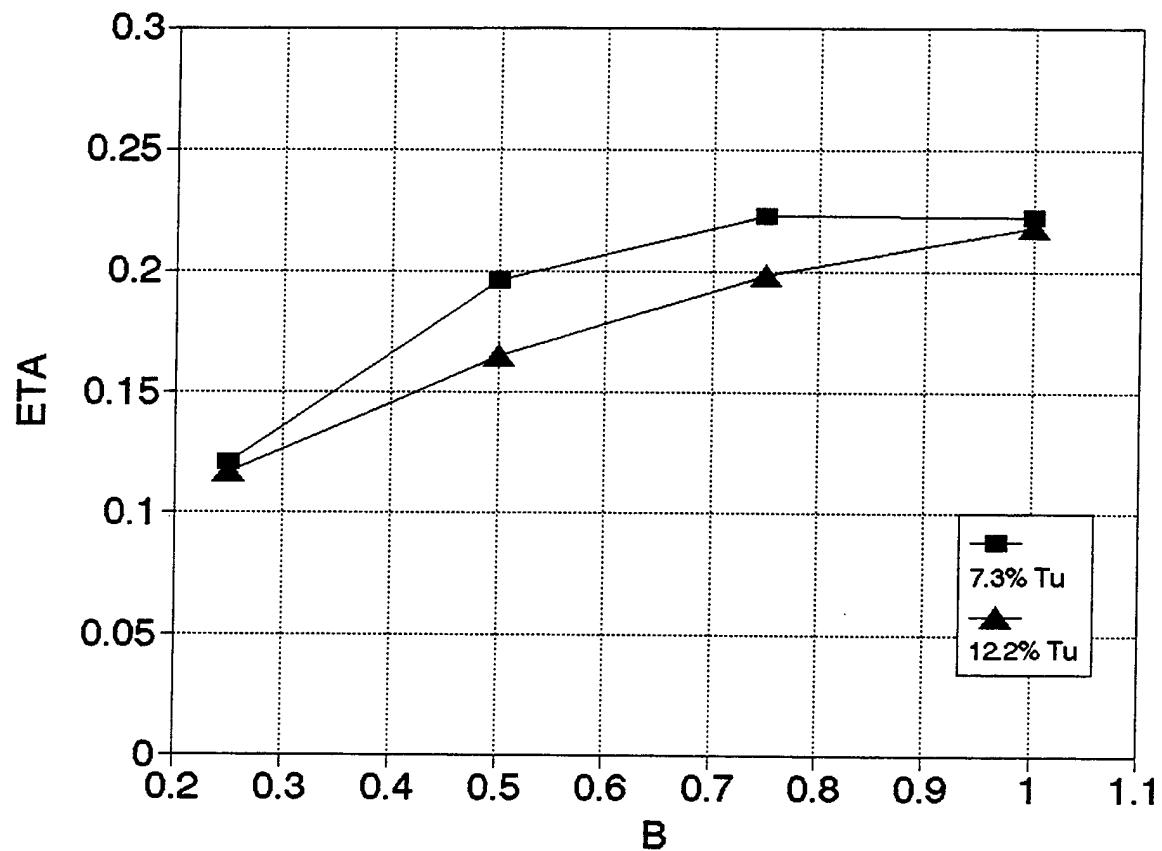
Figure E-36. Effect of Free Stream Turbulence on Film Cooling Effectiveness
X/D = 15, Free stream velocity at injection = 37 m/s
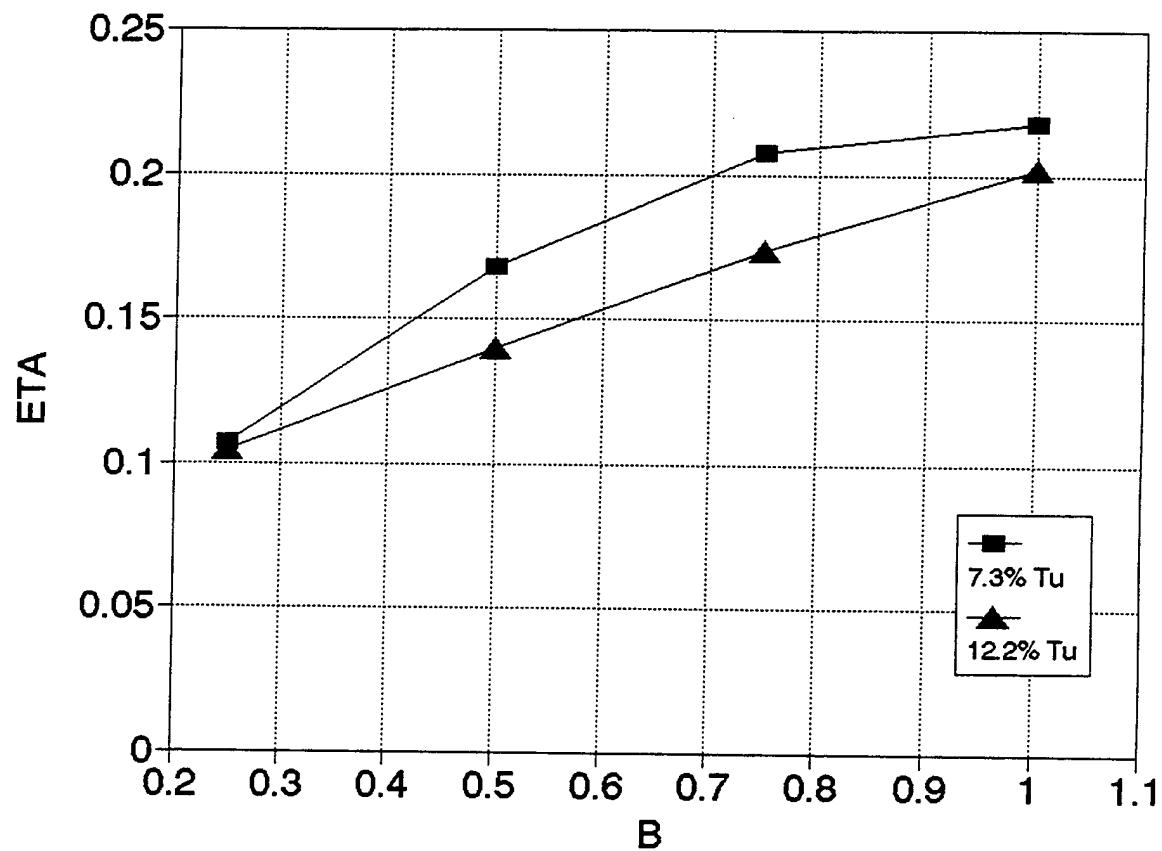
Figure E-37. Effect of Free Stream Turbulence on Film Cooling Effectiveness
X/D = 20, Free stream velocity at injection = 37 m/s
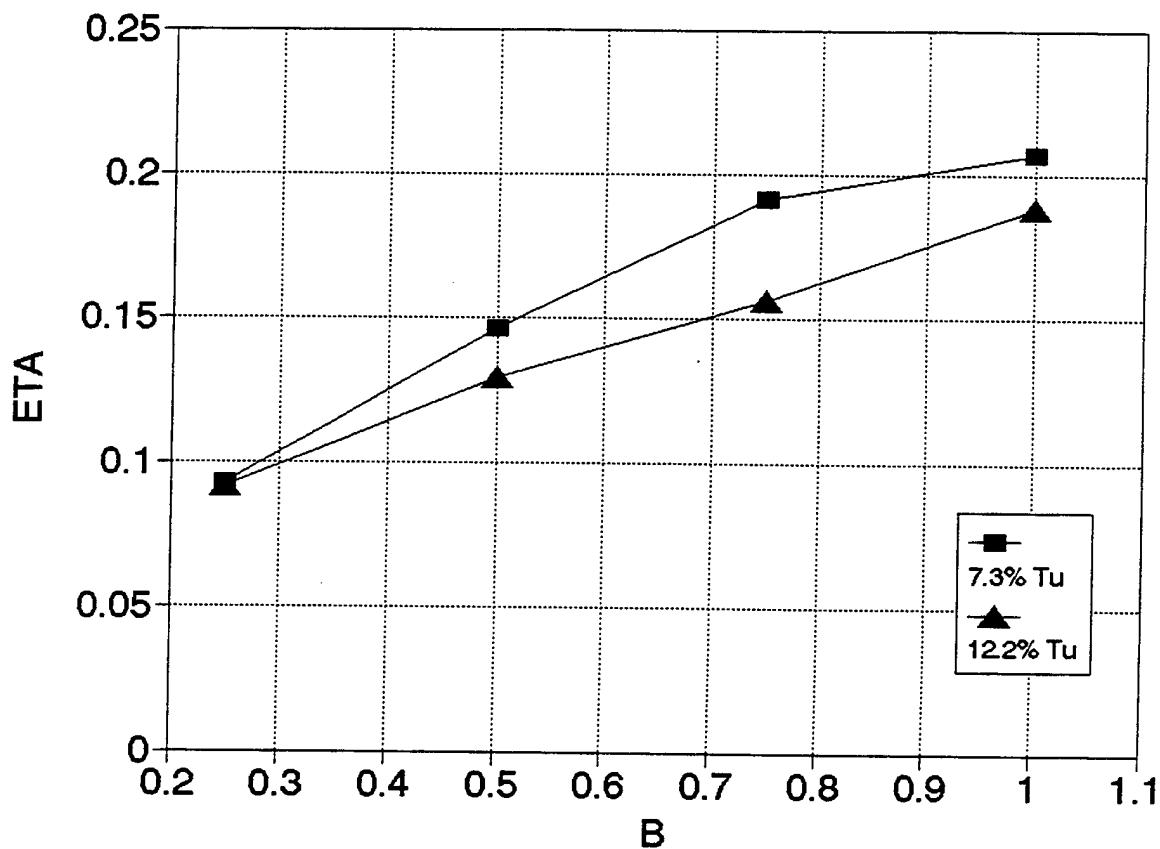
Figure E-38. Effect of Free Stream Turbulence on Film Cooling Effectiveness
X/D = 25, Free stream velocity at injection = 37 m/s
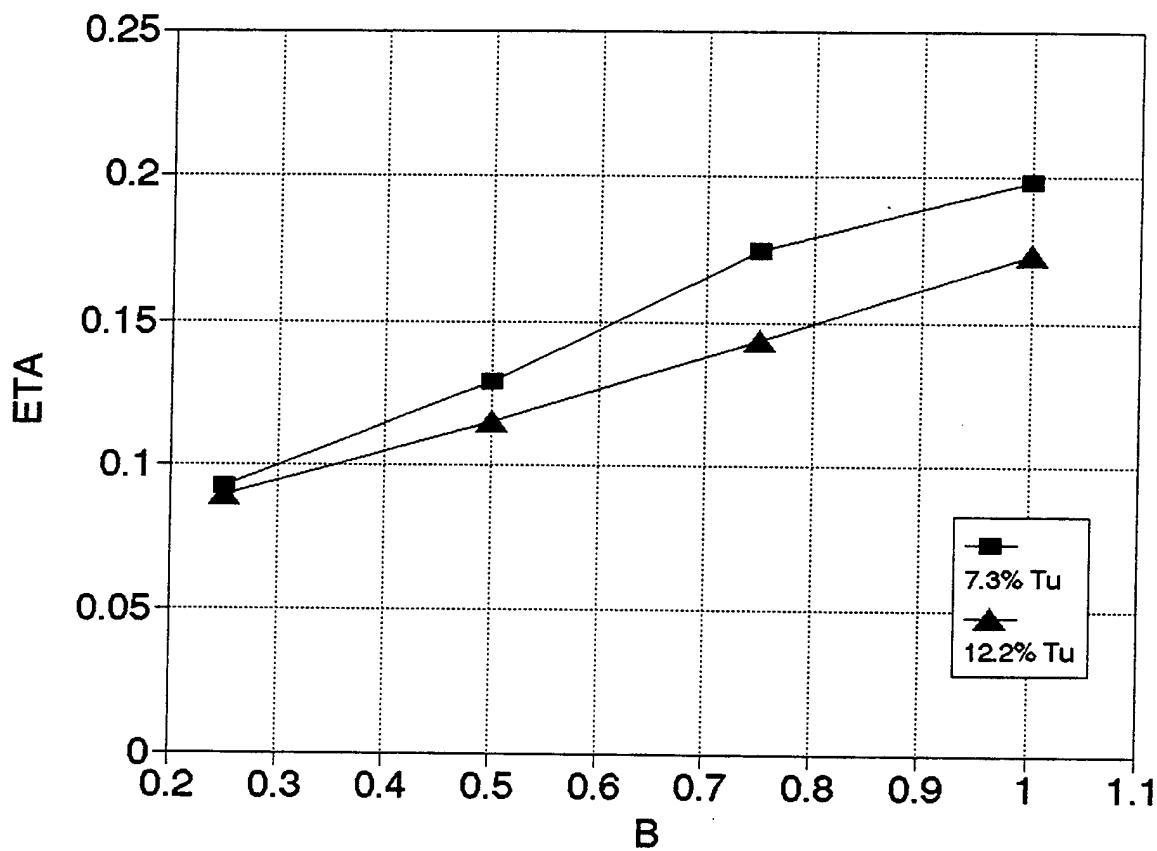
Figure E-39. Effect of Free Stream Turbulence on Film Cooling Effectiveness
X/D = 30, Free stream velocity at injection = 37 m/s
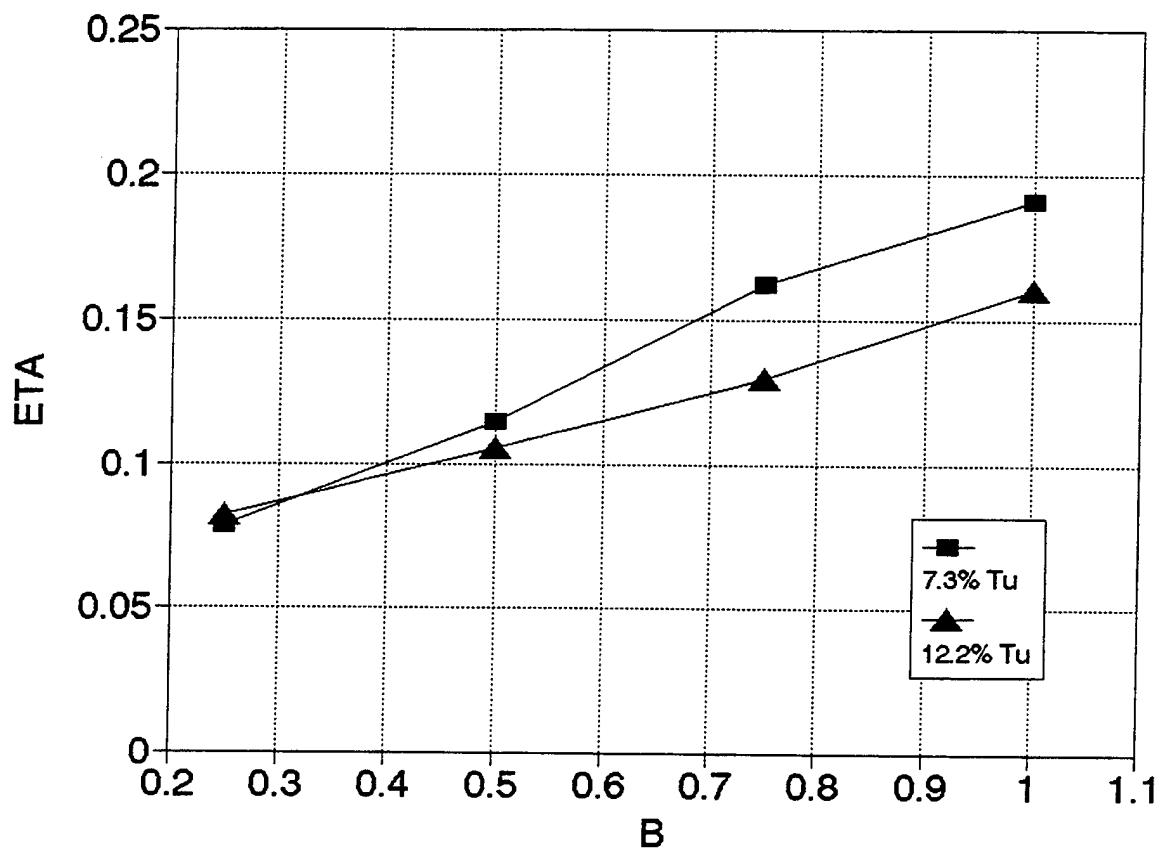
Figure E-40. Effect of Free Stream Turbulence on Film Cooling Effectiveness
X/D = 35, Free stream velocity at injection = 37 m/s
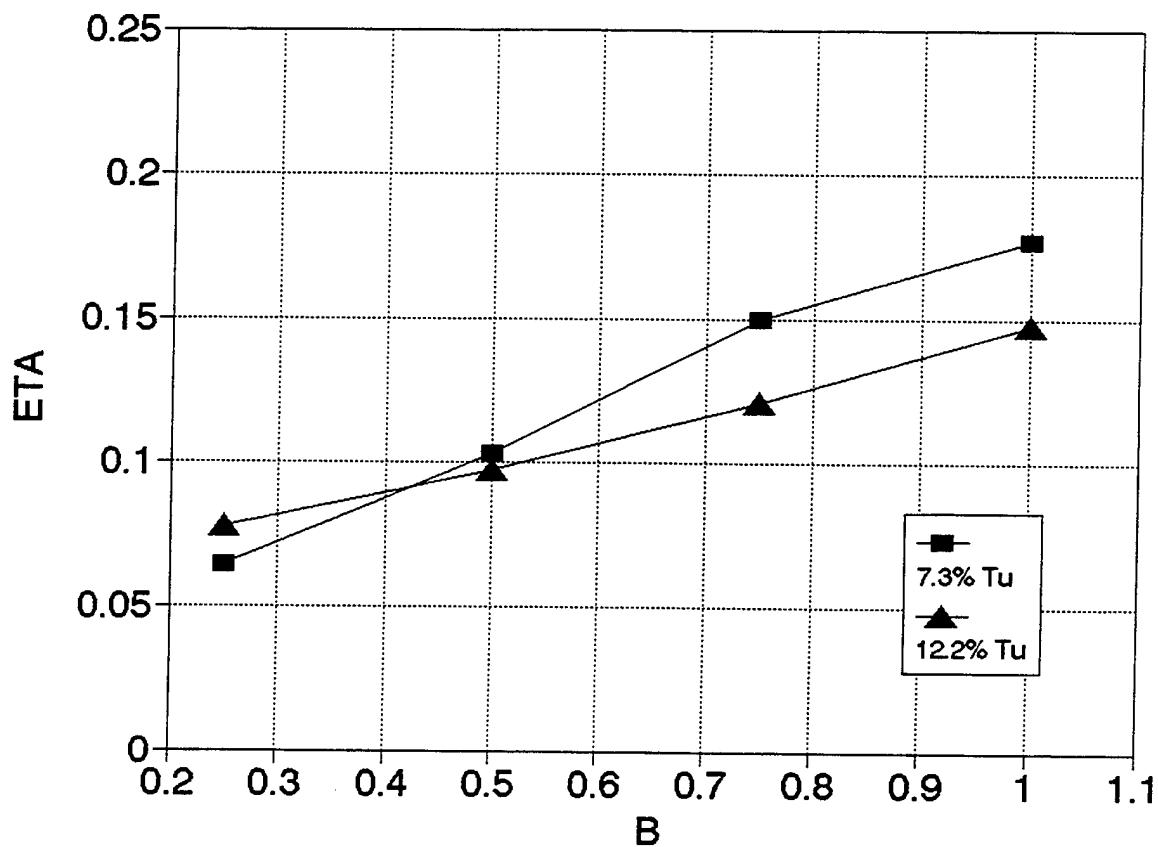
Figure E-41. Effect of Free Stream Turbulence on Film Cooling Effectiveness
X/D = 40, Free stream velocity at injection = 37 m/s
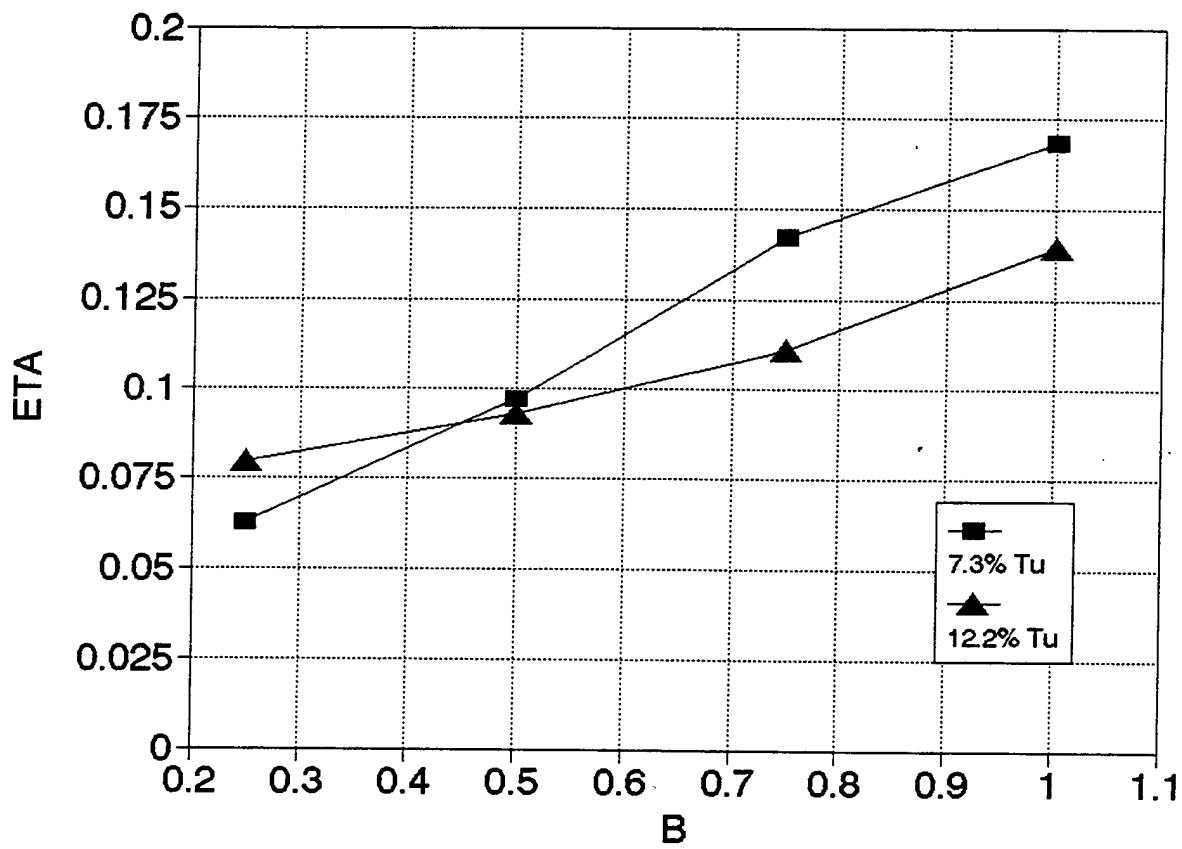
Figure E-42. Effect of Free Stream Turbulence on Film Cooling Effectiveness
X/D = 45, Free stream velocity at injection = 37 m/s
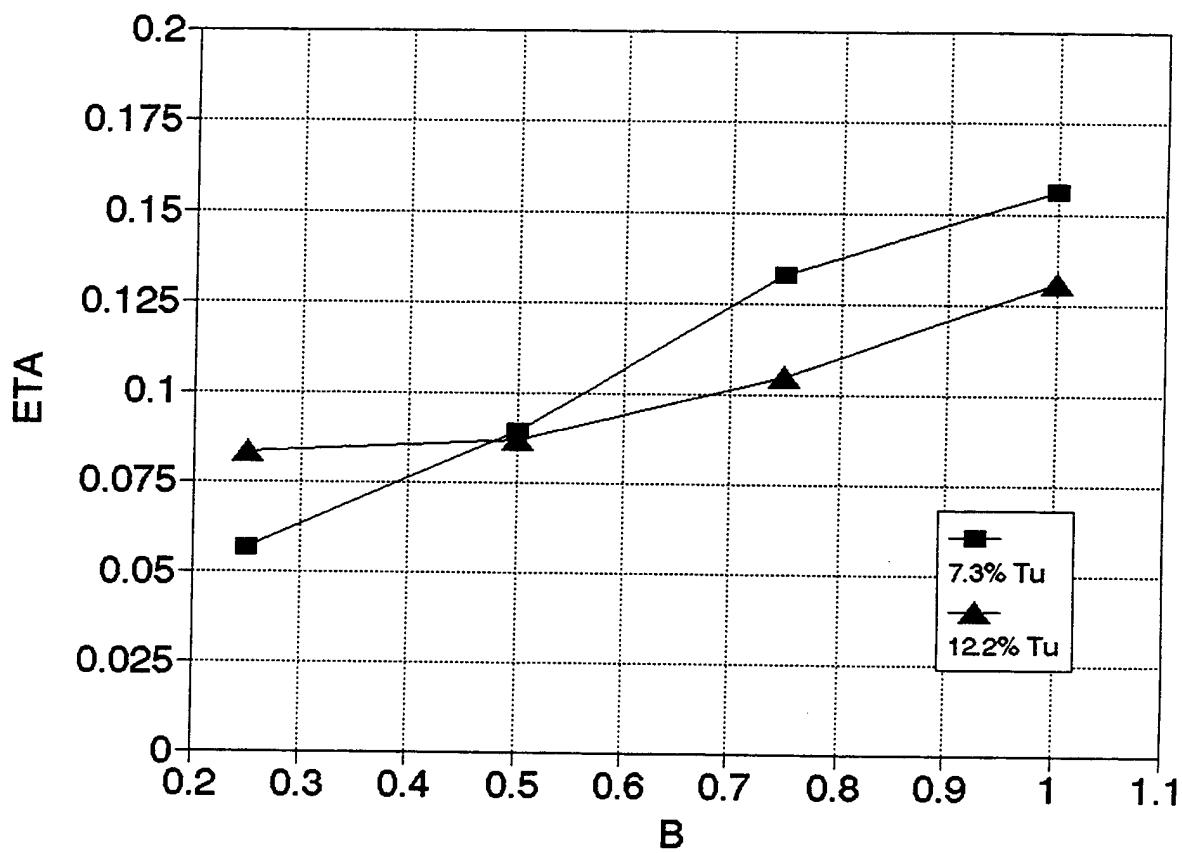
Figure E-43. Effect of Free Stream Turbulence on Film Cooling Effectiveness
X/D = 50, Free stream velocity at injection = 37 m/s
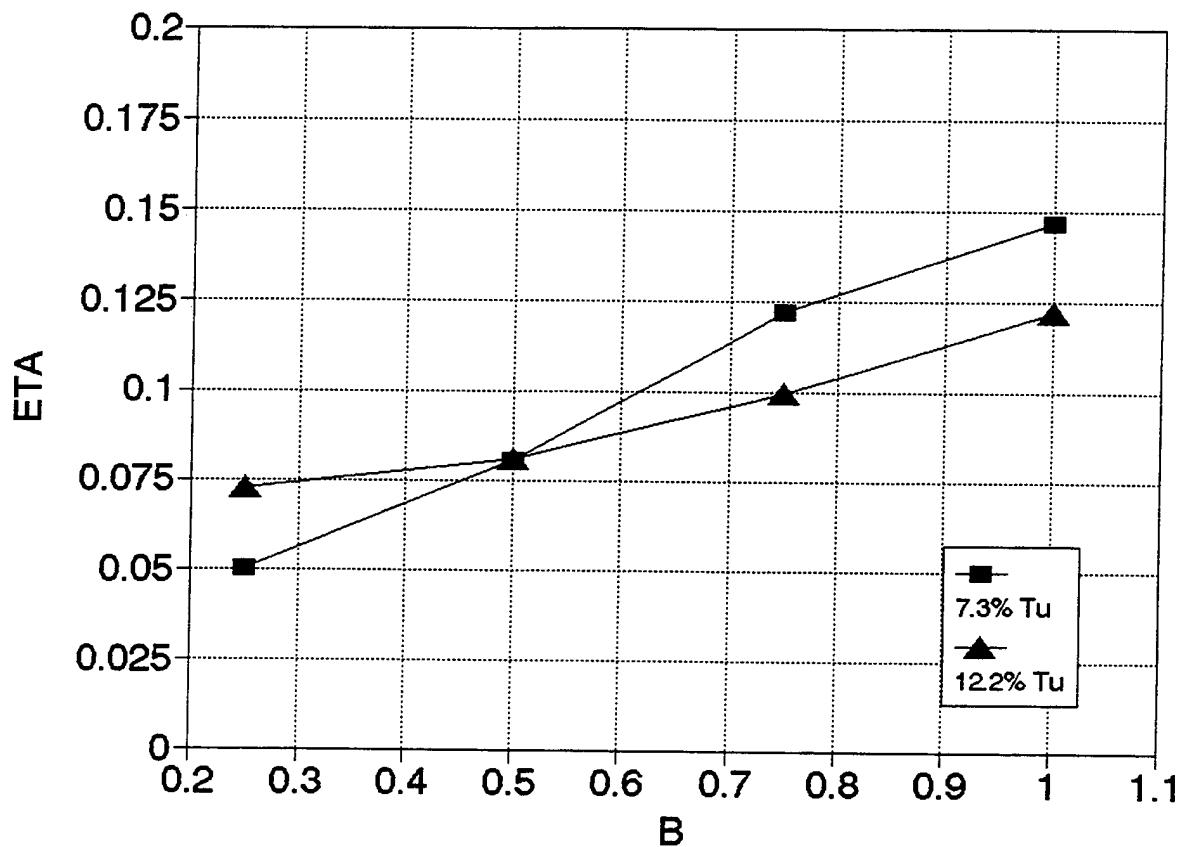
Figure E-44. Effect of Free Stream Turbulence on Film Cooling Effectiveness
X/D = 55, Free stream velocity at injection = 37 m/s
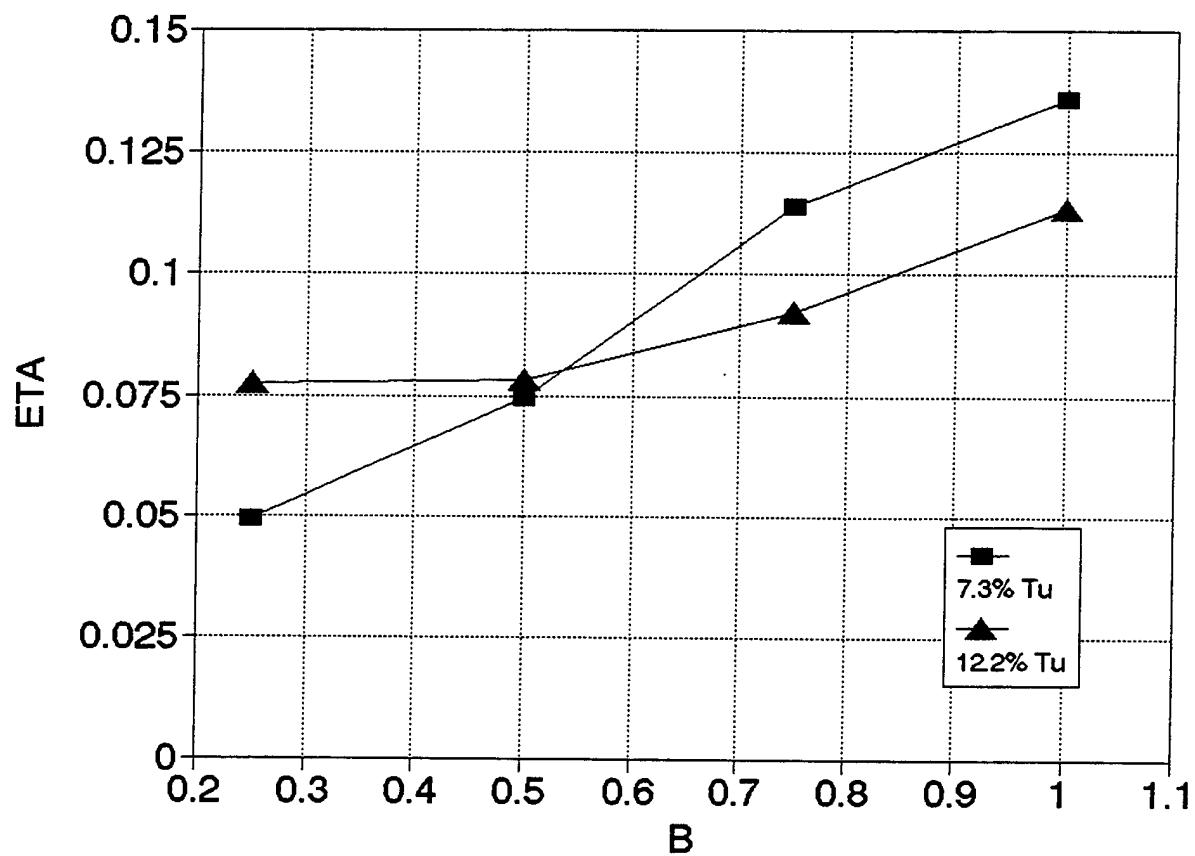
Figure E-45. Effect of Free Stream Turbulence on Film Cooling Effectiveness
X/D = 60, Free stream velocity at injection = 37 m/s
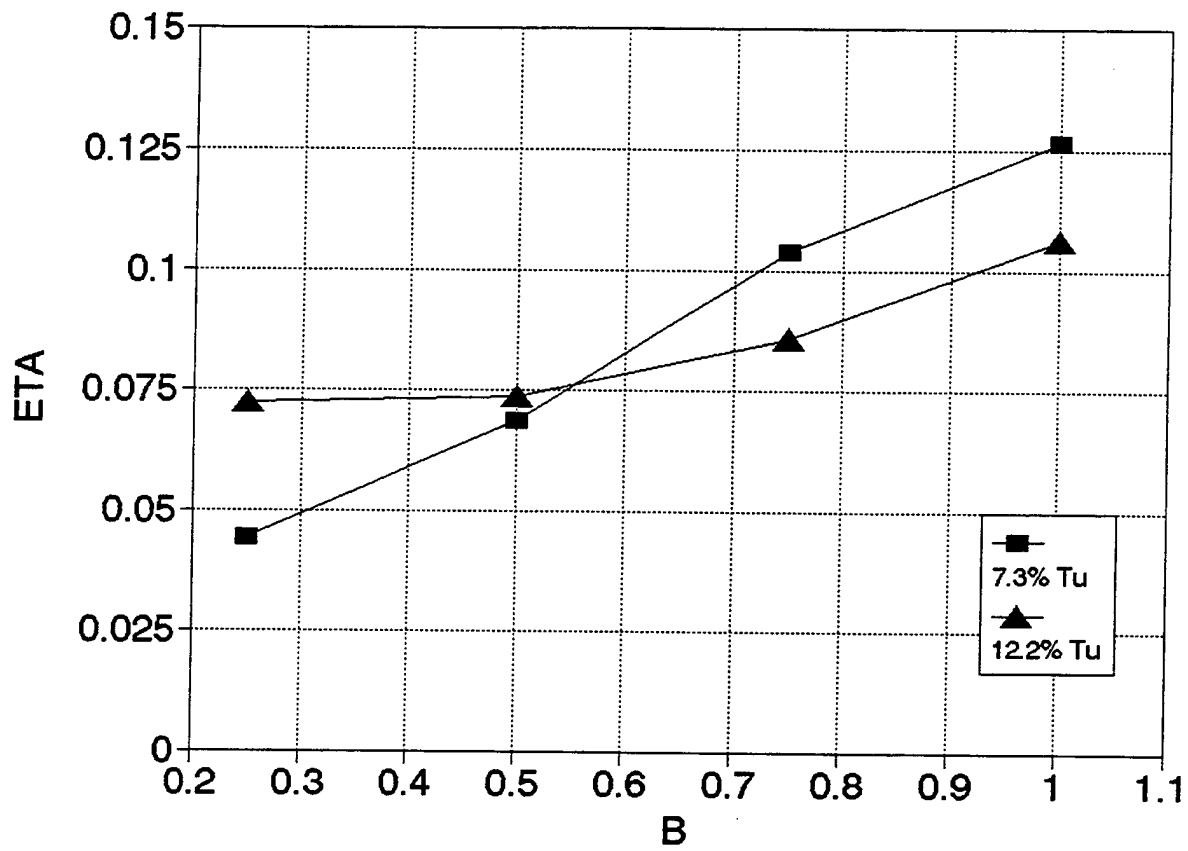
Figure E-46. Effect of Free Stream Turbulence on Film Cooling Effectiveness
X/D = 65, Free stream velocity at injection = 37 m/s
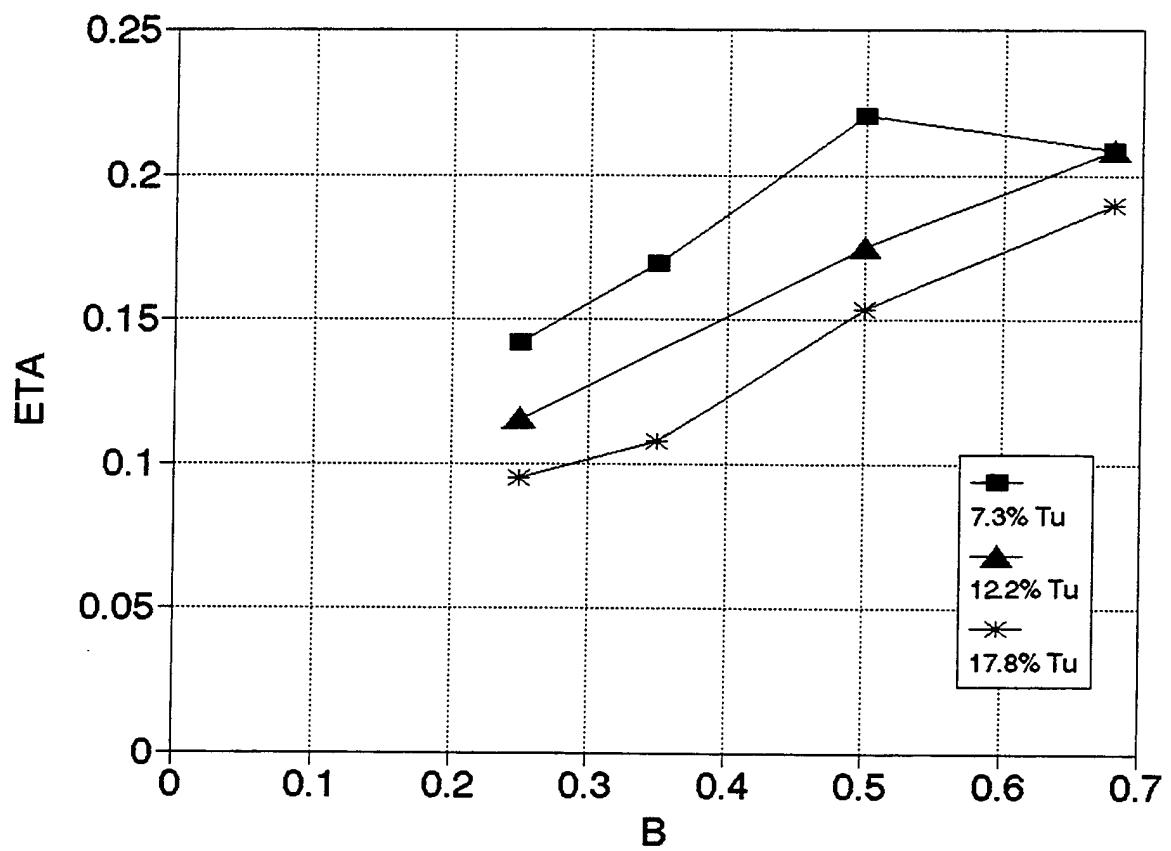
Figure E-47. Effect of Free Stream Turbulence on Film Cooling Effectiveness
X/D = 70, Free stream velocity at injection = 37 m/s
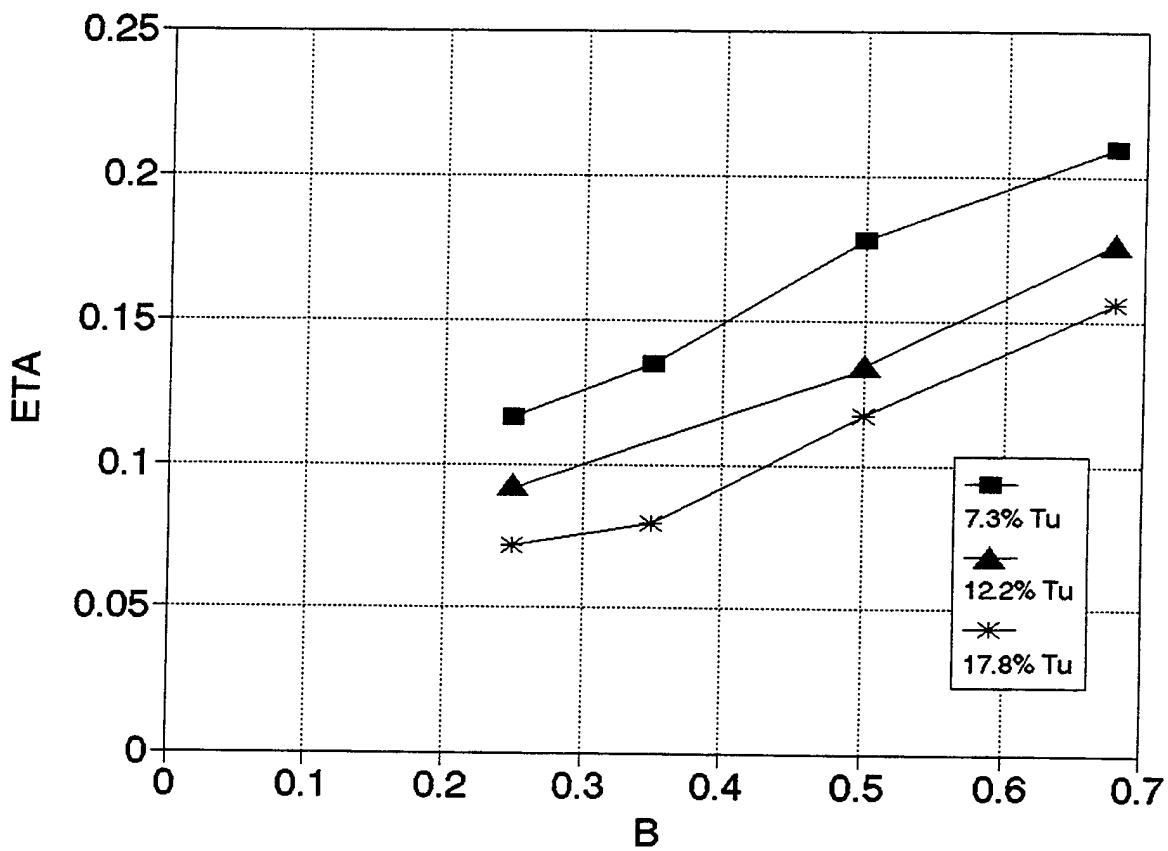
Figure E-48. Effect of Free Stream Turbulence on Film Cooling Effectiveness
X/D = 15, Free stream velocity at injection = 60 m/s
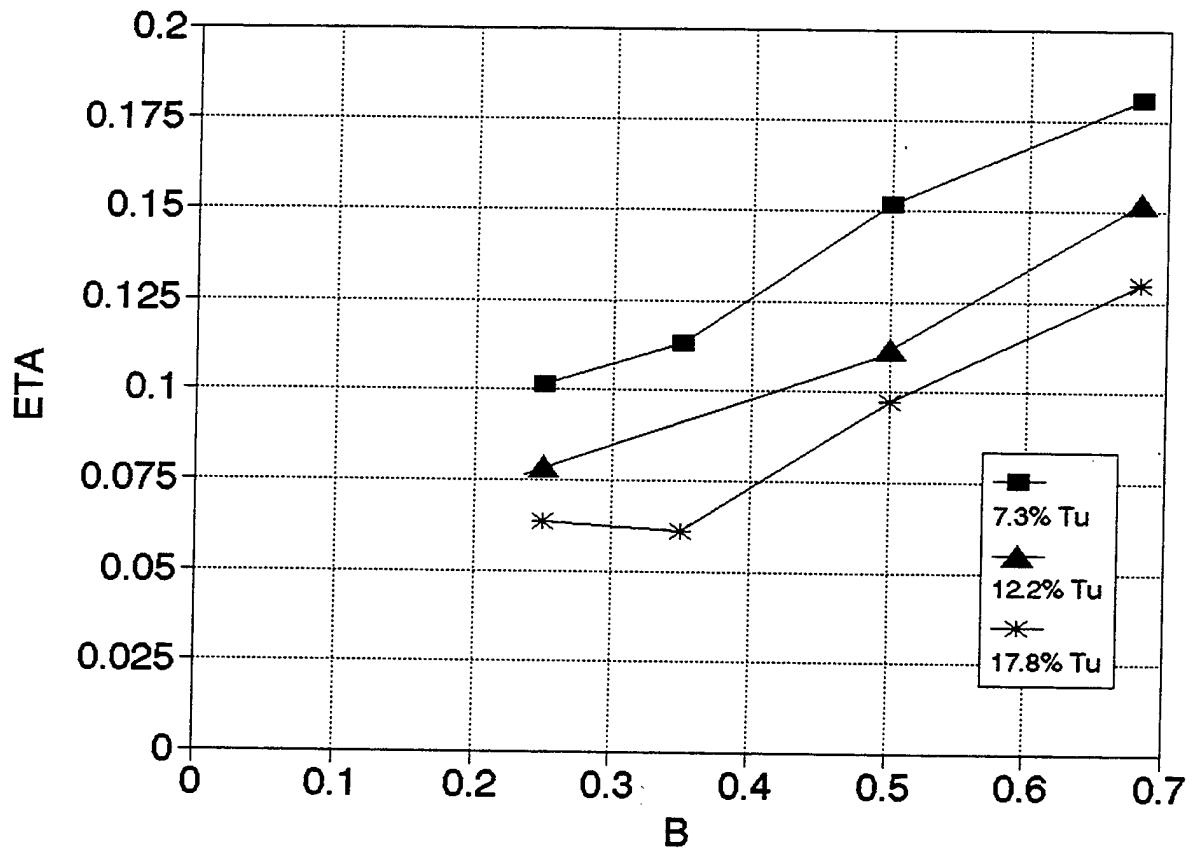
Figure E-49. Effect of Free Stream Turbulence on Film Cooling Effectiveness
X/D = 20 Free stream velocity at injection = 60 m/s
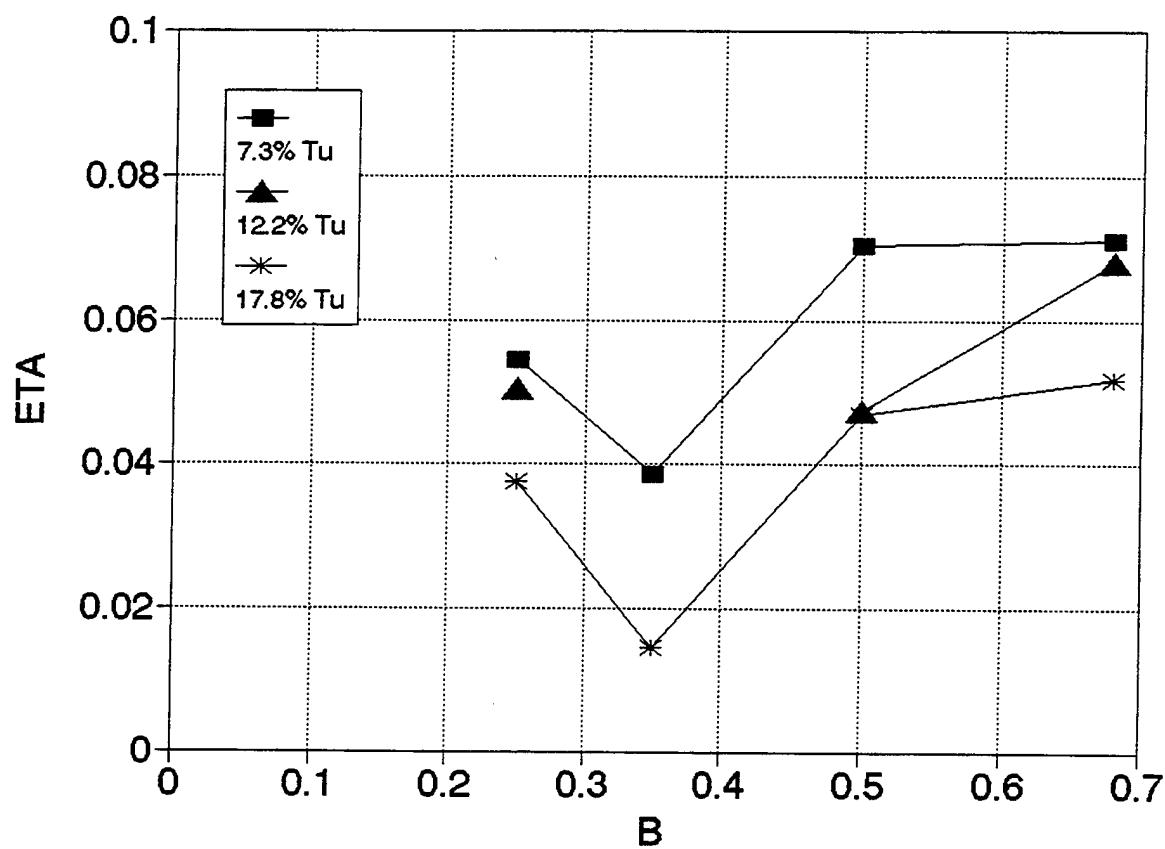
Figure E-50. Effect of Free Stream Turbulence on Film Cooling Effectiveness
X/D = 25, Free stream velocity at injection = 60 m/s
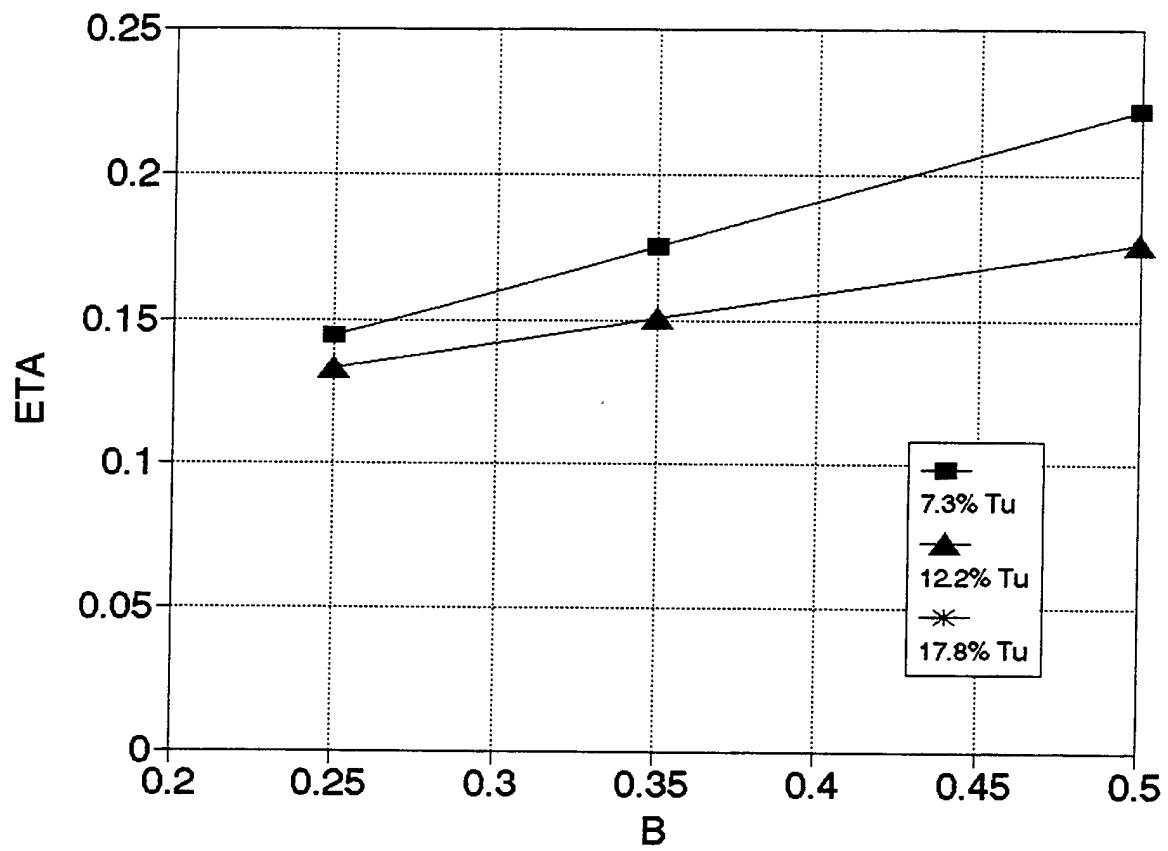
Figure E-51. Effect of Free Stream Turbulence on Film Cooling Effectiveness
X/D = 65, Free stream velocity at injection = 60 m/s
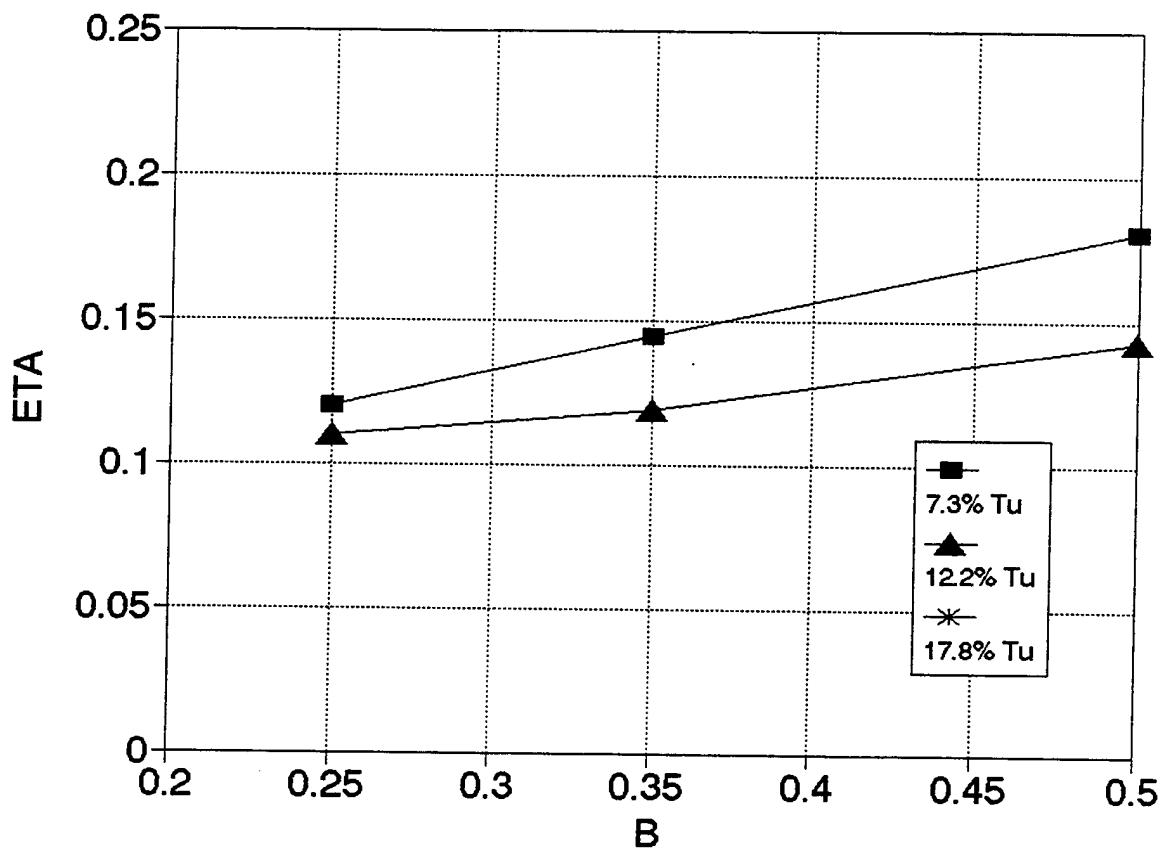
Figure E-52. Effect of Free Stream Turbulence on Film Cooling Effectiveness
X/D = 15, Free stream velocity at injection = 85 m/s
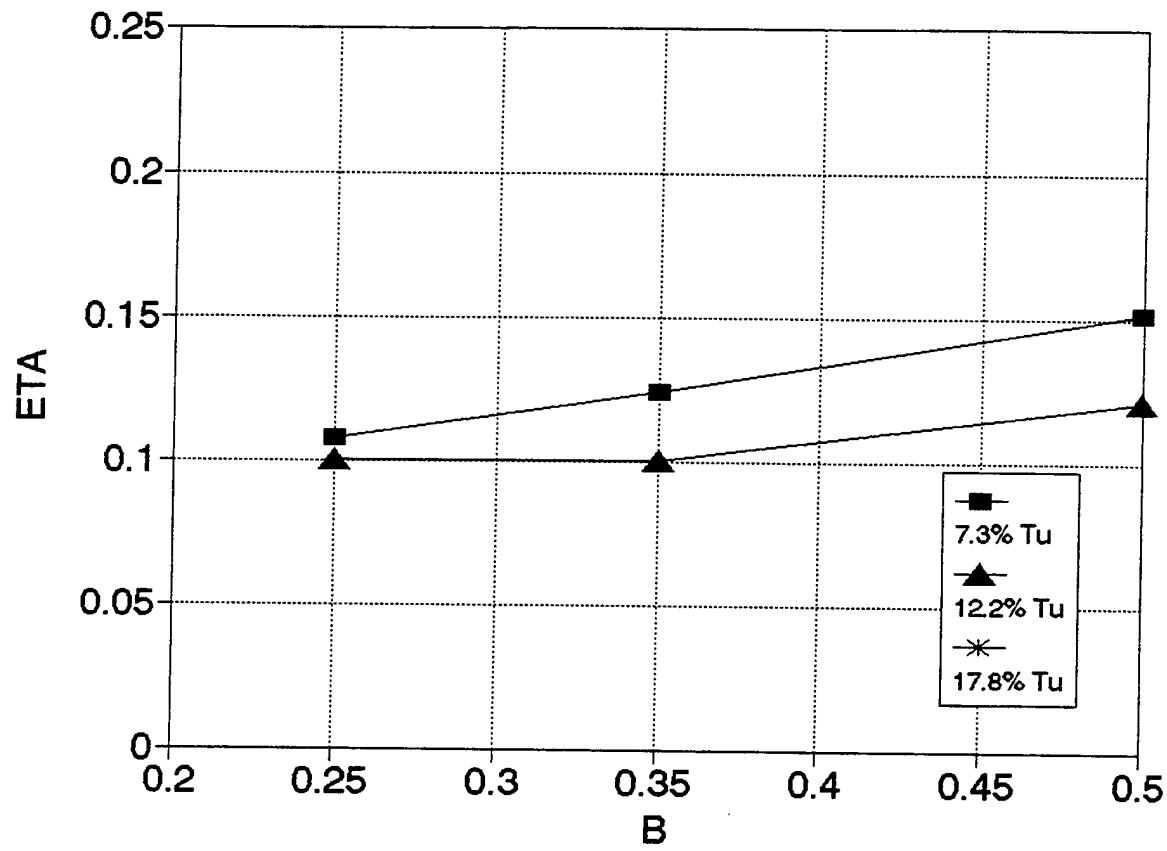
Figure E-53. Effect of Free Stream Turbulence on Film Cooling Effectiveness
X/D = 20, Free stream velocity at injection = 85 m/s
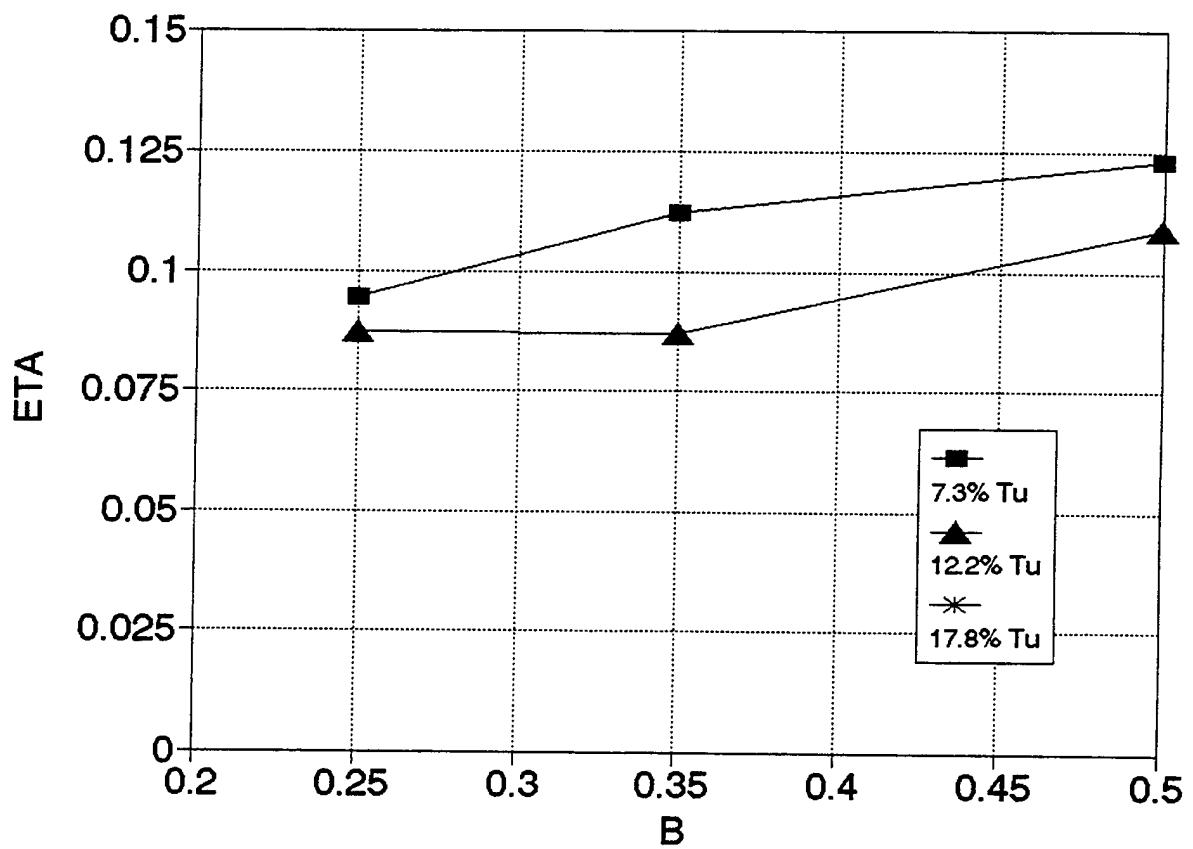
Figure E-54. Effect of Free Stream Turbulence on Film Cooling Effectiveness
X/D = 25, Free stream velocity at injection = 85 m/s
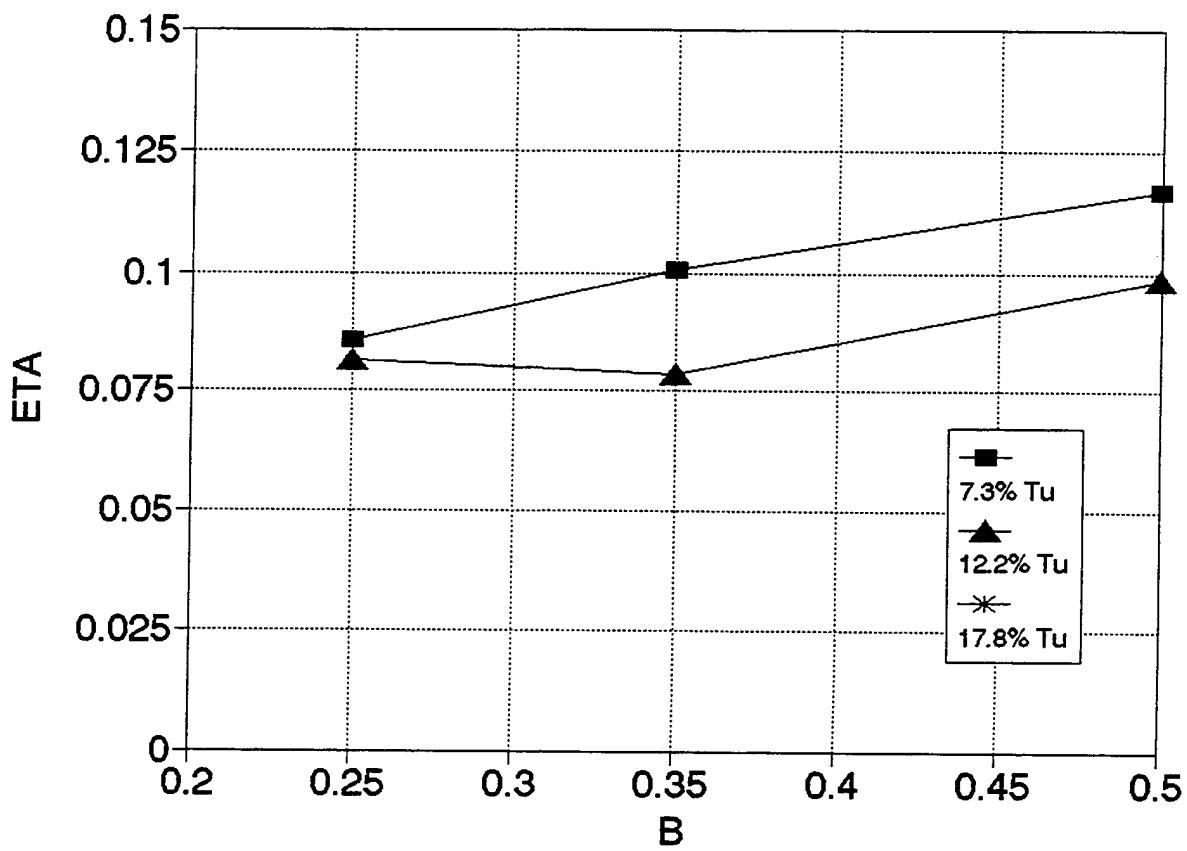
Figure E-55. Effect of Free Stream Turbulence on Film Cooling Effectiveness
X/D = 30 Free stream velocity at injection = 85 m/s
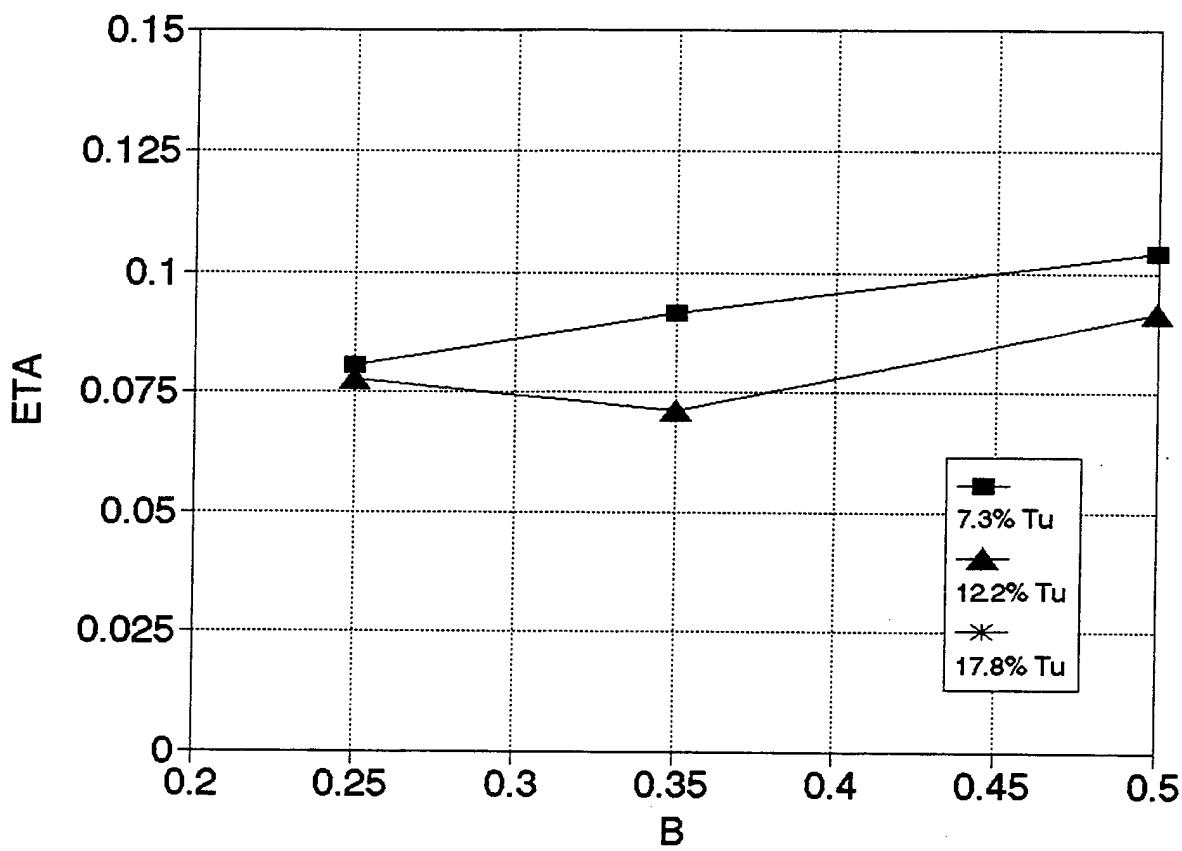
Figure E-56. Effect of Free Stream Turbulence on Film Cooling Effectiveness
X/D = 35, Free stream velocity at injection = 85 m/s
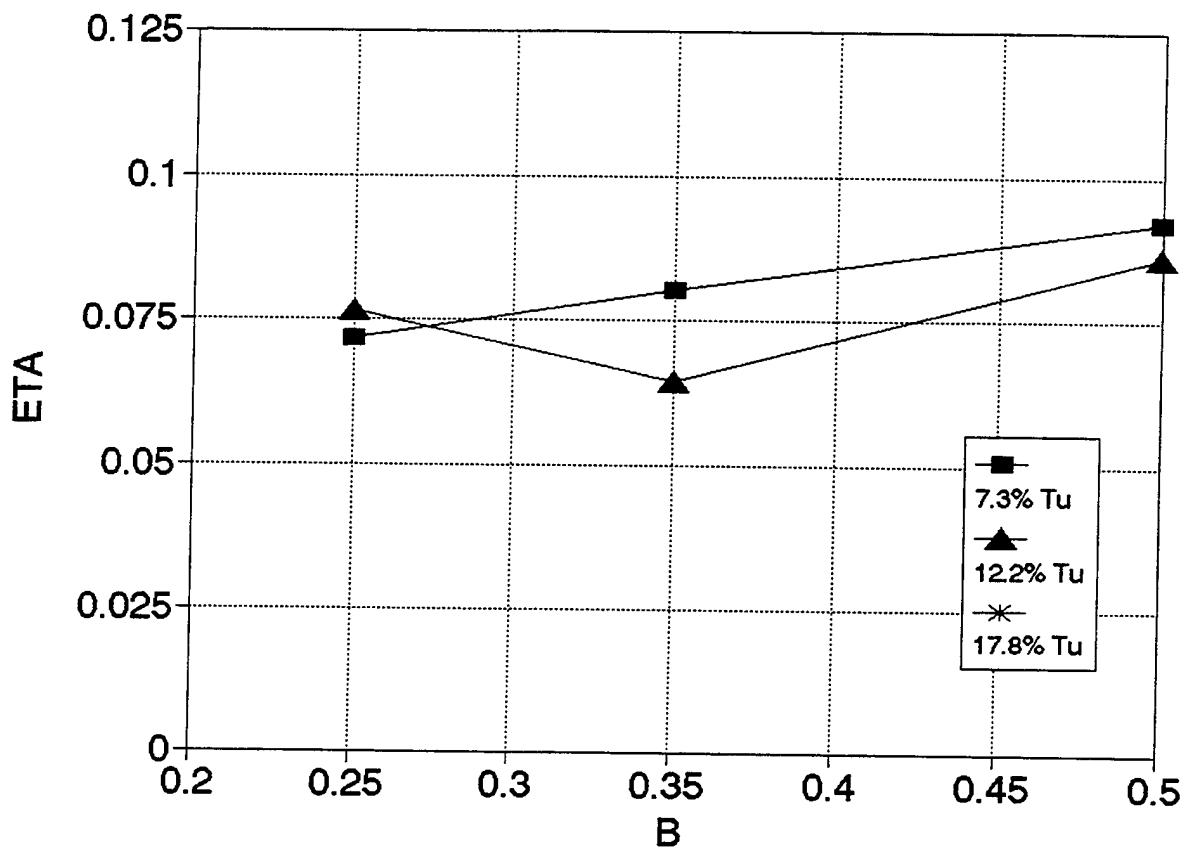
Figure E-57. Effect of Free Stream Turbulence on Film Cooling Effectiveness
X/D = 40, Free stream velocity at injection = 85 m/s
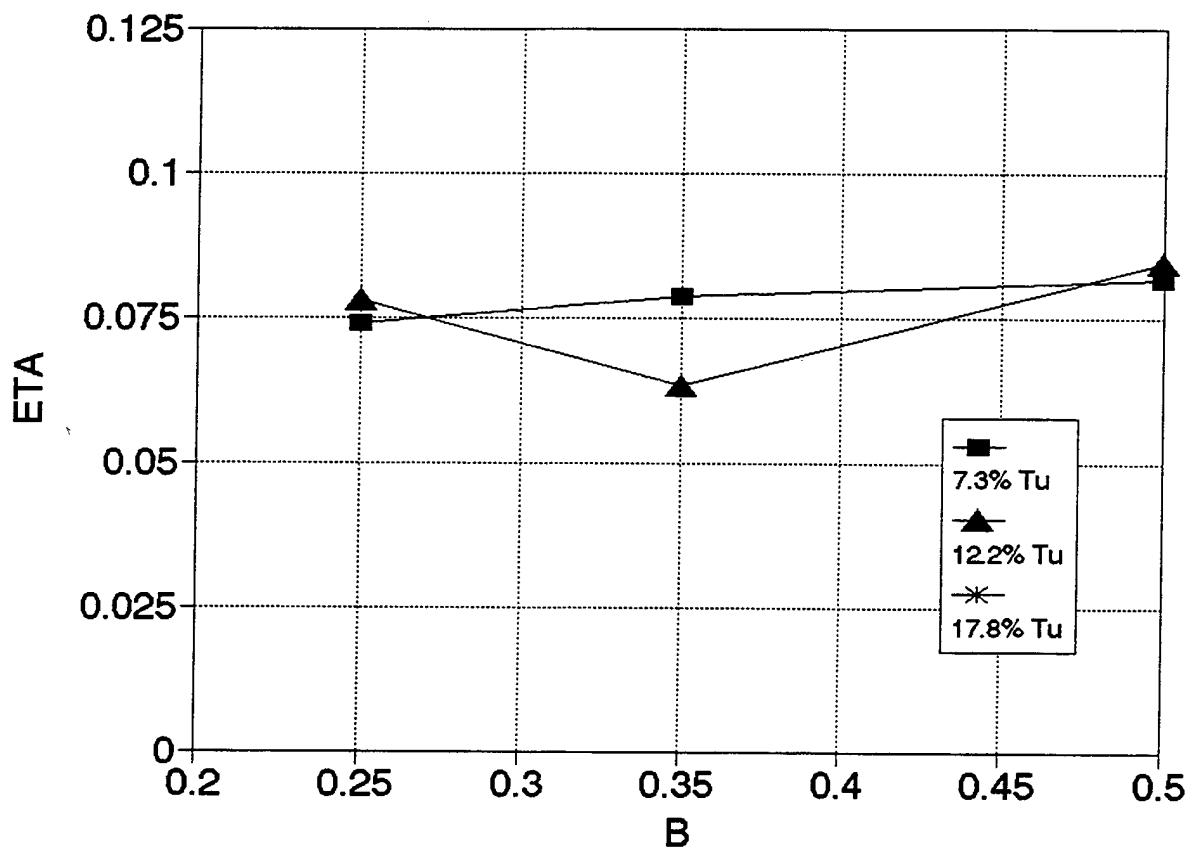
Figure E-58. Effect of Free Stream Turbulence on Film Cooling Effectiveness
X/D = 45, Free stream velocity at injection = 85 m/s
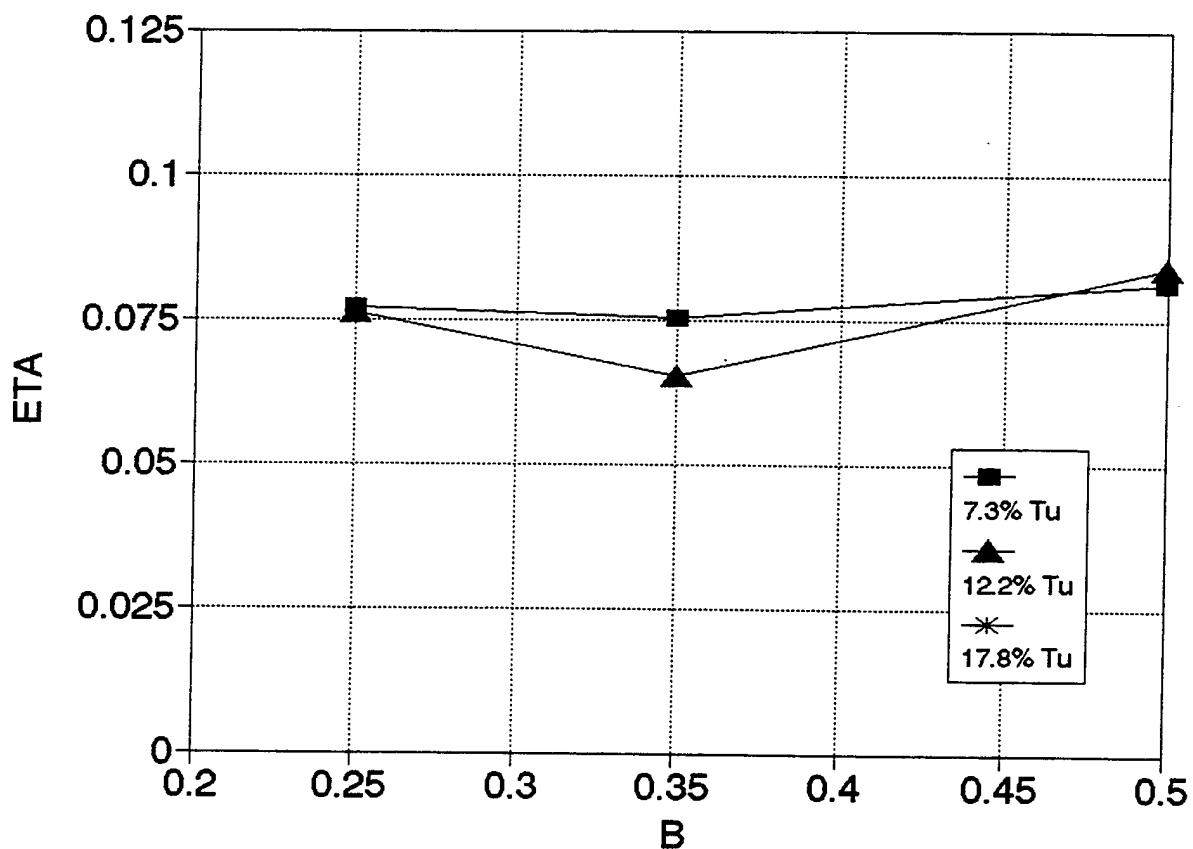
Figure E-59. Effect of Free Stream Turbulence on Film Cooling Effectiveness
X/D = 50, Free stream velocity at injection = 85 m/s
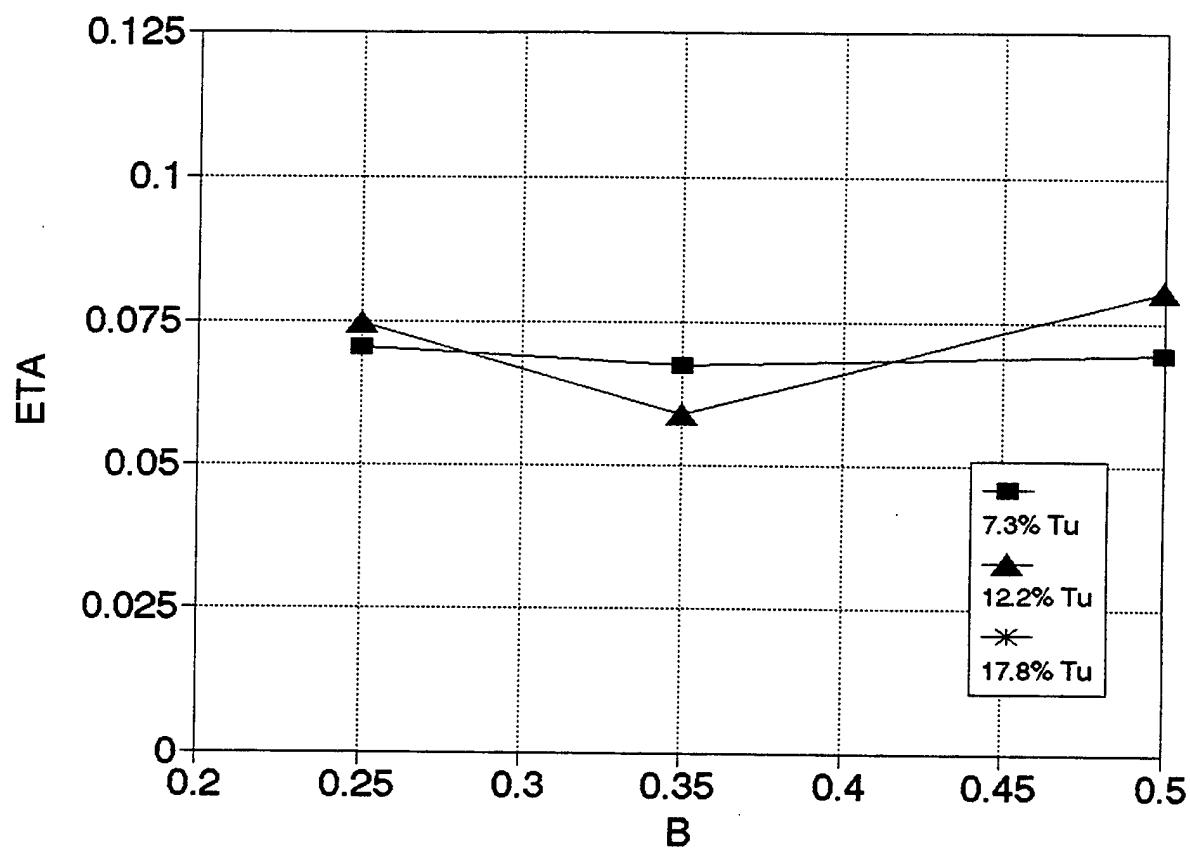
Figure E-60. Effect of Free Stream Turbulence on Film Cooling Effectiveness
X/D =55, Free stream velocity at injection = 85 m/s
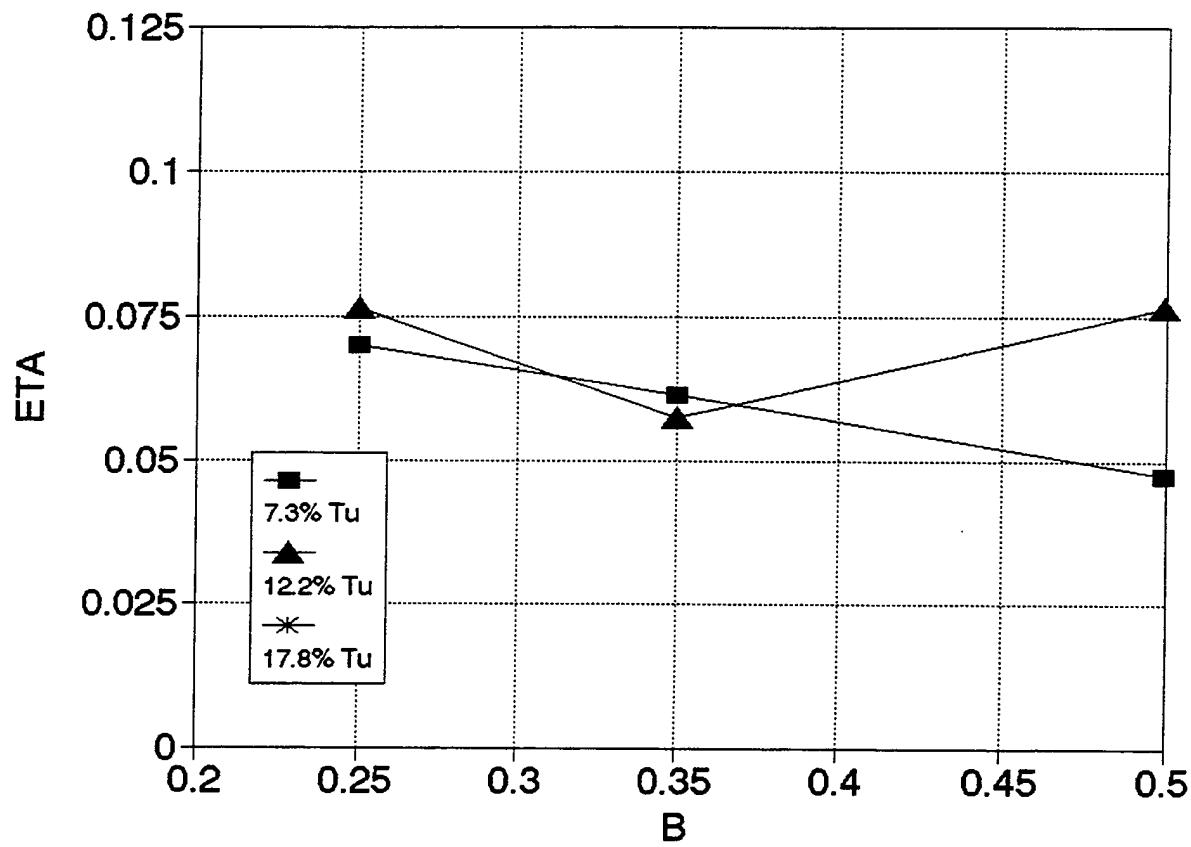
Figure E-61. Effect of Free Stream Turbulence on Film Cooling Effectiveness
X/D = 60, Free stream velocity at injection = 85 m/s
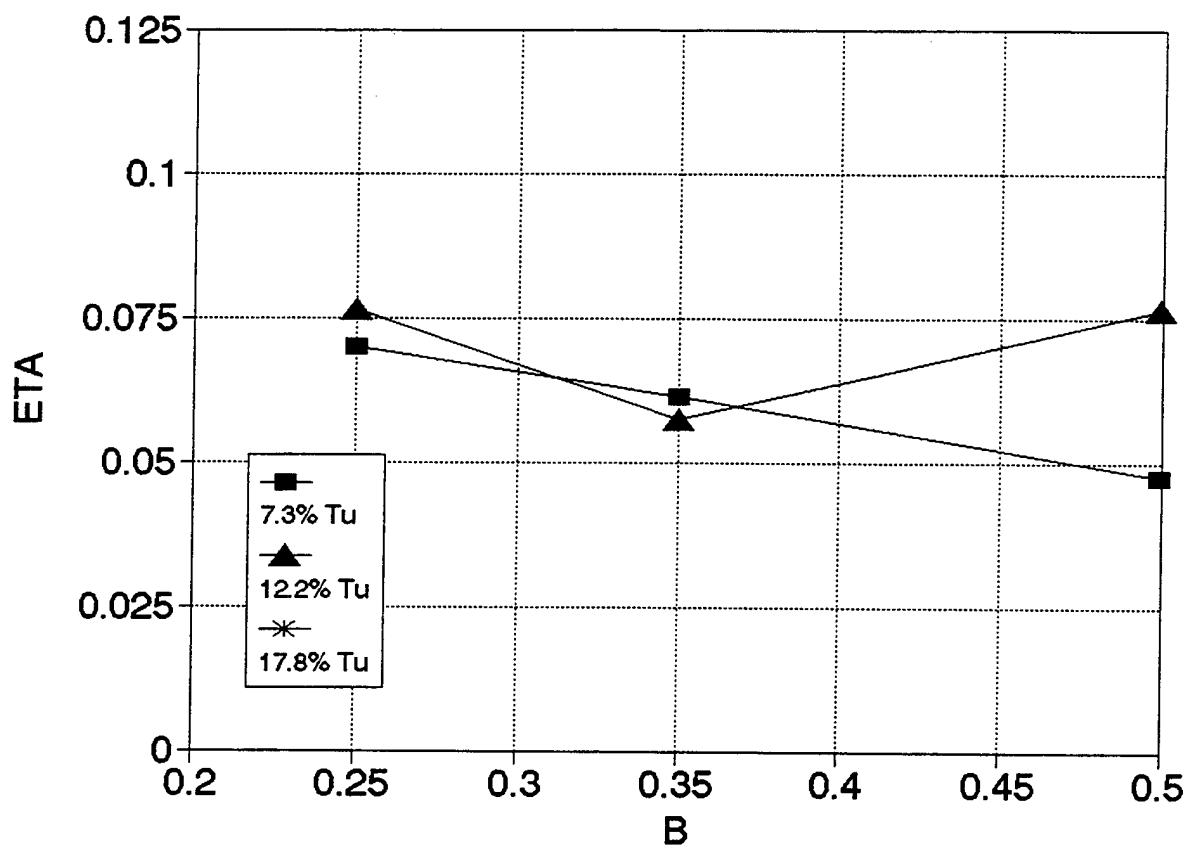
Figure E-62. Effect of Free Stream Turbulence on Film Cooling Effectiveness
X/D = 70, Free stream velocity at injection = 85 m/s

Appendix F : Effectiveness Correlation with B, X, I and S

A correlation of effectiveness with various non-dimensional combinations of parameters such as: blowing ratio (B), distance from injection to a station (X), momentum flux (I), and distance between injection hole centers (S), was attempted unsuccessfully. The specific combinations were, $\eta/B\sim XI/S$, $\eta\sim X/BS$, $\eta\sim XB/S$, $\eta/I\sim XI/S$ and $\eta/IB\sim XI/S$. These combinations were plotted for each blowing rate and all three Tu levels.

In research done by Cirrello (1991), with one and two rows of holes and no significant free stream turbulence, the first grouping, $\eta/B\sim XI/S$, came the closest to a collapse for blowing rates from 0.50 to 1.74. In the present research none of the groupings produced a collapse of effectiveness amongst different blowing rates or different Tu levels.

Appendix G : Sample calculation of τ_o and z_o

To obtain the kinematic shear stress, τ_o, the definition for the friction parameter

$$\gamma = \frac{\tau_0^{1/2}}{kU_0} \qquad (G\text{-}1)$$

was used, where U_o is the local maximum value of the velocity at a station. Solving equation (G-1) for τ_o yields

$$\tau_0 = \left(\gamma k U_0\right)^2 \qquad (G\text{-}2)$$

The value for the friction parameter in equation (G-2) is obtained from a plot of γ with Re_x (Figure 7.3 in Townsend, 1976). This plot displays several curves, each corresponding to a different velocity ratio defined as $V = U_1/U_o$, in which U_1 is the velocity of a free stream superimposed on the wall jet (for this research $U_1 = 0$, therefore $V = 0$). The value of U_o is obtained from the velocity profile at the x location where the self-preserving distribution is sought.

For example, at $x = 64.6$ cm: $U_o = 51.95$ m/s, $\gamma = 0.131$, $k = 0.41$. Substituting these values into equation (G-2) yields

$$\tau_0 = \left[(0.131)(0.41)(51.95m/s)\right]^2 = 7.79m^2/s^2$$

To find z_o at the x location in question, the self-preserving distribution equation

$$U = \frac{\tau_0^{1/2}}{k}\left[\log\left(\frac{z}{z_0}\right) - \frac{z}{\eta_1 l_0}\right] \qquad (5\text{-}2)$$

is solved for z_o by dividing both sides of the equation by the kinematic shear term and isolating the log term in the right hand side

$$U\left(\frac{k}{\tau_0^{1/2}}\right) + \frac{z}{\eta_1 l_0} = \log\left(\frac{z}{z_0}\right),$$

taking the log base 10 of both sides of the equation

$$10^{\left[U\left(\frac{k}{\tau_0^{1/2}}\right)+\frac{z}{\eta_1 l_0}\right]} = \frac{z}{z_0},$$

and finally multiplying through by z_0

$$z_0 = \frac{z}{10^{\left[U\left(\frac{k}{\tau_0^{1/2}}\right)+\frac{z}{\eta_1 l_0}\right]}} \qquad (G-3)$$

Next, an arbitrary point (U, z) in the profile at x = 64.6 cm is substituted into equation (G-3), along with the value of $\eta_1 l_0 = Y_m$ at that location. These quantities are: U = 51.52 m/s, z = 0.01524 m, and Y_m = 0.02035 m. The substitution yields

$$z_0 = \frac{0.01524m}{10^{\left[51.52m/s\left(\frac{0.41}{(7.79m^2/s^2)^{1/2}}\right)+\frac{0.01524m}{0.02032m}\right]}} = 7.373 \times 10^{-11}$$

Vita

Lilith I. Sorensen was born on June 9th 1965 in Manhattan, New York. She graduated form Ana Roque high school in Humacao, Puerto Rico in 1982 and attended the Interamerican University, Hato Rey, Puerto Rico then transferred to Embry Riddle Aeronautical University, Daytona Beach, Florida from which she graduated with a Bachelor of Science in Aeronautical Engineering in April 1989. Upon graduation she was employed as a Mechanical Engineer for ECC International, Orlando, Florida where she designed flight control components for the Air Force C-17 maintenance trainer. She later worked as an Electronics Engineer for the Defense Electronics Supply Center (DESC), Dayton, Ohio, performing audits and providing management oversight of the test and manufacture of electronics component to be used in military weapons systems. While at DESC she entered the School of Engineering, Air Force Institute of Technology, as a part-time student in July 1992. She is now employed as a Heat Transfer Engineer for TK Engineering, Springdale, Ohio where she performs heat transfer analysis of gas turbine engine components.

Permanent Address: 430 North Village Drive

Centerville, Ohio

REPORT DOCUMENTATION PAGE

1. AGENCY USE ONLY (Leave blank)	2. REPORT DATE	3. REPORT TYPE AND DATES COVERED
	March 1998	Thesis

4. TITLE AND SUBTITLE

Effect of High Free Stream Turbulence on Film Cooling Using Double Row of 30° Slant-Hole Injectors

5. FUNDING NUMBERS

6. AUTHOR(S)

Lilith I. Sorensen

7. PERFORMING ORGANIZATION NAME(S) AND ADDRESS(ES)

Air Force Institute of Technology,
2950 P Street
WPAFB OH 45433-7765

8. PERFORMING ORGANIZATION REPORT NUMBER

AFIT/GAE/ENY/98M-03

9. SPONSORING/MONITORING AGENCY NAME(S) AND ADDRESS(ES)

Dr. Richard Rivir   Phone: (937)255-7621
AFRL/POTT
1950 Fifth Street
WPAFB OH 45433-7251

10. SPONSORING/MONITORING AGENCY REPORT NUMBER

11. SUPPLEMENTARY NOTES
Advisor
Dr. Paul King

12a. DISTRIBUTION/AVAILABILITY STATEMENT
Approved for public release; distribution unlimited

12b. DISTRIBUTION CODE
A

13. ABSTRACT (Maximum 200 words)

In this study free stream turbulence levels from 7.3 % to 17.8 % are applied to film cooling over a flat plate with two rows of 30 ° slant-holes using a wall jet as the main stream air supply and source of turbulence. Blowing ratios are varied from 0.25 to 2.0 and free stream velocities at injection range from 10 m/s to 85 m/s. A constant density ratio of 1.07 is kept throughout the experiment. Results show that for different magnitudes of blowing ratio free stream turbulence has a different influence on effectiveness. At the forward stations, where blow-off was present at high blowing ratios, high free stream turbulence increased effectiveness. While at mid to aft stations for all blowing ratios high free stream turbulence decreased effectiveness. A correlation for effectiveness with a non-dimensional group of film cooling parameters is offered. The effectiveness correlated best 10 to 15 diameters after injection where blow-off effects are no longer present, and before the very far downstream stations where uncertainties in the measurements were greater.

14. SUBJECT TERMS
Film Cooling, Effectiveness, Blowing Ratio, Coolant Injection, Free Stream Turbulence, Discrete hole Coolant Injection, Flat Plate, Wall Jet, Slant-Holes, Mass Flux Ratio

15. NUMBER OF PAGES
200

16. PRICE CODE

17. SECURITY CLASSIFICATION OF REPORT	18. SECURITY CLASSIFICATION OF THIS PAGE	19. SECURITY CLASSIFICATION OF ABSTRACT	20. LIMITATION OF ABSTRACT
Unclassified	Unclassified	Unclassified	UL